

University of New Hampshire

University of New Hampshire Scholars' Repository

Doctoral Dissertations

Student Scholarship

Spring 2003

Design and in situ testing of a piezometer system to measure earthquake -induced pore -pressure changes

Robert Farrell

University of New Hampshire, Durham

Follow this and additional works at: <https://scholars.unh.edu/dissertation>

Recommended Citation

Farrell, Robert, "Design and in situ testing of a piezometer system to measure earthquake -induced pore -pressure changes" (2003). *Doctoral Dissertations*. 123.

<https://scholars.unh.edu/dissertation/123>

This Dissertation is brought to you for free and open access by the Student Scholarship at University of New Hampshire Scholars' Repository. It has been accepted for inclusion in Doctoral Dissertations by an authorized administrator of University of New Hampshire Scholars' Repository. For more information, please contact Scholarly.Communication@unh.edu.

INFORMATION TO USERS

This manuscript has been reproduced from the microfilm master. UMI films the text directly from the original or copy submitted. Thus, some thesis and dissertation copies are in typewriter face, while others may be from any type of computer printer.

The quality of this reproduction is dependent upon the quality of the copy submitted. Broken or indistinct print, colored or poor quality illustrations and photographs, print bleedthrough, substandard margins, and improper alignment can adversely affect reproduction.

In the unlikely event that the author did not send UMI a complete manuscript and there are missing pages, these will be noted. Also, if unauthorized copyright material had to be removed, a note will indicate the deletion.

Oversize materials (e.g., maps, drawings, charts) are reproduced by sectioning the original, beginning at the upper left-hand corner and continuing from left to right in equal sections with small overlaps.

ProQuest Information and Learning
300 North Zeeb Road, Ann Arbor, MI 48106-1346 USA
800-521-0600

UMI[®]

DESIGN AND IN SITU TESTING OF A PIEZOMETER
SYSTEM TO MEASURE EARTHQUAKE-INDUCED PORE-
PRESSURE CHANGES .

By

Robert Farrell

BS, University of Maine, 1969

MS, University of Maine, 1975

MS, University of New Hampshire, 1983

DISSERTATION

Submitted to the University of New Hampshire
in Partial Fulfillment of
the requirements for the degree of

Doctor of Philosophy
in
Engineering: Civil

May 2003

UMI Number: 3083728

UMI[®]

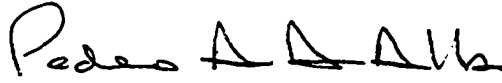
UMI Microform 3083728

Copyright 2003 by ProQuest Information and Learning Company.

All rights reserved. This microform edition is protected against
unauthorized copying under Title 17, United States Code.

ProQuest Information and Learning Company
300 North Zeeb Road
P.O. Box 1346
Ann Arbor, MI 48106-1346

This dissertation has been examined and approved.



Dissertation Director, Pedro A. de Alba
Professor of Civil Engineering



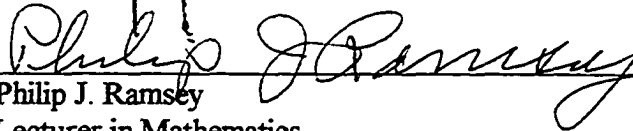
Jean Benoit
Professor of Civil Engineering



T. Leslie Youd
Professor of Civil Engineering
Brigham Young University



Thomas P. Ballester
Associate Professor of Civil Engineering



Philip J. Ramsey
Lecturer in Mathematics

May 9 2003
Date

ACKNOWLEDGEMENTS

The work described in this dissertation was made possible by grant No. CMS-9709334 from the National Science Foundation. This support is gratefully acknowledged.

Thank you Dr. de Alba. It is hard to explain how enjoyable it has been to have had the privilege to work with you over the past 5 years. I have never worked for someone that has so many excellent suggestions that always seem to be just the right ones at the just the right time.

Thanks to Dr. Benoit, Dr. Ballestero, Dr. Youd, and Professor Ramsey for providing critical review of this research.

Thanks to the Hedding Camp Meeting Association for making the Camp Hedding site available for testing. In particular, I would like to thank Barbara Fuller and James Odian.

I would like to thank the firemen on Treasure Island and their Assistant Deputy Chief Daniel A. Sullivan for their help in the field and hot coffee.

My thanks to Al Cramlet of the Caltrans Strong Motion Instrument Program for his help in the field and the California Department of Transportation, Strong Motion Instrument Program for access to the Treasure Island facility.

Thank you Kelly Hinton in the finance office for smoothing the way in so many things. Thank you Hui Chen for great discussions in the office and the valuable help in the field. Thank you Professor Baldwin for helping with the noise problems.

Thank you Bob Champlain for your help and ideas in the construction of numerous pieces of equipment.

I would like to extend a special thanks to Dr. Gress for giving me the encouragement to return to school. Your time and patience was critical.

Thank you Bobbi for your support over the last 5 years.

TABLE OF CONTENTS

LIST OF FIGURES.....	v
LIST OF TABLES.....	xiv
ABSTRACT.....	xv

Chapter	PAGE
I: Introduction and Literature Review.....	1
II: Pressure Vessel Testing.....	23
III: Pool Testing.....	51
IV: Field Testing Results.....	69
V: Frequency Analysis.....	100
VI Summary and Conclusions.....	126
List of References.....	143
APPENDIX A: Testing at Camp Hedding, April 2000	145
APPENDIX B: Testing at Camp Hedding, June and July 2000.....	164
APPENDIX C: Testing at Treasure Island, August 2000.....	173
APPENDIX D: Testing at Camp Hedding, October to December 2000.....	201
APPENDIX E: Testing at Treasure Island, March 2001.....	226
APPENDIX F: Numerical simulation.....	250

LIST OF FIGURES

Chapter I

Figure I.1 Acceleration and pore pressure record for the 1980 Mid-Chiba earthquake, Owi Island.	5
Figure I.2 Copy of Ishihara et al. (1989) Figures 18, 19, and 21 showing the upward ratcheting of pore pressures with ground acceleration	6
Figure I.3 Measured ground accelerations and pore pressure increases measured by USGS piezometers	8
Figure I.4 Increases in pore pressure during the 1995 Hyogoken-Nambu earthquake, Japan.	10
Figure I.5 Locations of the USGS piezometers, signal wells, and reference piezometers installed at the Wildlife site.	12
Figure I.6 Wildlife site air test (Hushmand et al, 1994)	14
Figure I.7 An example of the signal generated by the 1300-lb weight dropped for a height of 42 inches (Scott et al., 1996)	18
Figure I.8 Location map for piezometers used in Figure I.7 for drop tests 8 and 9. (Scott et al. 1996).	19
Figure I.9 Correlation of drop height to pressures measured in the piezometers.	22

Chapter II

Figure II.1 Pressure vessel design.	25
Figure II.2 Pass-through insertion sleeve in the bottom of the pressure vessel for inserting piezometer tip.	26
Figure II.3 Triaxial pressure chambers are used to regulate pressure within the test vessel.	27
Figure II.4 Sieve analysis for sand used in pressure vessel testing.	29
Figure II.5 Protective tip as designed by Youd (1996).	31
Figure II.6 The arrangement of the sand pressure vessel and pressure cells for manual cycling of pressure.	33

Figure II.7 Setup for creating dynamic pulse through the backpressure system using a shot actuated hammer (shot hammer).-----	35
Figure II.8 The Keller 1 transducer with the protective tip responds nearly identically as the reference transducer.-----	38
Figure II.9 Normalize signal received by Keller 1 transducer during tests.-----	39
Figure II.10 FFT for Keller 1, 7-30-99 data. -----	41
Figure II.11 FFT for Keller 1. Servo cycling of water pressures.-----	42
Figure II.12 Dynamic pressure signal generated by the cycling of the servo in a sand specimen. -----	43
Figure II.13 Shot hammer creates the maximum rate of change in pressure per second.-----	47
Figure II.14 Agreement between the Keller 1 transducer and the reference transducer.-----	48
Figure II.15 Digging the protective tip out of sand after testing. -----	49
Figure II.16 New protective tip design allows access to the piezometer screens after installation.-----	50

Chapter III

Figure III.1 Pool testing-Signal generating system. -----	54
Figure III.2 Roctest YEP 3.65/5.25 Packer used to seal the well casing below the well screen. -----	55
Figure III.3 Surge Block Design. -----	56
Figure III.4 Anvil drop distance.-----	57
Figure III.5 Pool Testing. Signal generating system.-----	61
Figure III.6 Pool Testing, Roctest #2 located in the signal well.-----	62
Figure III.7 Impact wave.-----	65
Figure III.8 Impact wave pressure decreases by the inverse square of the distance from the source well. -----	67

Figure III.9 Keller 1 transducer in protective tip located 16" from the signal well.	68
--	----

Chapter IV

Figure IV.1-Signal generating system as used in the testing at Camp Hedding and Treasure Island	75
---	----

Figure IV.2-The arrangement of strings used to lift and hold the 140 lb. SPT hammer.	76
--	----

Figure IV.3- Keller 2 at Camp Hedding, filtered confined pressure wave.	78
---	----

Figure IV.4 Surge block on NQ rods.	79
-------------------------------------	----

Figure IV.5 Comparison of data for Keller 3 on 8-11-00 and 4-14-01.	80
---	----

Figure IV.6 Camp Hedding impact wave arrival times at the various piezometers with distance from the signal well (Data 6).	84
--	----

Figure IV.7 Arrival times for the confined pressure wave at Keller 1 and Keller 2.	85
--	----

Figure IV.8 Change in velocity of the confined pressure wave with distance from the signal well at Treasure Island and Camp Hedding.	87
--	----

Figure IV.9- Unfiltered Keller 3 data is from Data 14 on 8-11-00 use for determining the velocity of the confined pressure wave from the impact wave and the arrival time of the confined pressure wave at the Keller 3 piezometer.	88
---	----

Figure IV.10 Filtered data for Keller 3, D-18, and D-33 "far" from Data 14 on 8-11-00 used to calculate the velocity of the confined pressure wave from the signal well to the piezometers.	89
---	----

Figure IV.11 Internally normalized confined pressure curves for Keller 1 and Keller 2.	91
--	----

Figure IV.12 Internally normalize data for Data 14.	92
---	----

Figure IV.13 Internally normalized data, for Data 3.	95
--	----

Figure IV.14 Internally normalized data for Keller 2 at Camp Hedding.	98
---	----

Figure IV.15 Comparing Druck 18 data for 8-11-00 and 3-14-01.	99
---	----

Chapter V

Figure V.1 Fourier transforms of acceleration records for several earthquakes.-----	101
Figure V.2 The signal detected by the Keller 1 transducer buried in sand within the pressure vessel. -----	104
Figure V.3 FFT for Test 2, 7-13-99, shown in Figure V.2.-----	105
Figure V.4 Keller 1 in the sand filled pressure vessel. A shot actuated hammer created the pressure change. -----	106
Figure V.5 FFT of shot-hammer signal shown in Figure V.4.-----	107
Figure V.6 Keller 1 record at 19 inches from the signal well-----	109
Figure V.7 FFT for the impact wave shown in Figure V.6.-----	110
Figure V.8 Signal detected by Keller 1 was located 16 inches from the signal well screen in the pool. -----	111
Figure V.9 The FFT for combine signal of impact wave and confined pressure wave for Test 4, 3-2-00, pool testing shown in Figure V.8. -----	112
Figure V.10 Impact wave detected by the Keller 1 transducer located in the PVC well 32 feet from the signal well (Data 7, 6-14-00, logged at 500 Hz). -----	113
Figure V.11 FFT for impact wave shown in Figure V.10 for the Keller 1 transducer installed in the PVC well 32 feet from the signal well.-----	114
Figure V.12 Filtered confined pressure wave signal from Keller 1 at Camp Hedding.-----	118
Figure V.13 FFT for confine pressure wave signal from the Keller 1 piezometer at Camp Hedding.-----	119
Figure V.15 Confine pressure wave signal from Keller 3 piezometer.-----	120
Figure V.16 FFT for Keller 3 confined pressure wave signal.-----	121
Figure V.16 Internally normalized confined pressure waves for Keller 1 and Keller 2.-----	122
Figure V.17-Confined pressure wave signal from Keller 3 piezometer.-----	123

Figure V.18 FFT for Keller 3 confined pressure wave signal.-----	124
--	-----

Appendix A

Figure A.1 Location map for Camp Hedding testing site in Epping, New Hampshire.-----	146
--	-----

Figure A.2 Boring log for signal well.-----	148
---	-----

Figure A.3 Sieve analysis of samples from the 18 to 30 foot zone -----	149
--	-----

Figure A.4 Location map of wells, piezometer locations, and observation well (OW).-----	151
---	-----

Figure A.5 Roctest #1 transducer with drive tip.-----	153
---	-----

Figure A.6 Adjustment of Rt#1 to ambient water pressure at the depth of 20 below the ground surface-----	154
--	-----

Figure A.7 Roctest #1 piezometer located 6.2 feet from the signal well at location R-2. -----	157
---	-----

Figure A.8 The setup of the signal generating system at Camp Hedding.-----	158
--	-----

Figure A.9 Keller 2 is installed at location K-2 5.6 feet from the signal well to a depth of 20 feet. -----	160
---	-----

Figure A.10 Change in signal amplitude with distance from the signal well.----	161
--	-----

Appendix B

Figure B.1 Modifications made to the signal generating system.-----	165
---	-----

Figure B.2 The pressure changes measured by the Validyne transducer in the signal well. -----	167
---	-----

Figure B.3 Impact (P) waves measured by the Keller 2 piezometer located 20 feet from the signal well and the Keller 1 transducer located in the PVC well 32 feet from the signal well.-----	168
---	-----

Figure B.4 Confined pressure waves for Keller 1 in PVC well 32 feet from the signal well and Keller 2 twenty feet from the signal well. -----	171
---	-----

Figure B.5 Data for June-July 2000 testing has been added to Figure A.10 of the April 2000 testing at Camp Hedding.	172
---	-----

Appendix C

Figure C.1 Location map for Treasure Island.	174
Figure C.2 Boring log for signal well.	175
Figure C.3 Sieve analysis of samples from the 18 to 30 foot zone in which all the testing was done.	176
Figure C.4 Location map for wells and piezometers, Fire Station Site.	179
Figure C.5 All Druck 17 (D-17) signals for 8-11-00.	185
Figure C.6 All Druck 18 (D-18) signals for 8-11-00.	186
Figure C.7 Unfiltered data from Druck 18 showing the impact wave.	187
Figure C.8 All Druck 33 "near" signals for 8-11-00.	189
Figure C.9 All Druck-33 "far" signals for 8-11-00.	190
Figure C.10 Signal from Keller 3 transducer located in the inclinometer casing.	192
Figure C.11 Signal from Keller 3 located in the water table well.	194
Figure C.12 Signal from Keller 3 piezometer is located in the new boring.	195
Figure C.13 Enlargement of the signal shown on Figure C.13.	196
Figure C.14 Change of signal strength with distance from the signal well.	197

Appendix D

Figure D.1 The screen of Roctest #1 was clogged with silt/clay after being advanced to a depth of 20.5 feet.	202
Figure D.2 The Keller 1 transducer and protective tip were modified for installation at Camp Hedding 10 feet from the signal well.	204
Figure D.3 Developing Keller 1 piezometer by the injection of deaired water through the screens.	207

Figure D.4 The arrangement of strings used to lift and hold the 140 lb. SPT hammer. -----	208
Figure D.5 Impact of hammer on anvil. -----	209
Figure D.6 The PCB transducer exited the bottom of the NQ rods through hole in the bottom plate. -----	211
Figure D.7 The responses of the PCB transducer located in the PCB well and the GEMS transducer located in the signal well are compared. -----	213
Figure D.8 Responses of the PCB transducer in the PVC well and the GEMS transducer in the signal well are compared.-----	214
Figure D.9 The response of the GEMS transducer in the signal well.-----	215
Figure D.10 Response of the PCB transducer located in the PVC well.-----	216
Figure D.11 Differences in the response of PCB transducer located in the signal well.-----	217
Figure D.12 The response of the PCB blast transducer located in the signal well. - -----	218
Figure D.13 Unfiltered signal received form the Keller 1.-----	220
Figure D.14 Filtered signal from Keller 1 logged at 5000 Hz.-----	221
Figure D.15 Keller 1 signal detected on 11-15-00. -----	223
Figure D.16 Response of the Keller 2 piezometer located 20 feet from the signal well. The signal is unfiltered.-----	224
Figure D.17- Response of the Keller 2 piezometer located 20 feet from the signal well. -----	225

Appendix E

Figure E.1 Signal generating system set up over the signal well-----	227
Figure E.2 Signal from PCB blast transducer located in the signal well.-----	230
Figure E.3 Signal from the PCB blast transducer located in the signal well.---	231
Figure E.4 Signal from Keller 3 data logged at 3300 Hz.-----	232

Figure E.5 Signal from Keller 3-----	233
Figure E.6 Filtered signal from Keller 3 data logged at 500 Hz. -----	235
Figure E.7 Unfiltered signal from Druck 18 logged at 3300 Hz.-----	236
Figure E.8 Unfiltered signal from Druck 18 logged at 500 Hz..-----	237
Figure E.9 Filtered signal from Druck 18 logged at 3300 Hz-----	238
Figure E.10 Filtered signal from Druck 18 logged at 3300 Hz.-----	239
Figure E.11 Confined pressure waves from Druck 18 data. -----	240
Figure E.12 Druck 17 pressure signal logged at 3300 Hz.-----	241
-	
Figure E.13 Druck 17 pressure signal logged at 3300 Hz.-----	243
Figure E.14 Druck 17 data 7 corrected for drift in the base-----	244
Figure E.15 Druck 33 "far" unfiltered data logged at 3300 Hz.-----	245
Figure E.16 Druck 33 "far" unfiltered data logged at 500 Hz.-----	246
Figure E.17 Filtered signal from Druck 33 "far" data logged at 3300 Hz.-----	247
Figure E.18 Druck 33 "far" logged at 500 Hz. -----	248
Figure F.19 Change of signal strength with distance from the signal well for all the testing at Camp Hedding and Treasure Island.-----	249

Appendix F

Figure F.1 Keller 3, Treasure Island, Data 3, 3-14-01, logging rate is 3300 Hz.-----	254
Figure F.2 Arrangement of various components of the signal generating system as used in the Smith (1955) model for the compressional wave.-----	257
Figure F.3 Modeling results show the force generated by the hammer striking the anvil being transferred down the NQ rods to the surge block.-----	260
Figure F.4 Modeling the signal generated 20 feet from the signal well.-----	264

Figure F.5 Variation of parameters in the PLASM model to get different shape response curves 20 feet from the source.-----265

Figure F.6 Calculating the arrival times of the confined pressure waves at Keller 1 and Keller 2 at Camp Hedding.-----266

Figure F.7 Modeling the confined pressure wave for T-4450 gpd.-----267

LIST OF TABLES

Chapter I

Table I.1 Comparison of drop height and pressure measured by the Caltech and USGS piezometers #175365.-----	21
---	----

Chapter V

Table V.1 Summary of the frequency of the signal detected at various piezometers.-----	129
--	-----

APPENDIX C

Table C.1 Calibration Check of Piezometers Based on Ambient Conditions.--	182
---	-----

Table C.2 Sequence of Testing at Treasure Island, August 10 and 11, 2000.---	184
--	-----

APPENDIX F

Table F.2 Input Data for Smith (1955) Model -----	256
---	-----

ABSTRACT

DESIGN AND IN SITU TESTING OF A PIEZOMETER SYSTEM TO MEASURE EARTHQUAKE-INDUCED PORE-PRESSURE CHANGES

By

Robert Farrell

University of New Hampshire, May 2003

Pore pressure changes have been measured in fine sand deposits that are known to have liquefied during earthquakes. Some of the measured signals have not been similar to what was expected during earthquake-induced liquefaction. Using artificially generated signals, several investigators have attempted to determine if existing piezometer fields designed to measure earthquake induced pore pressure changes are operating correctly. The signals generated during one investigation were not similar to those expected from an earthquake. In another investigation, while the generated signals were similar to ones expected from an earthquake, the results were not reproducible; the generated signals damaged the aquifer being tested and damaged or destroyed some piezometers being tested. This thesis describes the design and field-testing of a piezometer system that allows in situ testing of the screens on the piezometer, and in situ calibration of the transducer. An integral part of this system is a signal generating system that generates a signal with frequencies similar to those expected from an earthquake. The generated signal has been detected in piezometers at least 20 feet from the source and at depths of at least 15 feet deeper than the source. The signal has been demonstrated to be reproducible through time with no measurable damage to the

aquifer or the piezometers. It has been possible to investigate the ability of an existing piezometer field to detect earthquake-like signals and to demonstrate changes over time of some piezometers in their ability to detect earthquake-like signals. A detailed procedure for installing a piezometer array for liquefaction studies is presented.

CHAPTER I

INTRODUCTION AND LITERATURE REVIEW

I.1-Introduction

Liquefaction is one of the most important effects caused by the shaking of the ground generated by earthquakes. The 1964 Alaska's Good Friday and Japan's Niigata earthquakes focused attention on the spectacular effects of liquefaction-induced damage to buildings, waterfront facilities, roads and bridges; as well as slope failures, and flotation of buried structures. Much has been learned in the nearly forty years since these earthquakes.

Mechanically, liquefaction can be explained as follows. The shear strength (τ) of a soil is equal to the effective stress (σ') times the tangent of the friction angle (ϕ),

$$\tau = \sigma' \tan \phi.$$

The effective stress (σ') is equal to the total stress (σ) minus the pore pressure (u),

$$\sigma' = \sigma - u.$$

Liquefaction of soil occurs when the pore pressure (u) approaches the total stress (σ)

As the u approached the total stress the effective stress (σ') approaches zero.

As the effective stress approaches zero the shear strength of the soil approaches zero and soil losses its bearing capacity. Liquefaction occurs when a loose saturated granular

soil, subject to a load or shock, attempts to consolidate. This attempt causes a positive increase in pore pressure, which results in a decrease in effective stress within the sediment. Once the pore pressure becomes equal to the effective stress, the strength of the sediment is reduced to a small residual value.

As Ishihara et al. (1987) pointed out, to gain in-depth understanding for the mechanism of liquefaction, it is necessary to obtain exact time histories of accelerations and pore water pressures recorded in the field deposit during actual earthquakes. In order to gain this understanding, piezometers and accelerometers have been installed in several sites in Japan and California where liquefaction has been observed in the past. On two occasions, pore pressures have been measured when liquefaction has occurred during earthquakes. The first site to measure pore pressure change associated with liquefaction was the Wildlife site, in Imperial County California, during the 1987 Superstition Hills earthquake. The other occasion was the Port Island and Rokko Island Sites, Kobe, Japan during the 1995 Hyogoken-Nambu earthquake.

This study intended to determine if the piezometers installed at the Wildlife site and subsequently at the Treasure Island, California, National Geotechnical Experimentation Site could detect the type of water pressure signal generated by an earthquake. It was also desired to determine if there were problems with the method of piezometer installation at these sites. In order to evaluate the above, it was necessary to design and demonstrate a way of testing existing piezometers insitu to determine if they were capable of detecting a signal that would be consistent with that of an earthquake. The

study consisted of laboratory testing and field-testing. Two field sites were used. Both have similar sediment gradations and are fine to very fine-grained sand. The Camp Hedding site was located near the University of New Hampshire campus providing an opportunity for making numerous trips to the field to test out systems and methods. The Treasure Island, California, site is an existing piezometer and accelerometer field; carrying out field tests at this important location was a major objective of this study.

I.2-Literature Review

As early as the 1970's attempts were being made in Japan to measure the acceleration and pore pressures at sites that were expected to liquefy during earthquakes. Figure I.1 from Ishihara et al. (1981) shows the accelerations and pore pressures at Owi Island during the Mid-Chiba earthquake in 1980. The jump in pore pressures correlates with the maximum ground accelerations. This spike of pore pressures is followed by a long decay of the pressures back to the initial conditions. Liquefaction did not occur at this site during this earthquake and the observed maximum increase in pore pressures were 75 cm (1.065 psi or about 11% of overburden pressure) for the piezometer at a depth of 6 m and 132 cm (1.88 psi or about 9.5% of total overburden pressure) for the piezometer at a depth of 14 m.

Ishihara, Muroi, and Towhata (1989) show a similar relationship of pore pressures to maximum accelerations with some important differences between the arrival of the maximum accelerations and the build up of pore pressures. Figure I. 2 modified from Ishihara et al.. The pore pressures begin the rise up to 4 seconds before the arrival of the

maximum ground accelerations. The pore pressures increase until the maximum ground accelerations arrive at 15 seconds. After the peak accelerations pass the pore pressure begin to decrease. Figure I. 1 of Ishihara et al. (1981) has no pore pressure build up prior to the arrival of the maximum ground accelerations. The pore pressures in the two piezometers take only one large jump in pressure that occurs with the arrival of the maximum ground acceleration. In both cases, however, the maximum increase in pore pressures corresponds to the maximum acceleration. Again, no liquefaction occurred during this earthquake at this site.

This ratcheting up of pore pressures, once certain threshold acceleration has been passed, is the response expected by researchers based on their experience with laboratory undrained cyclic loading tests. From measurements such as shown in Figure I.1 and Figure I.2, this was certainly what appears to have been occurring in the liquefiable sediments during the earthquakes. Once this threshold is exceeded, the pore pressure can rise rapidly, as in Figure I.1, or more slowly, as in Figure I.2.

Holzer, Youd, and Hanks (1989) and Youd and Holzer (1994) presented data for the November 24, 1987 Superstition Hills earthquake for the Wildlife site, instrumented by the USGS, where both accelerations and pore pressures were measured at a site where liquefaction was observed to have occurred during the earthquake. The site showed sand boils and lateral surface cracking indicating liquefaction of a silty sand layer. Figure I.3 shows the measured ground accelerations and corresponding pore pressure increases. Holzer et al. (1989) indicated that maximum ground acceleration of 0.21g occurred at about 13.6 seconds and stated that:

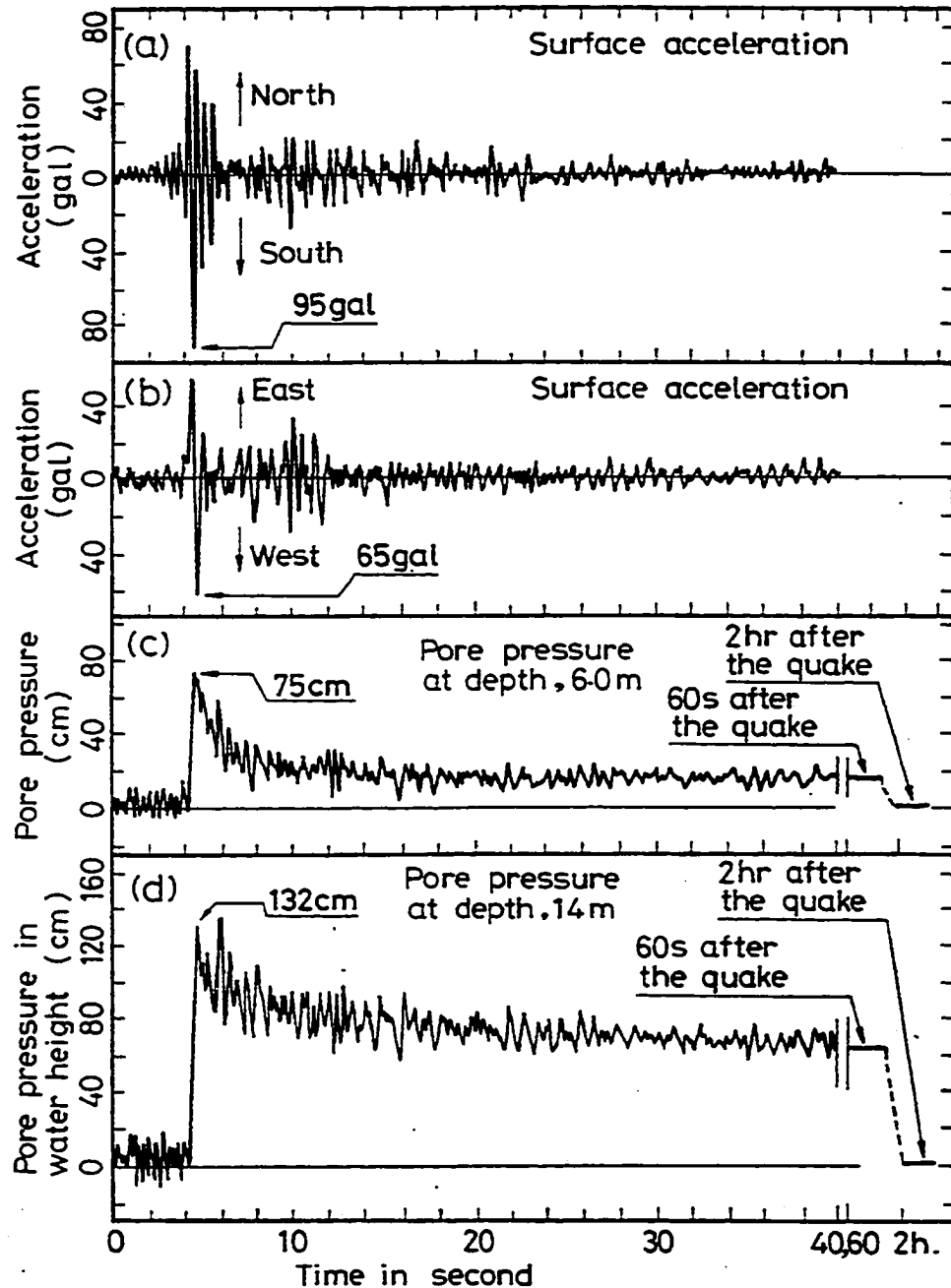


FIGURE 2-17 Instrument recordings of surface accelerations and pore water pressures at Owi Island recorded during the September 25, 1980, Mid-Chiba earthquake. Source: Ishihara et al. (1981).

Figure I.1- Acceleration and pore pressure record for the 1980 Mid-Chiba earthquake, Owi Island (from Ishihara et al. 1981, in *Liquefaction of Soil During Earthquakes*, NAS, 1985). The jump in pore pressure correlates with the maximum ground acceleration. Liquefaction did not occur at this site.

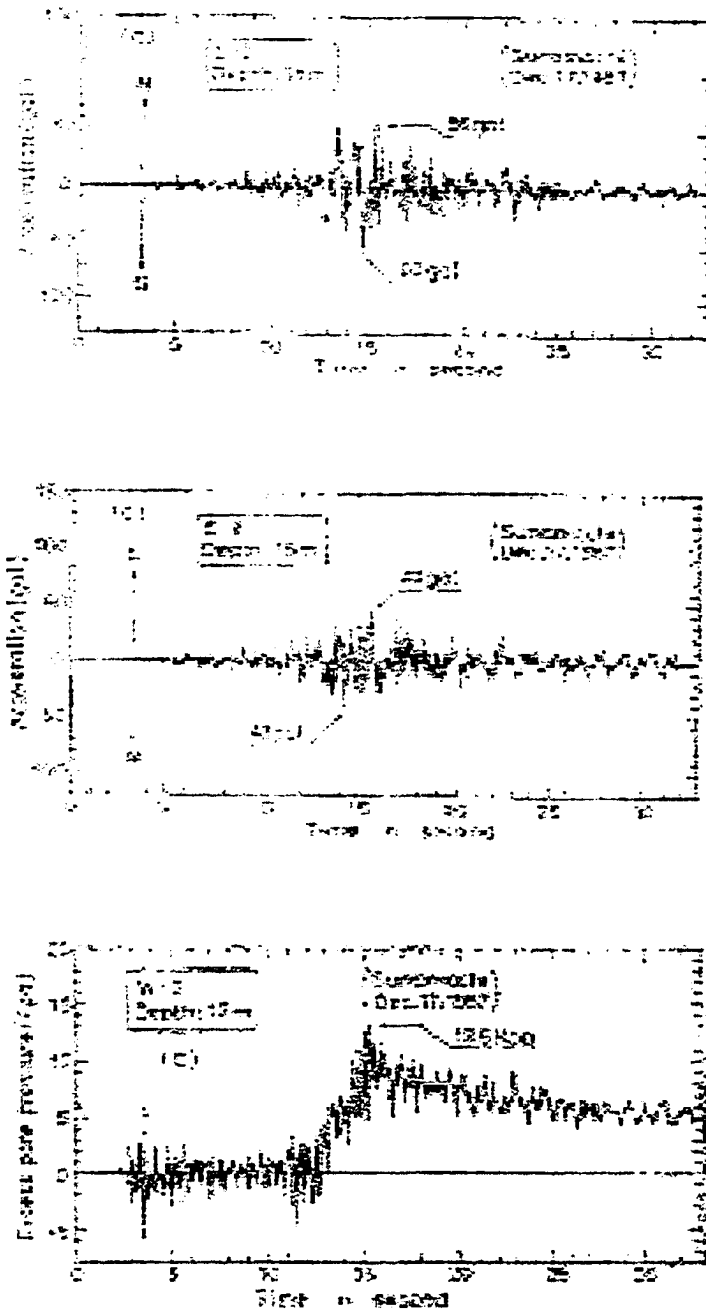


Figure I.2- The upward ratcheting of pore pressures with ground acceleration is shown for the pore pressure corresponding to the strong motion (Ishihara et al. (1989)). The maximum increase in pore pressures corresponds to the maximum acceleration. No liquefaction occurred during this earthquake.

“Pressures throughout the entire thickness of the silty sand increased slowly following the 0.21 g pulse, but at decreasing rate, until the end of the 97 second long record when the total pore pressure approached the vertical stress caused by the total weight of the overburden.”

They suggest that the change in the acceleration signal across the sand layer to low frequencies at 16 seconds is when liquefaction actually began in the sand layer rather than after the strong motion had stopped.

Holzer et al. proposed several possible causes for the delay in the response of the piezometers to the shaking: 1) migration of high pore pressures from outside the instrumented sand layer, 2) heterogeneities within the sand layer allowing only pockets of liquefaction, and 3) compaction around piezometers tips caused by pushing the tips into the sand. Youd and Holzer presented physical evidence indicating that pore pressures measured by the Wildlife piezometers during and after the earthquake were correct. Their reasoning is that seismic pore pressures were generated by cyclic shear deformation and that cyclic shear deformations increased with time after strong motion shaking ceased. By this reasoning the piezometer readings are consistent with the generating mechanism. Further, the study by Zeghal and Elgamal (1994) points out that, superimposed on the smooth pore pressure rise, are higher-frequency dynamic fluctuations and sudden pore pressure drops in the 0.5 to 1 Hz range. These strongly suggest that the four responding piezometers were capable of registering pressure signals in the dynamic range. Furumoto, Oka, Sugito, Yahima, and Fukagawa (1999) presented data for pore pressure increases from Port Island and Rokko Island during the 1995 Hyogoken-Nambu Earthquake. Figure I.4 is a copy of Furumoto et al. Figure 9

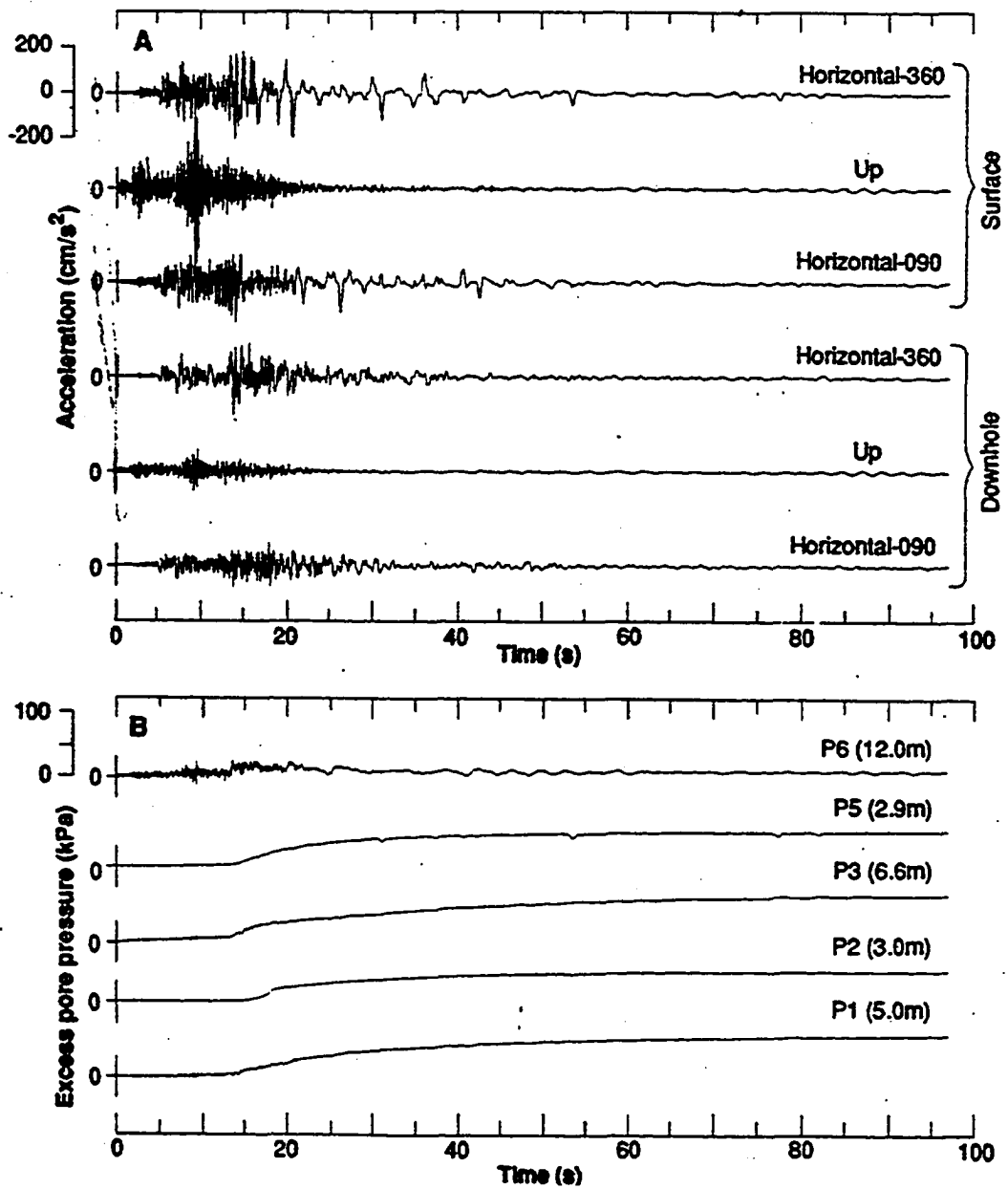


Figure I.3-Measured ground accelerations and pore pressure increases measured by USGS piezometers (from Holzer et al., 1989). The pore pressures begin a slow increase at 13.6 seconds. At about 97 seconds, the pore pressure approaches the total vertical stress.

tracing the build-up of excess pore pressures with time (in this case using the ratio of measured excess pore pressure to initial vertical effective stress). These records of pore pressure increase are similar to those shown at the Wildlife site. There is no large initial increase in the pore pressures that corresponds with the maximum acceleration as shown in Figure I.1. The pore pressure increases occur over 10 to 15 seconds for the Port Island records and for over 20 seconds for the Rokko Island records before the excess pore water pressure ratios approach 1. Roughly, the duration of the strong motion at Port Island was less than 10 seconds. Both sites have higher-frequency signals superimposed on these longer trends. The records do suggest an initial oscillating of the pore pressures both upward and downward particularly near the beginning. A similar oscillation is evident for piezometer W-3 on Figure 1.2. However, there are no net increases associated with these cycles of upward and downward pressures. Initially, for some of the records such as for the Port Island piezometer at 32 meters, the pore pressure oscillated above and below the static pore pressure for a few moments before moving upward. In summary, the Port Island and Rokko Island records also suggest that it is possible for earthquake-induced pore pressure to continue to rise after the end of strong motion.

A first attempt at systematically verifying the response of piezometer in the field was made by Hushmand, Scott, and Crouse (1994), who visited the Wildlife site. They did what they termed a preliminary investigation to determine whether the USGS-installed piezometers used to measure the pore pressures during the Superstition Hills earthquake were functioning properly during the earthquake. As noted, this was a first attempt to

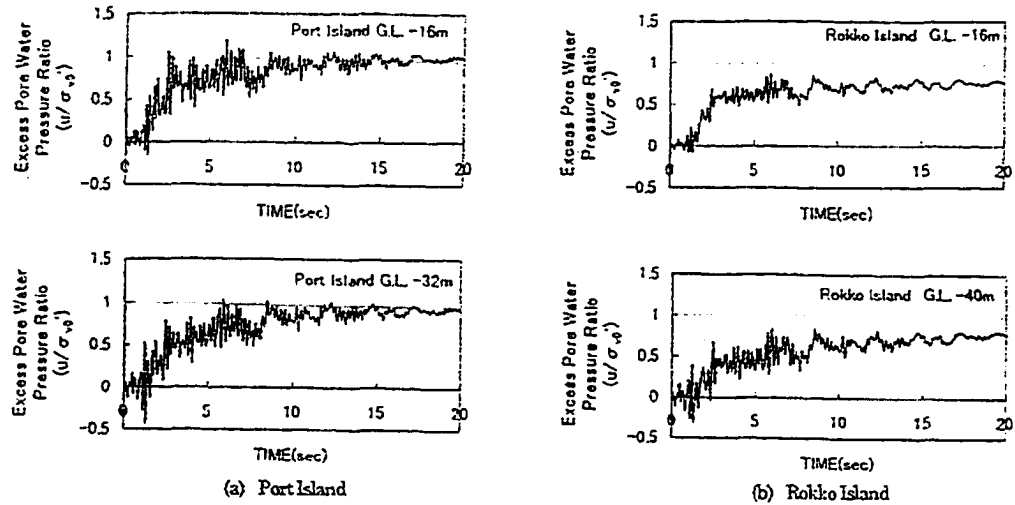


Fig.9 Time history of excess pore water pressure ratio.

Figure I.4: Increases in pore pressure during the 1995 Hyogoken-Nambu earthquake, Japan. Modified from Furumoto et al. (1999).

produce a dynamic signal in the ground water to check if the piezometers are operating in the field. The program set up to test the piezometers after the fact seemed to demonstrate that, three years after the earthquake, some of the piezometers were not functioning correctly. Their investigation undertook to 1) determine possible effects of installation on the piezometer responses, 2) specifically, to determine possible effects of installation on the pore pressure change measured during the earthquake of November 24, 1987, and, 3) examine and evaluate different ways of checking the conditions and performance of the installed USGS piezometers in situ. They used a compressed air

“popper” and compressed air pulses to create pore pressure changes in a signal well to activate the piezometers. New reference piezometers were installed to compare with the USGS piezometers during the application of pressure.

Figure I.5 is a copy of Hushmand et al.’s Figure 6 and 7 showing the array of USGS piezometers and the locations of the signal wells and reference piezometers installed for their study. The signal wells were installed 7 to 8 feet from the existing USGS and reference piezometers. Each signal well was drilled to the depth of the corresponding USGS piezometer and a 2-foot well screen installed opposite the piezometers. The reference piezometer was located 2 feet from the USGS piezometer and was pushed to the same depth as the USGS piezometer. The popper applied compressed air to the ground water at the level of the well screen in a series of bursts of compressed air within the well. The compressed air loading applied a sudden burst of compressed air to the top of the water column in the well. The top of the well was sealed to prevent leakage. The pressure was maintained for 30 to 60 seconds before the air pressure supply valve was closed and the relief valve was opened. Figure I.6, from Hushmand et al., indicates the pressure delivered by the popper was built up over nearly 100 seconds then allowed to decay. The single-burst compressed air test builds pressures up over about 10 seconds. The response of the corresponding reference piezometer (BAT) and the USGS piezometer were recorded. The USGS piezometer, P2 in this figure, did not match the rise recorded in the reference piezometer. Hushmand et al. determined that of the four USGS piezometers (P1, P2, P3, and P5), which provided data at the time of the

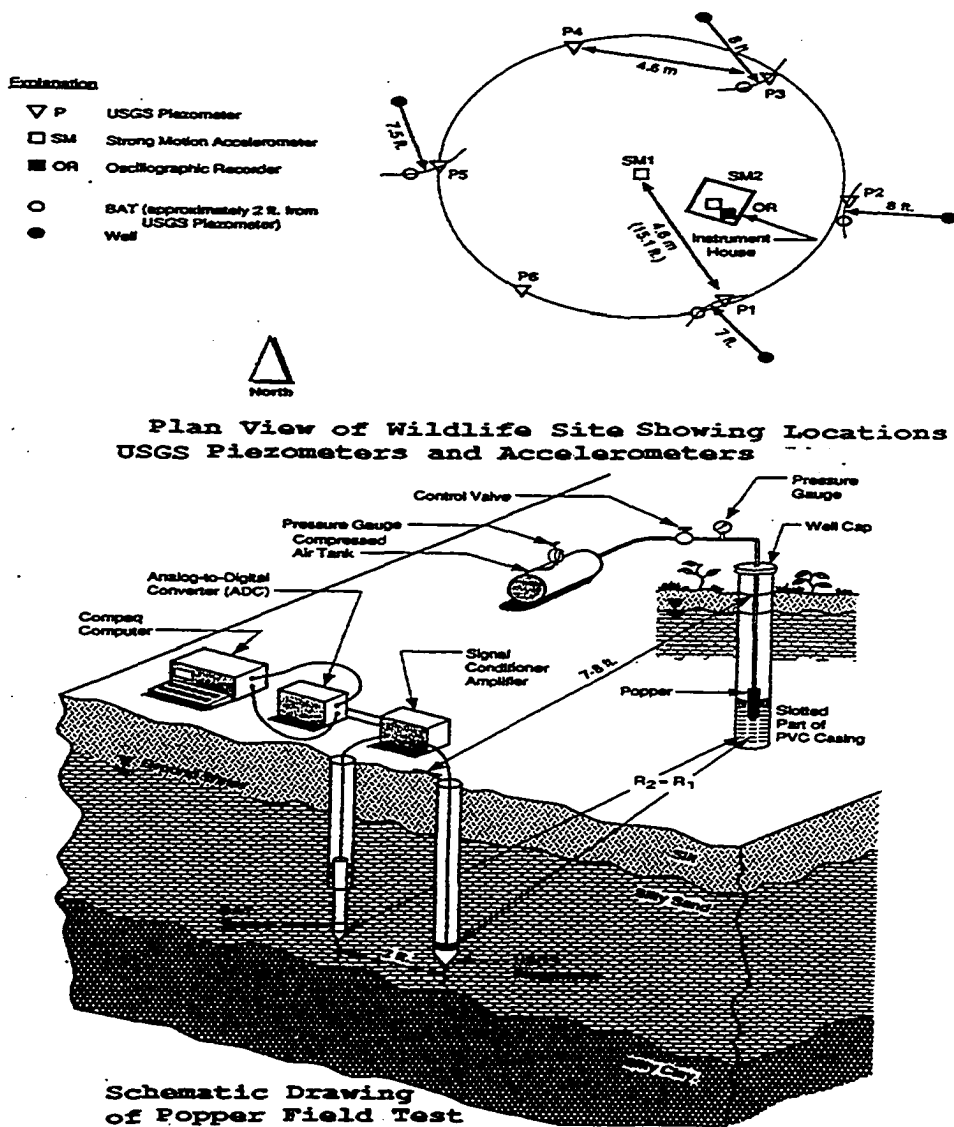


Figure I.5- Locations of the USGS piezometers, signal wells, and reference piezometers installed at the Wildlife site. The signal wells were installed 7 to 8 feet from the existing USGS piezometers and reference piezometers (from Hushmand et al, 1994).

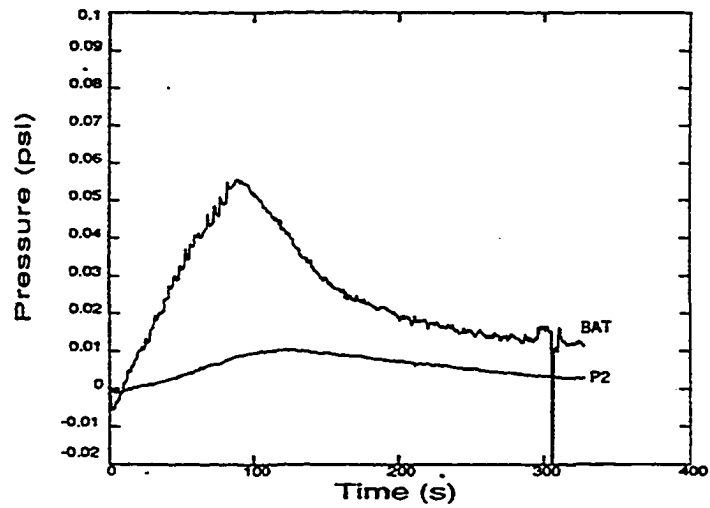
Superstition Hills earthquake, only P5 provided a response similar to the new reference piezometers. Hushmand et al. speculated that “Problems associated with transducer installation procedure were probably the major cause of their inconsistent response during the earthquake and the field testing.” They also speculated that potential problems were caused by installing the piezometers in silt or silty clay layers (i.e. at depths different from the intended depth of installation).

However, the signal delivered to the piezometers was a slow -rising signal not at all like the signal expected from an earthquake. The signal extends over many seconds and is related to the propagation of water from the signal well into the aquifer. The frequency of these signals is 0.01 Hz for the popper test to 0.1 Hz for the compressed air test.

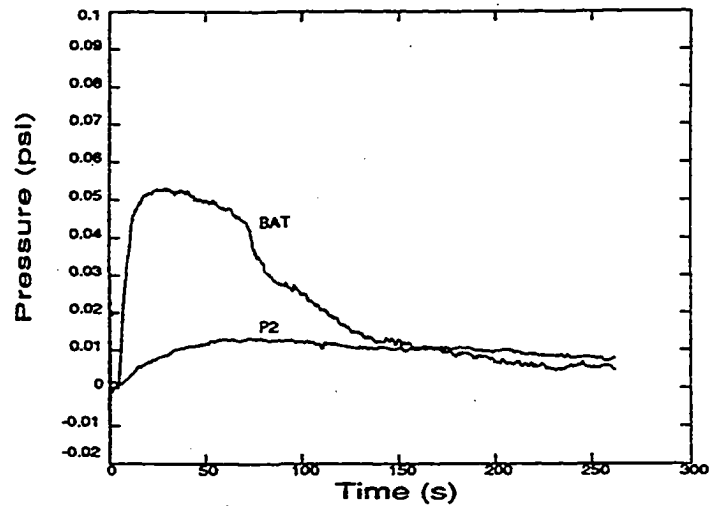
These are ten to twenty times slower than signals expected from an earthquake that might create liquefaction. As the data of Furumoto et al., shows in Figure I.4, signals with frequencies of several Hz occur at the initiation of the pore pressure rise.

Hushmand et al’s method does not tell us much about the ability of the USGS piezometers or the reference piezometers to detect earthquake-like signals if they were to occur in the range of several Hz.

The original record shown in Figure I.3 shows that the signals recorded by the 4 reported piezometers, at the time of the earthquake, were very similar. Hushmand et al. demonstrated that P5 was working at the time of their investigation. Given the similarity of the records of P1, P2, P3, and P5 during the earthquake, it is clear that Hushmand et



(8a) Popper Test P2BPOP02



(8b) Compressed Air Test P2COMP02

Figure 8. Comparison of Pore Pressure Time Histories Recorded by BAT and USGS P2 Transducers

Figure I.6-Results of varification tests by Hushmand et al. (1994).

al. are also demonstrating that P1, P2, and P3 were operating at least as well as P5 at the time of the earthquake. The deterioration of P1, P2, and P3 piezometers recorded by Hushmand et al. has to have occurred after the earthquake. It has to be considered that the damage to these piezometers or densification to the sediments may have resulted from Hushmand et al. driving their new reference piezometers too close to the existing USGS piezometers. More importantly, it still is not known if the USGS piezometers were capable of detecting earthquake-like signals during the earthquake or after the earthquake based on the work of Hushmand et al. If the Hushmand et al. investigation of the Wildlife site's piezometers had actually been capable of demonstrating that the piezometers were capable of detecting earthquake-like signals in the range of several Hz, it might have been possible to know if the sediments had somehow filtered out the higher frequency signals.

Scott and Hushmand (1996) undertook a subsequent investigation to demonstrate the ability to test in-situ for dynamic signals using a new piezometer design. Referring to Hushmand et al., (1994) Scott et al. stated that "One suggestion which resulted from this study was that it would be desirable to develop a standard procedure for testing current and future dynamic pore pressure installations in the field, after placement and, preferably, at regular intervals thereafter." The site selected for this demonstration was the Treasure Island National Geotechnical Experimentation Site where an array of piezometers and accelerometers have been installed with National Science Foundation funding in a deep soft soil deposit. Fortunately, the California Divisions of Mines and Geology-Strong Motion Instrumentation Program, which oversees the site, did not allow

the testing to be done in the area of the existing piezometer arrays, but required the testing to be done on new piezometers in adjacent areas. The methods chosen to generate signals were the dropping of a heavy weight on the ground surface or small explosive charges. The elevation of the weight drop and the amount of explosives used were varied between tests. "There was...an advantage in stimulating pore pressure change in the ground by generating ground motions similar, in some respects, to those produced by an earthquake." They developed a reference transducer that would be pushed into the aquifer to the desired level and then have its screen exposed to the aquifer (called Caltech piezometer). USGS pore pressure transducers of various designs were to be compared to the reference transducer.

The horizontal distribution of the piezometers for drop test 8 is shown in Figure I.7, and Figure I.8 (from Scott et al.) is an example of the signal generated by a 1300-lb weight dropped from 42 inches. The signal received by the piezometers has many similarities to Figure I.1. There is a sharp initial rise in pore pressure followed by a long decay. Scott et al. attributed the initial sharp rise to a compressional wave or P-wave and the second long decay to a pressure wave. Assuming the depths reported are depths below the ground surface, Figure I.8 shows distinct differences by depth for the signal received. The USGS piezometer at a depth of 15 feet has both positive and negative pressures that would be consistent with the impact of a compression wave on the piezometers. The reference piezometer (Caltech) at 15.5 feet does not show this oscillation of pore pressure. The shallower USGS piezometer (7.5 feet) shows the oscillating signal around

the static water level but does not show a rise in the pressure compared to the other two piezometers.

Scott et al. indicated that the dropping of the weight was capable of liquefying the sediments if the drop were sufficiently high. The dropping weight, even though landing on a steel plate, created depressions indicating compaction of the sediments. The use of explosive destroyed the sediments around them. Given these obvious problems that changed the properties of the sediments it would not be desirable to use these methods over the long term. Even in the short term, it can be shown that the testing causes irreversible changes in the sediments. The data for weight drops No. 1 to No. 5 are compiled in Table I.1. The reported increases in pore pressures for the reference piezometer and the USGS piezometer (S/N 175365) are shown. The test number (drop # on Table I.1) and the elevation of the weight drop are shown in the first two rows for each piezometer. The results for the first five drops are plotted in Figure I.9. Scott et al. attempted duplication of the data with the last two of these drops (#4 and #5 on Table I.1). For the reference piezometers, the same drop height of 62 inches results in a rise of 16.6 psi for the compression wave (P) produced by the initial 62-inch drop (drop #4) versus a rise of 1.7 psi for the second 62-inch drop (drop #5). The USGS piezometer also indicates decreases in pressure began from drop #3 onward. These results indicate, that as the testing continued damage was being done to the aquifer. It is likely compaction of the sediments was occurring as a result of high input of energy by the weight (dynamic compaction).

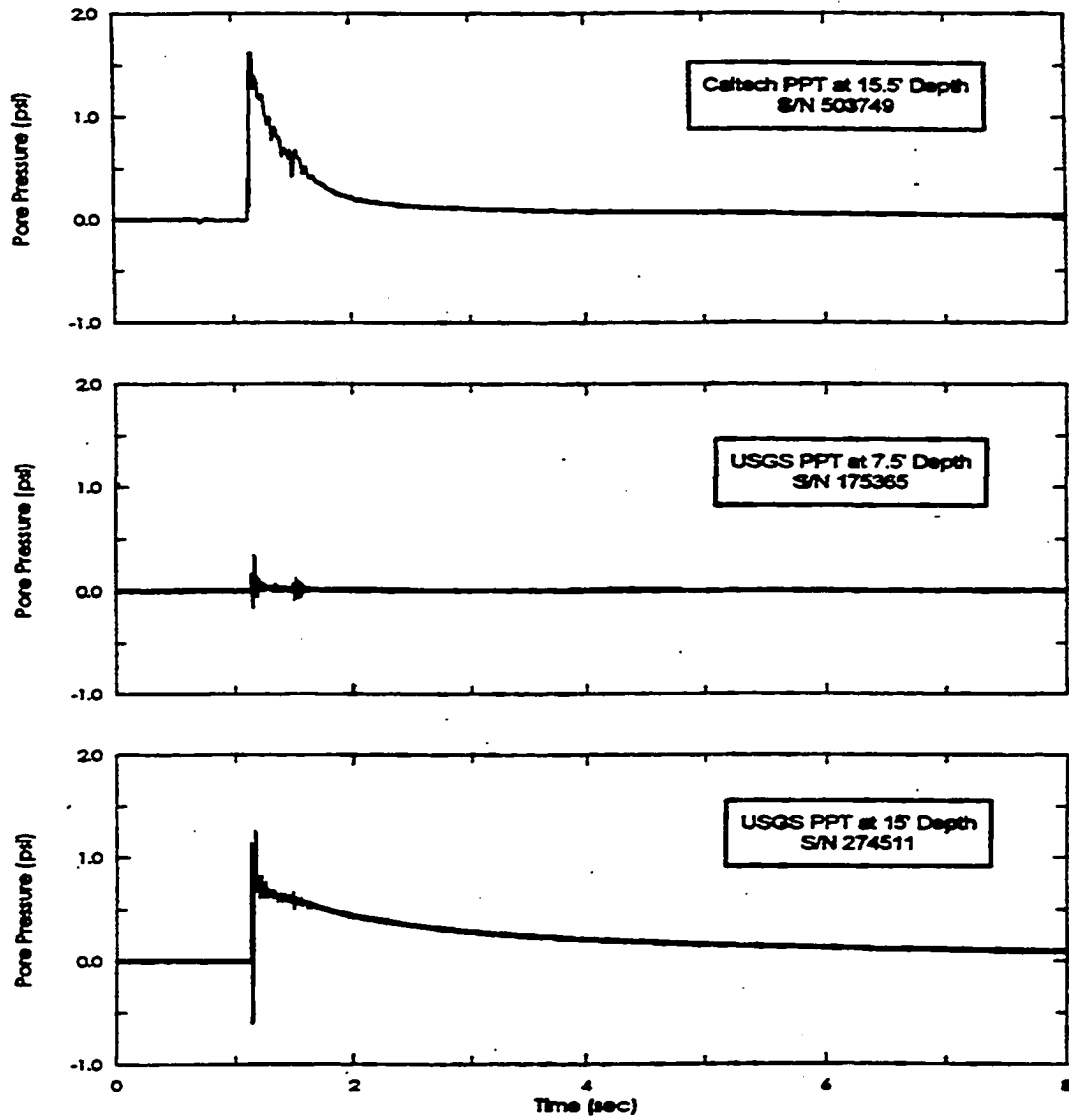


Figure 30. Time Histories of Pore Pressures Recorded during DROP8 Test

Figure I.7- This is an example of the signal generated by the 1300-lb weight dropped for a height of 42 inches (from Scott et al., 1996). The signal recorded by the various piezometers has many similarities to Figure I.1. There are distinct differences by depth between the signals received by the various piezometers.

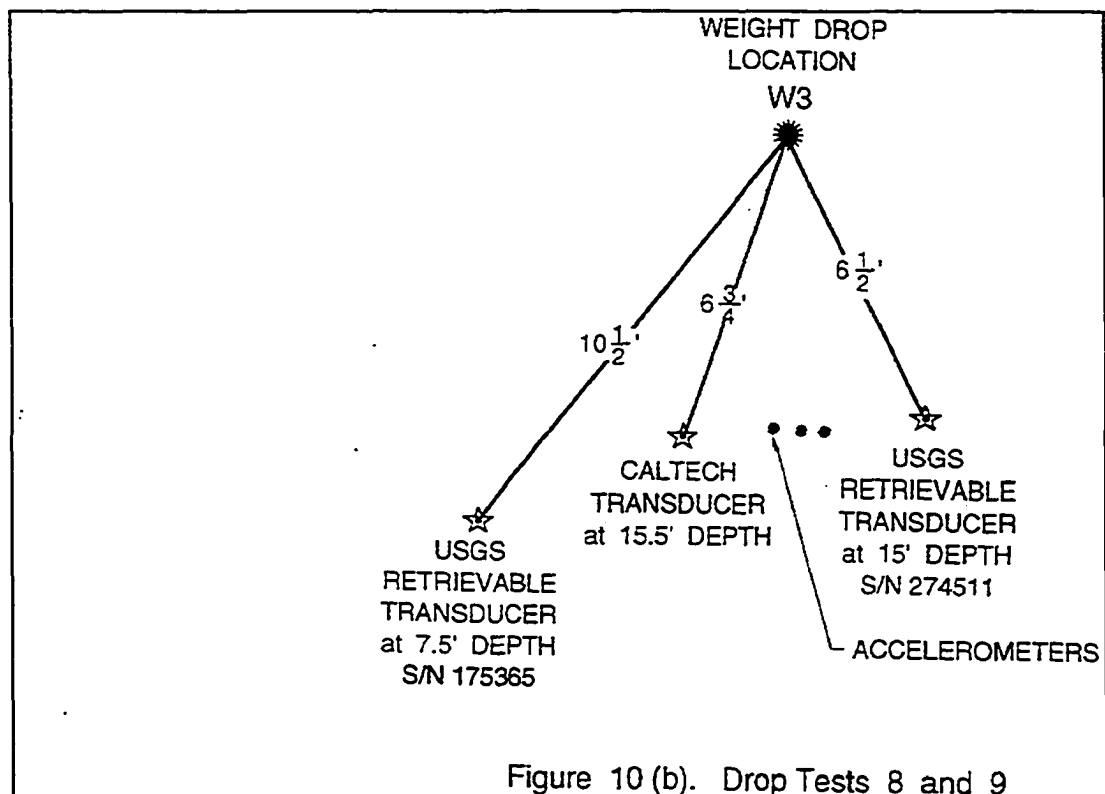


Figure I.8-Location map for piezometers used in Figure I.7 for drop tests 8 and 9. (from Scott et al. 1996).

The signals generated by the testing are similar to those expected by an earthquake.

However, the results cannot be duplicated. Drops of the same elevation were not reproducible and did not result in comparable pore pressure changes. The use of explosives damaged the sediments and did destroy one piezometer during the testing.

Therefore, these methods of signal generation cannot be used over the long term without damaging the very sediments to be tested and might result in destroying some of the piezometers. Consequently, a different signal generation system was required for field-testing of piezometers.

Cal Tech piezometer					
drop #	1	2	3	4	5
drop elevation (inches)	27	43	46.75	61.5	62
Distance from source (feet)	3.1	3.1	3.1	3.1	3.1
depth BGS (feet)	7.5	7.5	7.5	7.5	7.5
P-wave (psi)	4	4.1	10.6	16.5	1.7
Location	A	A	A	A	A
USGS piezometer (S/N 175365)					
drop #	1	2	3	4	5
drop elevation (inches)	27	43	46.75	61.5	62
Distance from source (feet)	3.4	3.4	3.4	3.4	3.4
depth BGS (feet)	7.5	7.5	7.5	7.5	7.5
P-wave (psi)	1.5	1.8	2.5	2	0.6
Location	A	A	A	A	A

Table I.1- Comparison of drop height and pressure measured by the Caltech and USGS piezometers #175365. The data was used in the construction of Figure I.9.

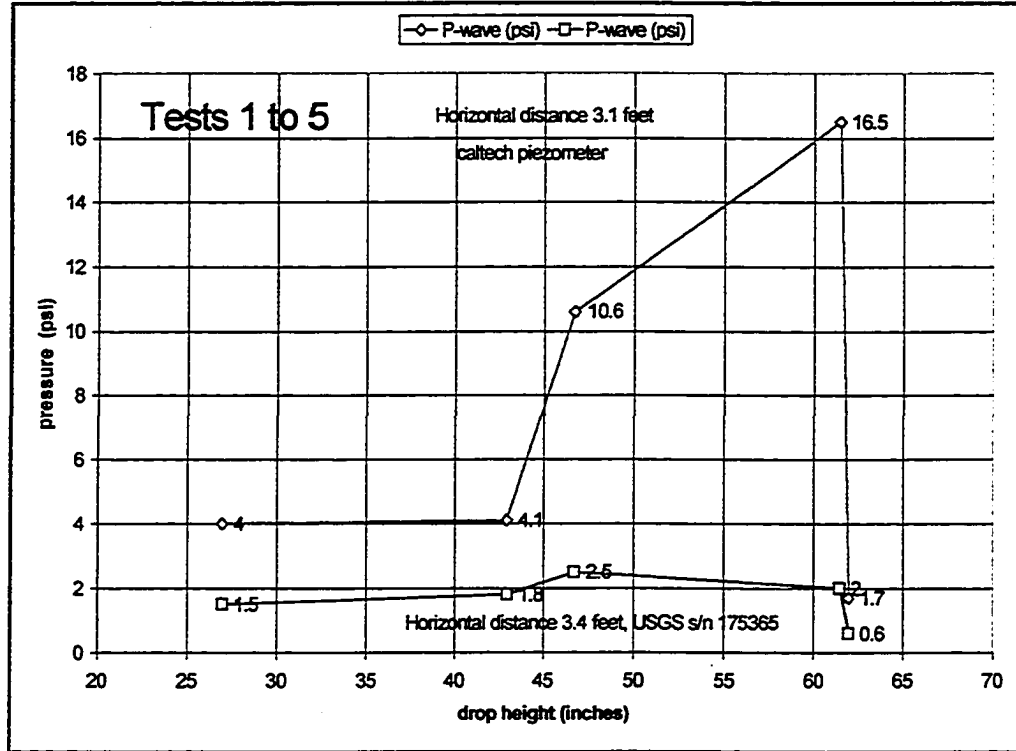


Figure I.9-Correlation of drop height to pressures measured in the piezometers. The attempts to repeat the drop of height of 62" results in very large differences in pressures being detected by the piezometers. The USGS piezometer begins to detect lower pressures after drop #3 at 47". Both would indicate the inability to duplicate results caused by damage to the soils.

CHAPTER II

PRESSURE VESSEL TESTING

The objectives of testing in the pressure vessel were:

- 1) to determine if the protective tip itself had an influence on the signal detected by the transducer,
- 2) to determine if the protective membrane placed on the protective tip was stripped off during insertion, and
- 3) to determine if any damage was being done to the protective tip during the insertion into the soil.

Testing in a large pressure vessel provided an environment as similar to a field site as could be obtained in the lab. Testing in the pressure vessel provided a controlled environment in which the proposed transducer, the influence of the protective tip, protective rubber membrane, method for logging the signal received by the transducer, and means for generating signals could be evaluated. Testing was done in deaired water and in saturated sand. Stringent controls were provided to insure saturation of the transducer and the screens on the protective tip on the transducer. Reference transducers were provided to check responses.

II.1-Description of equipment: Pressure vessel- The pressure vessel is a steel cylinder 24 inch diameter by 28.5 inch deep with flanges at the top and bottom mounted on a 40

inch high stand (Figure II.1). A bottom plate attaches to the bottom flange of the pressure vessel. An insertion sleeve (Figure II.2) was provided in the bottom plate, through which the transducer and the protective tip could initially be placed and then pushed vertically upward into the sand. This vertical upward push of 12 inches brought the tip opposite the reference transducer on the side of the pressure vessel (shown later in Figure II.15). The distance the protective tip was pushed into the sand in the pressure vessel was approximately the same distance the tips and transducers were to be pushed vertically below the bottom of the boring at the field sites (Camp Hedding, Treasure Island as examples).

A top chamber attached to the top flange of the pressure vessel. The upper chamber provided a confining pressure for the sand sample located within the lower chamber of the vessel. When the lower chamber was filled with sand, the upper chamber was separated from the lower chamber by a rubber membrane. Fluid pressure in the upper chamber applied the total vertical stress to the sand sample. A Validyne transducer (Model DP15-50) was attached to an access hole in the top chamber to measure the applied total stress. A second Validyne transducer was attached as a reference transducer to the side of the pressure vessel 12 inches from the bottom of the pressure vessel. The access hole on the side of the pressure vessel was covered with a porous stone.

Pressure control chambers – Three triaxial pressure chambers (Figure II. 3) were used to regulate the pressures within the upper and lower chambers. The air/water interface upon

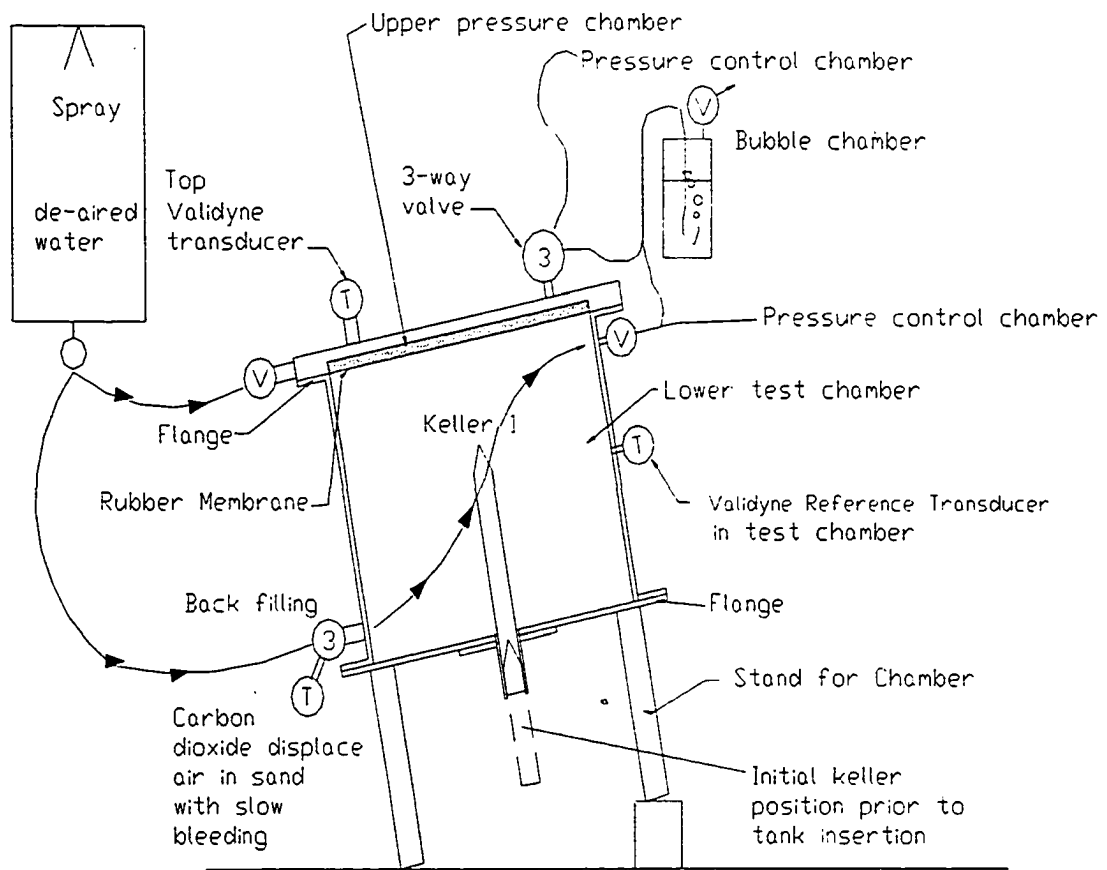


Figure II.1-Pressure vessel. The pressure vessel is divided into two chambers. The lower chamber, with the Keller 1, is filled with sand. The upper chamber is filled with water and is used to provide a confining pressure to the sand in the lower chamber. The two chambers are separated a rubber membrane. After filling the lower chamber with sand, the membrane separating the sand from the upper chamber is installed. A slight vacuum is applied to the sand in the lower chamber. The pressure vessel is tipped at an angle so that there is a valve at the lower and upper edge of each chamber. The sand is flushed with CO₂ and both chambers are filled with deaired water. A vacuum is maintained on the sample until all the air is removed. A 5-psi pressure is then applied to the upper chamber and the vacuum is released on the lower chamber. The sand can be tested at various effective confining pressures. A Validyne reference transducer (Model DP15-50) is located opposite the Keller 1 transducer in the lower chamber.

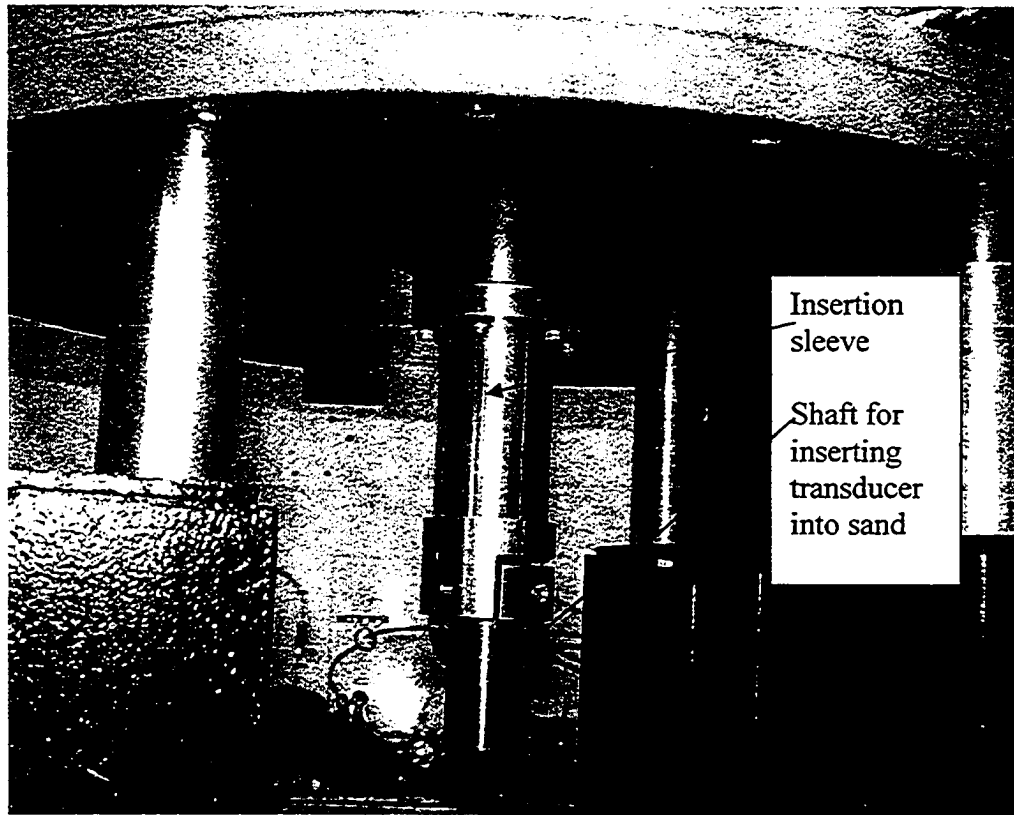


Figure II. 2: Pass-through insertion sleeve in the bottom of the pressure vessel for inserting piezometer tip.

which the pressure was applied was located in these chambers. This insured better saturation in the sand and no air traps in the upper chamber. Simulated earthquake-like water pressure signals were applied through the triaxial chamber system. Various techniques for producing signals were explored, as discussed in section II.4.

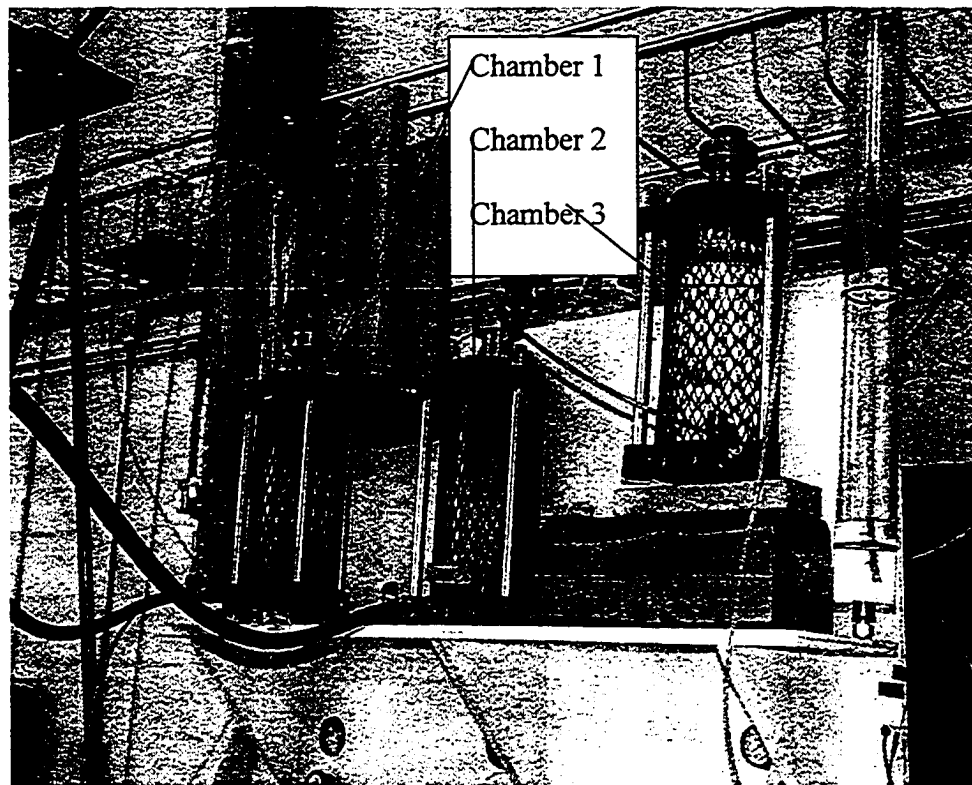


Figure II. 3: Triaxial pressure chambers are used to regulate pressure within the test vessel. Triaxial chamber 1) is where the signal generator sends pressure pulse into the lower chamber. Triaxial chamber 2) controls the confining pressure to upper chamber. Triaxial chamber 3) controls the backpressure for lower chamber.

A Keller Model 700 absolute pressure transducer, was placed in the protective tip used in this study. Sand gradation used in the pressure vessel is shown in Figure II.4. The sand is uniformly graded fine sand with 0.1% passing the #200 sieve. The minimum unit weight of the sand was 88.2-lbs/ ft³ and the maximum unit weight was 108.5 lbs/ft³ (personal communication, Dr. de Alba).

Sample construction: Sand samples of both low and high relative density were tested. The low relative density sand samples were constructed by dry air pluviation. The bottom of a large drum was perforated to form a sieve through which the sand could rain gently into the pressure vessel. The hole pattern consisted of $\frac{1}{8}$ -inch holes spaced on a 1-inch by 1-inch grid across the entire bottom of the drum. The pressure vessel was filled to the top of the flange. The pressure vessel was level at the time of filling. During the construction of the high relative density sample moist sand was placed into the pressure vessel in four lifts. Each lift was compacted with 25 blow/lift using a solid 3-inch diameter cylinder dropped 12 inches. Two loose samples with unit weights of about 92 pounds per cubic foot and relative densities of about 21% were tested. One sample at a relative densities of about 78% and unit weights of 103 pounds per cubic feet was also tested. Each was tested under numerous different effective stresses. The void ratio of the air pluviated samples tested was about 0.89 ($\gamma_d=92.6 \text{ lb/ft}^3$). The compacted sample had a void ratio of 0.59 ($\gamma_d=103.7 \text{ lb/ft}^3$).

After the lower chamber was filled with sand, the membrane separating the sample from the upper confining pressure chamber was installed on the pressure vessel, and the top chamber bolted on. A slight confining pressure was applied to the sand in the form of a vacuum in the lower chamber. The pressure vessel was tipped at a slight angle so that there was a valve in the lowest corner of each chamber and a valve in the uppermost corner of each chamber (see Figure II. 1). This minimized the amount of air that could be trapped in the chambers. In order to maintain confinement on the sample, the upper

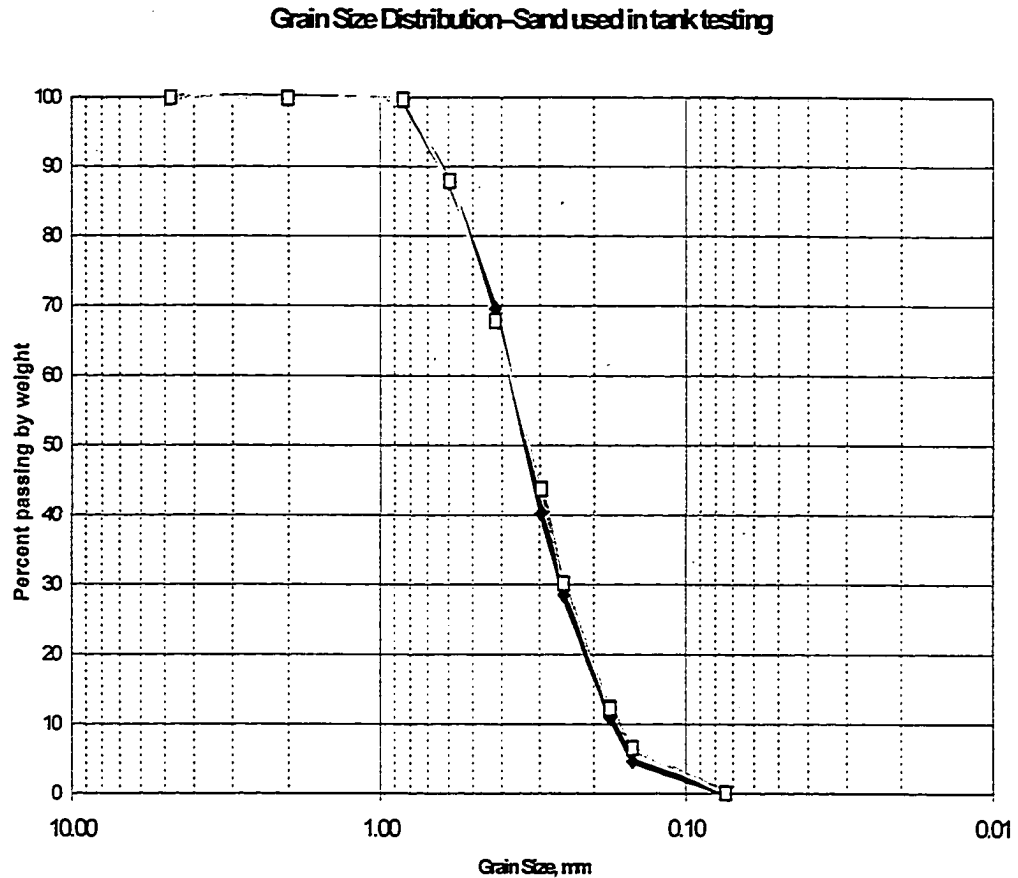


Figure II.4: Two sieve analyses of the sand used in pressure vessel testing.

chamber was filled with water and a 5-psi pressure applied to the upper chamber. The vacuum on the lower chamber was then released.

For experiments run with only water, no membrane separated the upper chamber from the lower chamber. The pressure vessel was filled from the lowest corner toward the uppermost corner.

Tip design-The protective tip placed over the Keller 1 transducer follows the original design of Youd (1996). It is a nylon tip with a 60° screw-on nose cone allowing the tip to be pushed into the sediments. The water has access to the transducer through 20 porous nylon plugs. The design of the protective tip used in the lab testing was similar to that shown in Figure II.5 (copied from: Figure 14, Faris and de Alba, 2000) except that a Keller transducer (Model 700, absolute pressure) is used and there was a screw plug on top through which the transducer cable was inserted.

The hydraulic conductivity of the tip averaged 2.9×10^{-2} cm/sec for five falling head tests. The tips subsequently installed on Keller 2 and Keller 3 field transducers had nearly identical hydraulic conductivities as the tip used in the lab. The protective tip used in the lab testing was eventually installed (with some modifications for an access tube and a check valve, see Chapter VII) with the Keller 1 transducer at the Hedding field site.

A thin rubber membrane (condom) covered the tip during installation. The membrane maintained saturation of the tip and transducer during installation. A great deal of effort went into insuring saturation of the tip and transducer prior to installation and while inserting the tip and transducer into the pressure vessel. The protective tip was saturated under vacuum in deaired water for at least 24 hours prior to installation. The protective tip and the transducer were assembled under deaired water to form the piezometer. The protective membrane was placed over the tip under deaired water. The assembled piezometer was moved to the pressure vessel in a bucket of deaired water. The

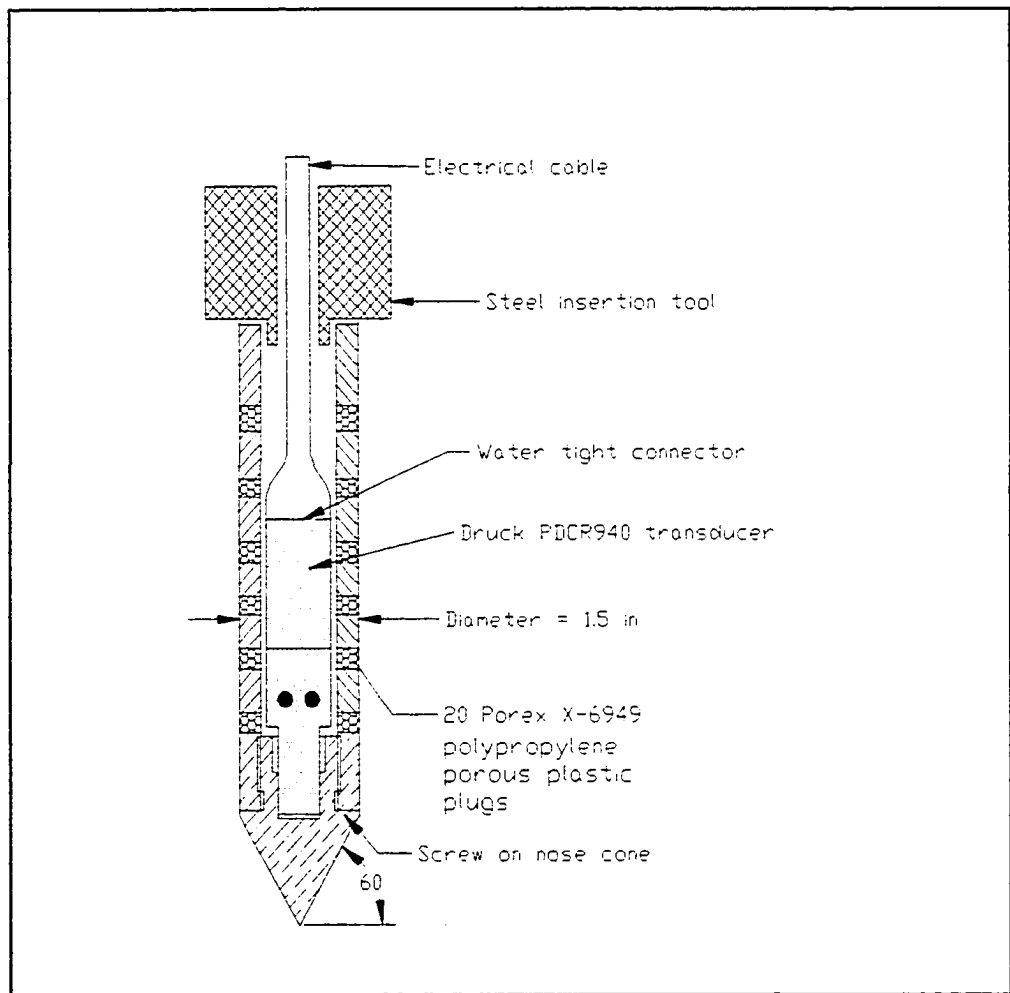


Figure II. 5- Protective tip as designed by Youd (1996). The protective tip place over the Keller 1 transducer is a nylon cylinder with a 60° screw on tip to allow pushing into place. Water has access to the transducer through 20 porous nylon plugs.

piezometer was removed from the deaired water and placed immediately in the insertion tube at the base of the pressure vessel (Figure II.2). The membrane and the O-rings in the insertion tube prevented any loss of saturation.

Two kinds of tests were carried out to check the transducer response and influence of the protective tip. Tests were performed in water alone and in specifically constructed sand samples. The sand samples were constructed as previously described. The Keller 1 transducer was placed in the insertion sleeve at the bottom of the tank but not projecting into the pressure vessel at that time. The transducer was held in place by a sleeve clamp and leakage was prevented by a series of O-rings on the inside of the insertion sleeve as previously described. After the sample was constructed and air removed from both chambers, the pressures were adjusted so that the top chamber had 10-psi higher pressure (confining pressure) than the sand chamber (backpressure). The effective pressure on the sand was the difference between the confining pressure and the backpressure. All tests were run on the sand with an effective confining pressure of at least 10 psi. After the sample was confined and saturated, the Keller transducer in its protective tip was advanced into the sand from the bottom. The B-value for the sand sample was checked to estimate the degree of saturation.

II.2--Signal generation: Dynamic pressure signals were generated using several methods.

1) Figure II.6 shows the arrangement of sand pressure vessel and pressure cells for manual cycling of pressure to lower sand chamber while leaving upper water chamber at constant pressure. The confining pressure on the sand in the upper chamber is maintained under constant pressure from the middle pressure cell. The pressure on the

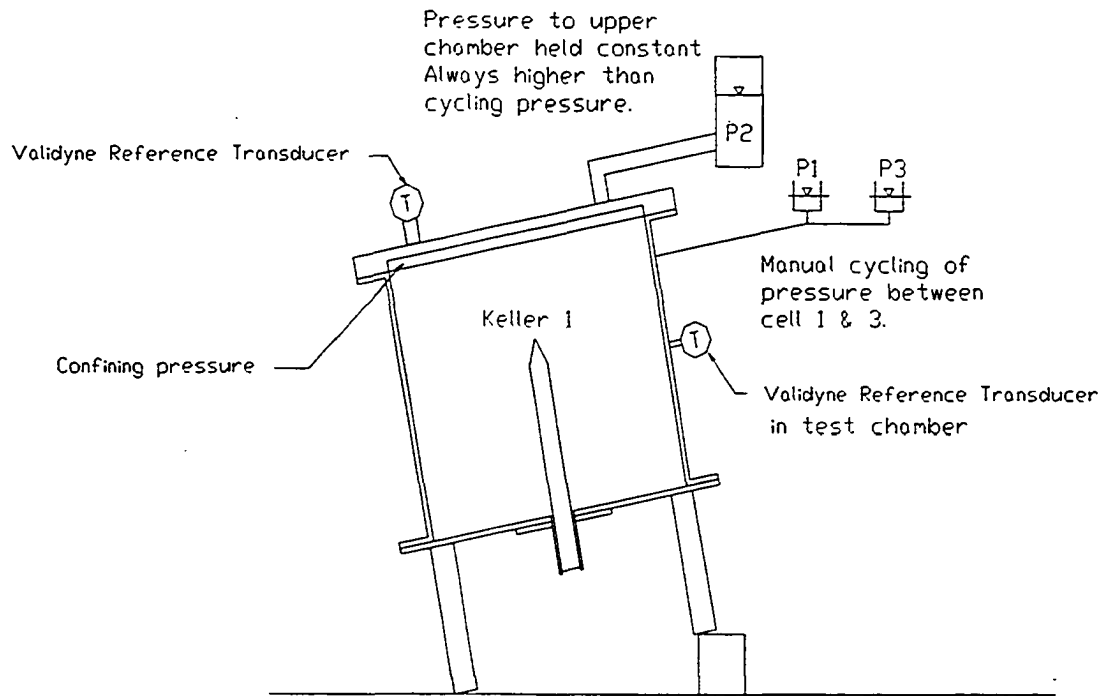


Figure II.6-The arrangement of the sand pressure vessel and pressure cells for manual cycling of pressure to lower chamber and for measuring the response of the Keller 1 and reference transducer in the lower chamber. The backpressure in the lower chamber cycled between two different pressures P1 and P2 by switching the valve on the lower chamber, changing the effective confining pressure. The pressure on the upper chamber was held constant.

lower chamber is cycled between two different pressures P1 and P3 that varied between the various tests. Pressure changes were created in the lower chamber by hand cycling of a three-way valve at the top of the lower chamber between two different pressures that varied between the various tests. At all times the maximum backpressure was at least 10 psi lower than the confining pressure on the sand. This prevented the membrane between the two chambers from flexing and prevented the sand from shifting.

2) Servo cycling of pressure is basically the same as shown in Figure II.6 except regulators set at different pressures take the place of P1 and P3. An electrically operated servo valve cycled the pressure between the two regulators onto the air-water interface in triaxial chambers 1 and 3.

3) To obtain a faster rise time for the dynamic signal than could be obtained by methods 1 and 2, a shot-actuated hammer (Figure II.7) or a hand-held hammer was used to drive a loading ram into a water-filled triaxial pressure chamber. This caused a rapid increase in water pressure in the lower chamber while maintaining a constant confining pressure in the upper chamber. This arrangement is shown in Figure II. 3. The ram is on cell 1. The initial pressure in cell 1 is controlled from cell 3 where the free surface is located. Cell 2 provided the confining pressure for the upper chamber. In order to prevent the signal from dispersing into cell 3 when the shot was delivered in cell 1 the valve between cell 1 and cell 3 was closed just before the shot was made.

The ram was driven forward either by a blow from a hammer on the top of the ram or by a shot-actuated hammer (Remington, Powder Actuated Tool, model #475 using a #4

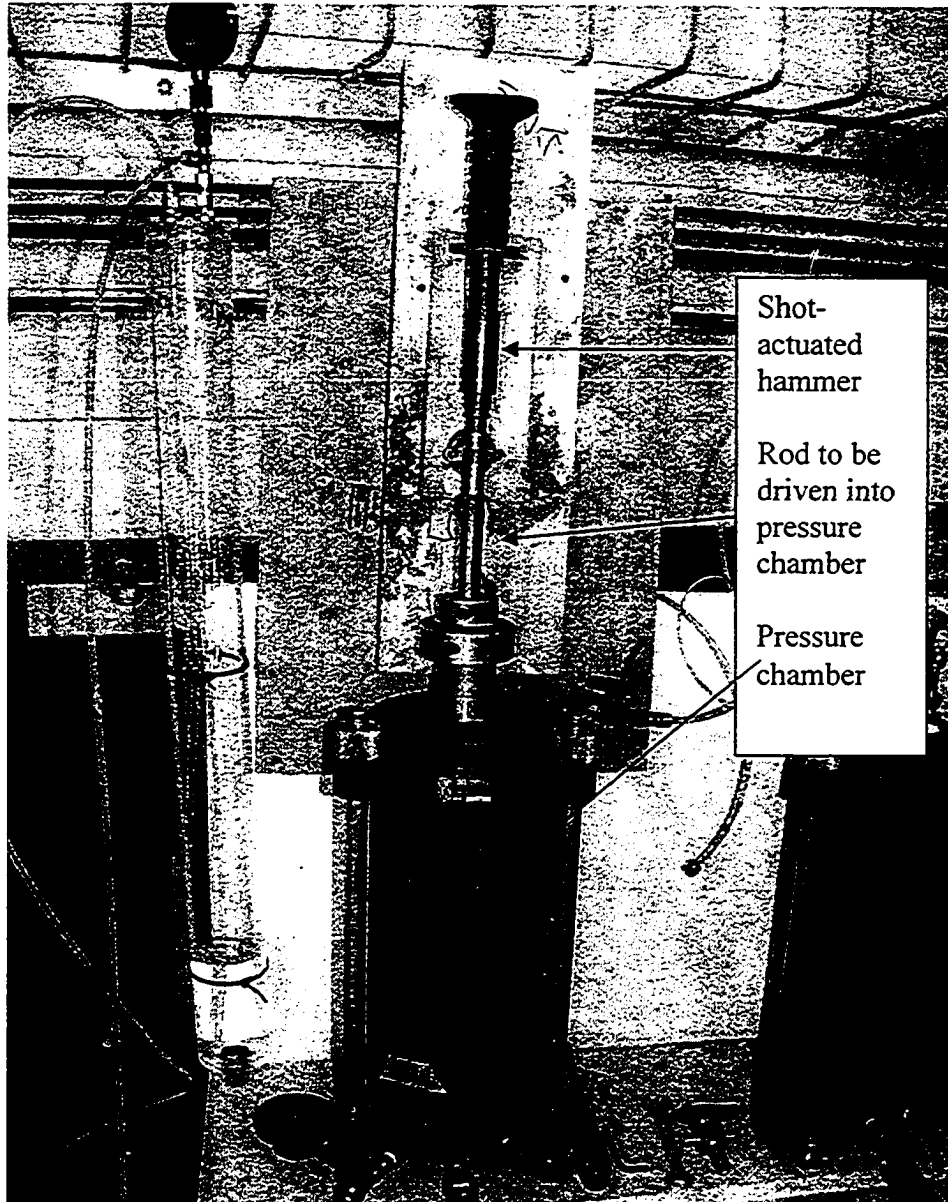


Figure II.7: Setup for creating dynamic pulse through the backpressure system using a shot-actuated hammer (shot hammer) to shoot a rod into the water-filled signal pressure chamber (chamber 1).

cartridge). The shot-actuated hammer (shot-hammer) gave a larger pressure change than did the hammer alone and both methods had similar rates of pressure rise. When the shot-actuated hammer was used to drive the ram, the shot-actuated hammer was placed at the top of the ram and clamped in place. The spring was removed from the hammer so that the bolt in the shot-hammer sat directly on the ram. When the firing pin was tapped with a hammer, the bolt pushed the ram down into the water column in the triaxial cell. The shot-hammer provided a consistent signal that was reproducible. Whereas the energy applied by using a hammer alone was variable.

II.3--Test Results: Water testing: In this case, the pressure vessel was completely filled with water, and both Validyne transducers (see Figure II. 1) were used as references to compare with the signal from the Keller piezometer transducer. The Keller 1 transducer, either alone or in its protective tip, was located at the mid-height of the pressure vessel at the same elevation as the Validyne transducer in the side of the lower chamber.

The initial water testing provided experience in the application of pressure to the sample inside the pressure vessel and a reference of the response of the transducers in a pure water environment. The side transducer provided a reference to compare the response of the Keller 1 when covered with the protective tip and to determine if the tip affected the signal received by the transducer. Only hand cycling of pressure change was done for the initial water testing.

The results of the initial water testing demonstrated that the Keller 1 with and without the protective tip detected the same hand cycled change in pressure signal and no influence from the tip was detected in these tests (6/15/99 data). The same was shown for the second set of water tests when the servo valve (7/2/99 data) performed the pressure cycling. Figure II.8 shows the similarity of the responses of the reference transducer compared to the Keller 1.

At this time, the method of signal generation was changed to the shot-actuated hammer. Problems had been noted with manual cycling and the servo cycling signals. The most important the relatively slow rise time of the signal, corresponding the low frequency of the signal, and the reproducibility of the manual signal. The use of the shot-hammer generated sharper rises in pressure than the servo cycling as shown in Figure II.9. Fourier analysis of the signals showed that the shot-hammer generated equivalent frequencies of 7 to 8 Hz (Figure II.10) compared to 2 Hz for the servo-generated signal (Figure II.11). The peaks could consistently reproduced with the shot-hammer.

Sand testing: Sand Saturation—Saturation of the sand was critically important to the propagation of the signal through the sand. The measure of the B- value for the sample was used to estimate the degree of saturation of the sand. B-values and percent saturation of sand during testing: For the two loose pluviated sand samples the B-values were 0.84 and 0.97. From Black and Lee's (1973) saturation of greater than 99% is indicated. For the higher relative density sample tested in October 1999, B-value was 0.68. This still indicated saturation greater than 99%.

Servo cycling of pressure to water in tank, 7-2-99

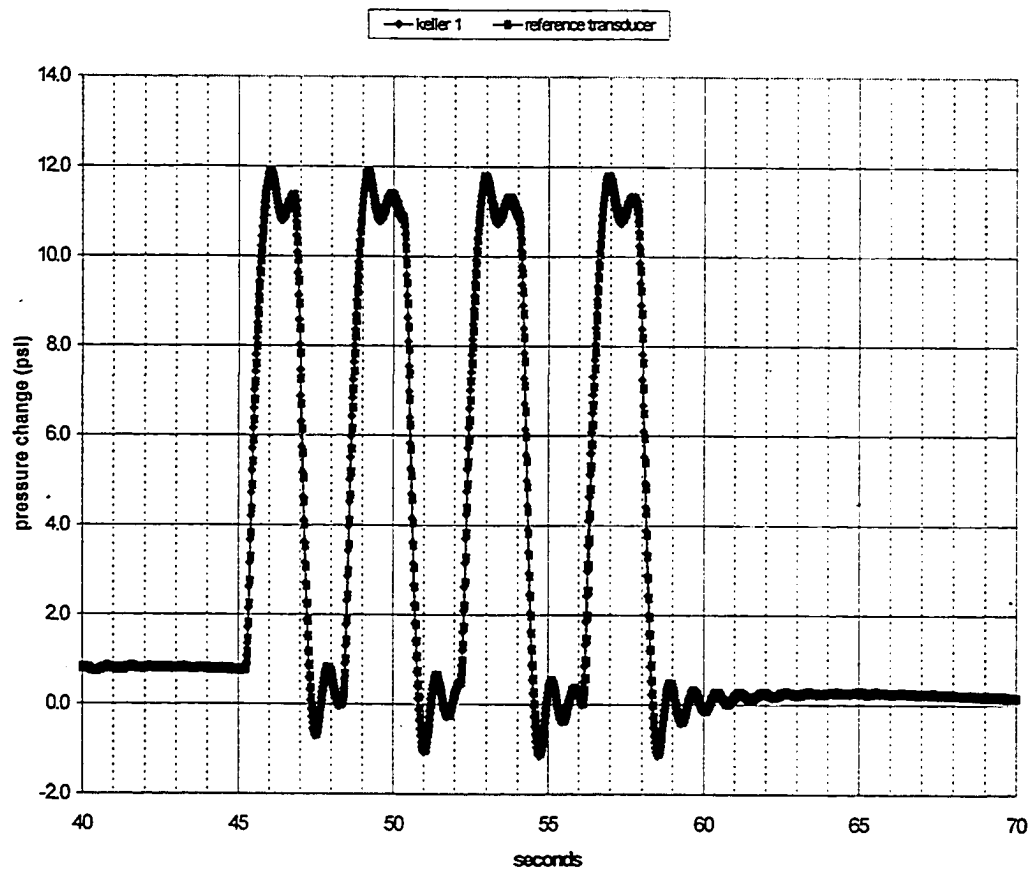


Figure II. 8-Water test. The Keller 1 transducer with the protective tip responds nearly identically as the reference transducer. The pressure is being cycled by the servo valve between two regulators set at different pressures.

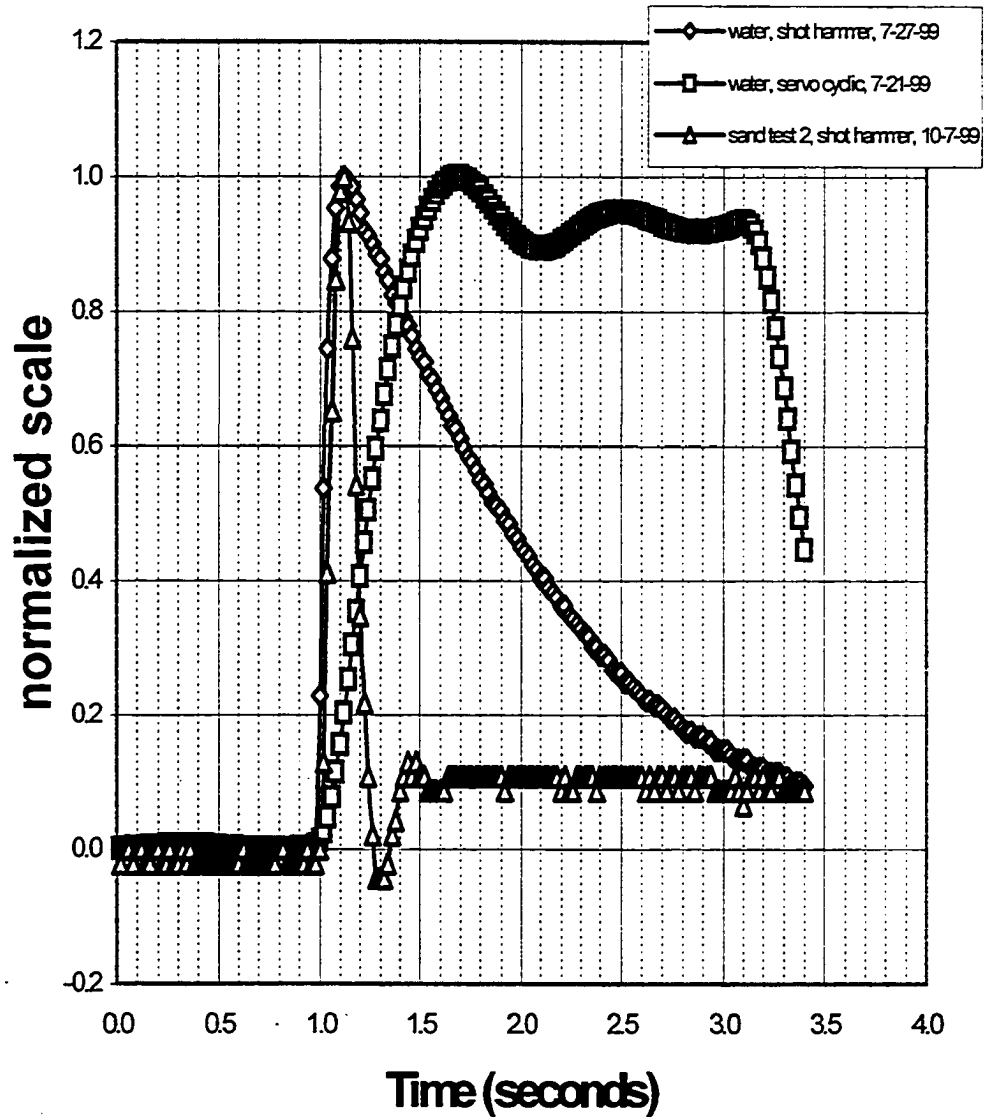


Figure II. 9: Normalized signal received by Keller 1 transducer during tests in water and sand. The signals are normalized by dividing the change in pressure at each data point by the maximum change in pressure for each signal ($\Delta u_i / \Delta u_{i \max}$).

The first set of sand testing was done with sand samples with relative densities of 25% and the pressure was cycled by hand and later by the pressure servo. As previously noted, the protective tip was covered with a membrane to maintain saturation during insertion. The transducer and tip were successfully inserted through the bottom of the pressure vessel into the sand. The membrane was scraped off the tip as the tip was installed. No damage was done to the protective tip, screens, or the Keller 1 transducer. The signal being received by the reference transducer was nearly identical to that received by the Keller 1. Frequencies as high as 2 Hz were generated and detected by the transducers buried in the sand. Figure II.12 is an example of the servo-generated cycles detected by the Keller 1. The frequency for this signal was about 0.7 Hz.

As previously noted, problems with manual cycling and servo cycling signals such as the relatively slow rise time of the signal and the low frequency of the signal. Therefore, the second set of sand testing carried out on low relative density sand used a shot-actuated hammer to create the pressure change in the sand. In all cases a #4-blank 22 cartridge was used. The shot-actuated hammer increased the rate of rise of the signal received by the Keller 1 and Validyne transducers. This was shown above in Figure II. 10 where the normalized initial rise of the servo cycling in water, shot hammer in water, and shot hammer in sand are shown. The pressure rise caused by the shot hammer in water and in the sand is distinctly steeper than the rise generated by the cycling the servo or by cycling by hand. Figure II.13 shows the slope of the pressure rise curves. The maximum slopes for the shot hammer in water is 15.5 psi/second compared to a

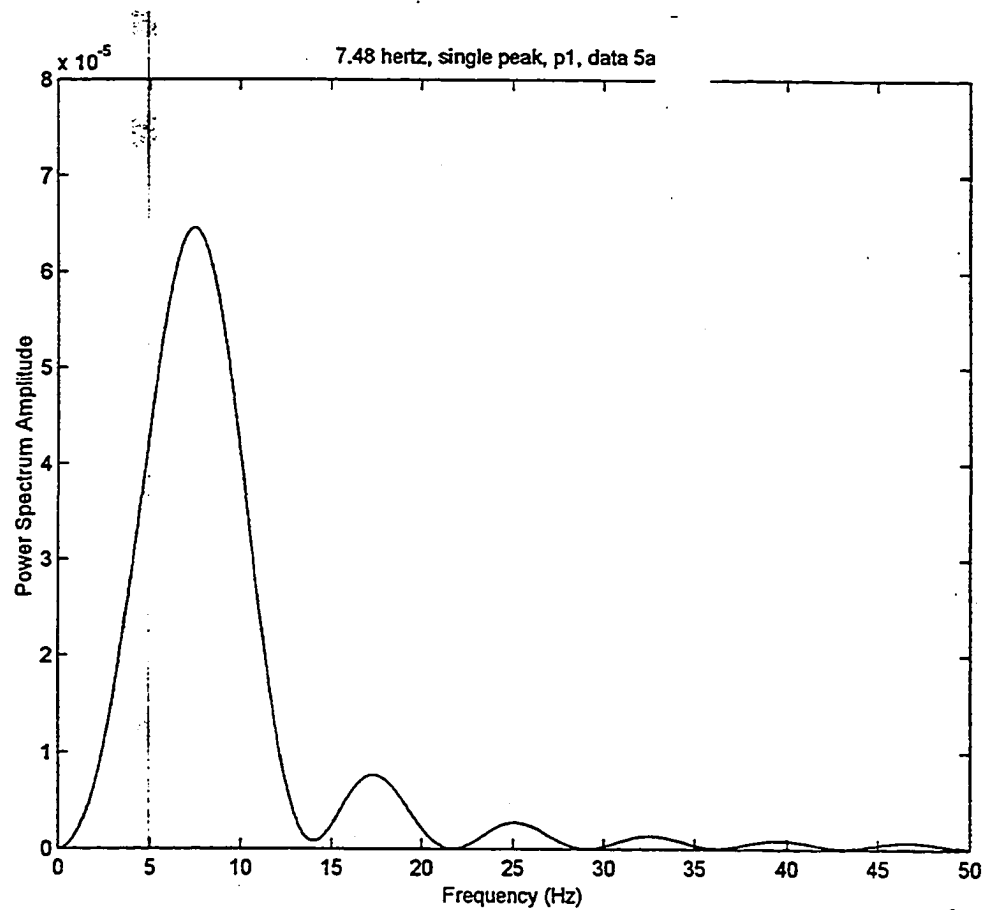


Figure II.10-FFT for Keller 1, water test (7-30-99). Analysis of the signal received by the Keller 1 transducer as a result of the impulse of the shot hammer.

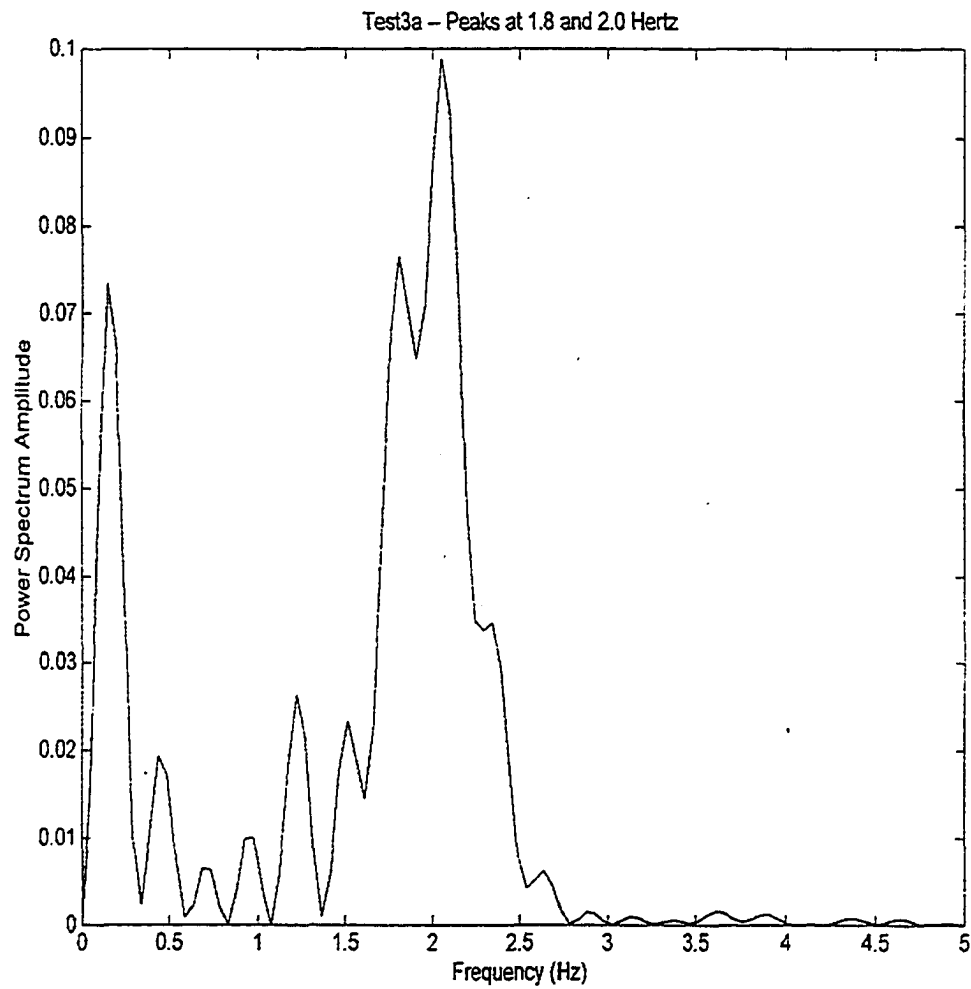


Figure II.11-Pressure vessel testing: FFT for Keller 1. Servo cycling of water pressures.

Sand Tank Testing, Pressure Change

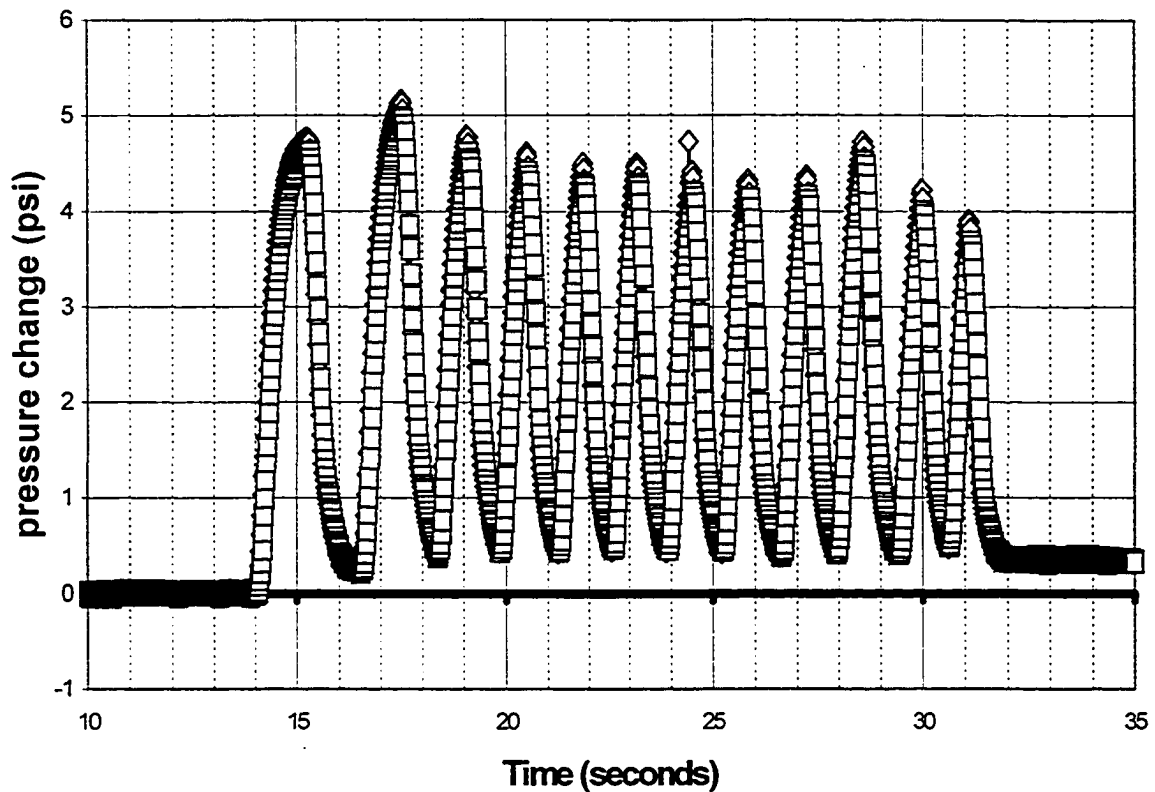


Figure II. 12: The dynamic pressure signal generated by the cycling of the servo in a sand specimen. The Keller 1 transducer in the protective tip (diamonds) and the reference transducer in the side of lower chamber (squares) recorded a signal at approximately 0.7 Hz.

maximum rate of rise for the servo of 2.7 psi/second. The maximum rate of rise for the hammer signal in sand is 13 psi/second. The Fast Fourier Transform (FFT) for the sand signal generated by the shot-hammer indicates frequencies of 7 to 8 Hz for the signal (Figure II.11).

In all cases, there was good agreement between the reference transducer and the Keller 1 in the protective tip. This is shown on Figure II.12 for the reference transducer and for the Keller 1 transducer during the cycling by the servo and for the shot hammer signal in Figure II.14.

In all the sand tests, after measuring the response of the Keller 1 transducer, the protective tip was slowly dug out of the sand to determine if the rubber membrane had been removed during insertion and if there was any damage to the protective tip. Figure II.15 shows the protective tip in the pressure vessel is intact with the rubber membrane having been scraped off during insertion. The porous stone for the reference transducer is located on the side of the vessel opposite the protective tip and the Keller 1 transducer. During one test, the force required to insertion of the piezometer tip into the sand against a vertical effective stress of 10 psi. was measured with a load cell. The load cell failed due to overload at 2000 lb., before the tip was completely inserted. No damage was ever noted to the transducer or the protective tip at any time during the testing.

II.4-Conclusions: Because the Keller 1 transducer in the protective tip received nearly an identical signal as the reference transducer the following were demonstrated:

- 1) The protective tip had no influence on the signal detected by the transducer.
- 2) No damage was done to the transducer or protective tip by the insertion into the fine sand in the pressure vessel.

- 3) That whatever compaction of the sand around the tip occurred during the inserted process it had no effect on the signal detected.
- 4) That the transducer in the tip could detect signals with rise times of 15 psi/second and frequencies of at least 7 to 8 Hz.

The uncovering of the tip after insertion and testing demonstrated that during insertion the rubber membrane was stripped off the protective tip therefore could not affect the signal received by the Keller 1 transducer and no visible damage was done to the protective tip.

II.5) Modification of tip for field application: During the testing of the Keller 1 and protective tip it became apparent that being able to check the calibration of the transducer insitu would be desirable. While this was possible to check the Keller 1 calibration in the pressure vessel because of the external pressure cells with pressure gages, the initial design of the protective tip would not allow access to the tip for calibration once installed in the field. Experience in environmental water quality sampling indicated that precipitation of metallic oxides, silting of the screens, and the build-up of biofilms on the screen are likely to occur on piezometer screens requiring periodic redevelopment to keep the piezometer fully functional.

In order to determine the effect of having an access tube into the protective tip several tests were run with the valve open between triaxial pressure cells. The energy of the shot hammer was dissipated in both directions resulting in a much-reduced signal being measured by the Keller transducer. Consequently, a check valve installed at the top of the protective tip, allowing flow only into the protective tip, was included in the new

design to prevent a signal entering the tip from being dissipated up the access tube. This modified tip is described in detail in the pool testing section and shown in Figure II. 16. The protective tip shown in Figure II.16, has the same screen area (4.06 cm^2), length of opening (screen thickness of 0.7 cm), but has increased outside diameter from 1.5 inches (3.8 cm) to 2 inches (5.1 cm). Hydraulic conductivity testing on the new tip showed the same permeability as the earlier tips ($2.9 \times 10^{-2} \text{ cm/sec}$).

Keller 1, Comparison of rate of change of pressure (psi/sec) of servo and shot hammer signals in water and sand

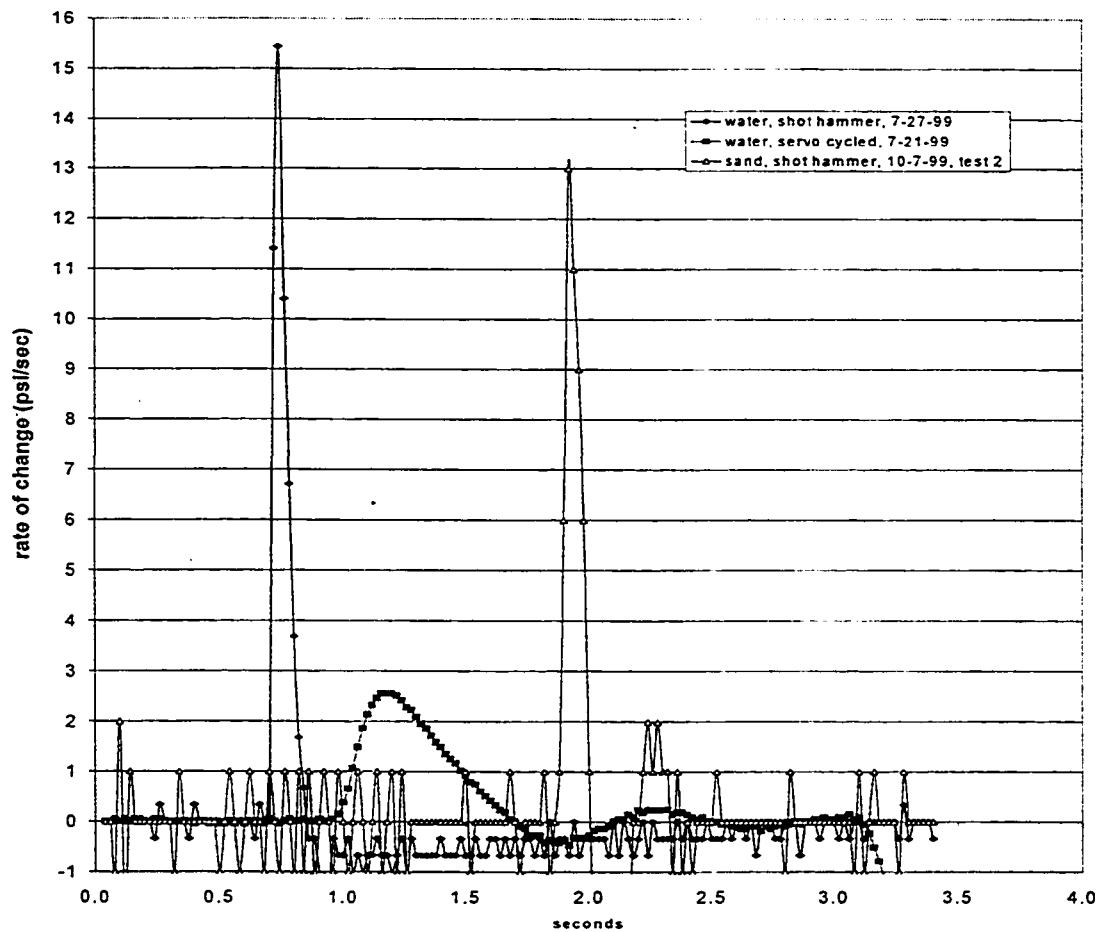


Figure II. 13: The shot hammer creates the maximum rate of change in pressure per second.

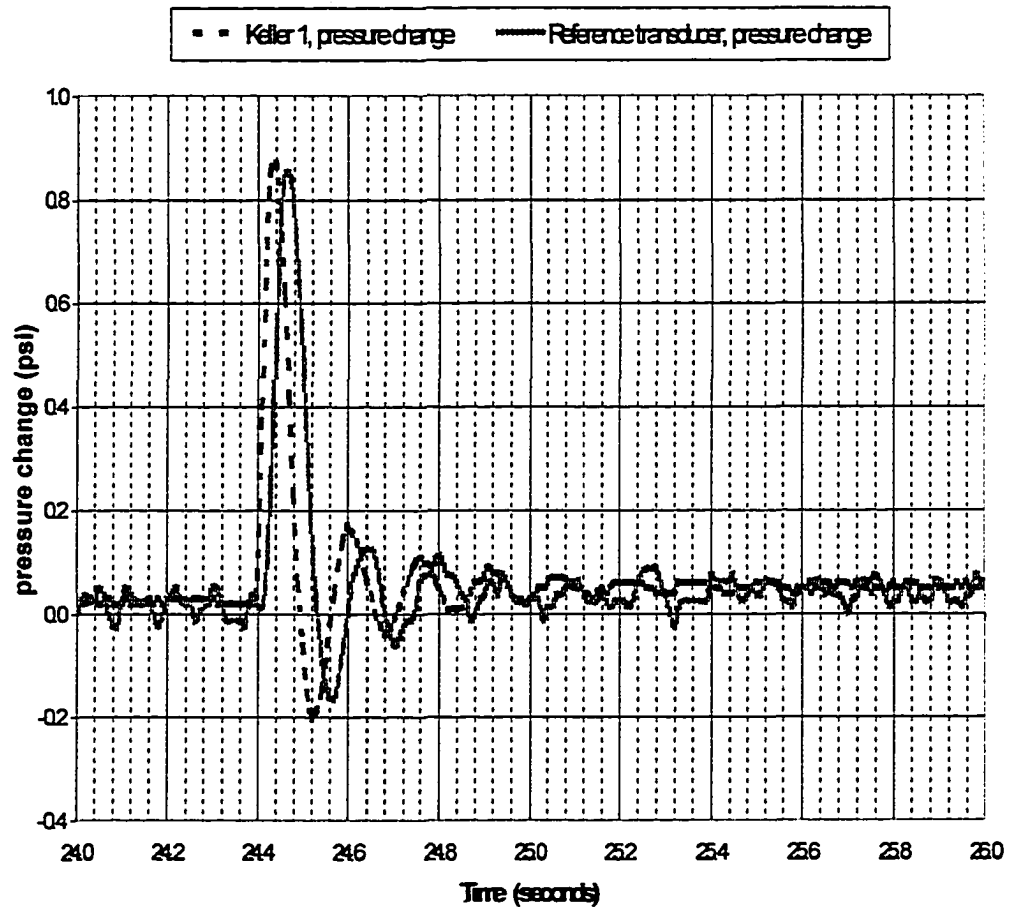


Figure II.14: Shot actuated pressure changes. During the pressure vessel testing there is good agreement between the Keller 1 transducer that has been pushed into the sand inside the protective tip and the reference transducer located in the side of the pressure vessel opposite the Keller 1.

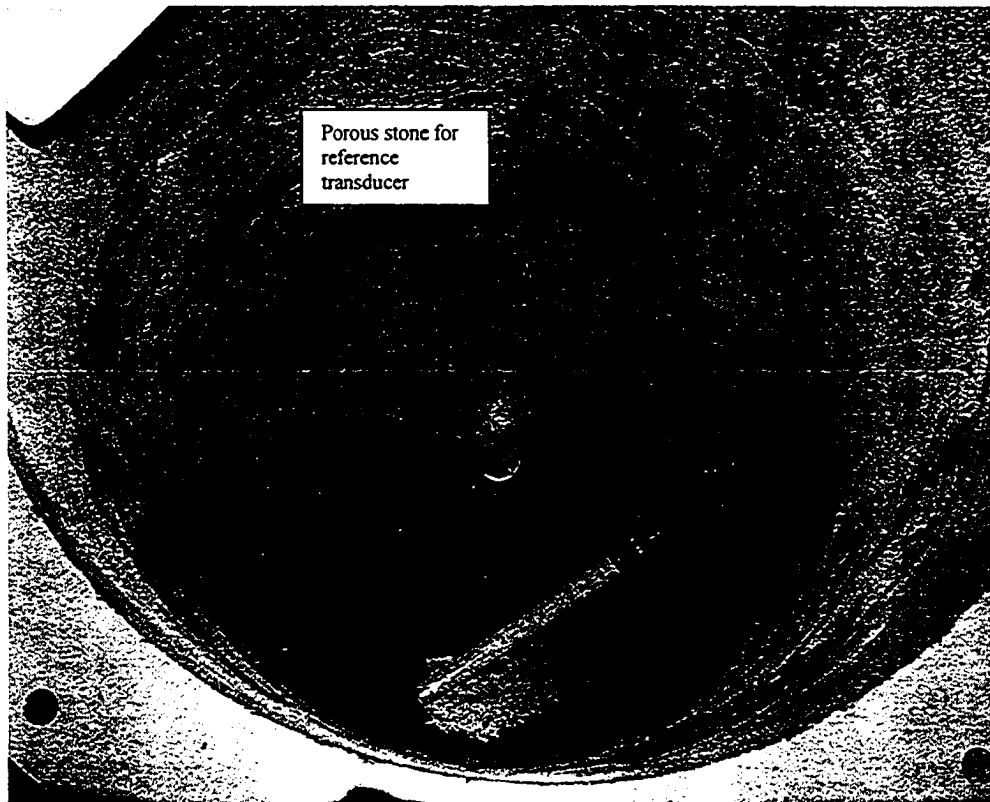


Figure II.15: Digging the protective tip out of sand after testing. The rubber membrane covering the protective tip was stripped off during insertion into sand. The protective tip and the enclosed transducer were undamaged by the insertion of the tip one foot into the sand. The porous stone for the reference transducer is in middle left of picture.

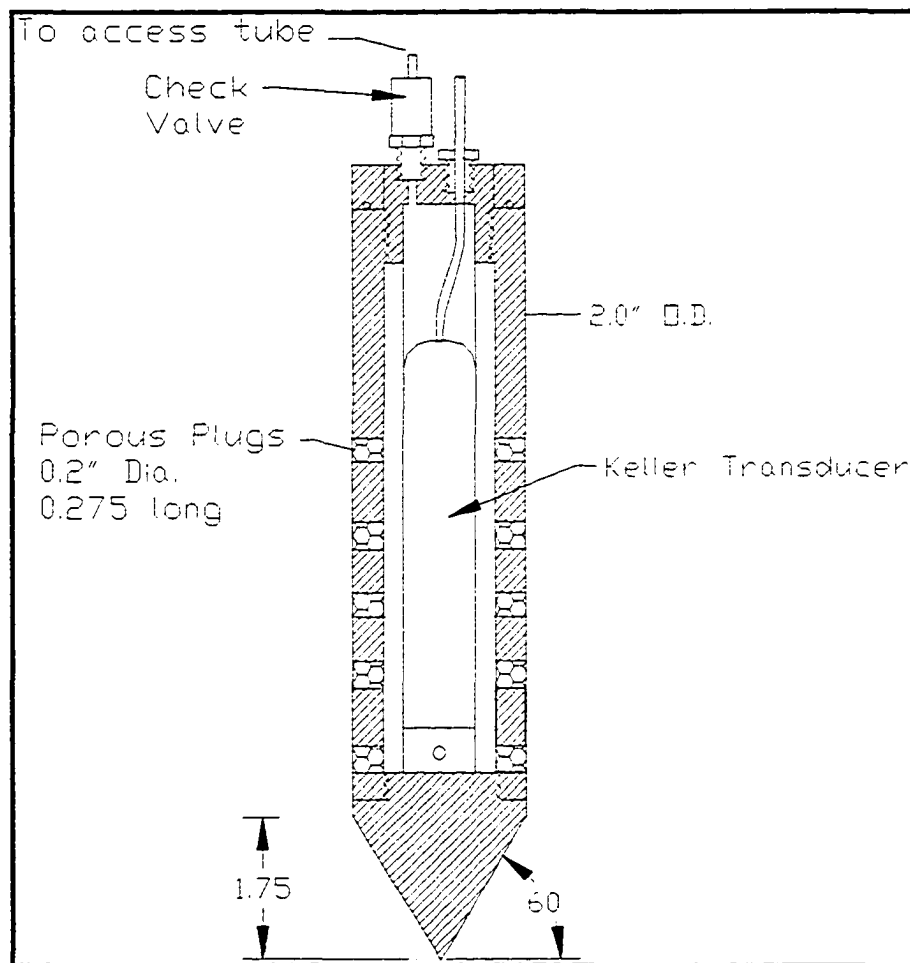


Figure II.16- New protective tip design allows access to the piezometer screens after installation. A check valve is attached to the top to prevent the signal from dispersing up the access tube. The screen area and permeability of the tip are the same as the earlier tip.

CHAPTER III

POOL TESTING

In order to test the protective tips and existing piezometers in the field, field-testing equipment was designed and built. To create a sharp fast-rising signal, a hammer/surge block signal-generating system was developed that would be placed some distance from the piezometers to be tested. It was envisioned that a 4-inch diameter PVC signal well would be placed with 2-foot screened intervals at several different depths below the water table. The locations of the screened interval would depend on the depths of the installed piezometers. As was discussed in the literature review, the use of compressed air as poppers or air pressure pulses applied to the top of the column of water did not provide signals with sufficiently rapid rise velocities to simulate the development of excess pore pressures expected during an earthquake. Other methods of developing a fast-rising signal in ground water such as dropping large weights on the ground surface or using explosives, while providing the rapid pressure rise to be expected, destroyed fabric of the very sediments needed for repetitive testing to determine the ongoing conditions in a piezometer field. Reproducibility of signal was an important concern in the development of the signal-generating device.

III.1-Objective of testing in the pool: Testing in the pool primarily was intended to try out field equipment and develop standard procedures to be used in the field.

Specifically, questions that needed to be answered while testing in the pool were:

- What is the nature of the signal generated by dropping a large weight on a column of water?
- Was the signal a fast-rising signal?
- Was the signal-generating equipment durable enough to withstand repeated testing?

The pool, like the water testing in the pressure vessel, provided an ideal setting where everything could be controlled. The results would provide a baseline against which field results could be compared.

The newly redesigned protective tip for the Keller 1 transducer was to be tested for use in the field. Procedures needed to be developed for testing the permeability of the screens of the protective tip. Two new Roctest transducers (FISO Technologies' fiber-optic) for use in the field were to be tested. The new Roctest transducers used their own signal conditioner (FTI-100i) and program for logging.

III.2-Signal generating system: The hammer, anvil, hammer guide rods are the same as the equipment used for standard SPT testing using a donut hammer. As is shown in Figure III.1 and Figure III.2, this equipment was modified to accommodate a string of NQ rods (2.75" OD and 2.375" ID) below the anvil, and a surge block attached to the bottom of the NQ rod. The surge block fits into a 4" inside diameter PVC schedule 40 well. A metal shroud was located below the well screen and held in place by a string of 1-inch pipes inserted down the middle of the NQ rods. The Roctest #2 transducer was located inside the shroud. The shroud provided protection for the transducer and allowed access to the water in the well screen through a hole in the bottom of the shroud. An inflatable packer (Figure III.2) was placed below the shroud to limit the

volume of water compressed by the surge block. The packer was lowered into the PVC well casing on 1" pipes so that it sealed the well casing below the well screen. The 1" pipe with the pressure line and the transducer cable extended up the middle of the NQ rods to just below the platform elevation. The internal transducer (Roctest #2) was placed in the shroud with the sensitive face of the transducer facing downward. The pressure in the packer was controlled with a tank of compressed nitrogen gas.

The signal was generated when the anvil was struck by the falling hammer, driving the NQ rods and surge block rapidly forward, forcing a surge of water through the well screen into the aquifer creating a pressure spike. This pressure spike was measured in the transducers located some distance horizontally from the well screen in the water. The intent was to duplicate as closely as possible the action of a hammer or shot-actuated hammer used in the pressure vessel testing.

The 140-pound SPT hammer rides on a 2.75" OD guide pipe that allows a maximum of a 5-foot hammer drop onto the anvil. A hole was drilled through the center of the anvil allowing the pressure line for the inflatable packer and the cable for the transducer to pass through. The surge block has a diameter of 3.75" (Figure III. 3). Two hard plastic disks fill the remaining quarter inch, in part, with a slightly larger diameter than the surge block. There is less than a sixteenth of an inch gap inside the 4" ID PVC casing.

To prevent the anvil from advancing too far, an arrestor was constructed that provides a stop about 6" above the well top and prevents the anvil from being driven into the top of the 1" pipe inside the NQ rods (Figures III.1 and III.4). The one-inch pipe is

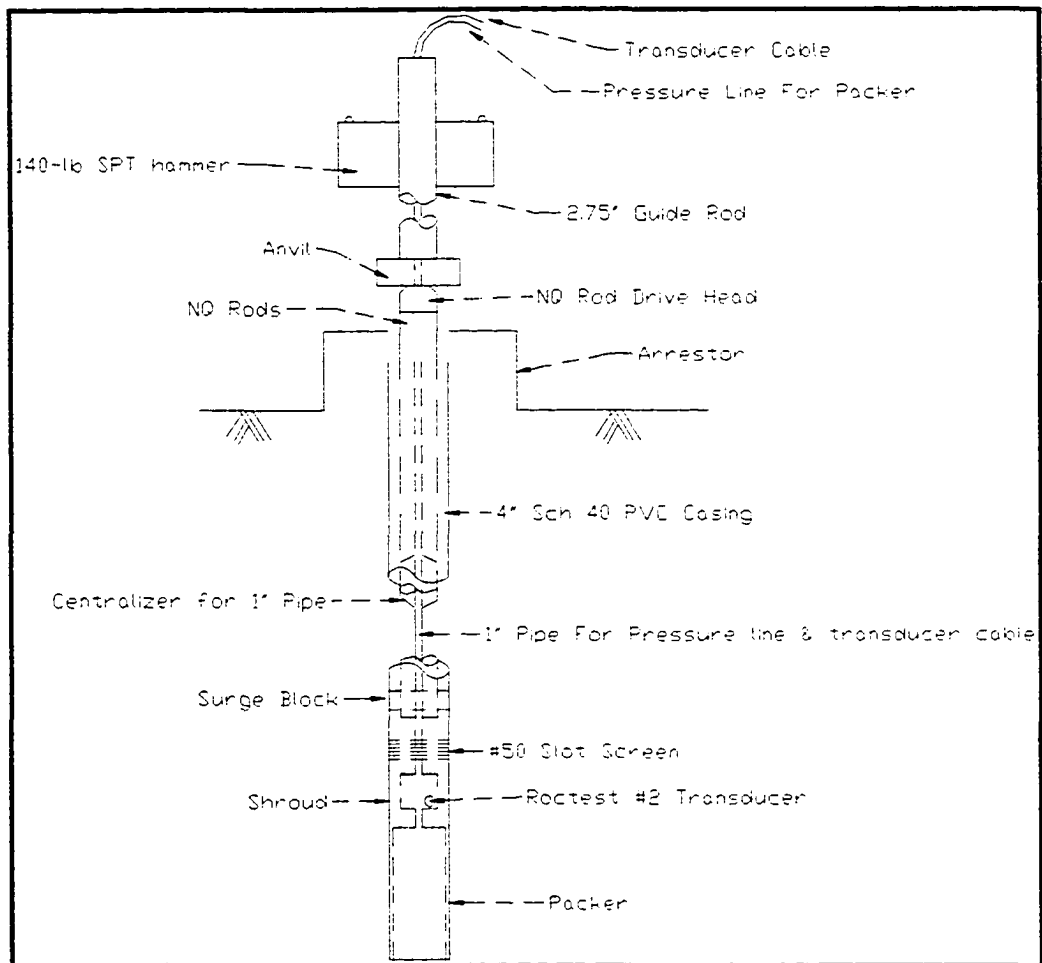


Figure III.1-Signal Generating System. The signal is generated when the anvil is stuck by the falling SPT hammer driving the NQ rods and surge block rapidly forward forcing as surge of water through the well screen into the aquifer creating a pressure spike.

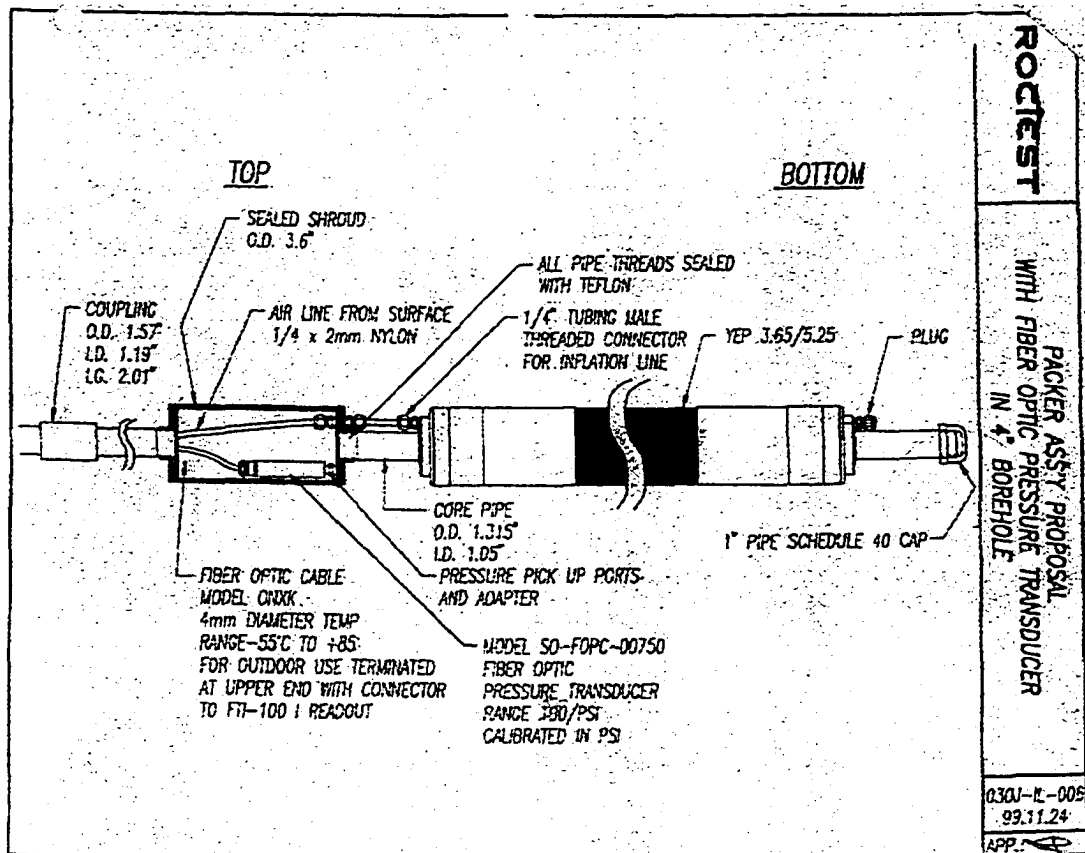


Figure III.2-Roctest YEP 3.65/5.25 Packer used to seal the well casing below the well screen. The shroud at the top of the packer houses the Roctest #2 transducer with a range of 500 psi.

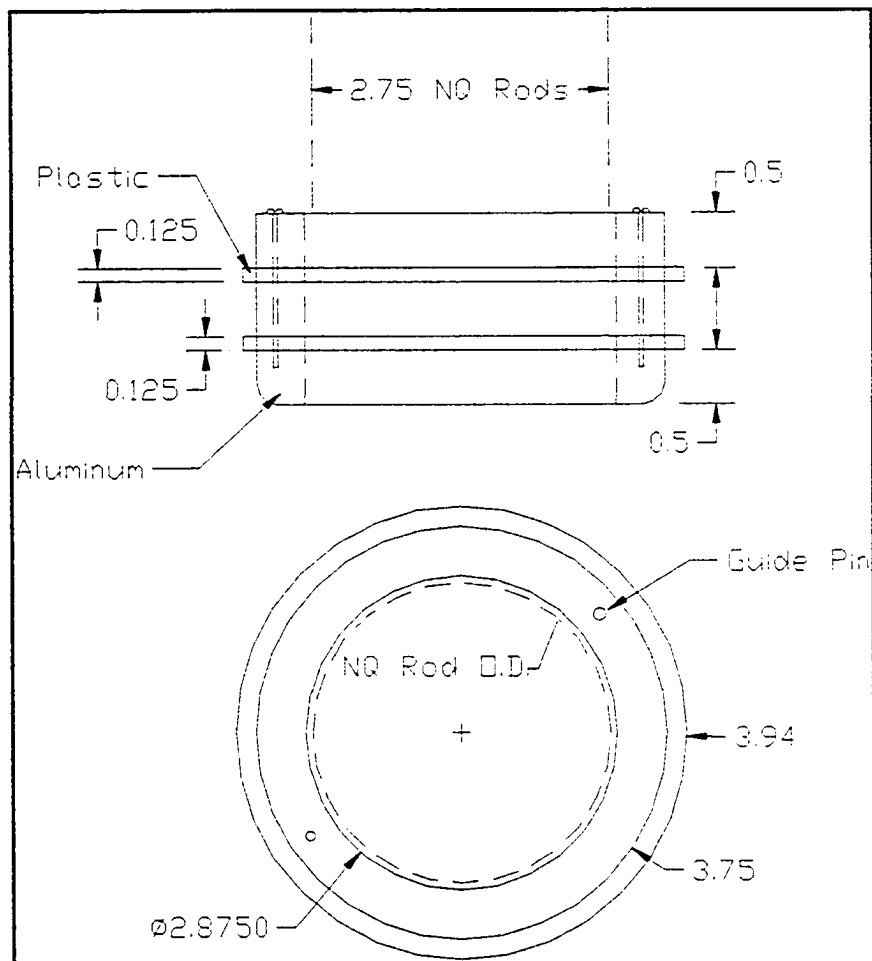


Figure III.3-Surge Block Design. The surge block is used at the end of the NQ rods to create a surge of water in the well casing after the anvil is struck by the SPT hammer. The surge block is made of three half-inch thick aluminum disks separated by two hard plastic disks of slightly larger diameter than the aluminum disks. The plastic disks are intended to have sufficient diameter so that there is less than a sixteenth of an inch space inside the 4-inch ID schedule 40 PVC casing being used for the well.

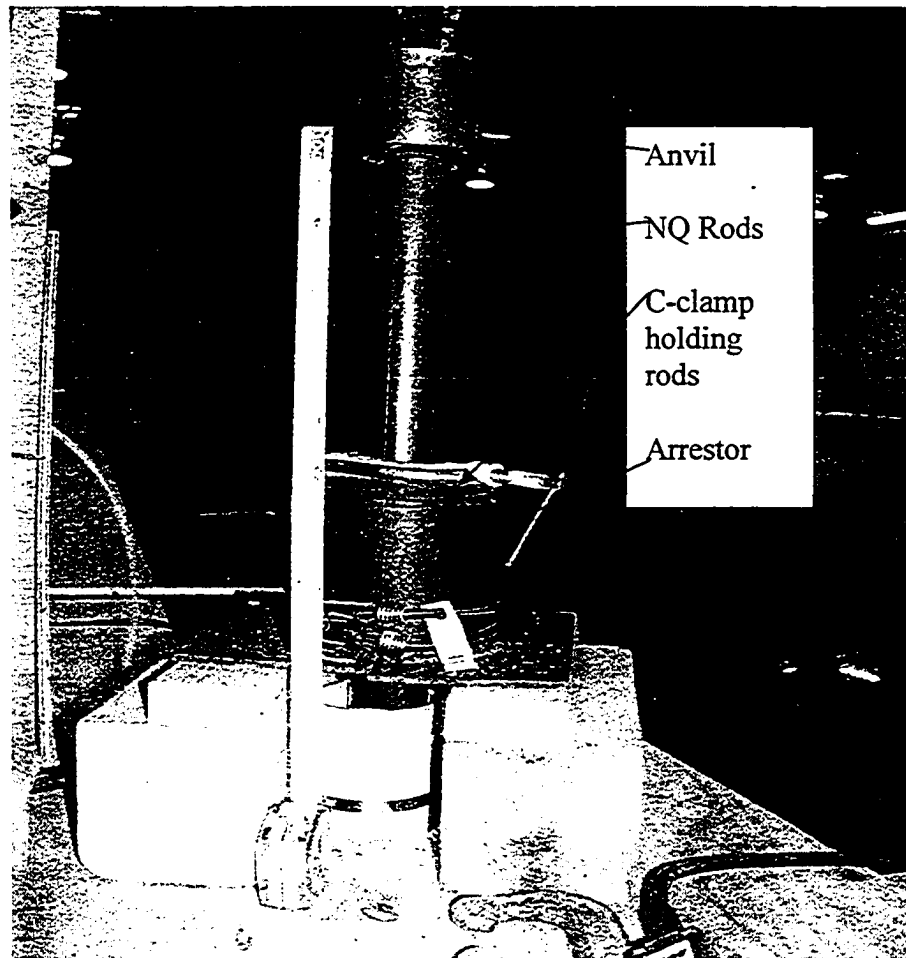


Figure III. 4: Pool Testing-Anvil drop distance. C-clamp is holding NQ rods up. The arrestor stops anvil before impacting the top of the 4" well casing.

kept centered on the NQ rods by a centralizer made of plastic. The centralizer acts as a guide for the NQ rods over the couplings in the 1" pipes and as a plug to prevent water pressure from surging up the center of the NQ rods. The SPT hammer, rods, and anvil were lifted with a crane. Initially a chain, attached to the eyes at the top of the hammer, was used to lift the hammer. A pipe coupling at the top of the hammer guide pipe allowed the lifting of the hammer, anvil, NQ rods, and surge block as a unit once the hammer reached the end of the guide pipe. Review of the videos made of the initial hammer drops showed that the anvil, without being restrained, was dropping too rapidly for the hammer to catch up to before the anvil hit the arrestor. Restraint was accomplished by attaching a C-clamp to the NQ rods so that the anvil, rods, and surge block rested on the hammer arrestor. Review of videos of the drops with the C-clamp holding the NQ rods and anvil up showed that the impact of the hammer on the anvil caused the C-clamp to fly off releasing the NQ rods. The hammer was then hitting the anvil at full velocity. The anvil, rods, and surge block were shot forward by the impact creating a gap between the hammer and the anvil. The hammer could drop 5 feet, once released, while the anvil, rods, and surge block remained stationary. Figure III.5 shows the hammer raised to the top of the guide rods. Figure III.4 shows the position of the C-clamp holding the NQ rods and the anvil.

The release mechanism that seems to work best for the hammer was the use of four overlapping strings through the eyebolts on the top of SPT hammer as shown in Figure III.1. The string was strong enough to lift the hammer and rods. Once the hammer and rods were at the desired elevations, the string was cut.

III.2-Pool: The pool used is located in the Jere Chase Ocean Engineering Center at University of New Hampshire and is 20 feet deep. As shown in Figure III.5 the signal well casing was located in the corner of the pool with the center of the two-foot screened interval at the depth of 13 feet. A Roctest transducer (500 psi, called Roctest 2) was located in the casing, below the well screen and under the surge block (Figure III.1). The Keller 1 and another Roctest transducer (100 psi, called Roctest 1 below) was placed in the pool opposite the well screen. Changing the location of the raft to which the transducers were attached varied the horizontal distance between the transducers and the well screen.

The Roctest #1(reference) and the Keller 1(piezometer) transducers were located opposite the well screen in the pool at a depth of 13 feet. These transducers could be set at various horizontal distances from the signal well, ranging from as close as 12 inches to 30 feet from the well screen.

The well casing used in the pool was 20 feet long. The top 12 feet was solid casing. The slotted interval was set from 12 to 14 feet below the water surface. The size of screen used was #50 slot (0.05-inch wide slots). The bottom 6 feet of the well was solid casing. The packer and shroud were located in this section.

The usual sequence of running a test was as follows:

- Raise the hammer to the top of the guide pipe (5 feet in most cases).
- Raise the hammer and rods 1.5 feet above the arrestor.
- Put the C-clamp on the NQ rods.
- Lower the hammer and rods slightly so the C-clamp supports the weight of the rods and anvil.
- Begin logging transducer signals.
- Cut the string holding the hammer.

III.3-Results: The packer pressure line was crimped several times during the testing causing loss of pressure in the packer. While crimping of the line did not occur on every test the problem was never satisfactorily overcome until the use of the packer was discontinued and replaced by a sealed 3-inch PVC pipe section set below the screen. Logging of the signal received by the transducers was done on a PC using LABVIEW program for the Keller-1. The Roctest transducers were logged using the signal conditioner provided with the optical fiber transducers and a program called FISO provided by Roctest to interface with the PC. The maximum logging rate provided by the FISO program was 100 Hz. The initial signal logging speeds of 50 Hz and 100 Hz were shown to be too slow to measure the signals generated by the hammer system. Examination of the signals demonstrated that more details of the shape of the signal were achieved with logging speed of 3000 to 5000 Hz (5000 Hz being the maximum logging rate for the system). The Roctest program limited to 100 Hz (10 ms) missed much of the data contained in a signal. This problem was overcome in later in field-testing when the output from the Roctest signal conditioner was taken as an analog signal and read directly by the LABVIEW program. It was expected that the pressures generated within the well casing by the surge block would be between 100 to 200 psi. As

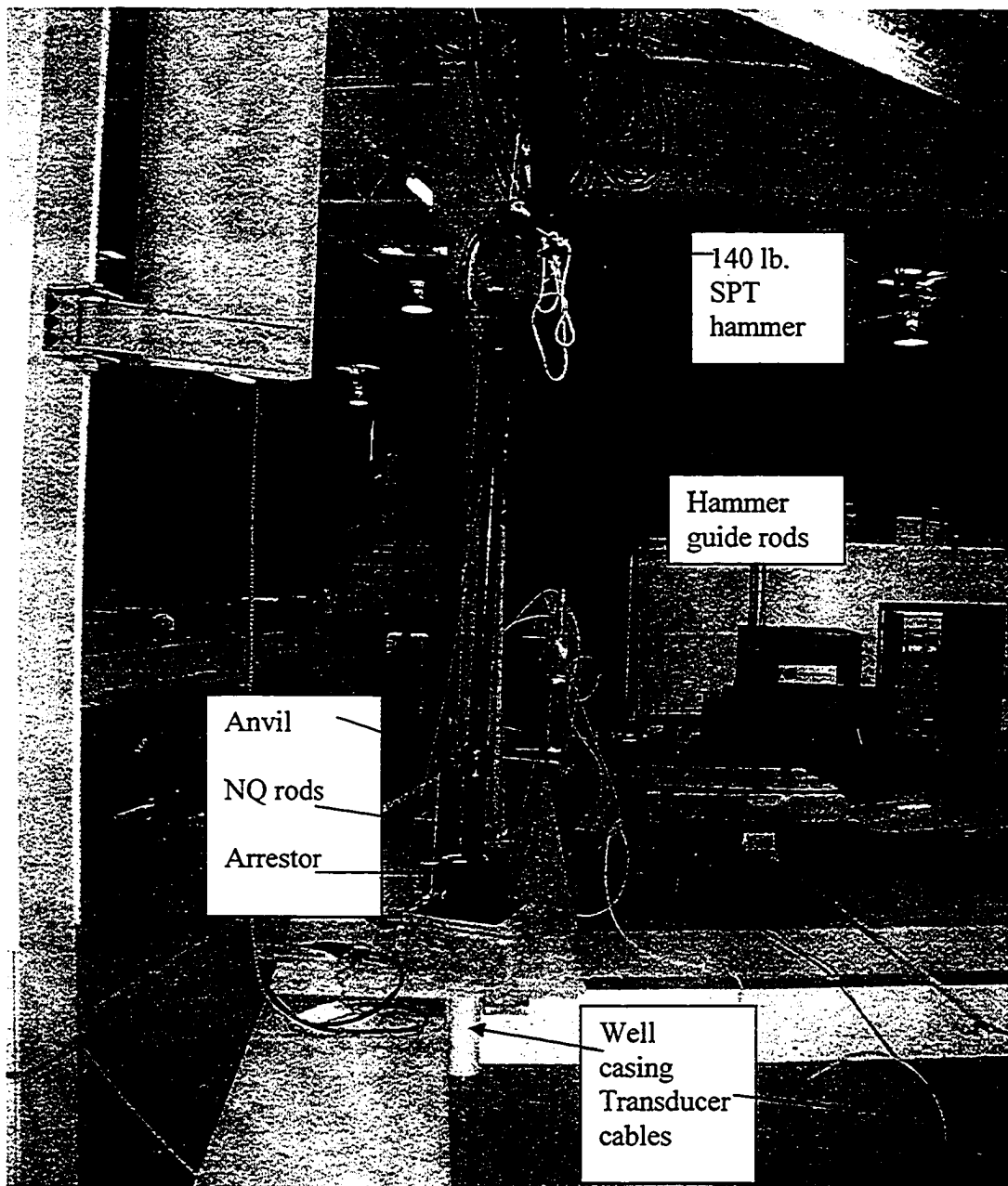


Figure III.5: Pool testing-Signal generating system. 5' hammer drop on 2.75" guide pipe, anvil drop is 15". NQ rods are held by C-clamp on top of the arrestor. String is holding hammer. Other ropes are safety lines.

previously noted the Roctest 2 transducer of 500-psi capacity was installed in the shroud to measure the pressures generated within the well screen area under the surge block. This transducer was overstressed in the first two hammer drops. The recorded pressures exceeded 825 psi. Figure III.6 is the recorded pressures by the Roctest 2 transducer during the first test in which it was used. The logging rate was 100 Hz. The test was duplicated because the first test so much exceeded the expected pressure it was assumed to be an error of some kind. The second test recorded a similar value of over 800-psi but went to zero after a few moments. The Roctest 2 transducer did not function at any pressure after the second test. Discussions with the technicians at Roctest indicated that for internal protection the transducer stopped recording data when the pressure exceeded about 800 psi. To actually destroy the transducer would require pressures in excess of 1200 psi.

During the first few tests the Roctest 1 and Keller 1 transducers were located 2 feet horizontally from the well screen. No pressure wave was detected but a large spike was observed in both the Roctest 1 and Keller 1 transducer. The pressure waves as observed in the pressure vessel testing were made of smoothly-rising positive pressure increases (see Figure II.12). The spikes were only made up of one or two data points when logged at 50 or 100 Hz and could be both positive and negative changes in pressure. The logging rate was progressively increased. With each increase more detail of the spike and its wave shape were observed. It became apparent that the hammer impact was producing a compressional (P) wave in advance of the “pressure wave” produced by water flowing out of the casing through the screen as the surge block

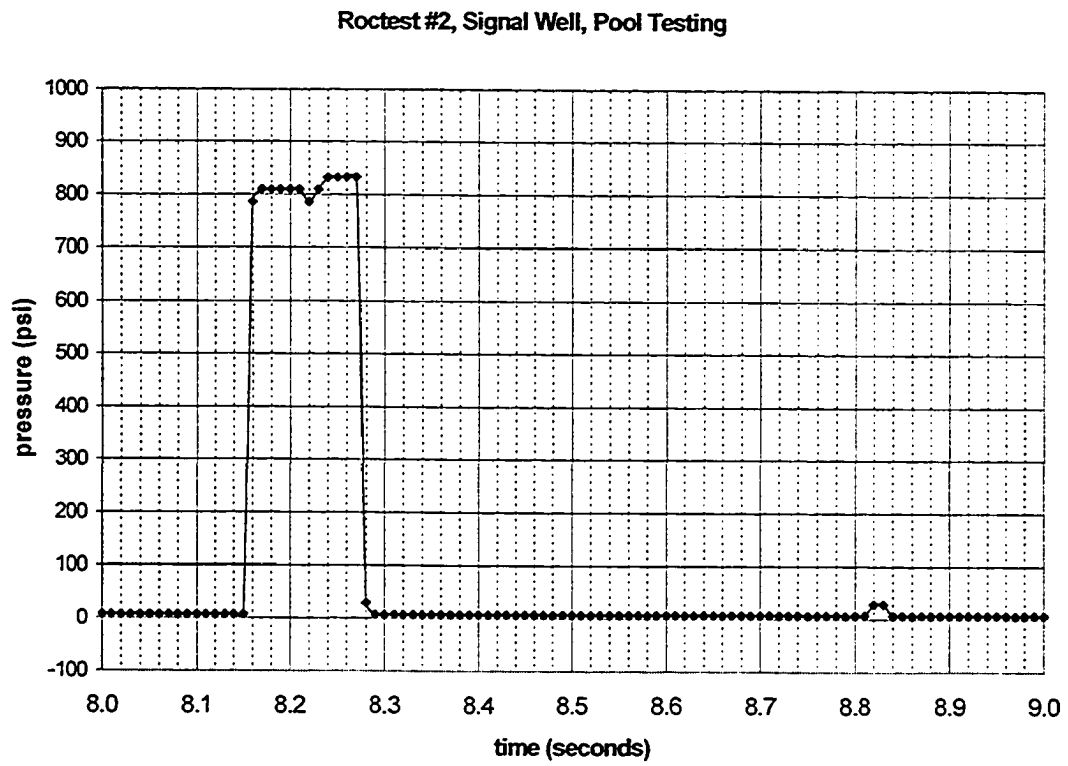


Figure III.6: Pool Testing, Roctest #2 signal, located in the signal well. The transducer is rated at 500 psi. It stops recording at about 825 psi.

advanced. Figure III.7 is a typical example of the P-waves detected by the Keller 1 transducer. Figure III.7 is logged at 5000 Hz. Three or more peaks are detected as a result of the interaction of the hammer, anvil, and arrestor. In viewing the video of this particular event, it was evident that the first peak was caused by the impact of the hammer with the anvil. The second event was caused by the impact of the anvil on the arrestor; i.e. the anvil bounced off the arrestor and impacted the hammer again creating the large middle peak. The hammer and the anvil were traveling in opposite directions during this impact. The last smaller peak, at 5.86 seconds, was the impact of the anvil and hammer on the arrestor again. The amplitude of the P-wave decreases with distance from the source well. Figure III.8 shows the decrease in the amplitude of the P-wave related to the inverse log of the distance from the signal well. The amplitude of the wave was measured as the difference in pressure between the maximum and minimum pressure (positive and negative) for largest peak at each distance from the source well.

Velocity of the P-wave could not be determined during the pool testing. After the failure of the Roctest 2 transducer and the inability of the Roctest 1 to log at a sufficiently fast rate it was not possible to determine the start time for the input of the signal or the travel time between two different transducers at different distances. A pressure wave caused by the injection the water out of the well screen could be detected if the transducer was close enough to the well. Figure III.9 is the signal received by the Keller 1 transducer positioned 16 inches from the source well. The

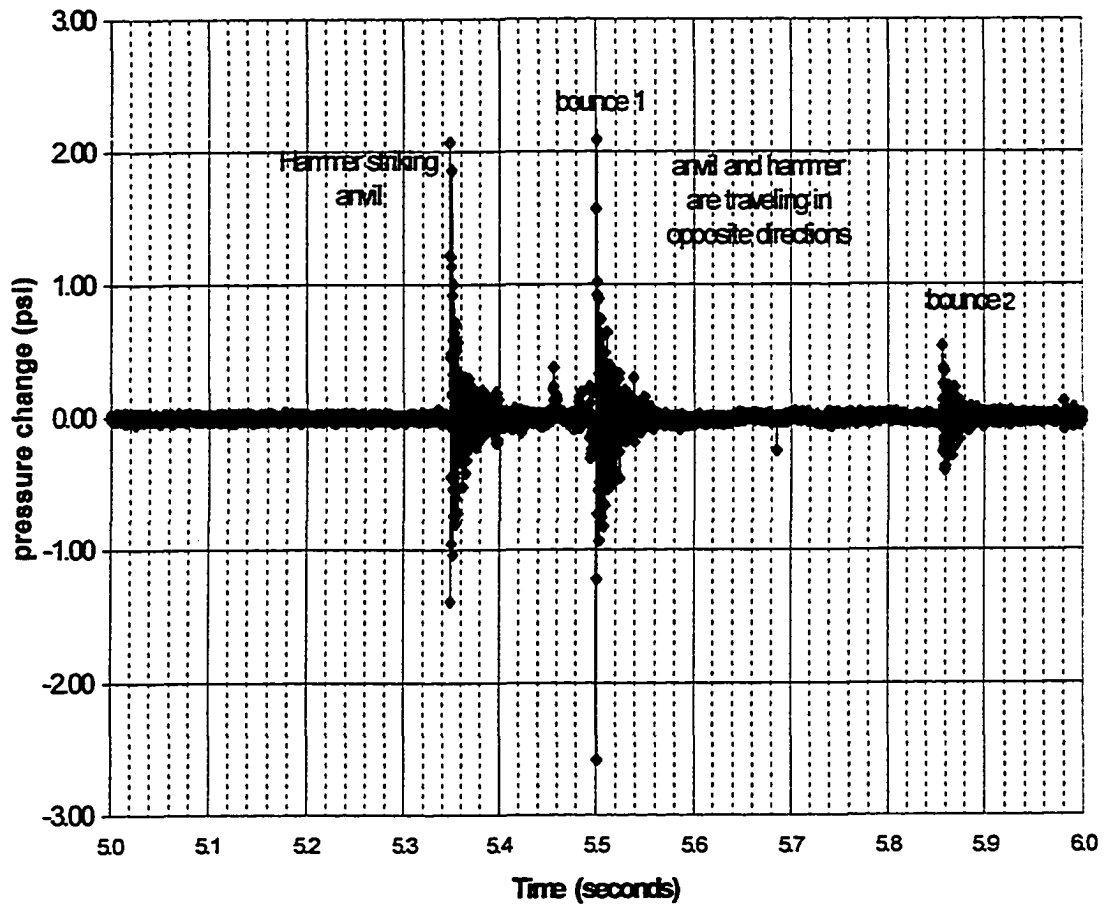


Figure III. 7: Pool Testing. Keller 1 Pressure change. Impact wave. Three impact waves are created by the impact of the hammer on the anvil. The first is created when the falling hammer strikes the stationary anvil. The second impact wave is created by the anvil bouncing off the arrestor and meeting the falling hammer. The third impact wave is the anvil again bouncing off the arrestor being hit by the falling hammer.

signal was logged at 5000Hz. The pressure wave could not be detected when the transducer was set more than 16 inches from the screen.

III.5-Conclusion: A P-wave generated by the hammer/surge block system was transmitted to the water in the pool. The energy of the signal decreased as the inverse log of the distance from the signal well. Logging speeds of 3000 Hz or more were necessary to detect the details of the P-wave. Source pressures of 1200 psi or more on the water column were likely being generated by the impact of the hammer on the anvil and surge block. The Keller transducer within the protective tip detected a pressure wave with a frequency of about 2 Hz and a P-wave at with a frequency of about 1000 Hz (see Frequency Analysis, Chapter V). A usable signal generating system and the procedures for operating in the field were developed.

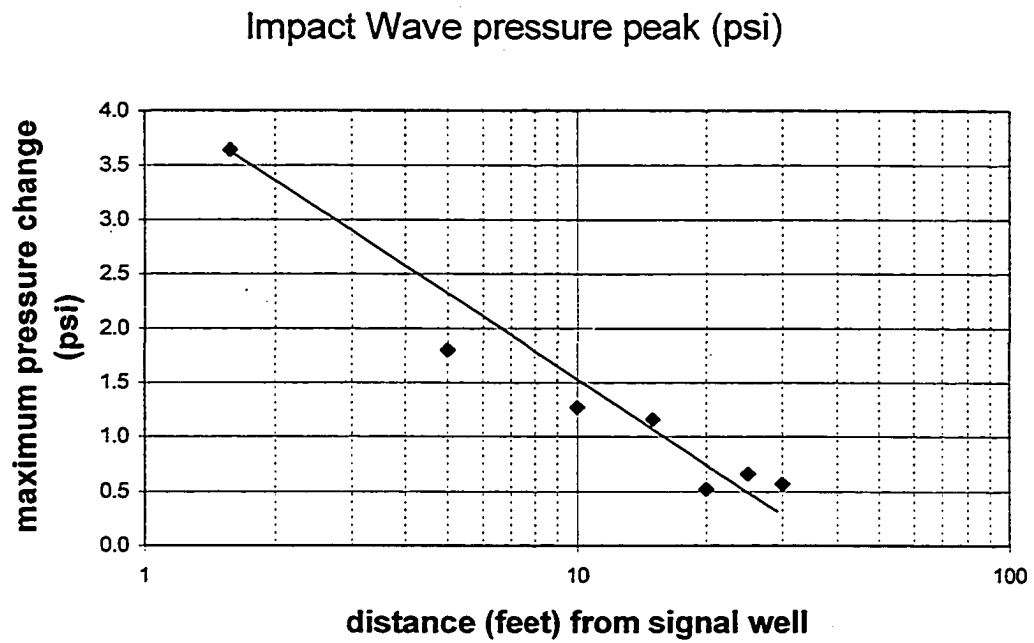


Figure III. 8: Impact wave (P wave) pressure decreases by the inverse square of the distance from the source well.

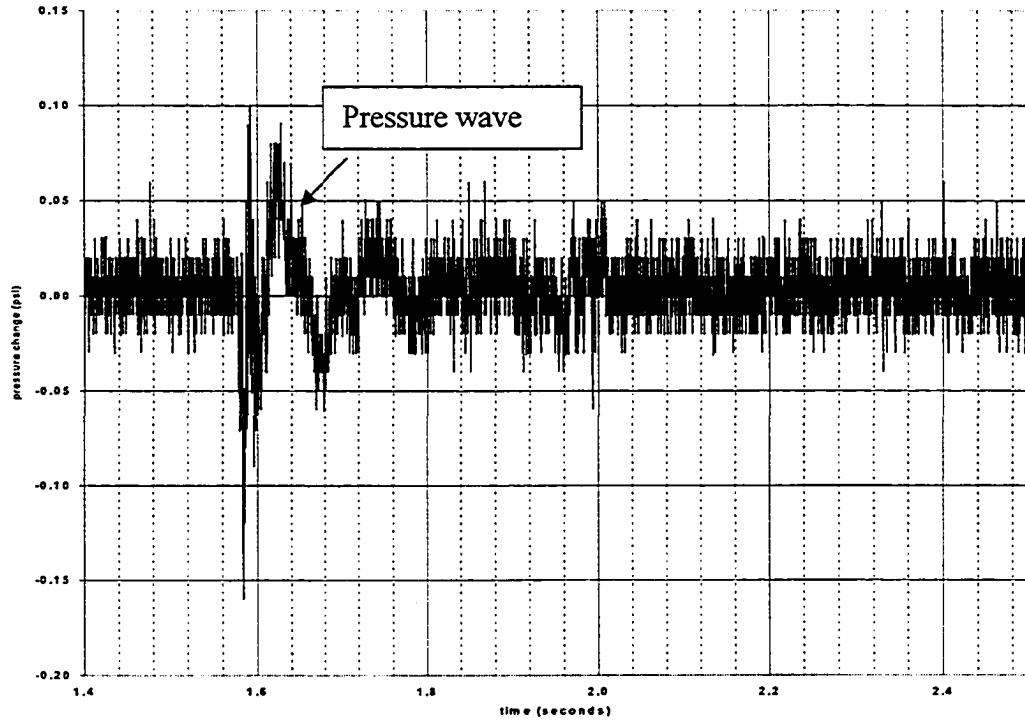


Figure III. 9: Keller 1 transducer in protective tip located 16" from the signal well (3-2-00). The initial signal received is the impact wave (P wave) followed by the confined pressure wave.

CHAPTER IV

FIELD TESTING RESULTS

IV.1-Introduction: This chapter summarizes the results from 5 field campaigns, three at Camp Hedding, New Hampshire, and two at Treasure Island, California. Each of the 5 testing programs is covered in detail in Appendices A-E. The Camp Hedding site is a deep fine sandy outwash plain located near the University of New Hampshire allowing easy access for testing changes in equipment design. Treasure Island is a man-made island in San Francisco Bay, California which has a piezometer array installed in 1994. The testing facility is an existing facility at which the piezometers were to be tested.

In the following are described the source, transducers, and data acquisition systems tested in the field. The evolution of the signal generating system is described in the Appendices as it developed through the field-testing campaigns. Through the testing campaigns, an understanding evolved of the signal generated by the system. Three different parts of the signal are identified covering a wide range of velocity and frequency content. These parts of the signal were designated the impact wave, the confined pressure wave, and the unconfined pressure wave. They are defined as follows:

Impact wave is a compressional wave or P-wave. The impact wave is generated by the SPT hammer striking the anvil. Part of the energy of the impact is transferred as a

compressional wave through the anvil down the NQ rods to the surge block located in the signal well below the water table. The compressional wave is transferred from the surge block into water column in the well and through the water column into the ground water. This compressional signal is transferred to the piezometers through the ground water. The impact wave is shown in Figure III.7. Its characteristics are a large initial oscillation of positive and negative pressures around the ambient hydrostatic pressure. The strength of the signal diminishes within a tenth of a second back to ambient pressures. As is noted on Figure III.7 several impact waves can be generated during a single hammer drop. The frequency of the impact wave is about 900 to 1000 Hz.

Confined pressure wave is a pressure wave created by the attempt of the surge block to push the water out of the signal well into the aquifer. As was shown in the pool testing, pressures of 1200 to 1500 psi are believed to be generated in the signal well. The water in the signal well is attempting to migrate out of the signal well so rapidly that the aquifer acts as a confined aquifer with a small storage coefficient. The aquifer cannot drain rapidly enough to accept the water attempting being ejected from the signal well in the first few tenths of a second after the hammer impact. The aquifer can only adjust to the increase pressure in the well by a slight expansion of the soil skeleton and a slight compression of the water. A typical confined pressure waves are shown in Figure IV.5. The signal is characterized by the rapid increase in pressure over a few tenths of a second followed by a rapid decrease in pressure until a slower decay curve is encountered. The frequency of the confined pressure signal varies from 0.5 to about 2

Hz. The velocity of this signal will be shown to be a function of the distance from the source. Higher velocities occur closer to the source.

Unconfined pressure wave is a pressure wave created later after the hammer impact as water actually is pushed into the aquifer from signal well. The aquifer acts as an unconfined or phreatic aquifer with a large storage coefficient. The aquifer adjusts to the actual movement of the water out of the well by physically allowing the redistribution of water rather than accommodating to just the pressure change. There is no expansion of the soil skeleton nor compression of the water in the aquifer. The unconfined pressure wave is believed to form the long decay curves detected after the confined pressure wave. An example of a confined pressure wave followed by a separate unconfined pressure wave is shown in Figure IV.12. It takes several minutes for the unconfined pressure wave to decay to background water levels. The frequency of the unconfined pressure wave is about 0.01 Hz. The demonstration that the parts of the signal are as defined above is left to Appendix J (Numerical Simulation) and Chapter V (Frequency Analysis). The definitions are presented to facilitate the discussions of the signals detected during the field-testing program.

IV.2-Objectives of Field Testing: A field testing program should be capable of :

- 1) demonstrating that the piezometers are functioning,
- 2) determining if the piezometers are in calibration,
- 3) demonstrating that the piezometers can detect the type and range of signals generated by an earthquake,

- 4) demonstrating the signals generating system provides repeatable results,
- 5) demonstrating the signal generating system is non-destructive to the soil and piezometers,
- 6) demonstrating the testing system can be easily handled, and
- 7) demonstrating the testing system can minimize the costs of new wells.

IV.3-Equipment taken to the field: Figure IV.1 shows the final configuration of the signal generating systems. The anvil and surge block were held by strings until the impact of the falling hammer on the anvil broke the strings (Figure IV.2). The hammer was lifted by strings and its release was achieved by cutting the strings holding the hammer. The hammer drop could be up to eight feet on the AW guide rods. A 3-inch PVC capped pipe formed a plug in the well casing below the screened interval in the signal well. The 3-inch PVC pipe was sufficiently long that it could sit on the bottom of the signal well. It was lowered and raised by in the well casing by a a string of 1" pipes that screwed into the top cap. The 1" pipes were removed during testing. A steel plate was welded to cover the bottom of the NQ rods. A hole was provided in the metal plate sufficient for a transducer cable to be placed in the space between the bottom of the NQ rods and surge block and the top of the PVC plug to measure pressures generated inside the well casing when the anvil was struck by the falling SPT hammer.

IV.4-Measuring pressure inside the signal well screen during hammer drops: The GEMS transducer (2600RGH2019M3HA, #76218) was utilized to measure the pressures inside the signal well. The GEMS transducer measured pressures in the well casing over 1200

psi (see Figure D.9). This would seem to be in agreement with values measured by the Roctest #2 in the pool testing

IV.5-Test Site Description: The site maps for Camp Hedding and Treasure Island showing the distribution of wells and piezometers used in the field testing are shown on Figure A.4 and Figure C.4 respectively. At both Camp Hedding and Treasure Island it was intended to use a Roctest transducer enclosed in a drive cone as a reference against which to compare the results for the various Keller transducers enclosed in the new protective tips. Special measures were taken at both Camp Hedding and Treasure Island to insure that the screens on the push cone were saturated, protective membrane enclosing the tips was not removed until the screens were below the water table, and that advancing of the push cone did not begin until a casing had been advanced and washed out below the water table. At the Camp Hedding test site the piezometers were installed initially by pushing to the final depths. On Figure A.4 the locations that the Roctest #1 transducer was installed are indicated by R-1, R-2, and R-3. At Camp Hedding the Keller transducer was initially pushed (as described in Appendix A) into at the same location as R-1. At all other locations the Keller transducers were installed at Camp Hedding and Treasure Island, the transducer in the protective tip was placed in the bottom of the boring and covered with a filter pack (see full description the Keller installing procedures in Appendix A).

IV.6-Effect of the equipment changes: Over time there have been numerous changes made to the signal generation system in an attempt to increase the energy released by the

dropping of the hammer and to make it easier to utilize the equipment. The changes have included the following:

- 1) increasing the drop height of the hammer from 5 feet to 8 feet,
- 2) increasing the drop height of the anvil from 15 inches to 36 inches,
- 3) changing from 2.75" hammer guide pipe to AW drill rods as a hammer guide,
- 4) changing the hammer release from (a) pulling a pin to (b) using a pelican hook, and finally to (c) cutting string,
- 5) changing the means for holding the anvil stationary while the hammer accelerated from using a C-clamp around the NQ rods at the top of the arrestor to using string through the top of the AW rod,
- 6) replacing the pneumatic packer with a 3" schedule 40 PVC pipe to provide a seal in the well casing below the screened interval being tested, and
- 7) utilizing a 300-lb. hammer rather than the 140-lb. hammer.

A 300-pound donut hammer was used for the last two tests at Camp Hedding on April 14, 2000. The use of the 300-lbs hammer was abandoned because of the damage the hammer did to the equipment without any noticeable increase in the measured signal.

All these changes were tested at Camp Hedding to determine their utility. Figure IV.3 is a comparison of the tests measured by Keller 2 through that period. The April 11th signals were generated using the original system design--2.75-inch guide rods, pneumatic packer, 5 foot hammer drop, 18 inch anvil drop, pelican hook release of the hammer, and C-clamp restraint on the NQ rods. The subsequent tests in June, July, October, and November 13, 2000 included changing from a pelican hook to string release of the hammer, use of AW rod as guide rods for the hammer, and increasing the hammer drop to 6 and 7 feet. In combination, these changes all decreased the signal strength. On November 15, 2000 the pneumatic packer was replaced with the 3-inch ID schedule 40 PVC providing the plug below the screened section in the signal well. With the removal of the 1" pipe necessary to provide a conduit for the pressure line for the

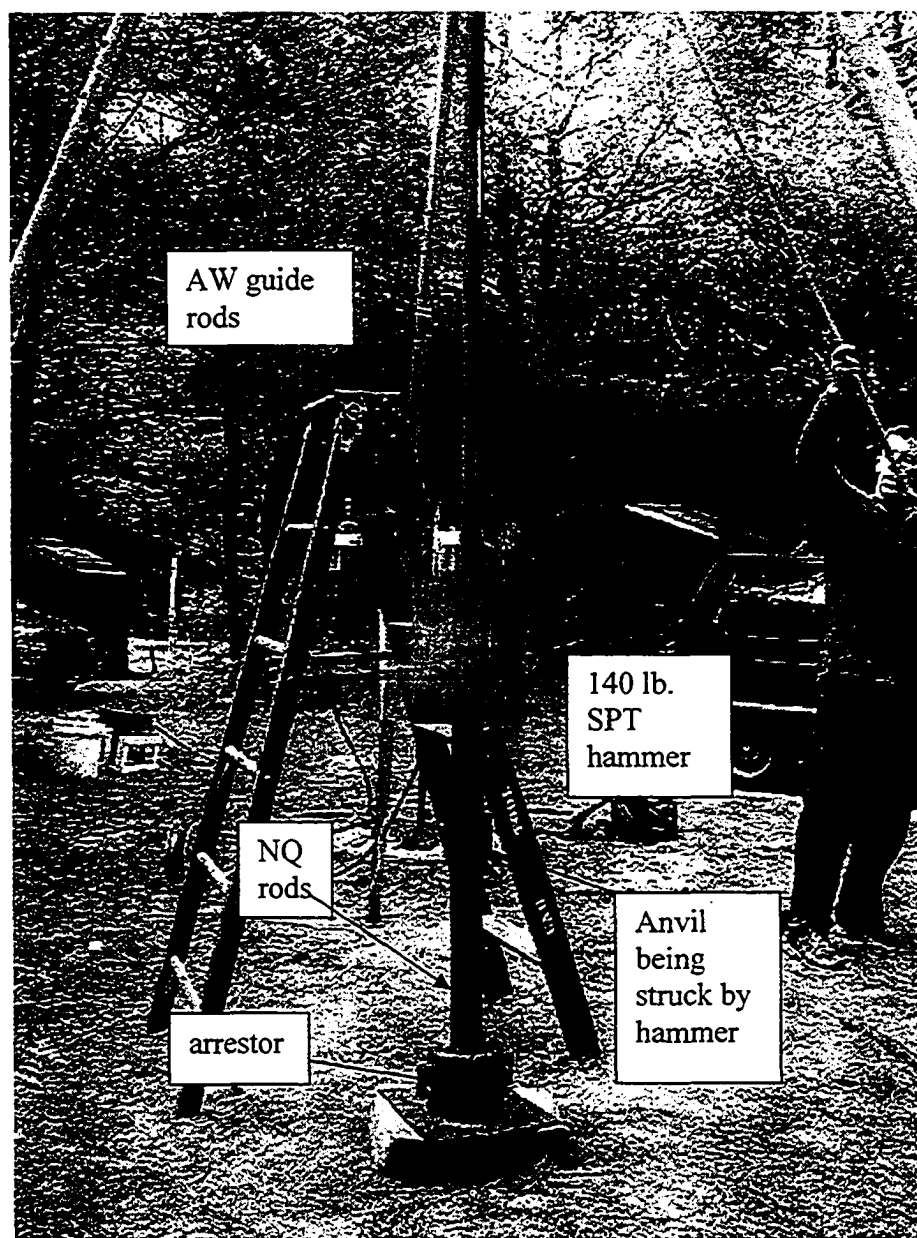


Figure IV.1-Signal generating system as used in the testing at Camp Hedding and Treasure Island. The string holding the hammer have just been cut and the hammer has impacted the anvil driving the NQ rods.

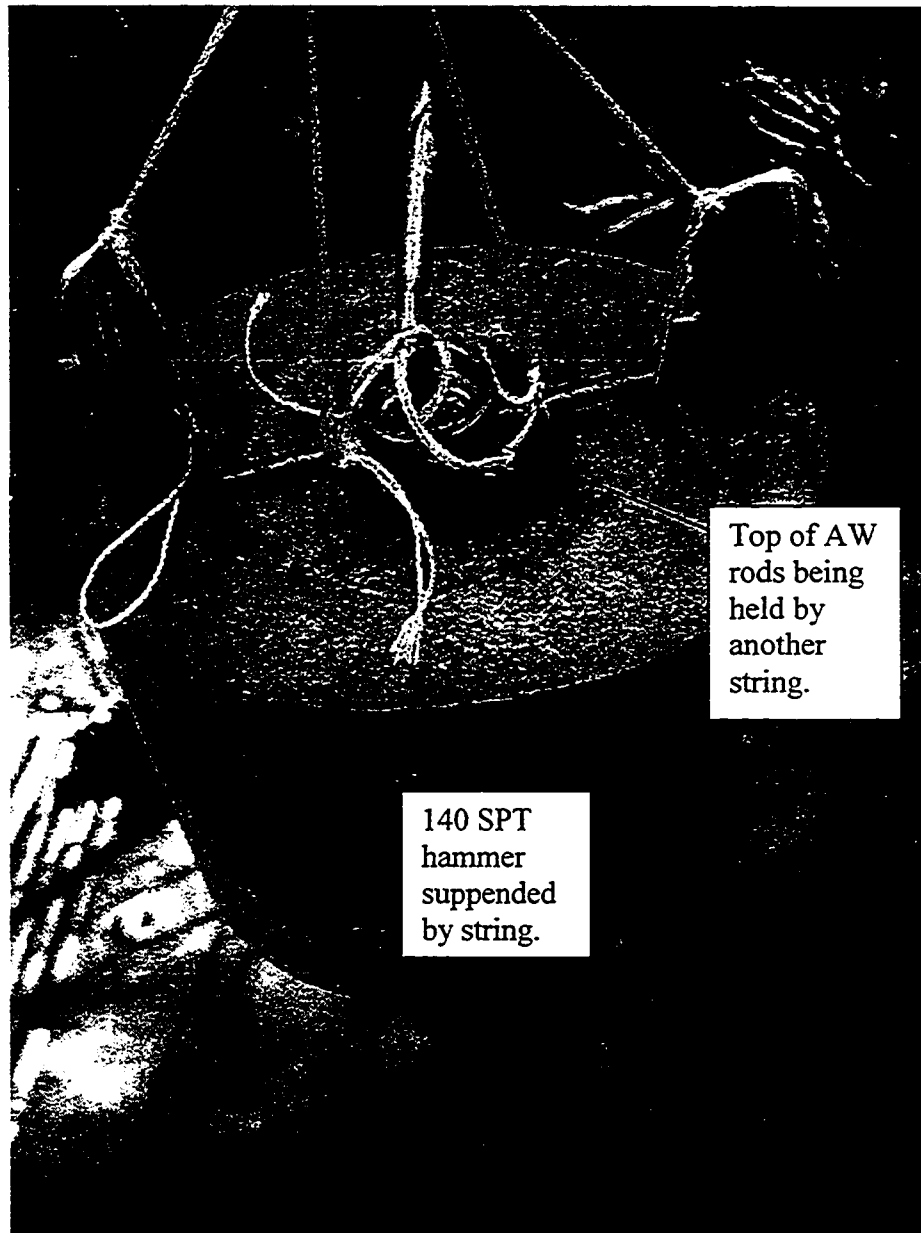


Figure IV.2-The arrangement of strings used to lift and hold the 140 lb. SPT hammer. Another set of strings, attached to the horizontal rod through the top of the AW rod, held the surge block/anvil while the hammer dropped. The strings holding the surge block/anvil were broken when the hammer struck the anvil. The cable to the GEMS transducer emerges from the center of the AW guide rods.

pneumatic packer it was possible to put a steel plate across the bottom of the NQ rods at the base of the packer (Figure IV.4). A hole was provided in the plate to allow the PCB transducer to be placed below the surge block within the screened interval. The November 15, 2000 data reflects the new combination of equipment which included 6-foot hammer drop, 36-inch anvil drop, plate at the bottom of NQ rods, AW guide rods, and 3" ID PVC plug below the screen in the signal well. This combination resulted in the larger pressures measured on November 15 compared to the earlier signals.

Figure IV.5 is the raw data for Keller 3 from Treasure Island for August 2000 and March 2001 testing. The August data was generated with the following conditions:

- 1) a 7-foot hammer drop,
- 2) using the AW guide rods,
- 3) using the pneumatic packer in the signal well,
- 4) utilizing the pelican hook to release the hammer,
- 5) an 18 inch anvil drop (with one exception, Data 14), and
- 6) the C-clamp restraining the advance of the anvil until struck by the hammer.

The March 2001 data was generated with the same equipment as was used on November 15, 2000 at Camp Hedding as described above with

- 1) an 8-foot hammer drop,
- 2) string replacing the pelican hook for holding the hammer, and
- 3) string replaced the C-clamp holding the anvil.

However, the 18-inch anvil drop was maintained in order to compare with the August 2000 tests. The impact waves locations and peaks are about the same between the dates. The confined pressure waves shapes and pressure changes are very similar. The shapes of the signals are visually the same between the two dates (spacing between the signals has been introduced to allow the characteristics of each signal to be seen). At Treasure

Camp Hedding, Keller 2, 20 feet from signal well, all 500 cps data

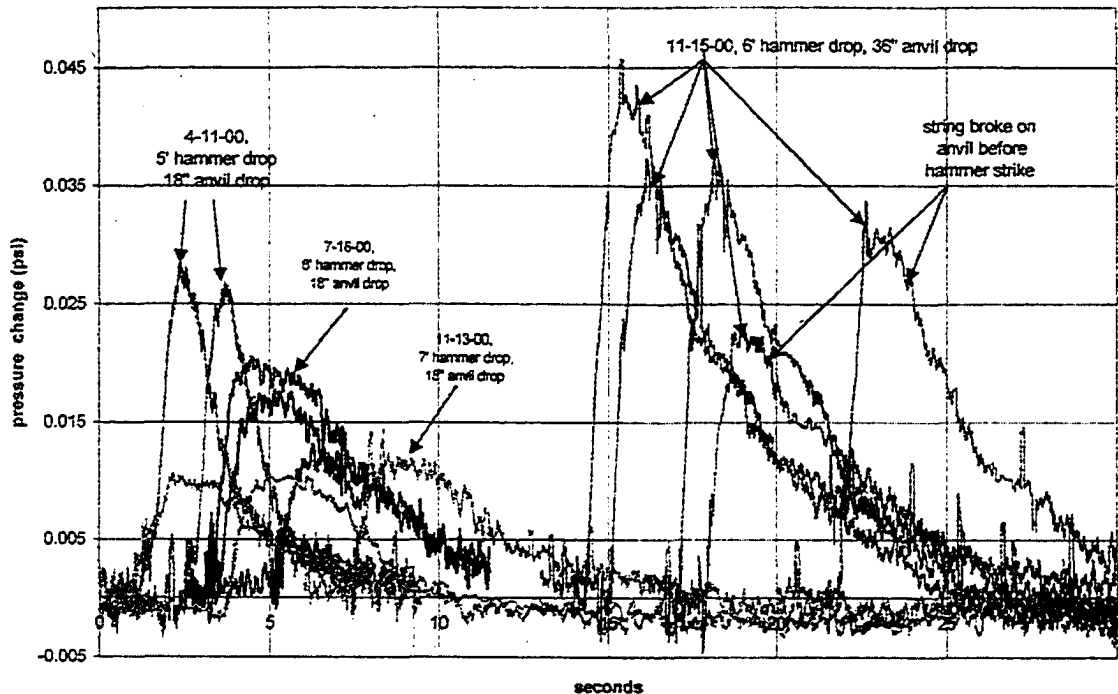


Figure IV.3-Keller 2 at Camp Hedding, filtered confined pressure wave. All data was logged at 500 Hz. The signals have been spaced out horizontally for comparison. The largest confined pressure waves were generated on November 15, 2000 with a combination of 3" PVC plug below the signal well screen, a hammer drop of 6', 36" anvil drop, and string release of both the hammer and anvil.

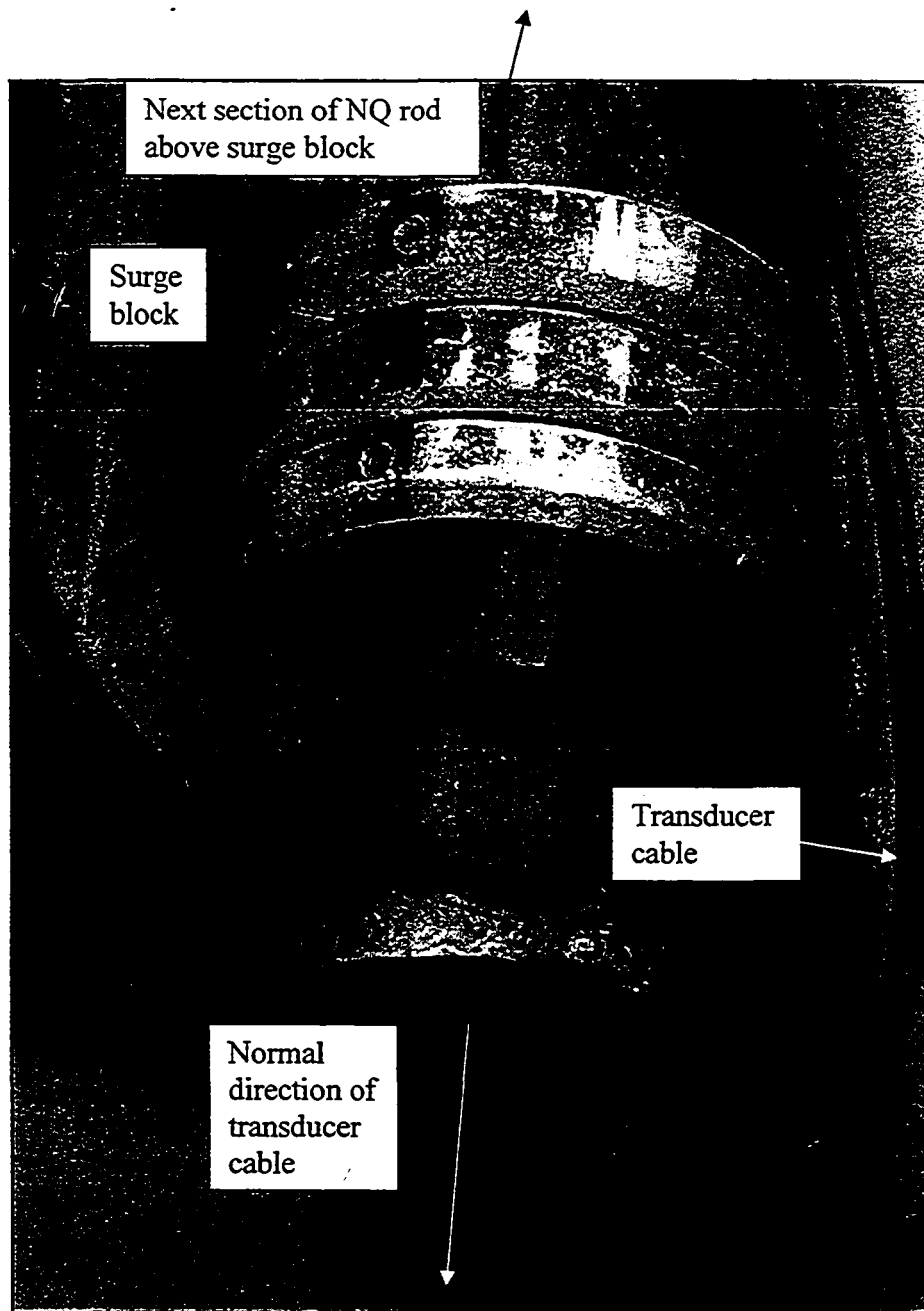


Figure IV.4-Surge block on NQ rods. The bottom of the NQ rod has a welded steel plate with a hole for the transducer. The bottom section of the NQ rod screws on to the next section of NQ rod and metal tabs hold the surge block in place. The transducer cable is folded back in picture but normally hangs below the bottom of NQ rod in the well screen.

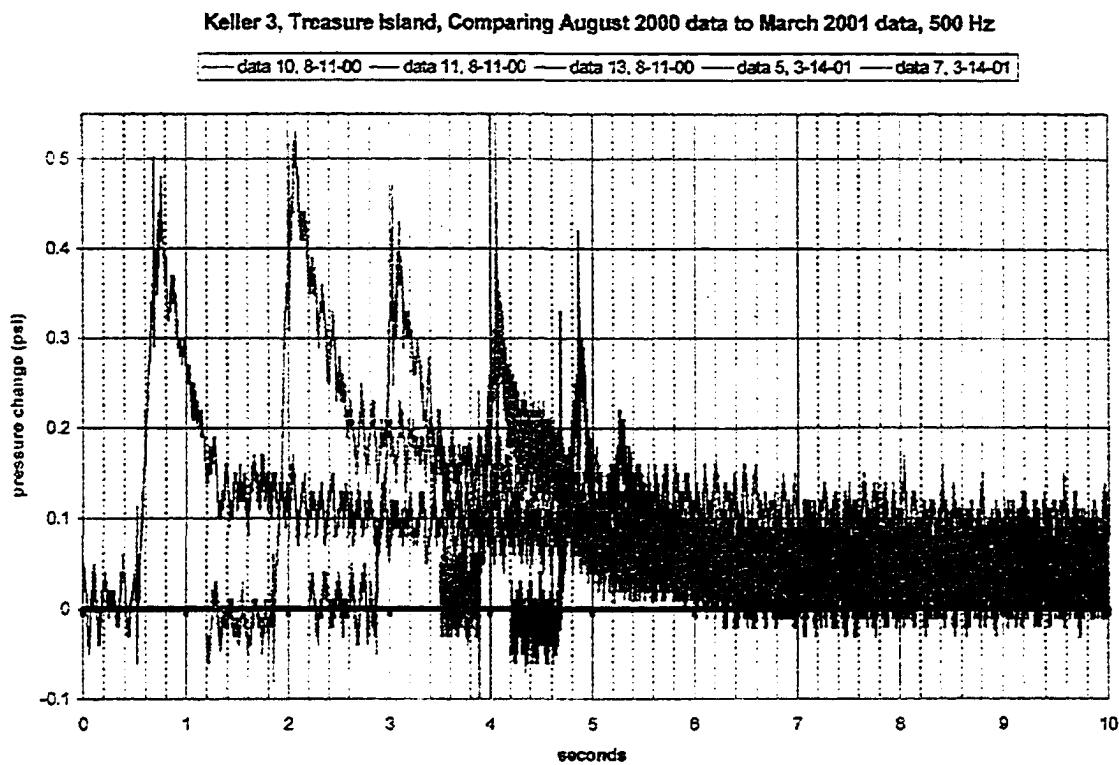


Figure IV.5-Treasure Island. Comparison of data for Keller 3 on 8-11-00 and 4-14-01. The anvil drop for both data sets was 18 inches and both were logged at 500 Hz. The horizontal separation has been added for clarity.

Island there does not appear to be any advantage to many of the changes made.

Obviously using the 3" PVC was easier to handle than the pneumatic packer was with the pressure line running up through the middle of the NQ rod and guide rods. The use of the 3" PVC plug saved significant field time with no failures occurring with the signal generating equipment during the March 2001 testing at Treasure Island. The greatest change that could be made to the confined pressure wave could be achieved by increasing the anvil drop height. This was demonstrated at both Treasure Island and at Camp Hedding. On November 15, 2000 testing at Camp Hedding the height of the anvil drop was increased to 36 inches with the corresponding increase in the confined pressure wave detected by the Keller 1 and 2 piezometers.

IV.7-Wave velocities vs distance: The velocities of the impact wave and the confined pressure wave were calculated from the arrival times of the signal at various piezometers. At Camp Hedding, it was possible to compare the arrival times between the signal well, Keller 1, Keller 2, and the PVC well (refer to Figure A. 4 for layout of piezometers). At Treasure Island, arrival times could be measured at the Keller 3, D-18, D-18, and D-33 "far" on the data collected on 8/11/00 (refer to Figure C.4 for layout). The data collected on 3-14-01 were not suitable for velocity determination because of the large amount of noise present on the D-18 signal (Figures E.7, E.8, and E.9) and the lack of response of D-33 "far" to the confined pressure wave (Figures E.15, E.16, E.17, and E.18).

As previously noted, the impact wave is a compression wave. The velocity of a compressional wave in water is about 4900 feet/second. Figure IV.6 is the plot of the arrival time against distance from the signal well at Hedding. The velocity for the impact wave is about 5000 ft/second. It should be noted, however, that because of the close well spacing, a change of one data point at a logging rate of 5000 Hz at the PVC well data would lower the velocity to 4100 ft/sec.

The confined pressure wave has a velocity that varies as a function of distance from the signal well. Data taken on 12-6-00, shown in Figure IV.7, is an example of how the velocity of the confined pressure wave was calculated between the PCB transducer in the signal well, Keller 1 ten feet from the signal well, and Keller 2 twenty feet from the signal well. The impact begins in the PCB transducer at 0.146 seconds. The Keller 1 piezometer is estimated to begin the rise due to the confined pressure wave at 0.18-seconds. This time was estimated based on a line drawn through rising part of the signal and extended through the normalized pressure line of zero. The velocity of the confined pressure wave is 303 ft/second between the signal well and Keller 1 ($10 \text{ feet}/\Delta t$). The rise in the Keller 2 piezometer is estimated to begin at 0.442 seconds. Again a line was drawn through the rising part of the signal. However, the baseline for the signal is higher than the zero normalized pressure line. This is caused by the higher signal noise and the remnants of the P-waves that occur ahead of the confined pressure wave at the Keller 2 piezometer. The baseline for the signal is taken as having a normalized pressure of 0.18. The velocity drops to 68 ft/second between the signal well and Keller 2 twenty feet from the signal well. Another example at Camp Hedding is the data collected on June 21,

2000 when the Keller 1 was placed in the PVC well. The velocity of the confined pressure wave was measured to be 20 feet/second between the signal well and the PVC well. The decrease in the velocity of the confined pressure wave with distance is seen at both Camp Hedding and at Treasure Island. Placing these distances and velocities of the confined wave on log-log plot (Figure IV.7) shows nearly a straight line for the velocity vs. distance.

Although conditions at Treasure Island were less favorable for accurate velocity measurements, approximated values of velocity decreases with distance were obtained as shown in Figure IV.8. The impact wave received by Keller 3 was used to approximate the start of the signal in the signal well (Figure IV.8). The impact wave arrived at about 2.300 seconds. The arrival time of the confined pressure wave is estimated to be 2.313 seconds. The velocity of the confined pressure wave over the 6.4 feet between the signal well and the Keller 3 piezometer is estimated as 493 feet/second. The estimate arrivals times (Figure IV.9) for D-18 is 2.355 seconds and for D-33 "far" is estimated as 2.394. Adjusting the arrival times for the effects of filtering the signals the arrival times of D-18 and D-33 "far" decrease to 2.344 seconds and 2.383 seconds respectively. The estimated velocity from the signal well to D-18 is 250 feet/second and to D-33 "far" is 222 feet/second for the confined pressure wave. This is the second line shown on Figure IV.7.

The slope or decrease in the velocity with distance is distinct at each site. The velocity of the confined pressure wave decreases much more rapidly at Camp Hedding than at

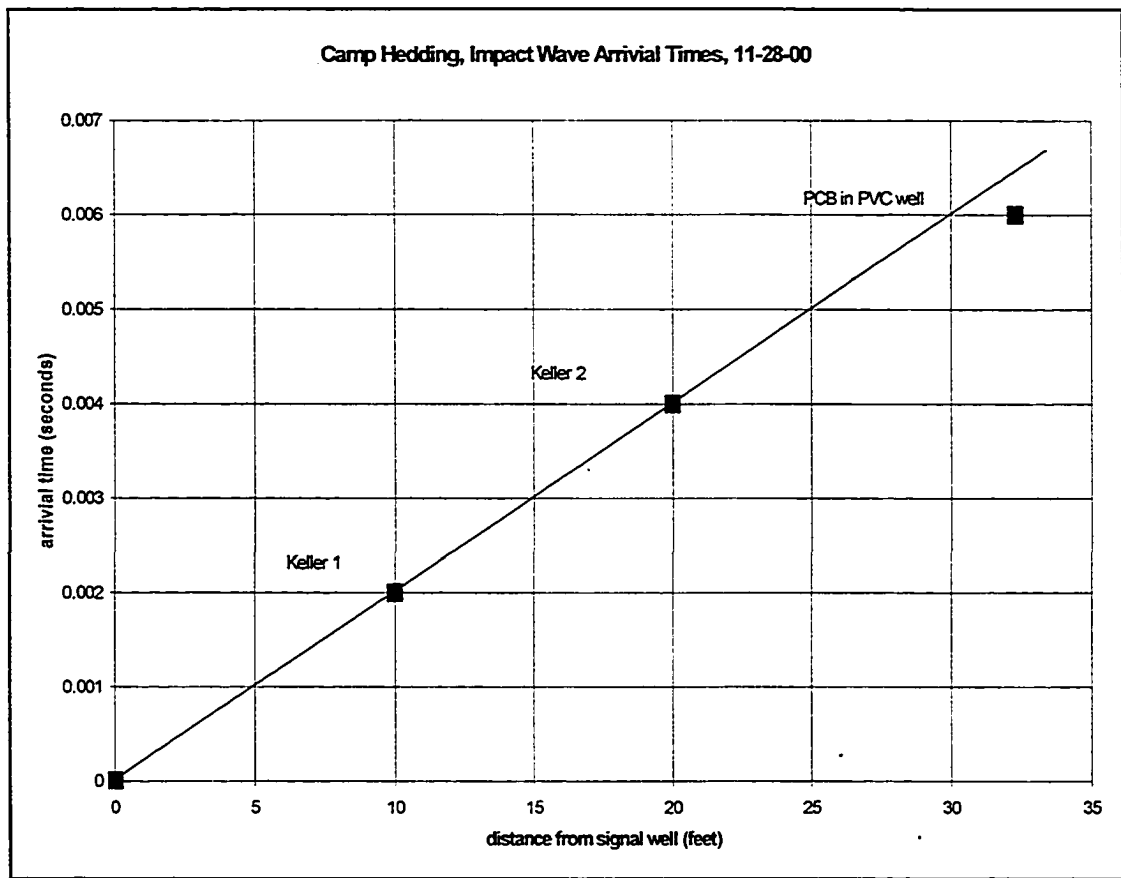


Figure IV.6- Camp Hedding impact wave arrival times at the various piezometers with distance from the signal well (Data 6).

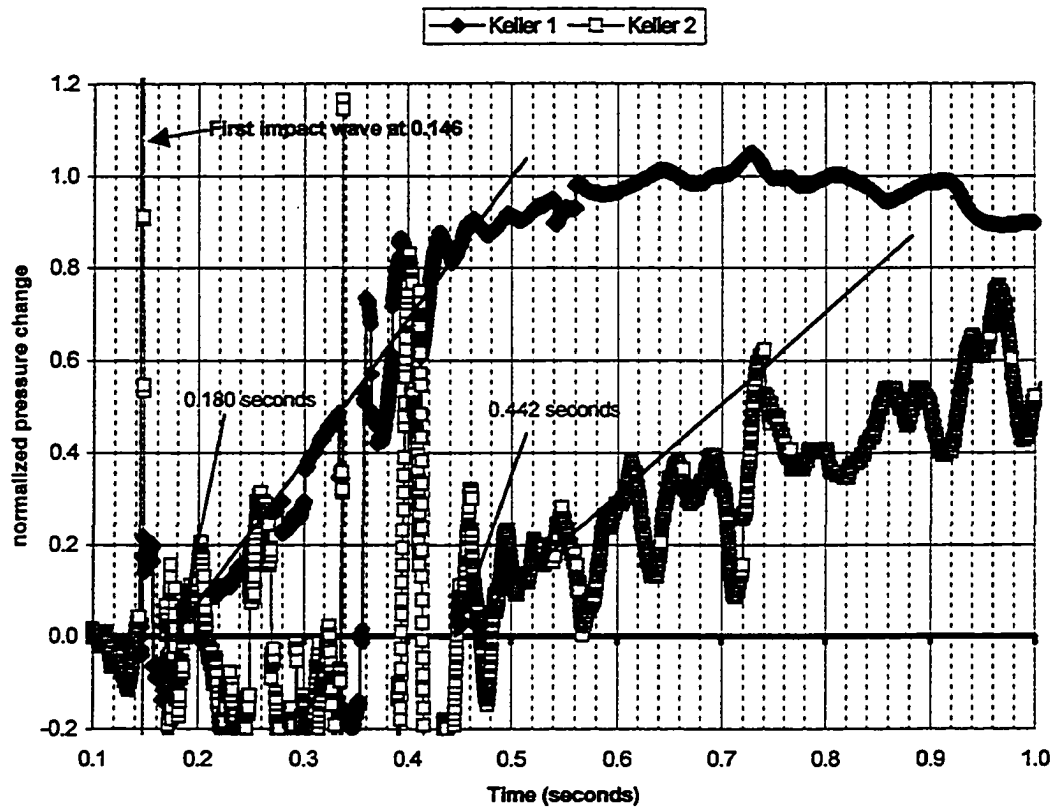


Figure IV.7-Camp Hedding, Data 4, 12-6-00: Arrival times for the confined pressure wave at Keller 1, 10 feet from the signal well, and Keller 2, 20 feet from the signal well. The signals have been internally normalized. The same amount of filtering has been done to each signal. Note that the “zero” for the Keller 2 data is estimated at 0.18. Remnants of the P-waves interfere with the identification of the initial rise of the confined pressure wave.

Treasure Island. A possible alternative way to evaluate the results is to place the five points, Keller 3, Keller 1, D-18, Keller 2, and the PVC well, on a separate single line. This would make the data for D-33 “far” at Treasure Island (165 ft/sec) an outlier. With what is known now it is not possible to resolve which best fits the available data. Based on the differences in geology (man-made vs naturally deposited sediments) it is believed likely that the attenuation of the velocity of the two sites should be different. What is not clear is why Treasure Island with its lower relative densities (based on blow counts) should have less attenuation of the velocity than the sediments at Camp Hedding. It may simply be the higher silt content at Treasure Island conducts this confined pressure wave at higher velocities than do the cleaner sands at Camp Hedding.

IV.8-Normalized data: Normalizing the data allowed comparing the shape and duration of each signal to determine if each is responding to the same event. Data was internally normalized by dividing all the data in the signal by its peak value. By this means, the highest pressure change was always 1 and all other data points were some fraction of the largest value. As the signal becomes smaller, the noise to response ratio increases, resulting in distortions to the shape of the signal as it is normalized. On small signals the noise to signal ratio becomes excessive. As will be seen in the figures below, average values are used in the peak area to establish the ratios. This means that some of the noise in the signal will be larger than 1.

Figure IV.10 is the normalized and filtered data for Keller 1 (10 feet horizontally from source) and Keller 2 (20 feet horizontally) at Camp Hedding on 12-6-00. Both data sets

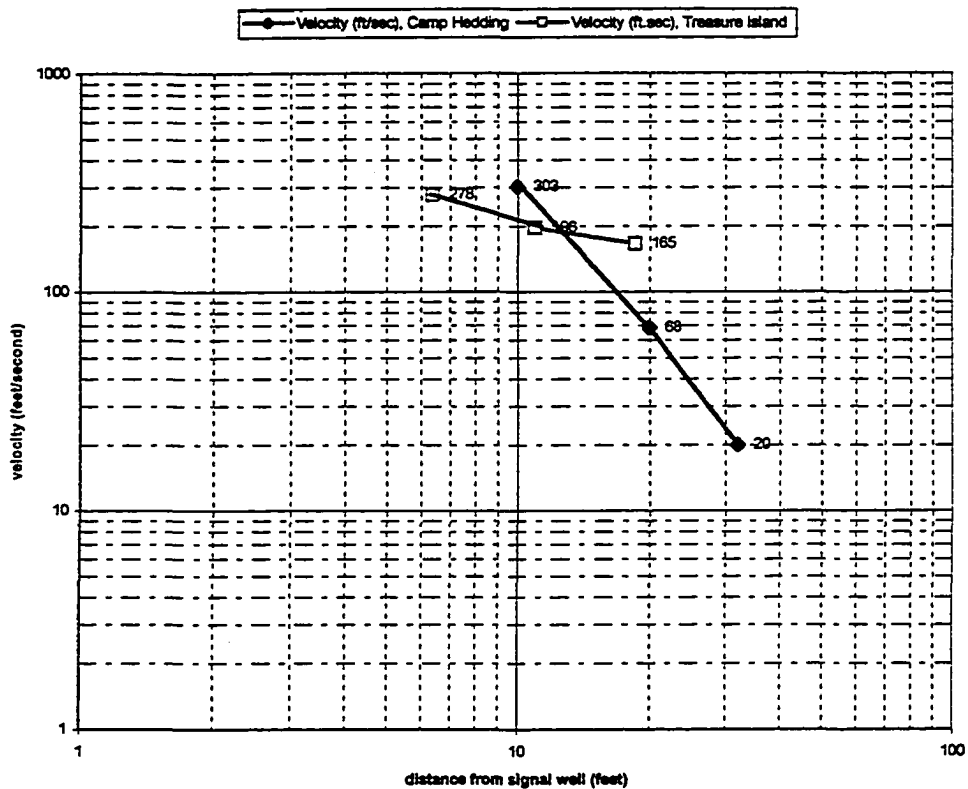


Figure IV.8-Change in velocity (ft/sec) of the confined pressure wave with distance from the signal well at Treasure Island and Camp Hedding. Data 14, 8-11-00 was used for calculating the velocities at Treasure Island. Data 4, 12/6/00 was used for calculating the velocities at Camp Hedding.

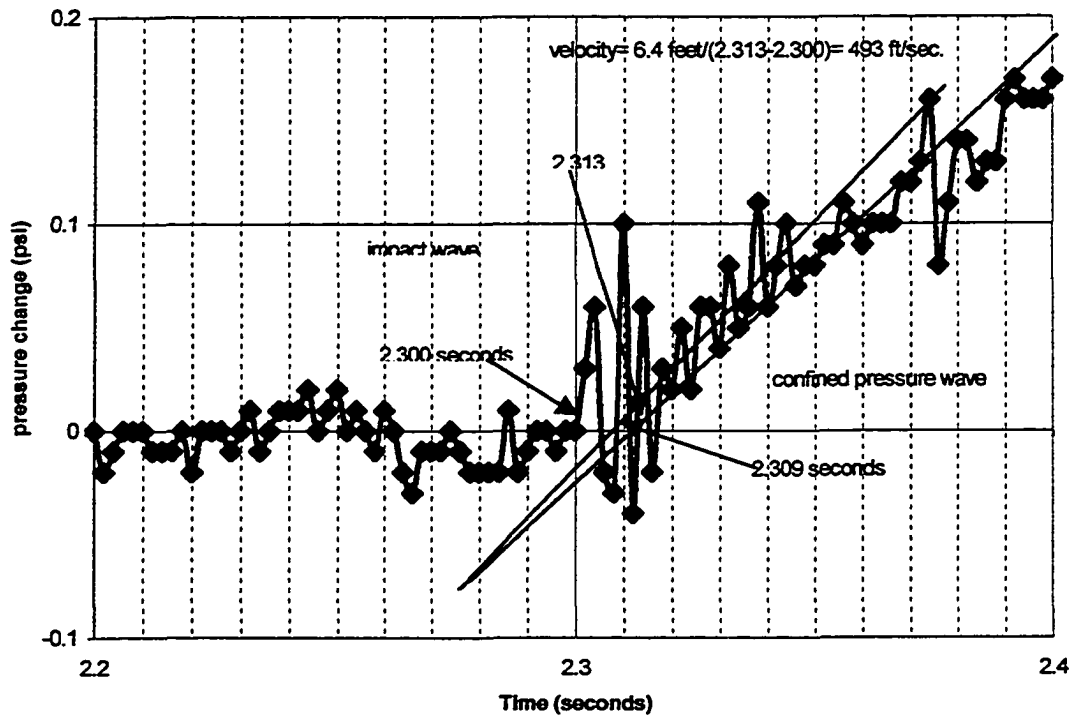


Figure IV.9- Treasure Island. Unfiltered Keller 3 data is from Data 14 on 8-11-00 use for determining the velocity of the confined pressure wave from the impact wave and the arrival time of the confined pressure wave at the Keller 3 piezometer.

Velocity determination for confined pressure wave, Data 14, Treasure Island, 8-11-00

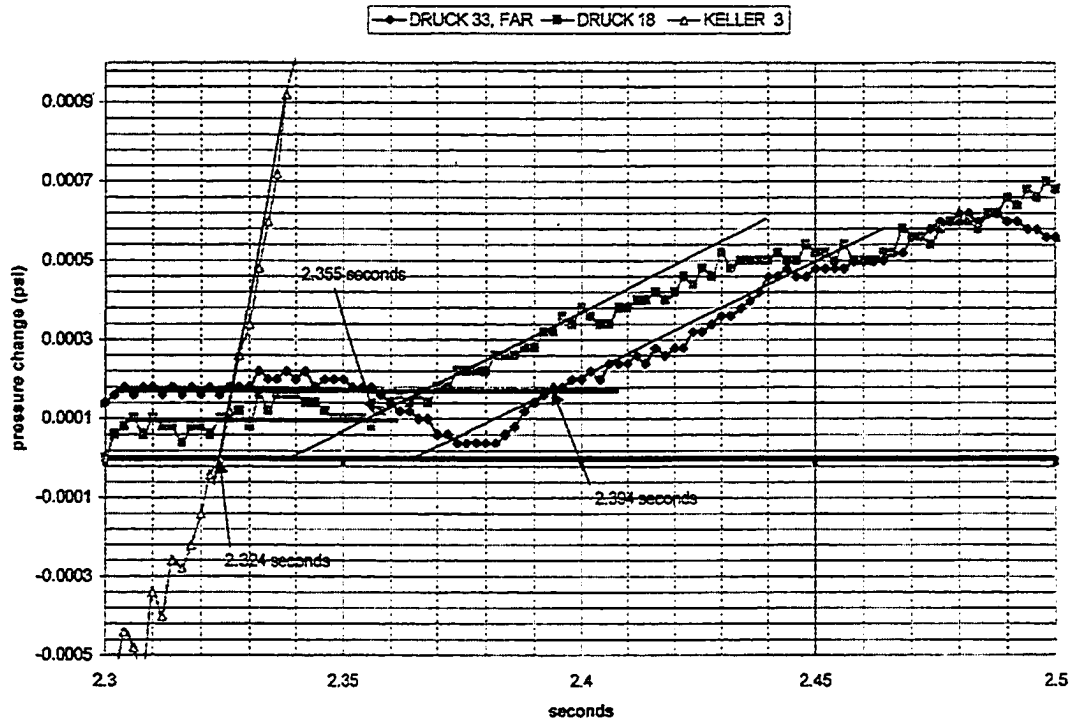


Figure IV.10-Treasure Island. Filtered data for Keller 3, D-18, and D-33 "far" from Data 14 on 8-11-00 used to calculate the velocity of the confined pressure wave from the signal well to the piezometers.

have the same amount of filtering. Both signals show some remnant of impact waves at 0.15 second and 0.33 seconds. The filtering process tends to diminish the extreme cycling of the impact wave and smooth the data. Keller 2 has a much higher noise to signal ratio than does Keller 1. The Keller 1 has a faster rise and a faster decay than the Keller 2 for the confined pressure wave. Distance from the source decreases the rate of rise of the signal and broadens the signal out and decreases the rate of decay of the signal.

Figure IV.11 is the filtered and internally normalized data for Data 14, 8-11-00 at Treasure Island. The entire data file for the first 60 seconds is shown and includes both the confined pressure waves for the Keller 3, D-18, and D-33 “far” (starting at 2.3 seconds) and the unconfined pressure wave for all the signals. Keller 3, D-18, and D-33 “far” have similar shaped confined pressure waves with rapid rise and with rapid decay. D-18 and D-33 ‘far’ also show the slower rise and then decay of the unconfined pressure wave. The nick point in the Keller 3 decay curve at 3.5 seconds probably is the arrival of the unconfined pressure wave. D-17 shows only the unconfined pressure wave. Since no other part of the signal is higher the highest change in pressure of the unconfined wave at D-17 has a value of 1 (at about 13.9 seconds) when internally normalized. All piezometers showed long decay curves taking several minutes for the pressures to return to background.

Figure IV.12 is the filtered and internally normalized data for Data 3, 3-14-01, at Treasure Island. The D-17 data has been adjusted to account for a drift in the baseline. It

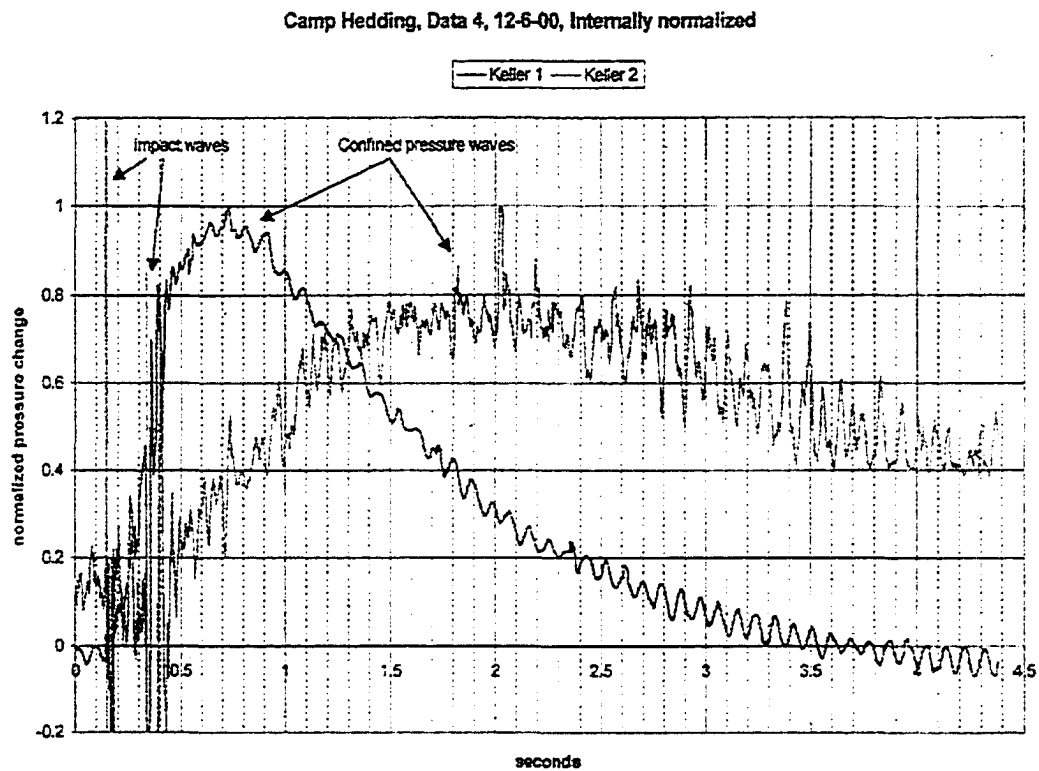


Figure IV.11-Camp Hedding. Internally normalized confined pressure curves for Keller 1 and Keller 2. The shape of the confined pressure wave becomes wider with slower rise and longer decay with distance from the signal well.

Internally normalized data, 8-11-00, Treasure Island, Data 14

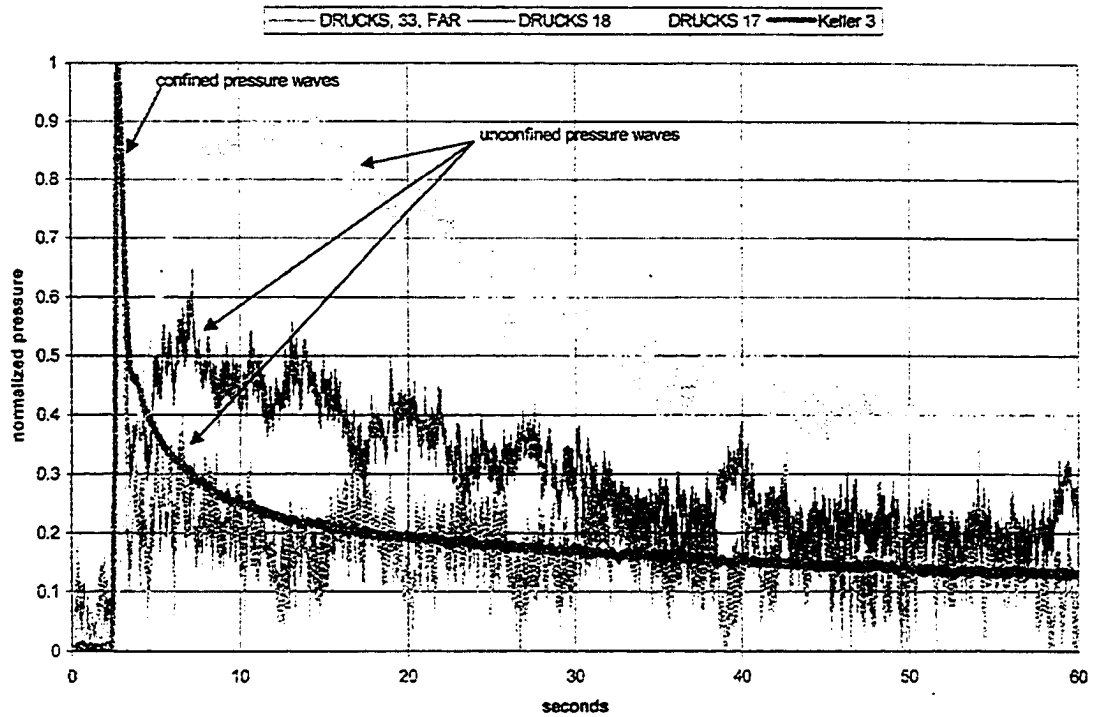


Figure IV.12-Treasure Island. Internally normalized data for Data 14, Treasure Island, 8-11-00. The Keller 3, D-18 and D-33 "far" detected the confined pressure wave and the unconfined pressure wave. D-17 detected only the unconfined pressure wave.

should be noted that Keller 3, D-18, and D-17 signals have the same shape for the confined pressure curve. This is a significant change for the D-17 from the August 2000 data, which only shows an unconfined pressure curve (Figure IV.11). The decay curves for D-18 and Keller 3 are similar. The drift in the baseline masks the decay of the confined pressure wave for D-17. D-33 “far” shows the confined pressure wave followed by the unconfined pressure wave that peaks at about 6.7 seconds. The 4-cycle noise discussed in Appendix E is apparent for all the signals but is most amplified for the D-33 “far” because it is the higher noise to signal ratio for this piezometer in March 2001.

IV.9-Change in signals received by Keller 3, D-18, D-17, D-33 ‘far’ at Treasure Island and Keller 2 at Camp Hedding over time: Figure IV.5 shows that the Keller 3’s response to the generated signal remained nearly identical in shape between the August 2000 and March 2001 testing at Treasure Island provided the same signal generation procedures are followed.

Druck 18 data from August 11, 2000 and March 14, 2001 are compared in Figure IV.15. The signals are very similar. Both have the initial sharp peak of the confined pressure wave followed by the unconfined pressure wave. The unconfined wave for the March data is more subdued than the August signal. It also peaks much later than the August data.

Druck 33 "far" signals are very different between the August and March. The August data shows both the confined pressure peak and the unconfined pressure peak. The March data does not show either. During the March 2000 testing at Treasure Island, only the impact wave was detected when logged at 3300 Hz.

At Treasure Island both the Keller 3 and D-18 had very similar results on the two testing dates. The D-33 "far" signal deteriorated between August and March with only the impact wave being detected in March testing. The D-17 piezometer in August 2000 detected only the unconfined wave. The data collected for D-17 in March is suspect because of the sloping baseline of the signal. Even though the signal was corrected for the sloping baseline, it makes no sense for the background water pressure to be changing consistently during the testing. None of the other piezometers record a sloping baseline as seen on D-17. The shape of the data collected in March 2001 suggests some type of failure of the D-17 transducer.

IV.10-Changes in signal due to equipment and testing changes: Numerous tests were performed at Camp Hedding from April to December 2000. Numerous changes were made during this period to the signal generating equipment. The signal received by Keller 2 piezometer at Camp Hedding located 20 feet from the signal well was shown to change if the anvil and/or the hammer drop distance was changed. Figure IV.1 shows plots of the filtered signals over the testing period. There are significant differences between the various dates. All the results shown were logged at 500 Hz and the same degree of filtering was applied to each signal. The 4-11-00 data was generated using the

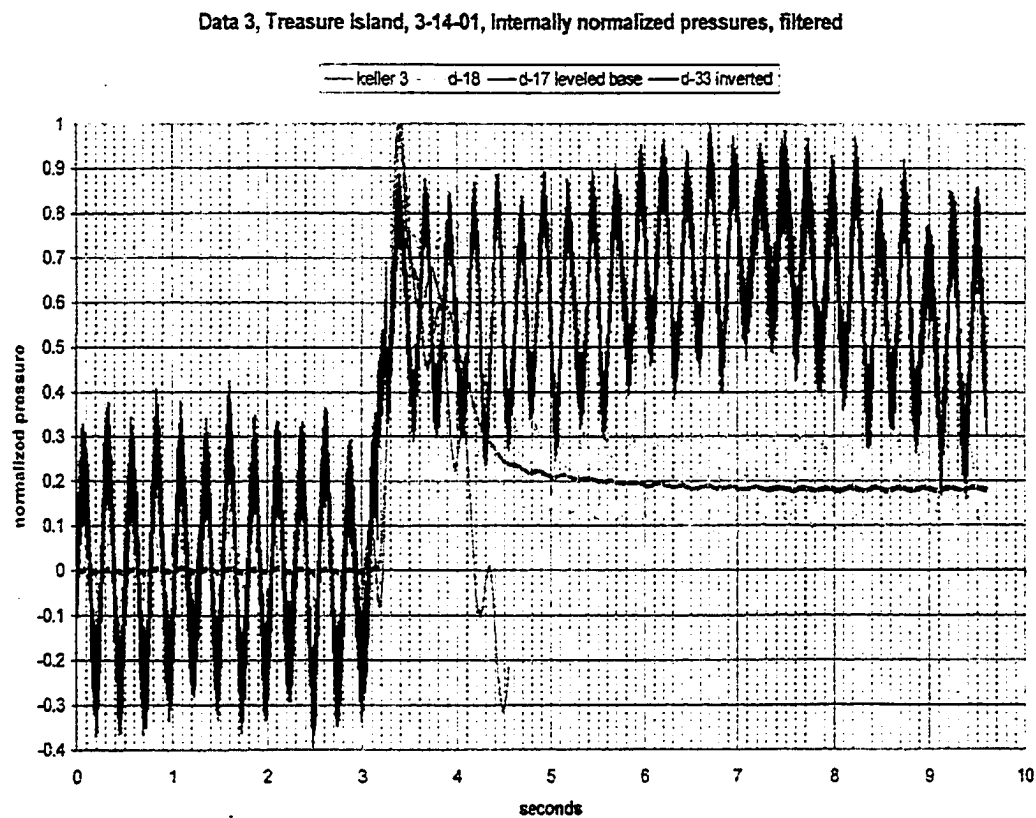


Figure IV.13- Internally normalized data, for Data 3, Treasure Island, 3-14-01. Data is time shifted for comparison of shapes. Note the similarity of the initial rise of each signal at about 3.1 seconds to 3.35 seconds. The 4 Hz noise is accentuated by the normalization of the data for D-33 "far" (called inverted here) and D-18. .

original signal-generating setup. Modifications made between April 11 and November 13 actually resulted in lower signals. This is primarily due to decreasing the drop height of the hammer and/or decreasing the anvil drop height during this period. The three highest peaks occurred on November 15 with a 6-foot hammer drop and a 36-inch anvil drop.

Figure IV.14 is the internally normalized data for some of the Keller 2 tests at Camp Hedding. The starting points were adjusted to about the same initial starting point. All the signals show the same rapid rise in pressure at the beginning. The rise is consistently in the range of 0.035 to 0.08 psi/second. The broadness of the top of the signal changes between the various period of testing. Taking the width of the signal at 75% of the maximum value indicates the sharpest peak occurred in the April data, with much wider peaks in July and November. The November 15 data has the longest decay of all the tests. The combination of increased hammer drop and anvil drop significantly increases the energy put into the ground water resulting in larger pressure rise over a longer duration. If, as shown in Figure IV.5, the same anvil drop is applied there is virtually no difference in the signals received by the piezometers.

IV.11-Conclusion: The testing at Camp Hedding demonstrated that by increasing the drop height of the hammer and the anvil increases the height of the impact wave. The data also shows that increasing the length of the anvil drop (after being hit by the hammer) increases the height of the confined pressure wave. This is shown particularly

well for the Keller 2 data shown in Figure IV.3. The Keller 3 data from Treasure Island, Figure IV.5, shows that nearly identical confined pressure signals were generated even though the March data was generated with a 2 foot higher hammer drop but with the same anvil drop of 18 inches on both dates.

The repeat performance of the Keller piezometers at both sites when drop conditions are the same demonstrates that the signal generating system produces a repeatable signal without damage to the aquifer. The data at Treasure Island demonstrates that D-33 "far" and D-17 changed significantly between August 2000 and March 2001. No similar change is evident at D-18 or Keller 3. Whatever occurred to D-33 "far" and D-17 piezometers to change the signals between the two testing dates either occurred to the piezometer screens or the electronics of the transducers. The inability to access the Druck piezometers prevents testing to determine where the problems lie in these piezometers.

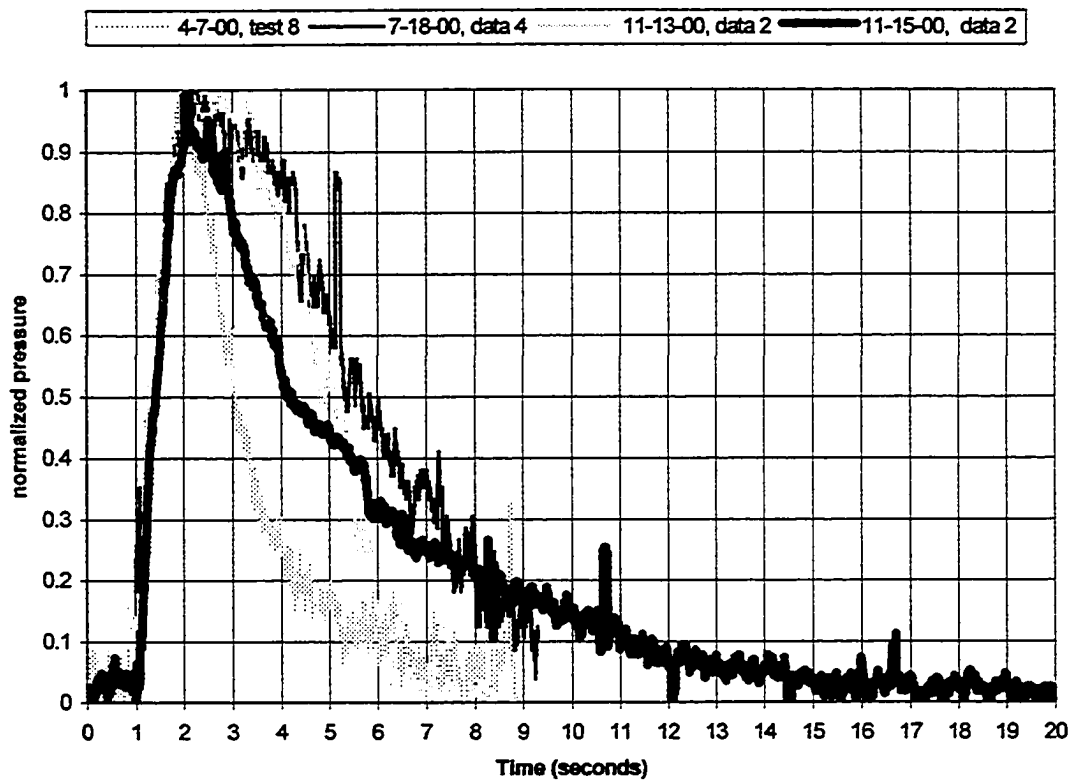


Figure IV.14—Internally normalized data for Keller 2 at Camp Hedding. The signals have been normalized to compare. As the hammer and anvil drop increase the signal becomes broader.

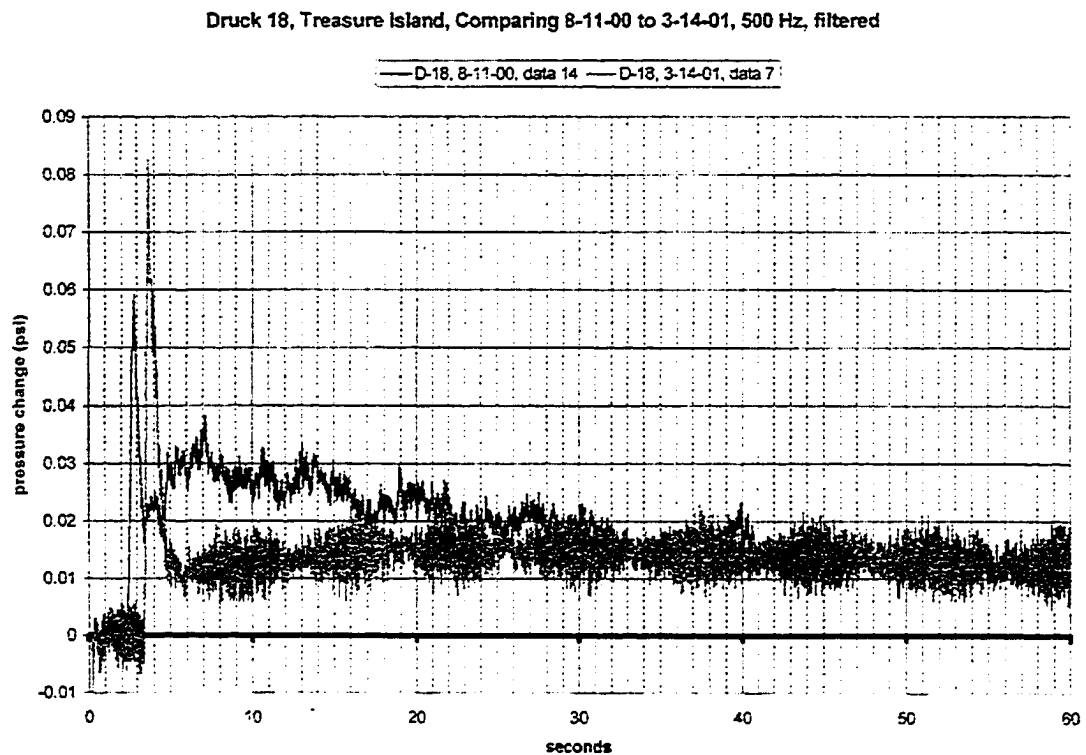


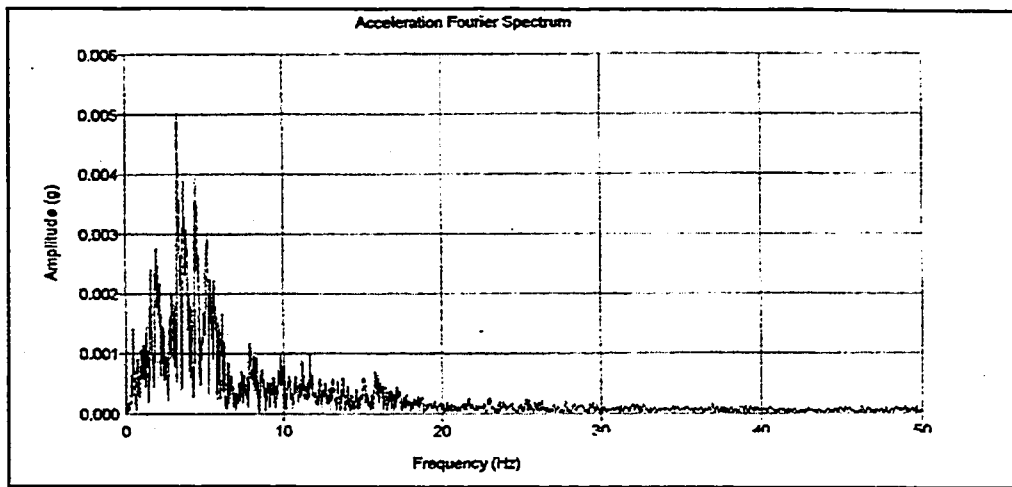
Figure IV.15-Treasure Island. Comparing Druck 18 data for 8-11-00 and 3-14-01. The peaks have been offset slightly for clarity.

CHAPTER V

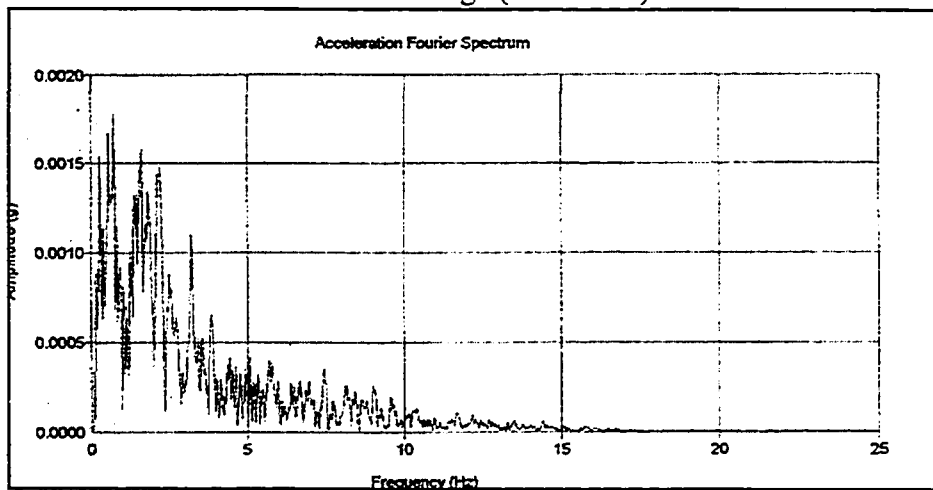
FREQUENCY ANALYSIS

V.1-Introduction: Frequency (FFT) response curves for Kern County (7/21/1952), Loma Prieta (10/17/ 1989), and Northridge (10/17/1994) earthquakes are shown in Figure V.1. Major frequencies range from less than 5 Hz to about 10 Hz. In order to measure pore pressure changes that may occur during earthquake-induced liquefaction, transducers have to be capable of detecting not only the rapid rise times of the pressure change (discussed in earlier sections) but the frequencies typical of earthquakes. In order to test the ability of a transducer to detect an earthquake-generated signal, the signal generating equipment has to be capable of producing signals that cover the range for frequencies expected from an earthquake. The following sections will show the frequency ranges of the signals detected during selected tests by the piezometers previously discussed. The results are summarized in Table V.1 at the end of the chapter. The intent of this chapter is to demonstrate that the hammer/anvil/surge block signal generation system is capable of generating signals with frequencies that cover the range of expected earthquake frequencies and that the piezometers are capable of detecting the generated frequencies.

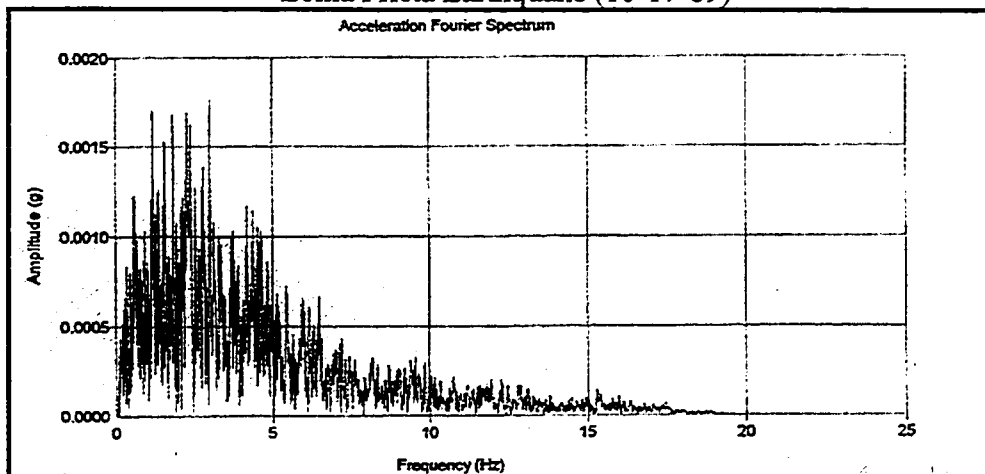
The Nyquist sampling rate [$T=1/(2f_c)$], where f_c is the highest frequency to be sampled in a waveform, requires that sampling rates be at least twice that frequency to prevent aliasing and recover the actual frequency of the signal. For a frequency



Northridge (1-17-1994)



Loma Prieta Earthquake (10-17-89)



Kern County (7-21-1952)

Figure V.1-Fourier transforms of acceleration records for several earthquakes. Largest frequencies are all below 10 Hz.

of 2 Hz the minimum sampling rate should be 4 Hz. A signal of 1000 Hz would require a minimum sampling rate of 2000 Hz to identify the actual frequency of the signal. Sampling rates below the Nyquist sampling rate will result in aliasing. So with the most common sampling rate of 500 Hz frequencies up to 250 Hz can be identified.

As discussed in other sections, the signals received at the transducers have three distinct components. The impact wave is the first component. The second component is the confined pressure wave and the third is the unconfined pressure wave.

To identify the signal under the noise it was necessary to filter the signals. This was done in all but a few cases by taking, for each point, the average of a specified number of the preceding data points. The number of points averaged was taken as one-tenth the signal-sampling rate. As an example, for a sampling rate of 500 Hz the preceding 49 points plus the current point were averaged for a total of 50 points. Every point in the data set was used and preserved by this filtering. The filtering worked well for data that systematically changed over time but for evenly spaced oscillating signals with a net near-zero average change between the highest and lowest values, the filtering would remove the oscillating signal and return only the change in the base curve. This was the case with the impact wave. The filtering process tended to shift the signal slightly forward in time. This was unimportant if the same filtering was applied to all the signals for a given test because they were all

shifted the same amount. If the same filtering was not used on all the signals then corrections had to be made to the signal in order to adjust for the shift in the signal.

V.2-Pressure Vessel Testing: As was discussed in Chapter II, a servo valve was one of the methods used to input alternating hydraulic pressures into the pressure vessel and to achieve frequencies consistent with earthquakes. Figure V.2 is a typical signal generated by cycling of the servo valve (p-1 being the same Keller 1 transducer used in the pool testing and later installed at Camp Hedding ten feet from the signal well). The maximum frequencies achieved by this method ranged from 1 to 2 Hz (Figure V.3). The biggest drawback to using the servo valve to input pressure change into the pressure vessel was the relatively slow rise time of the signal (see Figure II.13).

Faster rise times and higher frequencies were achieved using the shot-actuated hammer (see Chapter II) to drive a piston into the water source tank to create a pressure rise in the sample. A typical example of the resulting signal is shown in Figure V.4 for the shot hammer. The FFT, Figure V.5, shows that the Keller 1 transducer in the protective tip measured frequencies of 5 to 6 Hz.

V.3-Pool Testing: As discussed in Chapter III the primary purpose of the pool testing was to develop the field methods for the hammer drop and to gain experience into the logging of the signals. Because of the greater travel distance of the impact wave compared to the hydraulic pressure waves in the pool it was possible to

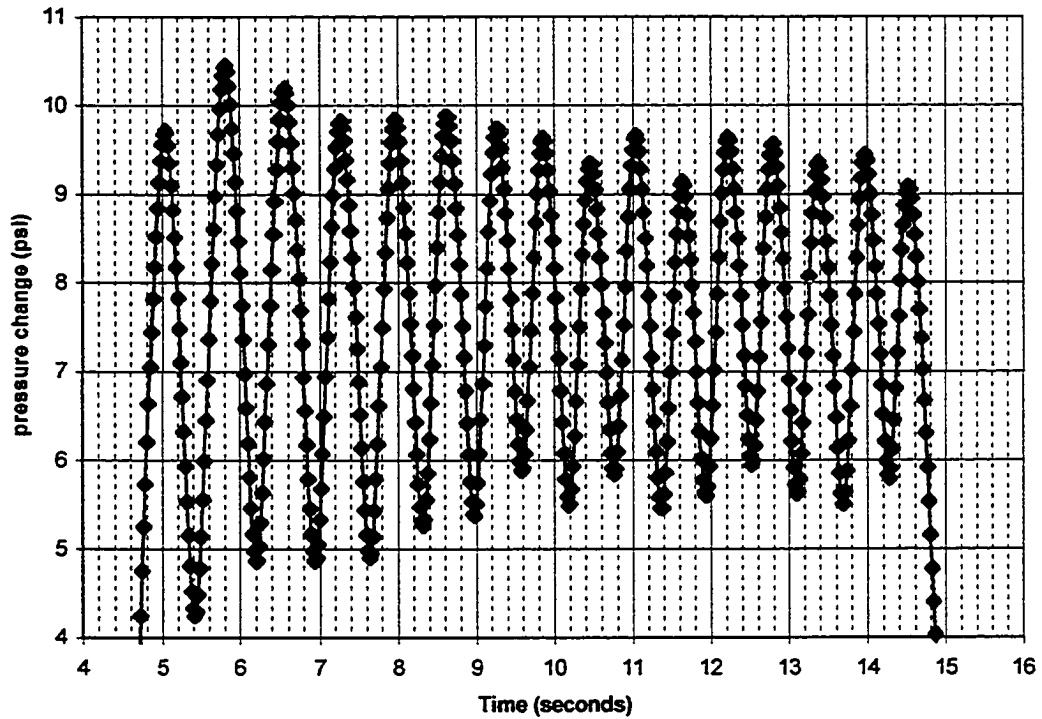


Figure V.2-The signal detected by the Keller 1 transducer buried in sand within the pressure vessel (Data 2, 7-13-99). The servo valve was cycled at its maximum rate between 20 and 30 psi while the confining pressure was maintained at 40 psi. The FFT for this signal is shown in Figure V.3.

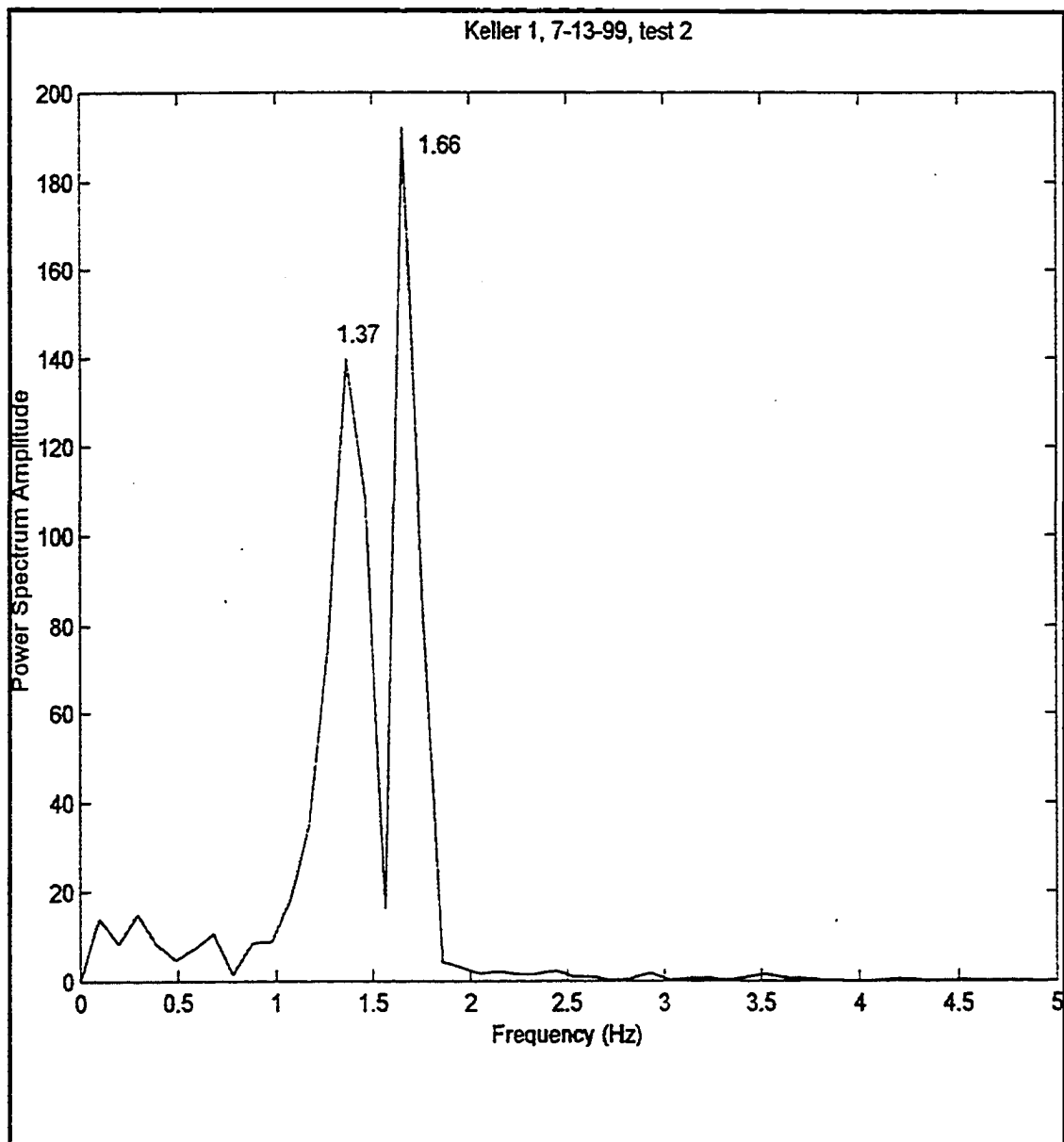


Figure V.3-FFT for Test 2, 7-13-99, shown in Figure V.2, cycling with the servo at the maximum rate.

**Keller 1 pressure change, Actuated Hammer shot,
Data 3, 7-30-99**

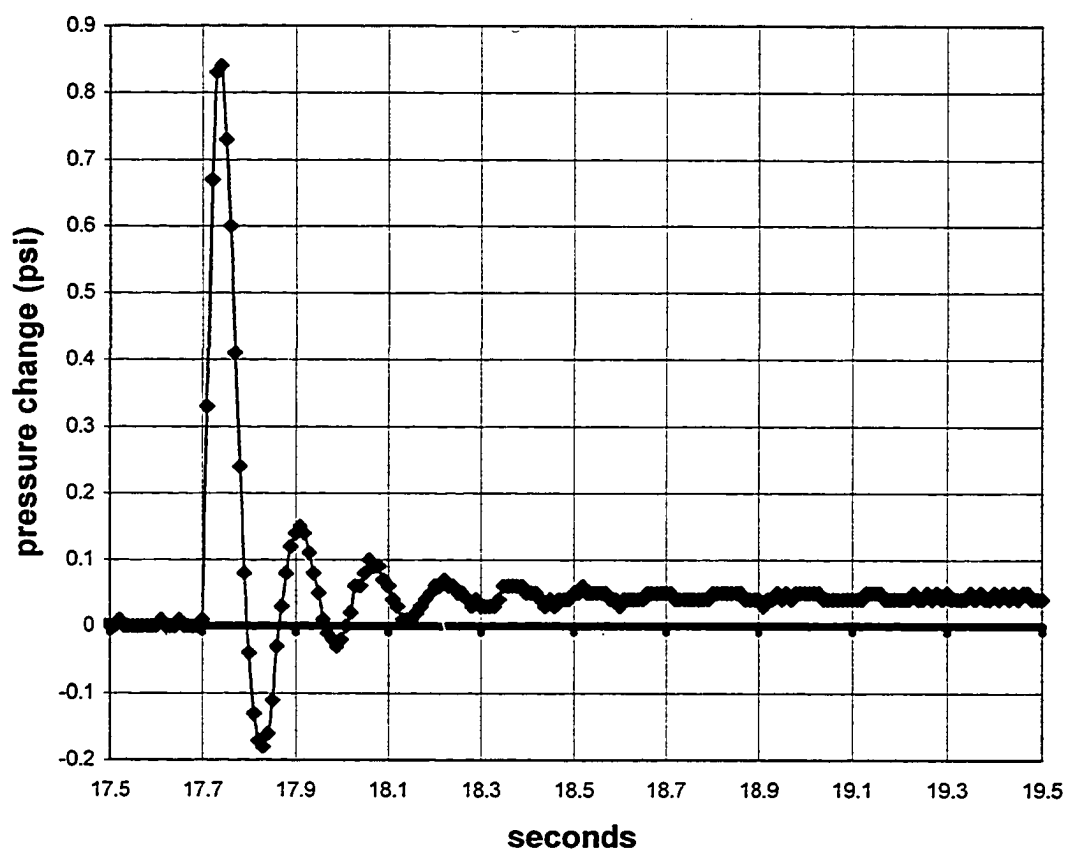


Figure V.4: Keller 1 in the sand filled pressure vessel. A shot actuated hammer created the pressure change. The confining pressure was 40 psi and the backpressure was 20 psi. The FFT for this signal is shown in Figure V.5.

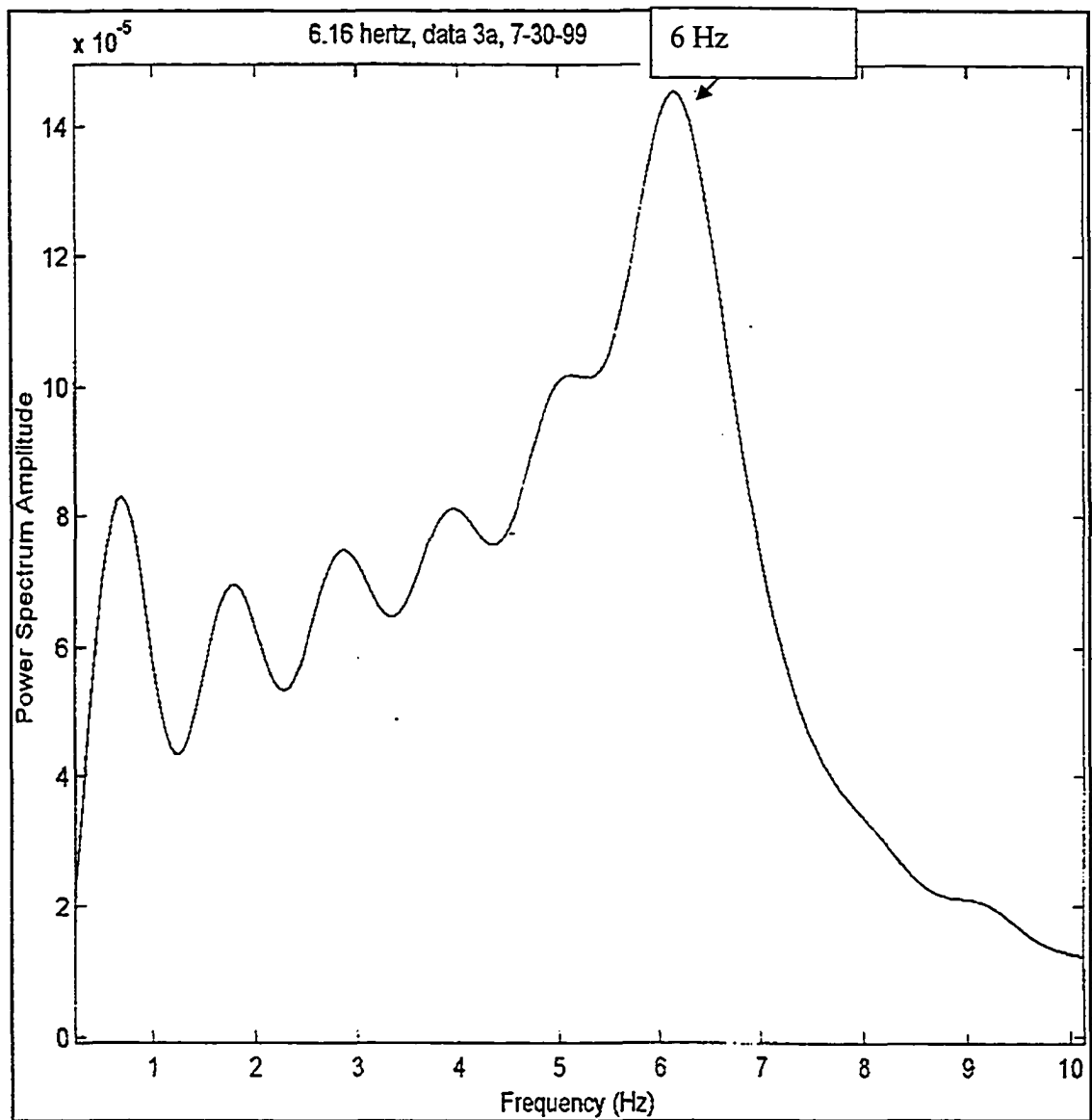


Figure V.5-FFT of shot-hammer signal shown in Figure V.4.

separate the impact waves from the confined pressure waves. The large storage of the pool relative to the discharge from the well screen limited the range for detecting the confined pressure waves to less than 19 inches from the signal well. Figure V.6 is the trace of the impact waves detected by Keller 1 transducer inside the protective tip located 19 inches from the well screen when logging at 5000 Hz. This signal was discussed in detail in Chapter III. The FFT, Figure V.7, of the first two sets of impact waves show a predominant frequency in the range of 900 Hz to 1000 Hz.

The confined pressure wave was measured in the pool when the Keller 1 transducer was placed closer to the well casing. Figure V.8 is the Keller 1 transducer record when the transducer was 16" from the well casing. Figure V.9 is the FFT of that signal. Predominant frequencies are 9.7 and 29 Hz. The 9.7 Hz is the frequency of the confined pressure wave and the 29 Hz is probably an alias frequency for the impact wave.

V.4-Camp Hedding: The Keller 1 transducer, when placed in the PVC well at Camp Hedding during the July/June 2000 testing, detected the impact wave without overlap with the confined pressure wave. Figure V.10 is the Keller 1 signal measured in the PVC well 32 feet from the signal well. Because the logging rate was only 500 Hz, aliasing has occurred. The frequency of 54.69 Hz, shown on the FFT

Keller 1, pressure change

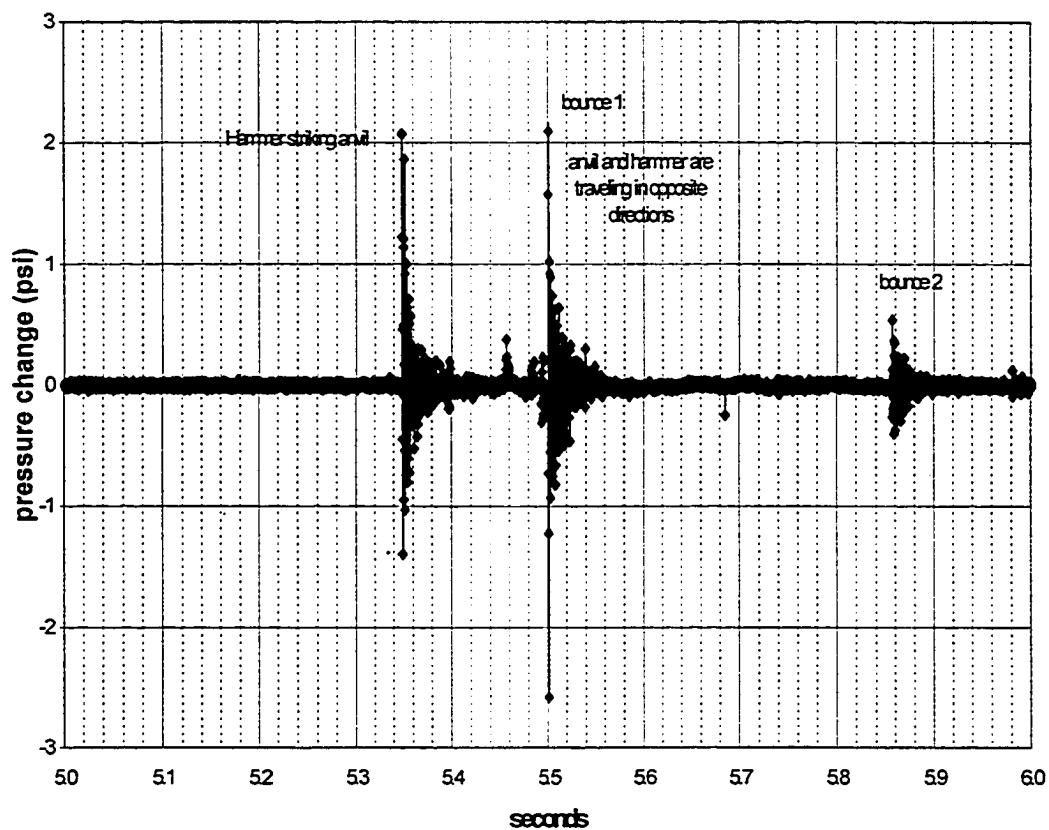


Figure V.6: Keller 1 record at 19 inches from the signal well. Three impact waves are created by the impact of the hammer on the anvil. The signal was logged at 5000 cps.

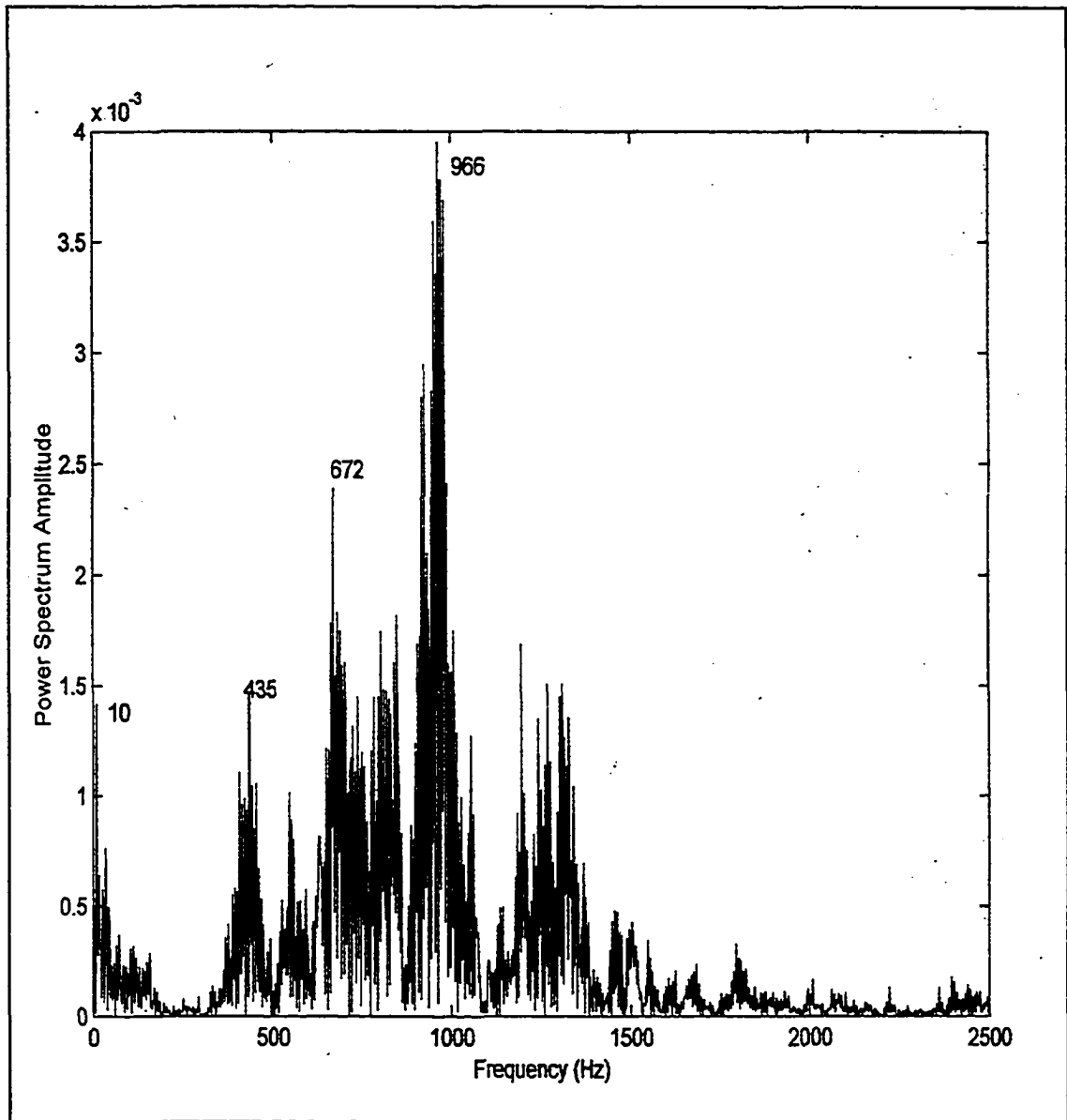


Figure V.7-FFT for the impact wave shown in Figure V.6. The Keller 1 transducer is in the protective tip 19 inches from the signal well.

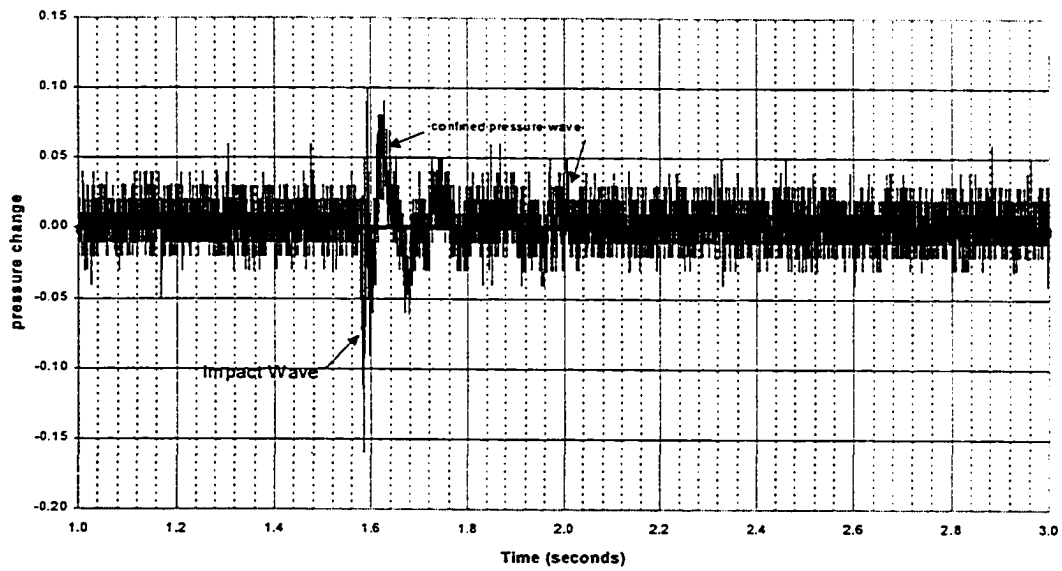


Figure V.8- Pool Testing. Test 4, 3-2-00. Keller 1 was located 16 inches from the signal well screen in the pool. The impact wave and the confined pressure wave are both detected if the transducer is close enough to the signal well.

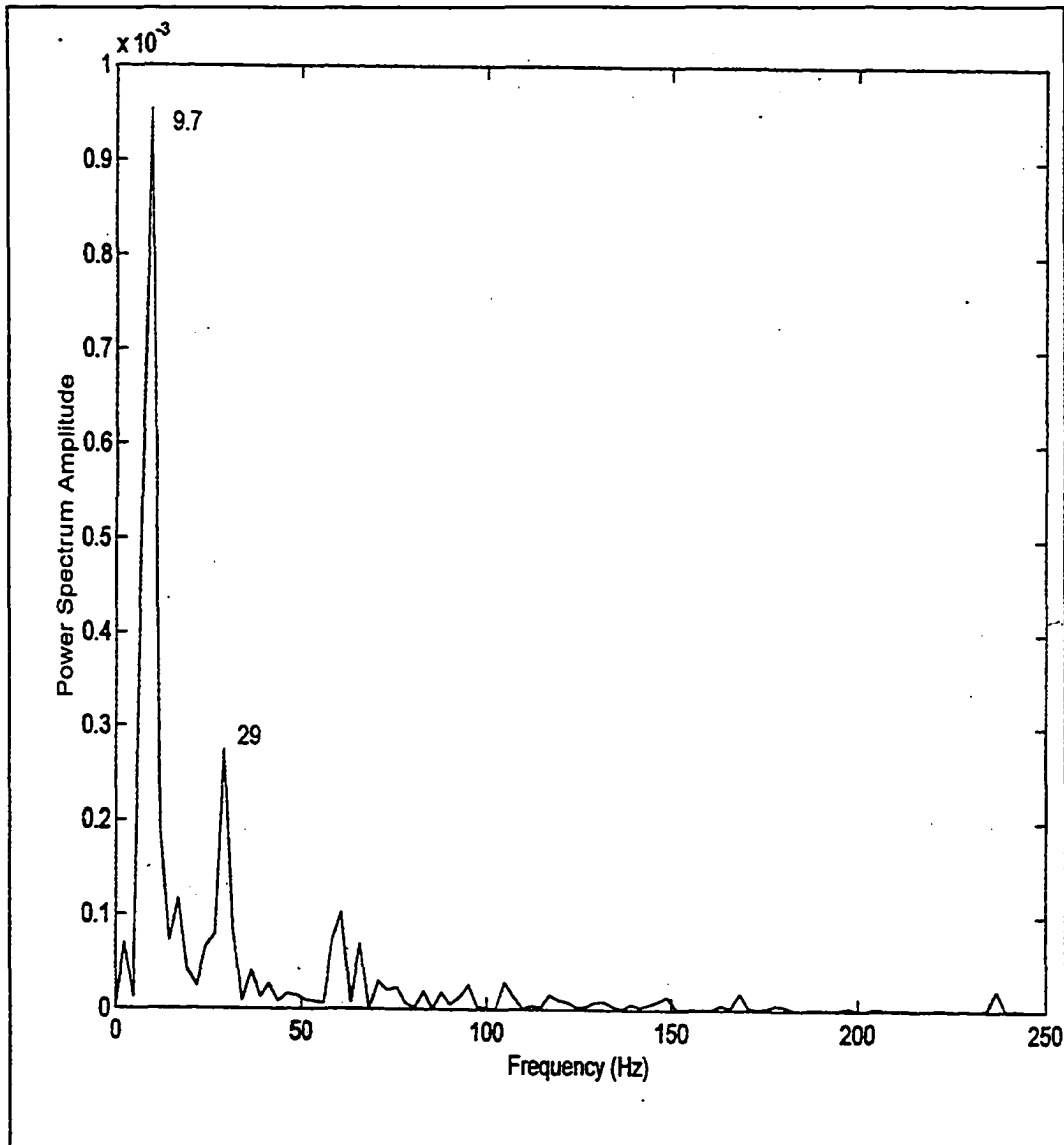


Figure V.9-The FFT for combined signal of impact wave and confined pressure wave for Test 4, 3-2-00, pool testing shown in Figure V.8.

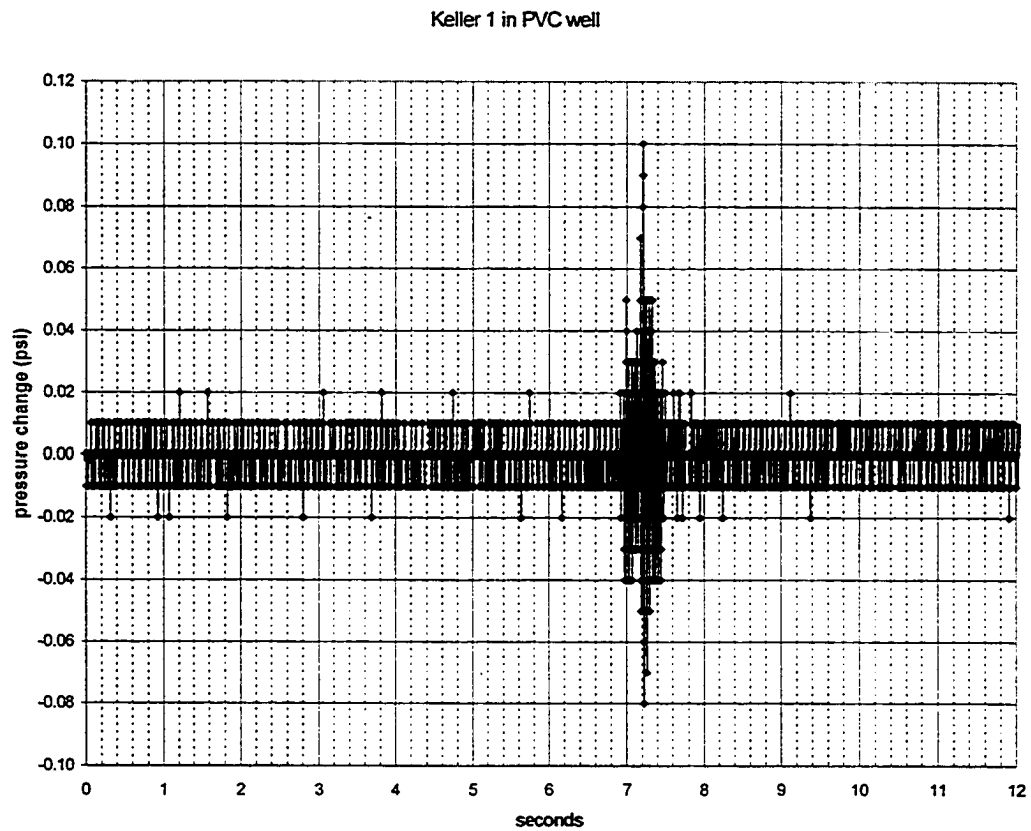


Figure V.10- Impact wave detected by the Keller 1 transducer located in the PVC well 32 feet from the signal well (Data 7, 6-14-00, logged at 500 Hz).

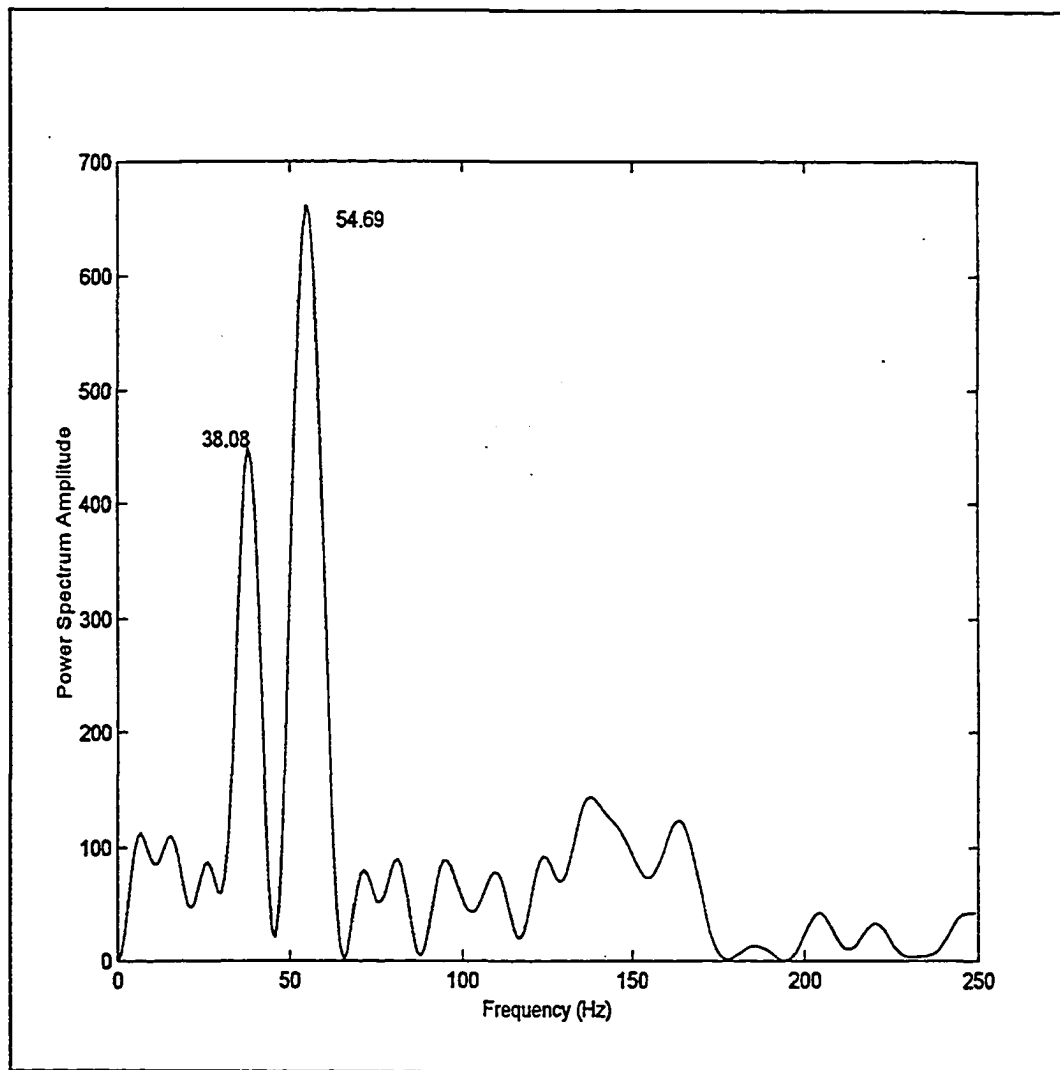


Figure V.11- FFT for impact wave shown in Figure V.10 for the Keller 1 transducer installed in the PVC well 32 feet from the signal well. The logging rate was 500 Hz.

for the signal, Figure V.11, has to be taken as a minimum frequency for the impact wave. The impact wave signal, received by the GEMS transducer while in the PVC well, appeared similar to those received by the Keller 1 in the PVC well. It was assumed, that because of their similarity in shapes, that their FFTs would be similar and because none of the signals were logged at a higher enough rate, all the frequencies would have been lower than the actual frequency as was detected in the pool. The only times the impact wave was logged at a higher rate and the signal was not interfered with by the confined pressure wave was while testing in the pool.

A lower frequency signal in the range of 0.1 to 2 Hz is caused by the confined pressure wave. Figure V.12 is the confined pressure wave measured by the Keller 1 located ten feet from the signal well. The FFT, Figure V.13, indicates a predominant frequency of 0.25 Hz for the signal. The confined pressure wave for the Keller 2 piezometer located 20 feet from the signal well is shown in Figure V.14. The FFT for that signal is shown in Figure V.15. Keller 2 has many major frequencies from 0.24 Hz to 3 Hz.

Even though the FFTs for the Keller 1 and Keller 2 suggest similar frequencies, the confined pressure wave broadens with increased distance from the signal well. To compare the shapes of the Keller 1 and Keller 2 signals both signals were internally normalized. Figure V.16 is the internally normalized confined pressure signals for Keller 1 and Keller 2. The broadening of the Keller 2 signal is clear even while both signal have nearly identical initial rates of rise.

V.5-Treasure Island: The impact wave was observed in the data from Keller 3 (final location 6.4 feet from the signal well), Druck 18, Druck 34 “far”. The Keller 3 when placed in the water table well and in the inclinometer casing detected the impact wave. Because of the relatively low logging rates of 500 Hz used when logging the signals on 8-11-00, no attempt was made to present the FFT for the signal from the water table well or the inclinometer casing.

The Keller 3 (in its final location 6.4 feet from the signal well), Druck 18, and Druck, 34 “far” piezometers detected the low frequency confined pressure wave. Figure V.17, 8-14-01 Data 5, is an example of the filtered data from Keller 3 piezometer located 6.4 feet from the signal well. Two impacts of the hammer/surge block system are evident. There is a long decay tail. The FFT for this test is shown in Figure V.18. Frequencies of 0.5 and 2 Hz are present in the signal. The total time necessary to achieve background pressures exceeded 60 seconds. The results for all the tests from the Keller 3 located 6.4 feet from the signal well appear similar to Figure V.17. This was shown in Figures IV.4 and similar Figures C.4, C.5, and C.6.

V.6-Conclusion: All the Keller transducers in their protective tips, whether used in open water (pressure vessel, pool testing, and open PVC well), in sand (pressure vessel), or installed in the field were capable of detecting signals with frequencies that ranged for under 0.1 Hz to nearly 1000 Hz. The Druck transducers are capable of detecting the same range of frequencies as the Keller if they are working properly.

The impact wave and the confined pressure wave were detected by D-18, D-33 'far' at Treasure Island. Both the impact wave and the confined pressure wave could be detected out to a distance of 32 feet from the signal well at Camp Hedding. Thirty-two feet appears to be close to the maximum limit that the confined pressure wave could be detected with the signal generating system used. The frequency of the confined pressure wave likely decreases with distance. The overlap of the impact wave with the confined pressure wave at Keller 1 and Keller 2 piezometer prevented a similar analysis to be made of the impact wave frequencies with distance from the source.

A summary of the frequency analyses presented in this chapter and in earlier chapters is given in Table V.1 below (pg. 125).

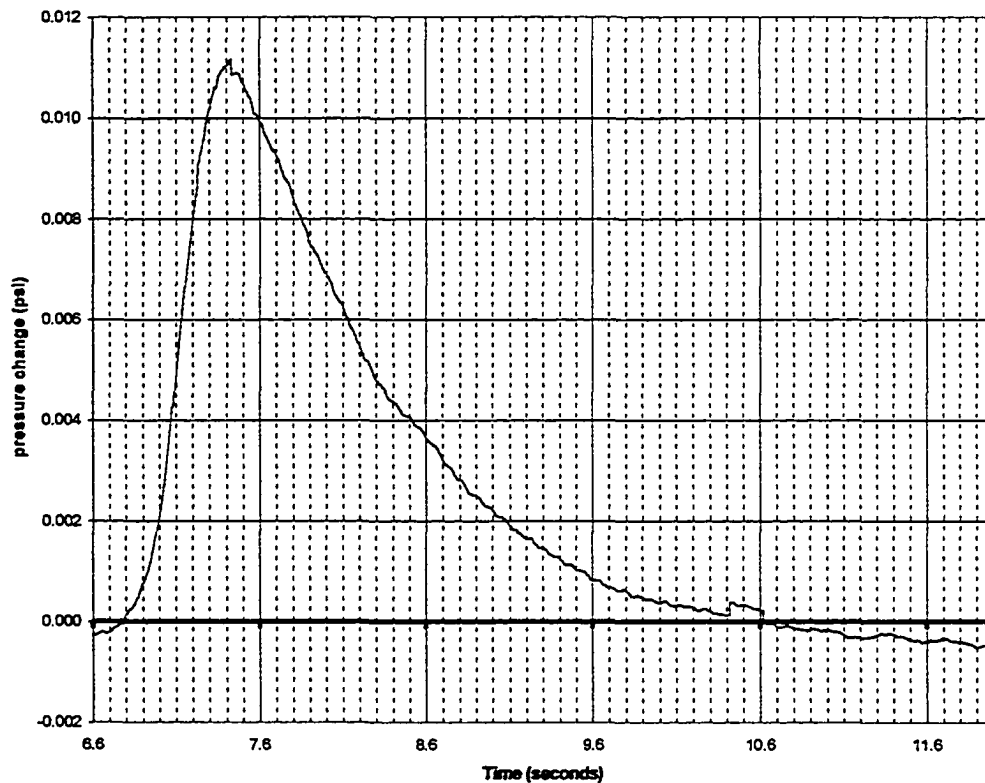


Figure V.12-Filtered confined pressure wave signal from Keller 1 (Data 5, 11-13-00) at Camp Hedding. The piezometer is located 10 feet from signal well. This portion of the signal was used to generate the FFT shown in Figure V.13. The signal was logged at 500 Hz.

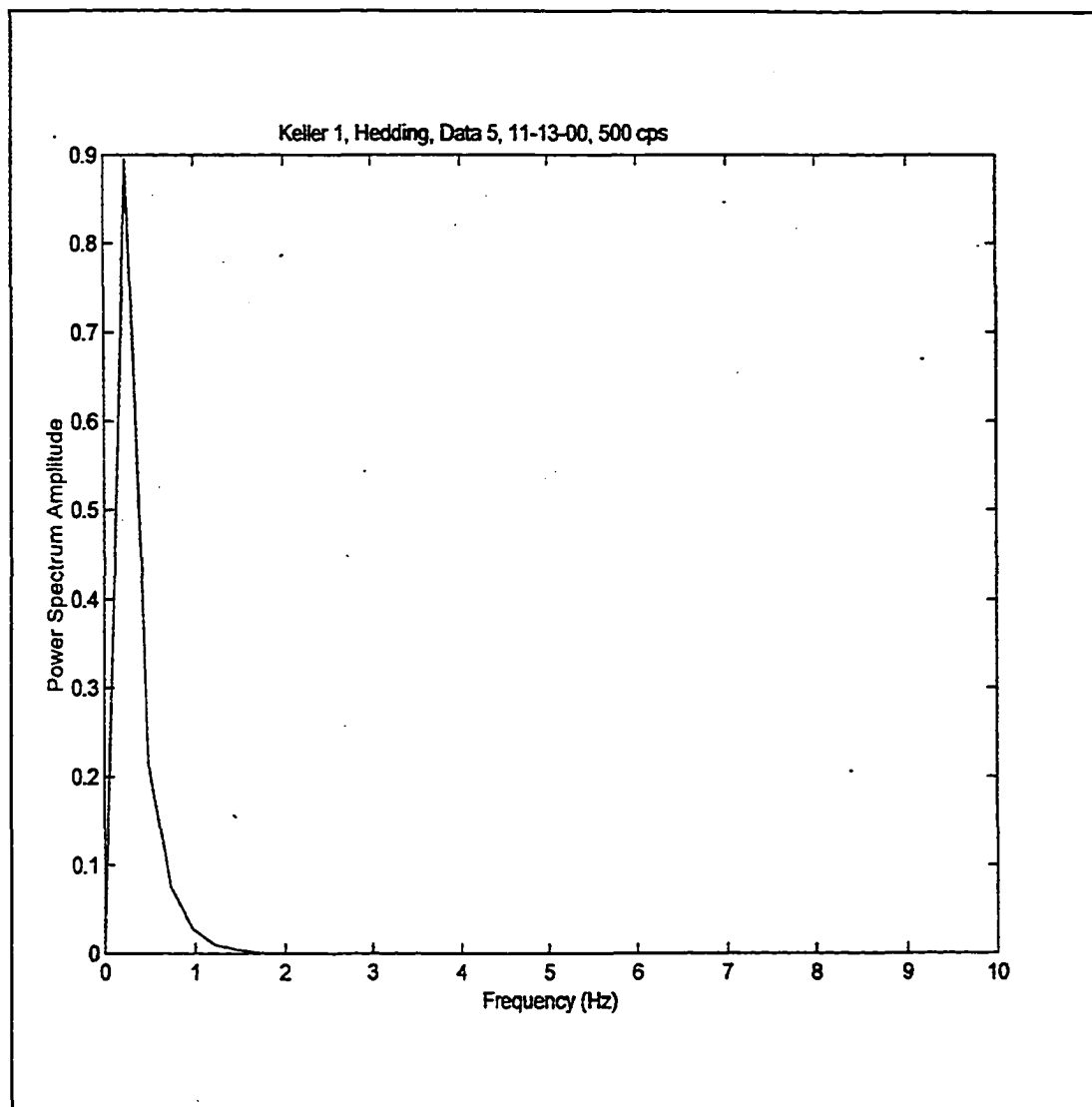


Figure V.13-FFT for the confined pressure wave signal from the Keller 1 piezometer at Camp Hedding. The signal for the FFT is shown in Figure V.12. Keller 1 is located 10 feet from the signal well.

keller 2 , Camp Hedding, Data 1, 6-27-00, filtered

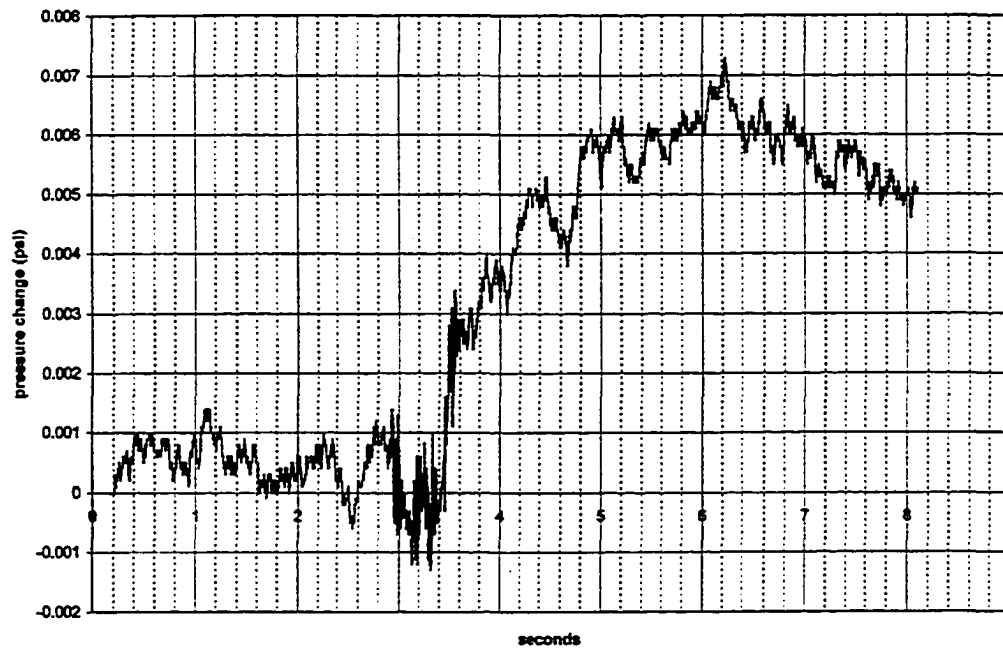


Figure V.14-Confined pressure wave detected by Keller 2. The FFT for the signal is shown in Figure V.15.

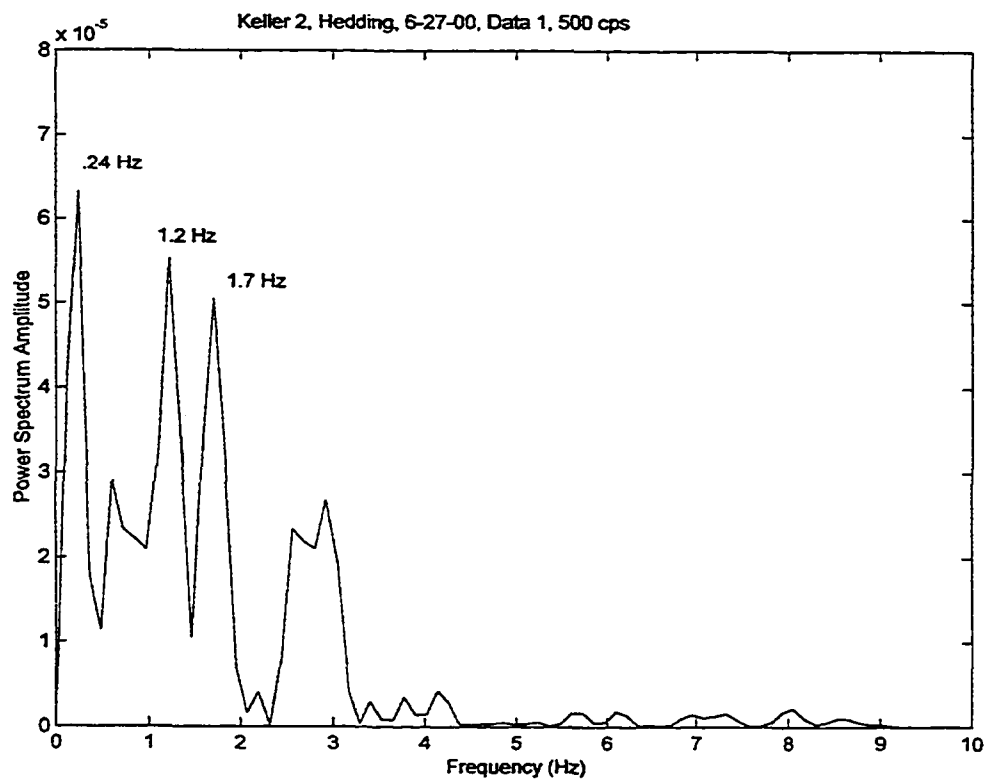


Figure V.15- Confined pressure wave for Keller 2 piezometer and the FFT for the signal.

Keller 1 and Keller 2, 11-13-00, Data 5. Internally normalized

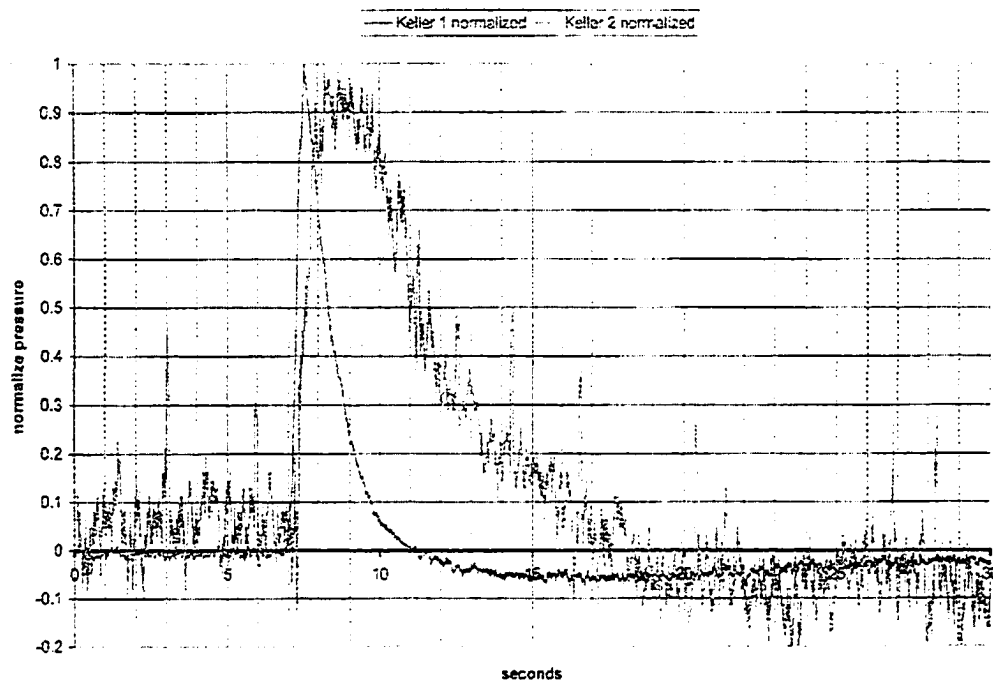


Figure V.16-Internally normalized confined pressure waves for Keller 1 (10 feet) and Keller 2 (20 feet). The confined pressure wave becomes broader with distance from the signal well. The initial rise of each signal is nearly identical. Keller 2 has been moved back slightly in time to allow between comparison of the shapes of the two signals.

Keller 3, Treasure Island, 6.4 feet from signal well, data 5, 3-14-01

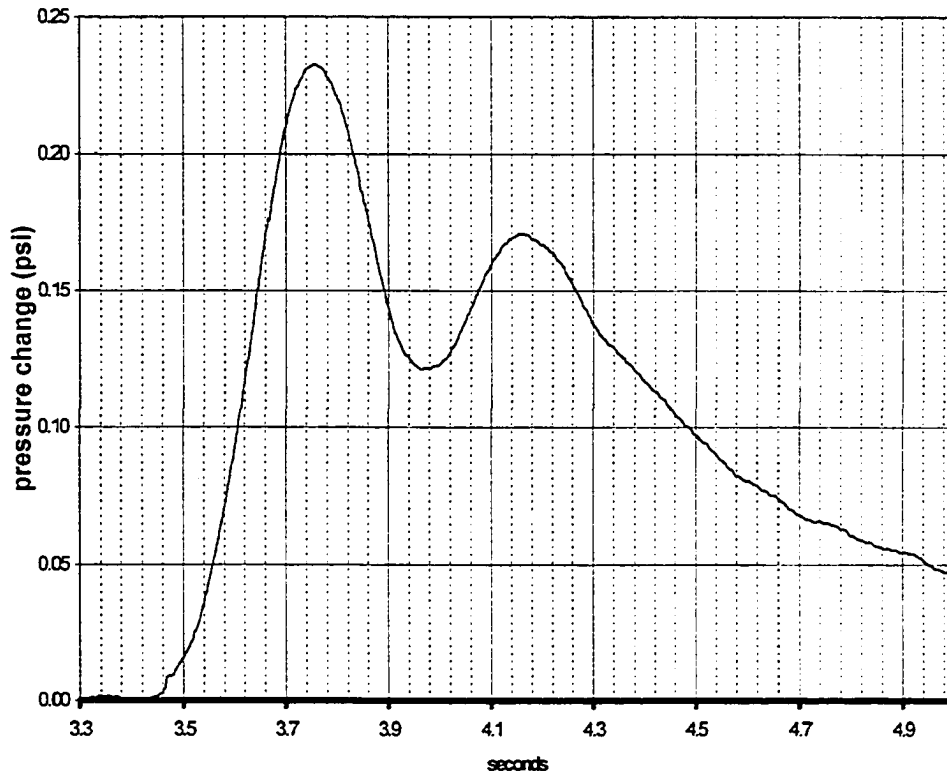


Figure V.17-Confined pressure wave signal from Keller 3 piezometer at Treasure Island located 6.4 feet from the signal well. This is the portion of the data was used for the FFT shown in Figure V.18.

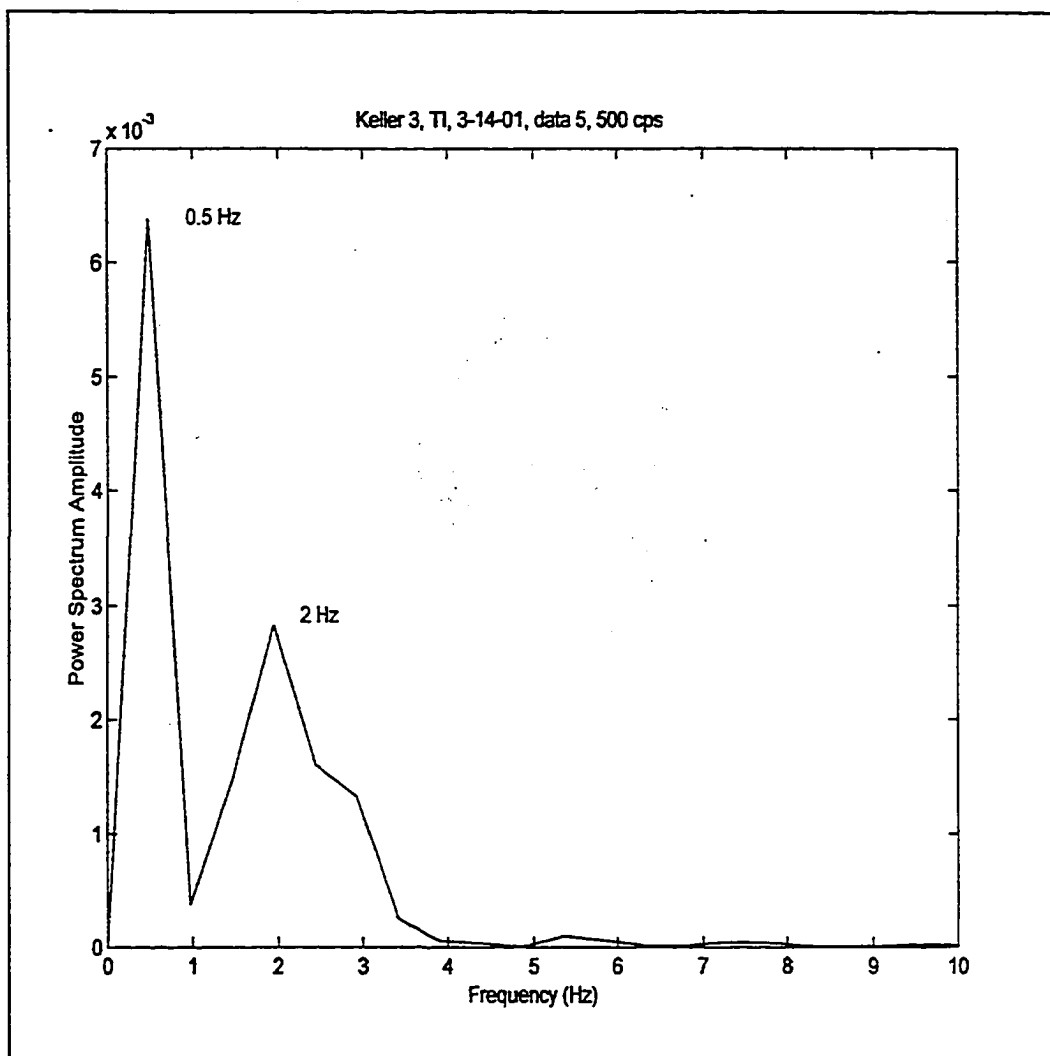


Figure V.18-FFT for Keller 3 confined pressure wave signal at Treasure Island shown in Figure V.18.

Table V.1
Summary of the frequency of the signal detected at various piezometers

Transducer	Location	Distance to signal well	Data of test	Wave type detected		Predominant Frequency (Hz)		Notes	Figures	material
				impact wave	confined pressure wave	impact wave	confined pressure wave			
Keller 1	pressure vessel	N/A	7/13/99	—	yes	—	1.66	servo cycling pressure	Figure V.2/3	water
Keller 1	pressure vessel	N/A	7/13/99	—	yes	—	2.0	servo cycling pressure	Figure II.11	water
Keller 1	pressure vessel	N/A	7/30/99	—	yes	—	6.16	shot hammer	Figure V.4/5	sand
Keller 1	pressure vessel	N/A	7/30/99	—	yes	—	7.48	shot hammer	Figure II.10	sand
Keller 1	pool	19 inches	3/14/00	yes	—	966	—	hammer drop	Figure V.6/7	water
Keller 1	pool	16 inches	3/2/00	yes	—	NA	9.7	hammer drop	Figure V.8/9	water
Keller 1	Camp Hedding	32 feet	6/14/00	yes	—	>54.69	—	Hammer drop	Figure V.10/11	Silty sand
Keller 1	Camp Hedding	10 feet	11/13/00	yes	yes	—	0.25	Hammer drop	Figure V.12/13	Silty sand
Keller 2	Camp Hedding	20 feet	6-27-00	—	yes	—	0.24/3	Hammer drop	Figure V.14/15	Silty sand
Keller 3	Treasure Island	6.4 feet	3/14/01	yes	yes	—	0.5/2.0	Hammer drop	Figure V.17/18	Silty sand

CHAPTER VI

SUMMARY AND CONCLUSIONS

VI.1-Introduction: A signal generating system has been designed, tested, and shown capable of producing a fast-rising pressure wave which models the rate of pore pressure rise expected during earthquake-induced liquefaction of fine sand. The signal generating system is easy to use, the signals are highly reproducible over time, indicating that no damage was being done to the aquifer, and are detectable by piezometers 20 feet or more from the source. Improvements have been made to the design and installation of piezometers to be used to detect pore pressure changes induced by earthquakes. Also presented are observations concerning piezometers and a suggested installation plan for piezometers to be used to detect earthquake-induced pore pressure changes.

XI.2-Types of signals observed-The signal generating system produces an impact wave, a confined pressure wave, and an unconfined pressure wave.

(a) Impact Wave: A typical impact wave is shown in Figure III.8. This wave was produced by the initial impact of the falling hammer on the anvil/surge block system. Impact pressure was approximated using the pile-driving model by Smith (1955) in Appendix F. The pressures produced by this model were consistent with those measured in the screened interval of the signal well. The velocity of the impact wave in the aquifer was consistent with that expected of a compressional wave in water. The impact wave

has frequencies in the 900 to 1000 Hz range. The energy of this signal was shown in pool testing to decrease by the inverse log of the distance from the source. Some piezometers, such as D-17 at Treasure Island, did not detect the impact wave. This is believed to be either because the sediments in which the piezometer tip has been installed are attenuating the impact wave before it can reach the piezometer, or the screen of the piezometer is clogged. It was shown with the clogging of the Roctest #1 piezometers that clogging of the screens will act to filter out higher frequency signals while allowing lower frequency signals to be detected.

(b) Confined Pressure Wave: The confined pressure wave is the signal that most resembles an earthquake-generated signal. This signal was produced by the large pressure increase created in the signal well during the advance of the surge block into the column of water in the signal well after the hammer impact. The pressure is applied so rapidly that the aquifer can only act as a confined aquifer with a low storage coefficient. The conditions could be numerically simulated by assigning a low storage coefficient to the aquifer (Appendix F). The numerical simulation signals had similar shapes and had similar arrival times at the same distances as the measured signals (see Figure F.1 for the confined pressure waves and Figure F.4 for the modeled confined pressure waves). Frequencies associated with the confined pressure wave varied from 0.25 to 8 Hz depending on the distance from the source and the sediments around the piezometers. Of the piezometers tested at Treasure Island, D-17 did not detect the confined pressure wave during the August 2000 testing at Treasure Island and probably was not operating correctly during the March 14, 2001 testing at Treasure Island. D-33 'far' did detect the

confined pressure wave during the testing in August 2000 but did not detect the confined pressure wave in the March 2001 testing.

c) **Unconfined Pressure Wave:** The unconfined pressure wave, which has the lowest velocity, is caused by the flow of the water out through the well screen into the aquifer and is related to the actual movement of water from the well into the aquifer. The aquifer has had time for drainage to occur and therefore the storage coefficient is much higher. Because of the long period of the unconfined pressure wave, no analytical time was spent on this part of the generated signal except to note its presence and visually estimate its period. In many cases, where rapid logging times were used, records were too short to record the unconfined pressure wave. The periods of the unconfined pressure wave vary considerably depending on the distance of the piezometer from the signal well. For piezometer(s) near the signal well, the unconfined pressure wave overlaps with the decay of the confined pressure wave. In the piezometers at Treasure Island such as D-18 (Figure C.14) and Keller 3, (Figure C.4) the period was about 2 minutes for the unconfined pressure wave. For D-17 (Figure C.11) the period of the unconfined pressure wave was about 1 minute. At the PVC well at Camp Hedding, no unconfined pressure wave was observed. This is likely because the distance to the well would result in dispersion of the signal and the velocity of the signal might move the signal beyond the 60 second window being logged (logging rate of 500 Hz) for each test.

VI.3-Reproducibility of Signals: The signal generation system was non-destructive. Duplicate testing could be done months later with virtually the same results. This was

shown with the data from Keller 3 and D-18 at Treasure Island. At Camp Hedding, repeated testing from April to December 2000 did not diminish the signal and the influence of individual changes made to the signal generating system can be shown. When the same hammer drop height, anvil drop height, and logging speeds were used, nearly identical results were obtained at the piezometers. Because of the reproducibility of the signal, it was possible to determine the effects of varying procedures and equipment. The signal generating system did not damage the sediments around the well screen. It was possible to demonstrate that increasing the anvil drop height was the most important factor in producing a larger signal from the signal generating system.

VI.4-Signal generating system assembly: After many modifications to the signal generating system it became fairly easy to set up and operate. At the final testing at Treasure Island in March 2001, using a drill rig, the signal generating system was installed in a few minutes. At Camp Hedding, where a tripod system was used, the signal generating system could be set up by one person in 2 hours. Much of the testing in June, July, and October 2000 at Camp Hedding was done with only one person to set up the signal generating system, drop the hammer, log the transducer, and break down the system. Once the tripod is set up the handling of the NQ rods, guide rods, anvil, and hammer are fairly straightforward. The trickiest part of the system is stringing the signal-well transducer cable through the center of all the rods in the reverse order in which they are to be installed in the signal well. Switching to 3" PVC pipe with a cap to plug the well casing below the screened interval to be tested eliminated the packer's pressure line and

all the attendant problems associated with keeping the packer inflated while installing all the various rods, anvil, and hammer in the signal well.

VI.5-Piezometer installation: It was shown with the Roctest #1 (Rt#1) push cone at Camp Hedding and Treasure Island and the pushing of the Keller 2 at Camp Hedding that even in relatively clean sediments there is a high rate of clogging of the screens on the piezometers that are pushed into place. These piezometers may be suitable for measuring ambient water pressures if sufficient time is provided for equilibration of the tip, however, they may not be capable of measuring dynamic signals. This is likely the case for D-17, D-10, D-33 'near', and D-33 'far' (March 2001 testing at Treasure Island). There is nothing inherent in the Druck transducers used at Treasure Island that prevents them from detecting the generated signal. This is shown by the performance of D-18 and D-33 'far' (August 2000 testing). The method adopted for the installation of the Keller piezometers (over-drilling and using filter pack around the tip) avoided many of the pitfalls associated with pushing the piezometer beyond the end of a boring.

VI.6-Piezometers vs. wells: The investigation of whether open wells and open piezometers were capable of detecting earthquake-like signals was not a focus of this investigation. Data collected on this issue grew out of a normal practice of maximizing the amount of data collected when doing field-testing. At both Camp Hedding and at Treasure Island there were open channels that could be used for logging, spare transducers that could be used, and places to put them that might be productive. At Camp Hedding, the 2-inch PVC well extended across the depth interval being tested and if

nothing else would have provided background information on water level changes during testing. As it turned out the Keller 1, Rt #1, and GEMS transducers detected both the impact wave and the confined pressure wave 32 feet from the signal well in the PVC well.

At Treasure Island the inclinometer casing and the water table well were instrumented using the Keller 3 before this piezometer was permanently installed in its current location. At both locations, the impact wave could be detected. The data from Camp Hedding suggest it is possible that open wells (i.e. wells with the casing open to the atmosphere at the top) with transducers installed have the potential for detecting signals generated by the signal generating systems with the same sensitivity as the installed piezometer (Figures C.2, C.3, and C.4, Appendix C). This would need to be tested by placing open wells at similar distances from the signal well as the buried piezometers. It is possible that open piezometers (i.e. piezometers that have short screened intervals of a few inches to a few feet with the top of the casing open to the atmosphere) might provide an accurate response for specific strata of concern. Better responses might also be obtained if the transducer was isolated in a small diameter piezometer screen by a packer located just above the screened interval in the casing. This would further limit the amount of water that would have to cross the screen to elicit a response by the transducer.

The advantage to using an open well, an open piezometer, or a piezometer isolated by a packer in a casing is the ability to check the calibration of the transducer and screens very rapidly. The simple process of measuring the static water level in the well or piezometer

with an electrical water tape would allow a quick check of the calibration of the transducer. Raising the transducer up and down in the water column in the well or piezometer would provide a more accurate check of the calibration of the transducer as was done at Treasure Island with Rt #1 during the August 2000 testing. A further advantage to their use would include using the in situ transducer to measure water pressures during falling head or slug testing on the screens.

Having access to the screen would also allow remediation of the screens if they become clogged or fouled. Replacement of a failing transducer would be rapid. It would also be practical to place two transducers in the same screened interval to compare performance and to provide redundancy in case one fails. The piezometer tip developed for this study (Figure II.16) and used on Keller 1, 2, and 3 has many of these characteristics except the ability for rapid and easy recovery. However, as previously noted, any open piezometer scheme would have to be verified by actual experience in a parallel installation as suggested above.

Another possible problem needs to be considered. It might be the very fact that a sediment is liquefying in the field that is causing failure of the piezometers that are attempting to measure the pore pressure changes during liquefaction. Liquefaction may be inducing clogging of the piezometer screens at the beginning of the pore pressure rise as fines are mobilized due to the initial increase in velocities around soil grains. The transducer becomes masked from the aquifer by the clogged screen and the transducer can only measure the slow changes of ambient pressure such as the unconfined pressure

wave generated by the signal systems with a cycle of minutes rather than fractions of a second. Personal experience at sites where dynamic compaction is being done show very muddy water being expelled into observation wells, piezometers, and on the surface. Some open piezometers at use at these sites, installed to monitor pore pressure changes, have become completely clogged with sediment.

There are many advantages to the use of wells or open interval piezometers if they can actually detect the signal generated by an earthquake. It should be noted that, as far as can be determined from the limited pore pressure data from sites that have actually liquefied during earthquakes, the existing system of sealed and buried transducers and piezometers has not provided the type of record of pore pressure change everyone is comfortable with. There is not the expected large initial increasing pore pressure toward liquefaction that matches the maximum ground acceleration or motions. These records have shown a slow build-up of excess pore pressure over tens of seconds at Port Island and over minutes at the Wildlife site. The existing signals have very slow rise times and do not have the “ratcheting” upward of pore pressures.

Two things are possible. First, it may be the lab cyclic shear test is not an accurate model for liquefaction in the field. Second, such factors as cementation, interlocking grain edges, relaxation of stress at grain boundaries by aging may delay the onset of excess pore pressures until the fabric of the soil is broken.

VI.7-Distance of source from piezometers to be tested: It was shown in the data from Camp Hedding that the confined pressure wave could be detected 32 feet from the signal well in an open well and 20 feet from the signal well in a buried piezometer (Keller 2). At Treasure Island the confined pressure wave could be detected in D-33 'far' 18.5 feet from the signal well in the August 2000 testing. During the March 2001 testing, the distance at which the confined pressure wave could be detected was reduced to 11 feet at D-18. In the August 2000, testing at Treasure Island, piezometers D-33 "far" and D-18, 18.5 feet and 11 respectively from the signal well, detected the confined pressure wave. During the same test piezometers D-33 'near' and D-17, located 10.4 feet and 7.7 feet respectively from the signal well, did not detect the confined pressure waves even though both piezometers reported as working (i.e. reporting the correct hydrostatic water pressure). Further, the signals detected by D-33 'far' and D-17 changed significantly between the August 2000 and March 2001 testing. This demonstrates that there are other factors that can influence the ability of a piezometer to detect a dynamic signal than just distance from the source. In this case, it is possible that as the transducer electronics deteriorated with time, they are not longer able to respond to dynamic signals.

VI.8-Type of transducer to be used: All the different makes of pressure transducers used in this study seem to provide adequate sensitivity to detect the signals generated by the system. Response of the transducer appeared to be related more to the condition of the screens or the sediments around the screens rather than to the ability of the transducer itself to measure the signal if it reaches the transducer. The Druck, Roctest #1, GEMS, and Kellers all worked well. The Roctest optical fiber lines were difficult to work with and required much more extra care to prevent damage to than the other transducers.

Eventually the signal conditioner necessary for the Roctest transducer to be read failed to be able to read the transducer. The connection on the signal conditioner for the optical fiber transducer cable was easily fouled and field repair was not possible once problems developed. Only the manufacturer could repair these problems. This meant the loss of valuable field time as well as additional cost. The only transducer cable to failed during nearly two years of the testing was on the fiber optic transducers. The GEMS failed only after being placed in the well screen of the signal well. The problem appeared to be the seal on the electronics not being capable of preventing wetting in the extreme environment of the signal well. The Keller transducers worked as they were intended in all cases; however, the Keller transducers were never subjected to pressure conditions in the interior of the signal well.

VI.9-Signal well pressures: Accurately measuring the initial pressures generated by the signal generating system was never satisfactorily done. The Roctest #2 transducer was over-pressured during the initial two pool tests (Chapter II). The Validyne transducer was not submersible and had to remotely measure the pressures within the signal well. The pressured recorded were low and sometimes responses lagged behind the responses recorded in the observation piezometers. The GEMS transducer when placed in the signal well provided some data that appears accurate but the electronics could not be protected. The transducer usually failed after a couple of hammer drops. Ultimately the transducer completely failed to respond.

The PCB blast transducer provided accurate start times of the pressure rise in the signal well but the measured pressures, of over 9000 psi, seem unlikely without damage to the well screen or the aquifer; since damage did not occur, pressures of 9000 psi or more have been discounted. The transducer was returned to the company for calibration check and the calibration was confirmed to be correct. Discussions with the company and providing the company with the recorded data did not lead to a resolution of why the transducer was recording such high pressures. Field calibration and lab calibration confirmed the calibration data provided by the company with the transducer. The PCB blast transducer when placed in the PVC well at Camp Hedding indicated pressure rises in the PVC well of over 100 psi. If this were the case, the pressure exceeded the overburden pressure at the PVC well (8 to 17 psi depending on depth) and damage would be expected to the sediments. The velocity of the signal from signal well to the PVC well at Camp Hedding, using the start time indicated by the PCB transducer is consistent with the velocity expected for the impact wave (about 5000 feet/second).

VI.10-Logging speed and details of signals being recorded: The rate of logging the signal has a good deal to do with the detail observable in the signal. In order to get details of the impact wave it was necessary to log the signal at rates over 2000 Hz. 500 Hz seemed adequate for the confined pressure wave. However, at this rate the ability to detect the impact wave was hit or miss and almost always, the impact wave would be removed during filtering of the signal. Slower logging rates could have been applied to the unconfined pressure wave.

VI.11-Suggested installation procedures for future piezometer installation at potential liquefaction sites:

- 1) It was shown in the use of Rt #1 at both Camp Hedding and Treasure Island and Keller 2 at Camp Hedding that advancing a piezometer tip by pushing has a high failure rate as far as its ability to detect signals in the range of frequencies generated by an earthquake. It is not recommended that piezometers be pushed into place if it can be avoided. Instead, it is recommended that the piezometer tip be placed in a boring at the depth desired and an appropriately designed filter pack be place and tamped around the piezometer tip. Driscoll (1986) is an example of a text containing standard methods for filter pack design. By using a boring to install the piezometer tip it is possible to take a soil sample at the projected depth where the piezometer is to be installed and thus it is possible to know exactly the sediments into which the tip is being installed, a critical point in sand deposits where there are thin layers or lenses of silt or clay. There may be instances where pushing of the piezometers is necessary. To do so would require exact knowledge of the zone of interest prior to installation to avoid advancing through or installing the piezometer in a silt or clay layer. A means of testing the piezometer after installation would be necessary to know if it can detect signals in the desire range of frequencies. The piezometer tip and the signal generating system developed in this study would be useful.
- 2) It is recommended that piezometers tips be used that allow access to the tip. The piezometer tip use for the Keller 1 and 2 at Camp Hedding and Keller 3 at Treasure Island were designed to allow the tip to be developed or redeveloped after

installation. It is possible to inject deaired water through the screens to develop the screen and filter pack around the screens. It was also possible to perform falling head tests on the tips to evaluate the permeability of the screens and to evaluate the calibration of the transducer. The transducer was used to monitor for water pressure change as the falling head tank was opened. The sensitivity of the transducer could be observed during the falling head test. As the head in the falling head tank drops, there is a corresponding lowering of the water pressure in the tip being measured by the transducer.

- 3) Further, with this design, if there had been a detected decrease in the permeability of the screens it would have been possible to redevelop them to re-establish the original permeability of the tip. If just flushing with deaired water does not restore the permeability of the screens appropriate redevelopment could be done with acids or bases to remove precipitants or biological growth that may have occurred on the screens.
- 4) In any piezometer field, it is desirable to have some redundancy. This is usually accomplished by the addition of multiple piezometers at the same depth as well as having piezometers at different depths if the deposit is sufficiently thick. While it was shown that it is possible to accurately measure the impact wave and the confined wave to at least twenty feet from the signal generating system and at depths up to 15 feet deeper than the source screen, the noise measured by the piezometer increases with distance. The greater the distance from the signal well the more filtering is

necessary to see the underlying signal. Increasing the strength of the signal increases the possibility of damage to the aquifer. Since the confined pressure wave, the signal most like that expected for an earthquake, decreases as the inverse log of the distance from the source, decreasing the distance between the piezometers and the signal well results in a log increase in the strength of the signal detected by the piezometer.

Large, easily identifiable signals were received by the Keller 3 at 6.4 feet for the signal well at Treasure Island and at the Keller 1 at 10 feet from the signal well at Camp Hedding. All components of the generated signal could be seen in the unfiltered signal. For example, a circle of wells, installed around a signal well at a distance of 6.4 feet, would allow six piezometers to be installed 6.4 feet from the signal well and 6.4 feet from each other. Extending the radius from the signal well to 10 feet allows 9 piezometers to be installed 7 feet from each other and 10 feet from the signal well. Differences created by details in the strata could be evaluated by such an installation and redundancy included in the piezometer field.

- 5) Logging speeds of 500 counts/second gave good detail of the confined pressure wave at the Keller transducer. The logging speed of 500 cps is a good compromise. While not sufficiently rapid for discerning details of higher frequency signals, it allows you to know if an impact wave is present while providing good detail of the confined pressure wave and not producing extremely large data files.
- 6) There should be a means for periodically testing the piezometer field for its ability to detect earthquake-like signals. The signal generating system developed for this study

is such a system and has many desirable characteristics for a signal generating system. These are:

- a) consistency of the signal over time,
- b) the aquifer is not damaged by repeated testing,
- c) the system generates an earthquake-like signal covering frequencies for .01 Hz to nearly 1000 Hz,
- d) the system can be constructed of readily available standard equipment,
- e) the system is easy to use in field operations, and
- f) the system is easily transported in a van, pickup truck, or, as was done as part of this research, shipped across the country.

The same equipment that is used to drill the piezometer borings can be use to drill the signal well and install the signal generating system. Such a signal generating system as used in this study with the signal well having screens open to the sediment of interest, allows testing specifically in the strata in which the piezometers are located as well as strata some distance above and below the screened interval.

Assuming there is a clear understanding of the strata of interest and it is known what the variations are in local geology and hydrology, a piezometer field and testing system might be installed using the following steps:

- 1) piezometers installed within a 10 feet radius of the signal well.
- 2) install piezometer tips that allow access to the screens and testing the transducer after installation.

- 3) Preferred not to install a piezometer intended to detect an earthquake-like signals by pushing.
- 4) Bring the saturated piezometer tips to the field for installation under water and sealed in a protective membrane.
- 5) Take a soil sample from the zone in which the piezometer is expected to be installed.
- 6) Over-drill the boring by 1 foot below the depth that the piezometer is to be installed.
- 7) Place 1 foot of filter pack below the proposed depth of the piezometer.
- 8) Fill the drill casing to the surface with water.
- 9) Assemble the piezometer tip and transducer under water in the filled drilling casing.
- 10) Remove the protective membrane under the water in the drilling casing.
- 11) Lower the piezometer to the top of the filter pack insuring that the piezometer remains vertical.
- 12) Fill around, and 1 foot above, the piezometer with filter pack.
- 13) Tamp the filter pack.
- 14) Install a firm seal above the filter pack. A three-foot bentonite plug above the filter pack worked well in this study.
- 15) Fill the remainder of the boring with native material.
- 16) The depth and number of piezometers to be installed will depend on the site geology and the amount of redundancy with which the investigator is comfortable.
- 17) Maintain at least 5 feet between piezometers to avoid interference and damage to the sediments.
- 18) Install the signal well: a 4-inch diameter, schedule 40 PVC casing with a screwed on bottom cap worked well in this study.

- 19) A 2-foot length of screen in the signal well at each depth to be tested worked well in this study.
- 20) A plug or packer should be used to seal the well casing just below the 2-foot screen to be used. In the case of our study, we found it convenient to use a 3" schedule 40 PVC pipe and cap to provide a seal below the well screen. Additional pipe was added below the cap so the 3" PVC pipe stood on the bottom of the well casing.
- 21) The surge block and hammer system with a hammer drop height of 5 feet and anvil drop of 36 inches described in this study generates a signal that covers a range of frequencies to be expected for an earthquake, provides a fast rising signal, is reproducible, does not damage the aquifer, and is easy to handle in the field.
- 22) Record the signal at the piezometers at 500 Hz. If it is suspected that some part of the signal is being missed or perhaps a screen is clogged, increase the logging rate to 3000 Hz or more to allow the necessary detail of the signal to be detected.
- 23) Check the conditions of the piezometer field at least once a year using the signal generating system and determining the hydraulic conductivity of the screens. If changes occur redevelop the piezometer screens and recheck the piezometers with additional tests. Continue redevelopment until the original parameters have been restored.

LIST OF REFERENCES

- Black, David K., Kenneth I. Lee (1973), "Saturating Laboratory Samples by Back Pressure", *J. Soil Mechanics and Foundations*, ASCE, 99(SM 1), 75-93
- Bouwer, H., and R.C. Rice (1976), "A slug test for determining hydraulic conductivity of unconfined aquifer with completely or partially penetrating wells." *Water Resources Research*, 12 (No. 3), 423-428
- Daily, J.W. and D.R.F. Harleman (1966), *Fluid Dynamics*, Addison-Wesley Pub., NY, 454 pg.
- Driscoll, Fletcher G. (1986), *Groundwater and Wells*, Johnson Division Pub., St. Paul, MN, 1089 pg.
- Das, Braja M. (1999), *Principles of Foundation Engineering*, 4th ed., PWS, Boston, 862 pg.
- Faris, J. Richard, Pedro de Alba (2000), "National Geotechnical Experimentation Site at Treasure Island, California", *National Geotechnical Experimental Sites, Geotechnical Special Publication #93*, Jean Benoit and Alan J. Lutenecker, eds. , ASCE, 52 - 71
- Furumoto, Y., Oka, F., Sugito, M., Yahima, A., Fukagawa, Y. (1999), "Proceedings of the Seventh U.S.-Japan Workshop on Earthquake Resistant Design of Lifeline Facilities and Countermeasures Against Soil Liquefaction"; Technical Report MCEER-99-0019, Thomas D. O'Rourke, Jean-Pierre Bardet, Masanour Hamada, eds.
- "Handbook of Physical Constants" (1966), *GSA Memoir 97*, Sydney P. Clark Jr. Ed
- Holzer, T. L., Youd, T. L., Hanks, T. C. (1989), "Dynamics of liquefaction during the 1987 Superstition Hill, California, earthquake", *Science*, 244, 56-59
- Hushmand, B., Scott, R. F., Crouse, C. B. (1994), "In-situ calibration of USGS piezometer installations", *Recent Advances in Instrumentation, data acquisition, and testing in soil dynamics: Geotech. Spec. Pub. #29*, S. K. Bhatia and G. W. Blaney eds. ASCE, NY, NY
- Ishihara, K., Muroi, T., Towhata, I. (1989), "In-situ pore water pressures and ground motions during the 1987 Chiba-Toho-Oki earthquake", *Soils and Foundations*, Japanese Society of Soil Mechanics and Foundation Engineering, 29, (No. 4), 75-90
- Kramer, Steven L. (1996), *Geotechnical Earthquake Engineering*, Prentice and Hall, NJ, 653 pg..
- Lambe, T. William, Robert V. Whitman (1969), *Soils Mechanics*, John Wiley and Sons, NY

Lee, Charles H, Michael Praszker (1969), "Bay mud developments and related structural foundation", *Geologic and Engineering Aspects of San Francisco Bay Fill, Special Report 97, Calf. Div., of Mines and Geology*, Harold B. Goldman, ed., 43 - 85

Lew, Marshall (2001), "Liquefaction evaluation guidelines for practicing engineering and geological professionals and regulators", *Environmental and Engineering Geoscience*, VII, (No. 4), 301-320.

Liquefaction of soils during earthquakes, (1985), Committee on Earthquake Engineering, Housner, George W., Chairman, National Academy Press, Washington, D.C., 240 pg.

Moore, Richard Bridge (1992), "Geohydrology and ground-water quality data for stratified-drift aquifers in the Exeter-Lamprey, and Oyster River basins, southeastern New Hampshire", *USGS Open File Report 92-95*

Prickett, T.A., and C.G. Lonquist (1971), "Selected digital computer techniques for groundwater resource evaluation", *Illinois State Water Survey Bulletin 55*, 66p.

Smith, E.A.L. (1955), "Impact and Longitudinal Wave Transmission", *J. Transp. Engr.* ASME, 77, 963-973

Youd, T.L. (1996), "Treasure Island, California, National Geotechnical Experimentation Site"

Youd, T.L., Thomas L. Holzer (1994), "Piezometer performance at Wildlife liquefaction site, California", *J. Geotechnical Engineering*, ASCE, V. 120, No. 6, 975-995

Zeghal, Mourad, Ahmed-W. Elgamal (1994), "Analysis of site liquefaction using earthquake records", *J. Geotechnical Engineering*, ASCE, V. 120, No. 6, 996-1017

APPENDIX A

CAMP HEDDING, APRIL 2000

A.1-Introduction: In the following Appendices A to E are described the source, transducers, and data acquisition systems tested in the field. The evolution of the signal generating system is described through four field-testing campaigns at two different sites. The demonstration that the parts of the signal are as defined above is left to Chapter V and Appendix F. The definitions are presented to facilitate the discussions of the signals detected during the field-testing program.

A.2-Site Description-Camp Hedding is located in Epping, New Hampshire (Figure A. 1). The Camp Hedding site is located on a glacial outwash plain overlaying glacial marine sediments of the Presumpscot Formation (personal observations). Braided stream channels are present in the surface of the sand plain. There are suggestions of shallow kettle holes in the surface of the outwash plain. The sediments were deposited at the end of the last glaciation of the area about 10000 to 12000 BP.

The Camp Hedding site had been investigated by the USGS as part of a water supply investigation of the New Hampshire coastal plain (Moore, 1992). A 2" PVC well was installed at the site as part of their investigation. The boring log for the 2 inch PVC well (Moore, 1992) indicates sand is present from the surface to a depth of 34 feet below ground surface. Between 34 feet and 79 feet is clay. Till is present below 79 feet.

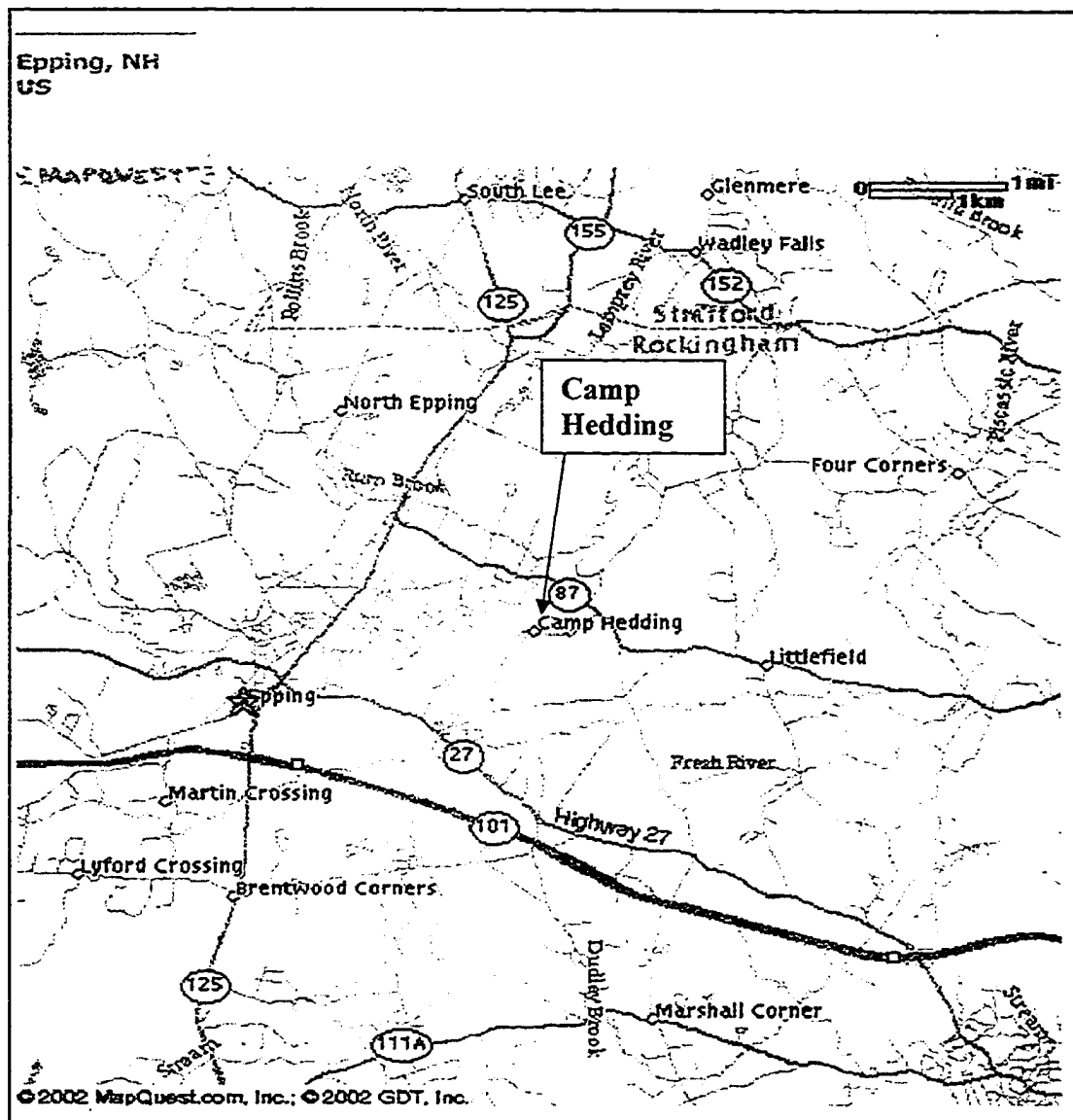


Figure A. 1-Camp Hedding Testing, April 2000: Location map for Camp Hedding testing site in Epping, New Hampshire

The two seismic refraction traverses, performed as part of this study, crossed in the area of the PVC well showed velocities consistent with saturated sand in the area of the PVC well to the full depth of the soundings, or about 40 feet. During the boring for the signal well, located 33 feet north of the existing PVC well, samples (Figure A. 2) taken to a depth of 32 feet were generally poorly graded sand (SP). Scattered silt layers were encountered from a depth of about 21 feet below ground surface down to 32 feet below ground surface. The sieve analysis for all the samples taken in the 18 to 30 foot proposed test zone below the ground surface are shown in Figure A.3. The sediments vary from poorly graded sands (SP) to silty sand (SM) with as much as 27% fines.

A.3-Hydrology: The water table was measured between 5 and 7 feet below the ground surface throughout the testing period from April to December, 2000. In order to determine the hydraulic conductivity of the aquifer, three one inch diameter observation wells were installed to depths of 10 feet below the ground surface as shown on the site map (Figure A.4). Slug tests on each observation well indicated hydraulic conductivities (k) in the range of 3×10^{-3} cm/second.

A four-hour pump test on the PVC well at 5 gpm resulted in less than 1 foot of drawdown over the period of the test. No drawdowns were recorded in the three observation wells used in the pumping. Slug tests on the PVC well yielded hydraulic conductivities in the range of 1×10^{-3} cm/sec. to 5×10^{-3} cm/sec. using the methods of Hvorslev, 1949, as presented in Lambe and Whitman, Table 19.4 (pg. 285) and Bouwer and Rice (1976). The Bower and Rice method yielded lower values of k than the Hvorslev method for the

Camp Hedding		NH Boring		Field N-count			Skempton's correction factor	short rod correction	Corrected and normalized N-count
depth (feet)	blows/6" hammer used is automatic 140 lb.	recovery (inches)	soil description	Nf	depth	effect stress (tons/ft. sq.)	Cn	Cr	N ₁ /60
10 to 12	2-2-2-2	12	Sand, SP, fine sand, no fines, micaceous, poorly graded (uniform grain size), no layering evident	4	11	0.6168	1.237011381	0.7296	5
12 to 14	2-2-3-4	8	Sand, SP, fine sand, no fines, micaceous, poorly graded (uniform grain size), 1/4" layer iron stain	5	13	0.6744	1.194457716	0.7542	7
14 to 16	3-5-4-5	10	Jar 1- 0 to 6" from bottom-Sand, med. sand, SP, iron stained, grades upward Jar 2 sand Jar 2- 6"- 10", Sand, SP, fine sand, light color grey, no fines	9	15	0.732	1.154734411	0.7788	12
16 to 18	5-5-6-5	20	Jar 1- 0 to 13" from bottom-Sand, med.sand, SP, highly iron stained, no fines Jar 2-13" to 20", Sand, SP, Alternating layers of iron stained and grey sand, the iron stained layers are coarser sand than lighter colored layers	11	17	0.7896	1.117568172	0.8034	14
18 to 20	3-4-5-7	10	Sand, medium sand, SP, iron stained, not as red a spoon above, 1" lighter red layer six inches from bottom of spoon, no other layers evident, micaceous	9	19	0.8472	1.082719792	0.828	12
20 to 22	3-6-7-5	6	0 to 2": alternating layers of red stained medium sand and lighter red layers, red sands are coarser than lighter layers 2" to 5": SM, olive colored sand with layer 1/4", darker and lighter layers, silt is evident in this layer. 5" to 6": SM, Slightly reddish sands, fines evident in this layer.	13	21	0.9048	1.049979	0.8526	17
22 to 24	4-5-5-6	16	Jar 1- 0 to 7", SM, silty sand, light color, 1" layer of reddish sand in middle. Jar 2- 7" to 16", SP, medium sand, reddish color	10	23	0.9624	1.019160212	0.8772	13
24 to 26	2-3-3-4	3	SM, light grey silty sand, very sensitive, quick's easily.	6	25	1.02	0.99009901	0.9018	8
26 to 28	2-3-3-4	23	SM, all light grey fine sand with minor fines	6	27	1.0776	0.962649211	0.9264	8
28 to 30	4-6-7-7	7	Jar 1, 0-3", SP, reddish sand, no fines Jar 2, 3"-7", SP/SM, light colored fine sand	13	29	1.1352	0.936680405	0.951	17
30 to 32	7-6-7-7	16	Jar 1, 0 to 4", SP, light colored fine sand, grades upward to reddish sand. Jar 2, 4" to 6", SP, dark reddish iron stained medium sand 6" to 7.5", SM and SP layer, alternating layer of fine light color sand and dark reddish medium sand, 1/8" pebble in red layer (only pebble seen so far). Jar 3, 7.5" to 14", SP, slightly reddish medium sand, some 1/8" grains. 14" to 16", SP, light color fine sand.	13	31	1.1928	0.912075885	0.9756	17

Figure A. 2-Camp Hedding, April 2000: Boring log for signal well.¹

¹ The field N-count, Nf, has been corrected for depth, $C_n = 1/(1 + \sigma'_{v0})$ (Skempton's correction factor), and hammer energy ratio correction factor ($C_e = 0.88$). Short rod corrections (C_r) were made according to values suggested in Lew (2001). $N_{1/60}$ was calculated as $N_{1/60} = N_f * C_n * C_r * (C_e / 60)$ from Lew (2001).

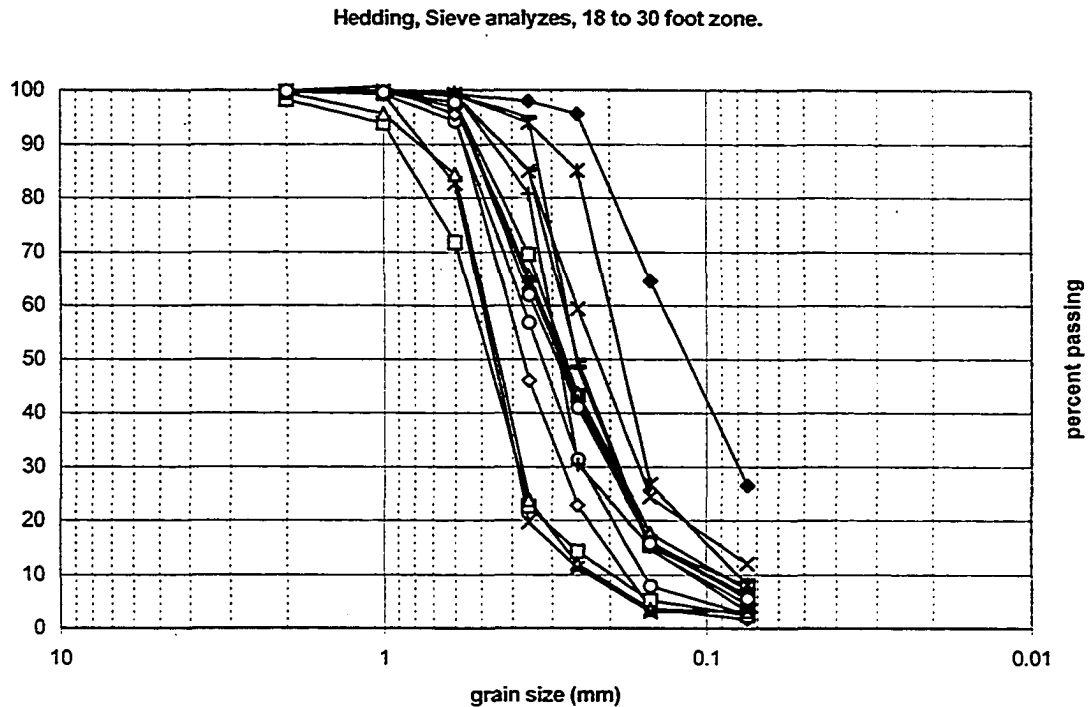


Figure A. 3: Camp Hedding, Sieve analysis of samples from the 18 to 30 foot zone.

same data. The full results of the slug tests and calculations are in Appendix K. The testing at Camp Hedding took place over about a year. The Camp Hedding site was used to test all the changes to equipment and methods of testing prior to use at the existing piezometer field at Treasure Island. Testing began in April 2000 with the same equipment and procedures developed during the pool testing. Modifications based on the April testing were made and additional testing was done in June and July 2000 (Appendix B) prior to testing at Treasure Island in August (Appendix C). As a result of testing at Treasure Island, additional modifications were made to the system and further testing was done at Camp Hedding in November and December 2000 (Appendix D) prior to testing at Treasure Island in March 2001 (Appendix E).

All the testing at Camp Hedding was done utilizing a tripod to lift the hammer and surge block system. The testing in April, June, and July 2000 utilized a pelican hook to release the hammer. In later testing in November and December the use of string for lifting the hammer and surge block was reintroduced.

In an attempt to increase the size of the signal generated by the surge block, a 300 lb. hammer replaced the 140-lb. hammer in the last few tests done in April 2000. In two drops, the 300-lb hammer causes a separation to occur between the anvil and the 2.75" guide rod or pipe. The pressure signal generated by the 300-lb hammer was smaller than the signal made with the 140-lb hammer. Because of the damage caused by the 300-lb hammer and the lack of apparent increase in the signal strength, all the reported tests are for the 140-lb. SPT donut hammer.

A.4-Signal well construction: A map of the testing locations at Camp Hedding is shown on Figure A.4. The boring log for the signal well was presented in Figure A.2. The signal well was sampled to a depth of 32 feet below ground surface (bgs) and drilled to 37 feet bgs. A six-foot long 12-inch OD hollow stem auger was used as a surface casing of the well. The auger was advanced to below the water table. A 6-inch OD steel casing was advanced through the bottom of the auger. A roller cone bit was used to wash out the

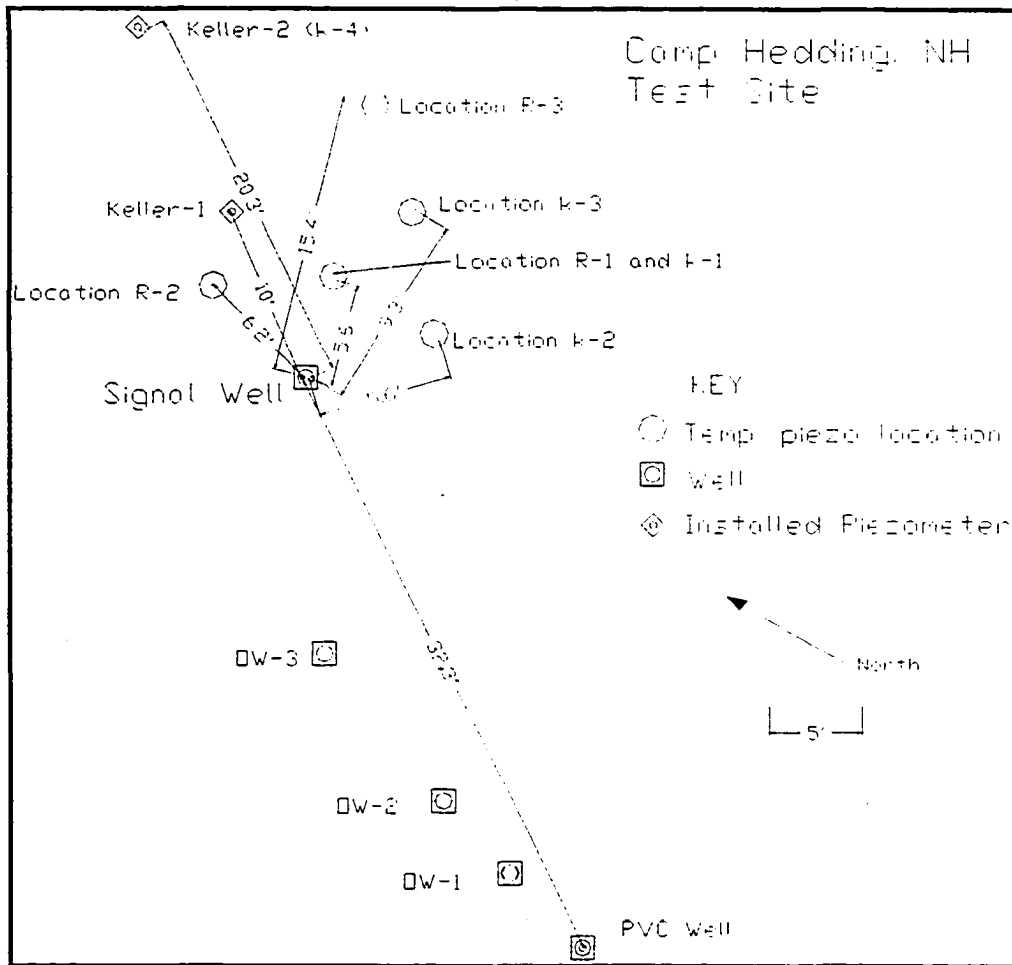


Figure A. 4-Camp Hedding, April 2000: Location map of wells, piezometer locations, and observation well (OW). The circles are permanent well, observation well or piezometer locations. The squares are temporary piezometer locations.

casing. Split-spoon samples were taken ahead of the casing. The well was constructed of 4-inch ID schedule 40 PVC with #50 slotting from 19'-21' and 29'-31'. The screens have filter packs that extend one foot above and below the screen intervals. Bentonite chips were placed below the bottom filter pack, between the screened intervals, and for three feet above the top filter pack. All material was placed with tremie pipe and the filter packs were tamped before the addition of the bentonite. Prior to placing the upper 3 feet of bentonite chips the well was pumped to insure the filter packs were settled and no gaps were present in the filter pack. Native fill was used to fill the casing above the top bentonite seal. All signals were generated using the well screen at 19 to 21 feet for the April 2000 tests.

A.5-Testing Results: The Roctest #1 transducer was sealed in a drive-cone as shown in Figure A.5. The screens were carefully saturated and brought to the field in deaired water. A thin latex membrane was fitted over the tip to maintain saturation and to allow transferring the drive-cone from the deaired water into the water in the casing. The initial testing location, R-1, was located 5.6 feet from the signal well. A 4-inch casing was pushed to below the water table and washed out. The Roctest #1 with the membrane was place below the water level in the casing. The piezometer was then pushed through the bottom of the casing to a depth of 10 feet. After initial background reading and a check made that the ambient pressure being measured by the piezometer was consistent with the depth of the piezometer below the water table, a signal test was run using the procedures developed in the UNH pool. No response was measured by the Roctest #1 piezometer at this depth. The piezometer was advanced to 20 feet. The background check of the

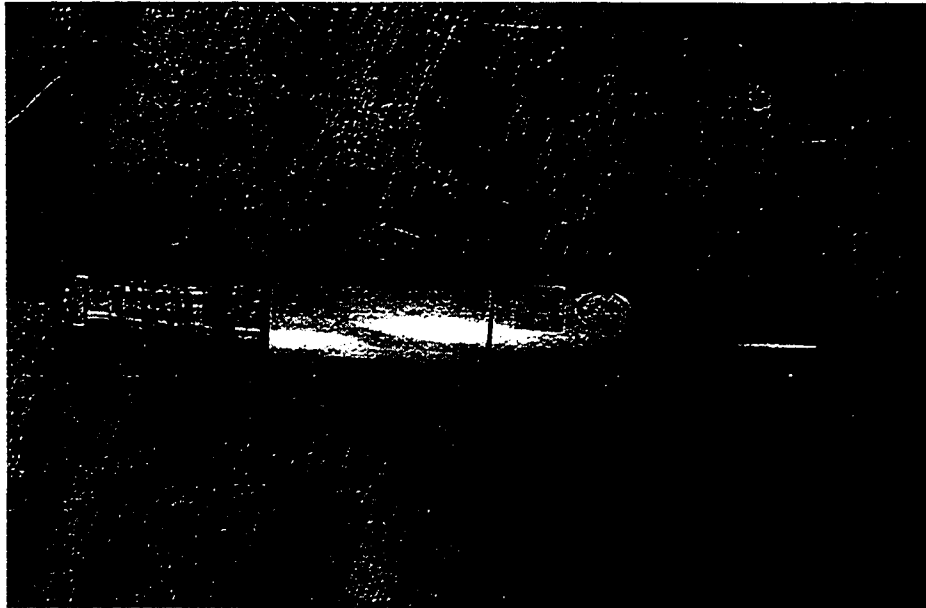


Figure A. 5: Camp Hedding-Roctest #1 transducer with drive tip.

Roctest #1, filtered, Location R-1, Adjustment of piezometer to ambient conditions after being advanced to 20 feet bgs

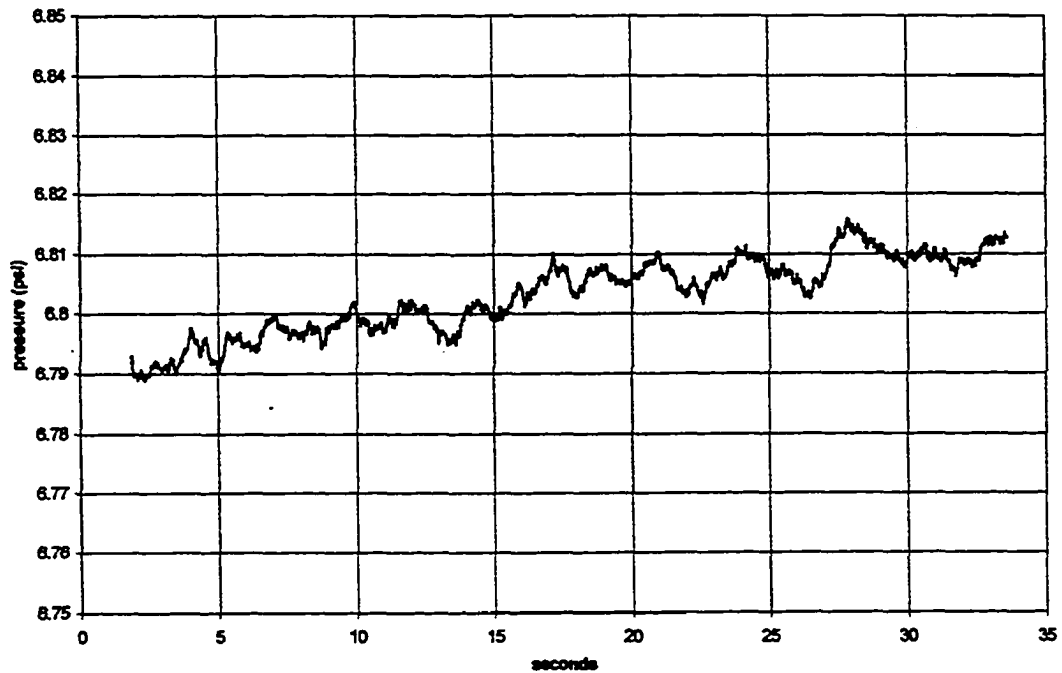


Figure A.6-Adjustment of Rt#1 to ambient water pressure at the depth of 20 below the ground surface.

pressure indicated slow equilibrium of the Roctest #1 to the ambient pressure (Figure A.6). The pressure slowly rose over the period of the background check. Dynamic signal tests were performed but Roctest #1 detected no signal at location R-1.

Several possibilities were debated. The most likely seemed to be air in the piezometer. There are two possible ways air could be trapped in the piezometer. The first is a lack of saturation of the drive-point screens. The second is that an air bubble could be present in the small cup just under the pressure diaphragm of the transducer (Figure A.5). The

screens on the drive-point were covered with silt or clay when retrieved. At the time this did not seem to be significant and was attributed to pulling the point back through the shallower sediments, which might have included thin silt layers. It was also possible that the tip had been installed in a silt lens. The slow equilibrium of the tip to the ambient conditions would be consistent with any of these conditions.

The Roctest #1 piezometer was replaced by the Keller 2 piezometer at the same location. The Keller 2 transducer was in the same protective tip as tested in the pool. A 4-inch casing was driven and washed out to a depth of 19 feet bgs. The piezometer was then placed on the end of drive rods and pushed ahead to its final depth at 20.5 feet bgs. Again, as with Roctest #1, care had been taken to insure saturation of the Keller 2 protective tip. The piezometer was assembled in deaired water after saturation of the screens and brought to the field in deaired water with a protective membrane. The tip would not be exposed until being advanced through the sediments below the end of the casing. A foot penetration into sand had been demonstrated in the pressure vessel testing to be more than sufficient to strip off the protective membrane.

A muted response was measured in the Keller 2 piezometer at this location. The same debate of possible causes for lack of response as had occurred with the Roctest #1 occurred. The additional possibility was discussed the signal from the signal well was being attenuated before traveling 5 feet from the source.

The procedures for installing the Roctest #1 and Keller 2 piezometers were modified slightly in order to enhance the possibility of detecting any signals from the signal well and to insure saturation of the screens on the tips. After saturating the tip and drive-point again overnight, the Roctest #1 piezometer was installed at the R-2 location 6.2 feet from the signal well. The Roctest #1 piezometer was installed through the bottom of a 4-inch casing that had been driven to a depth below the water table and washed out. On this attempt, the casing was filled with water to the top of the casing. The membrane covering the piezometer tip was removed by hand in the casing below the water level in the casing before beginning to push the drive-point. The drive-point was then advanced at a rate of 2 cm/second from 10 feet to 20 feet while recording the changes in pressure. Signal testing of the new installation began. A large response signal was received by the Roctest #1 piezometer at the R-2 location. Figure A.7 is an example of the unfiltered signals measured by Roctest #1 at the R-2 location. For this test, the pressure rise was about 0.55 psi with the event lasting about 1 second before returning to background water pressures..

The location of the signal well, the Keller 2 at location K-1 (same as R-1), and Roctest #1 at location R-2 are shown in Figure A.8. The 4-inch steel casings used for installing both piezometers are shown. The drive-rods and drive-head used for advancing Roctest #1 are shown at the background location.

The Keller 2 piezometer was removed from the K-1 location and installed at the K-2 location 5.6 feet from the signal well. The procedures for installing the piezometer were

Roctest 1, location R-2, 6.2 feet from signal well

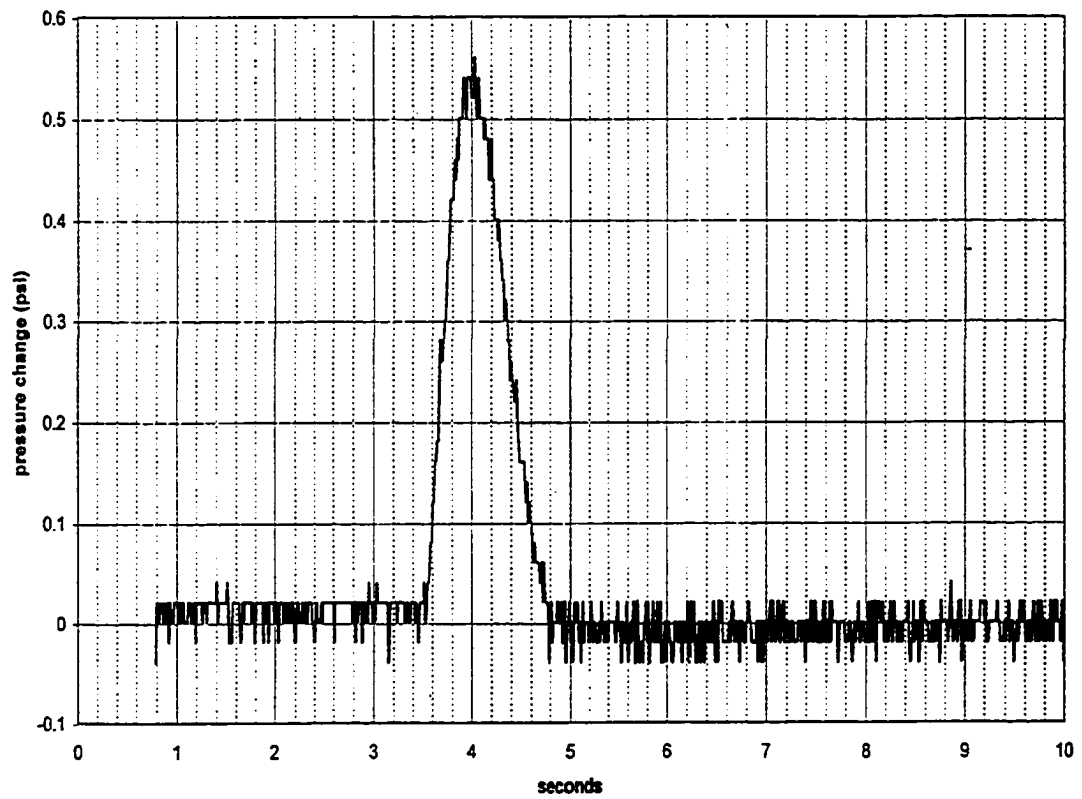


Figure A. 7-Roctest #1 piezometer located 6.2 feet from the signal well at location R-2. The Rt #1 was installed using alternative procedures than those used at location R-1.

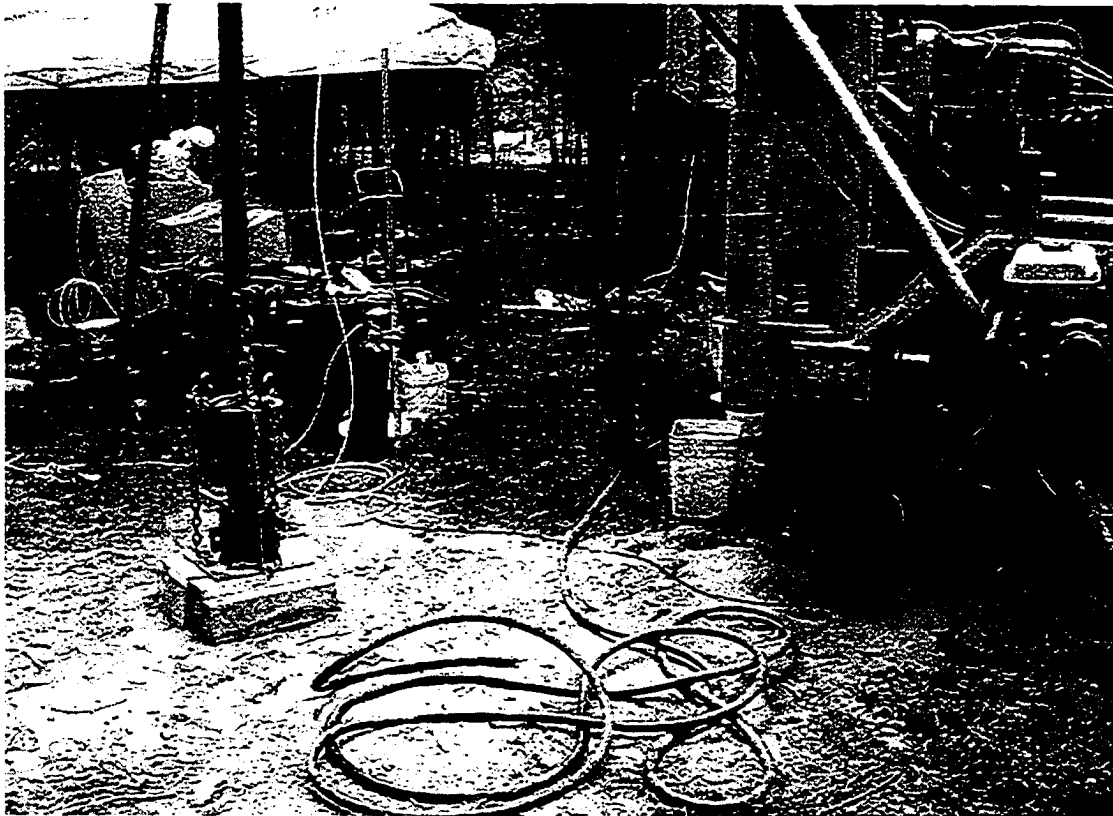


Figure A. 8: Camp Hedding Testing, April 2000: The setup of the signal generating system is at left. Locations K-1 with Keller 2 is at right 5.6 feet from signal well. Location R-2 with Rt#1 is in center 6.2 feet from the signal well. At good signal was received at location R-2 and a poor signal was received at K-1. Both are located at the same depth.

modified so that the steel casing was advanced and washed out to a depth one foot deeper than the depth at which the piezometer was to be installed. One foot of filter pack sand was placed at the bottom of the washed casing. The casing was filled with water to its top. The Keller 1 piezometer was placed below the water level in the casing and the membrane removed. The piezometer was then lowered on rods inside the casing and placed at the top of the filter sand. Additional filter sand was added around the piezometer. Once the piezometer was buried in filter sand, the rods used to place the piezometer were pulled leaving the piezometer in a vertical position in the sand.

Additional filter pack sand was added so that there was a foot of sand above the top of the piezometer. The sand was then tamped. The casing was pulled back so that the bottom of the casing was above the piezometer but still in the sand filter above the piezometer.

Bentonite chips were added and the casing pulled further back. This was continued until there were 3 feet of bentonite chips above the sand. For temporary installations such as K-2, and K-3 at Camp Hedding, the steel casing was left in place during testing at these locations. For permanent locations such as Keller 2 at distance of 20.3 feet horizontally from the signal well, the steel casing was replaced by 3-inch schedule 40 PVC casing. It was shown by the recovery of the Keller 2 piezometer at locations K-2 and K-3 that it is possible to wash out the sand and bentonite and remove the piezometer without damage to the transducer or the protective tip.

Figure A.9 is an example of the signal detected by the Keller 2 at location K-3, 5.6 feet from the source well. The signal has a longer tail than the Roctest #1 at location R-2 and

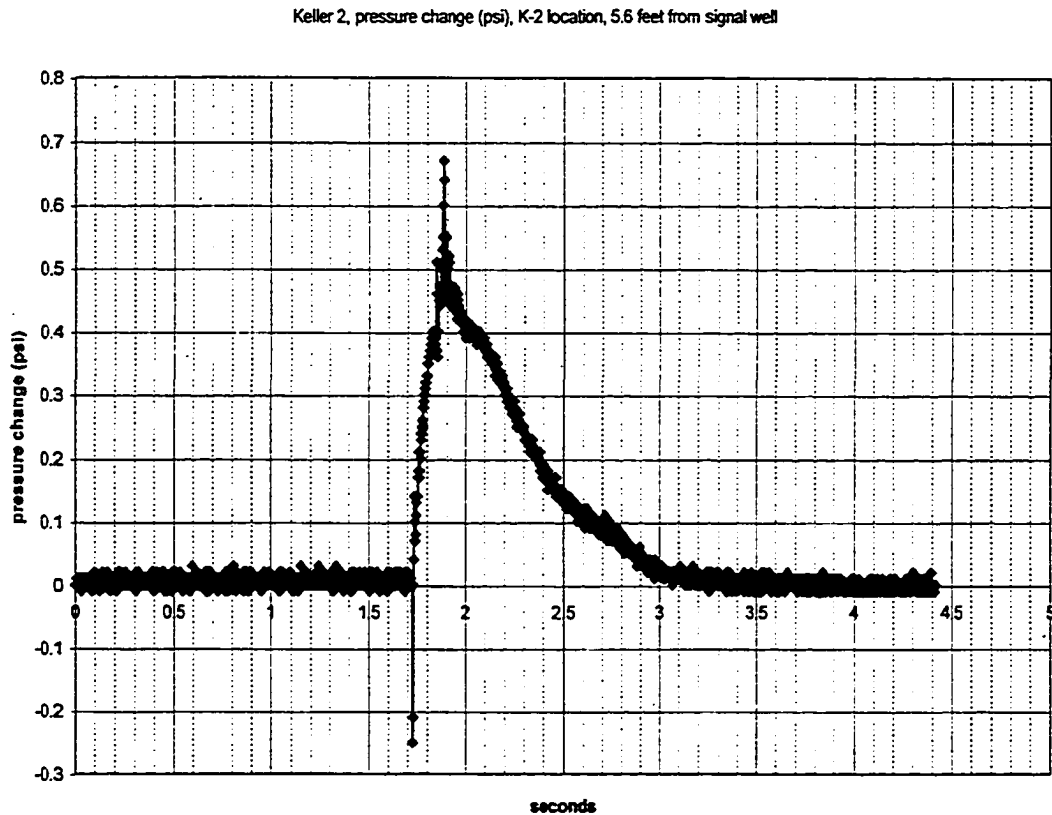


Figure A. 9-Camp Hedding testing April 2000: Keller 2 is installed at location K-2 5.6 feet from the signal well to a depth of 20 feet. Impact waves are seen at 1.7 seconds and 1.9 seconds. The hydraulic pressure signal is 1.25 seconds long. Logging rate is 500 cps.

the event lasted about 1.25 seconds. There are indications of a P-wave at the start of the signal at 1.7 seconds and at 1.9 seconds, however, because of the slow logging rate (500 Hz) the P-wave lacks detail. This P-wave is produced by the initial impact of the plunger on the water in the casing, as previously discussed. The amplitude of the signal

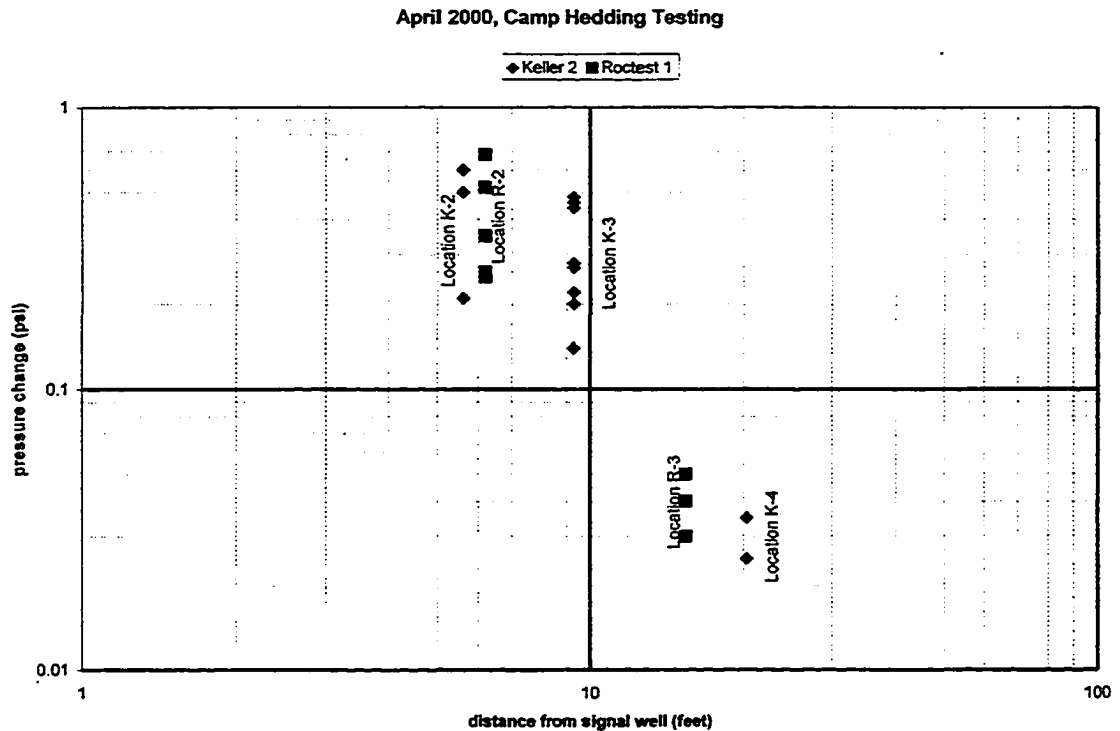


Figure A.10-Change in signal amplitude with distance from the signal well. The amplitude of the signal decreases with distance from the signal well. The distance is plotted as a log scale.

decreased with the distance from the source well. As shown in Figure A.10 the amplitude of the signal detected by Roctest #1 and Keller 2 piezometers decreased in amplitude with the change of its position from 5 feet to 20 feet from the source well. It is not clear what the nature of this decrease is because there is considerable scatter in the amplitudes at each distance. Distances in Figure A.10 are plotted on a log scale. Further, the signal to

noise ratio increases with distance and filtering becomes increasingly important with distance.

A.6-Discussion: The low response at the R-1/K-1, and R-3 locations suggests the influence of geology on the response of the piezometers. It is likely that either the screens on the Roctest #1 were clogged during the process of pushing forward or silt or clay layers were encountered that attenuated the signal. The possibility that the screens on the Roctest #1 drive point were clogged was investigated further while installing the Keller 1 at a distance of 10 feet from the signal well in November 2000 (Appendix D).

The April 2000 testing at Camp Hedding demonstrated that it was possible to detect the signal generated by the hammer/anvil/surge block system to at least 20 feet from the signal well. P-waves (impact waves) were detected with the Keller 1 piezometer during the April testing even though the maximum logging rate for the Keller 1 was 500 Hz.

The unfiltered data for the Keller 2 at K-3 location suggests a P-wave (Figure A. 9). No hint of a P-wave was suggested in any of the Roctest #1 data. The logging rate for the Roctest #1 was limited to 100 Hz (10 ms between readings). Problems at locations R-1 and R-3 appeared to have occurred with the driven tip on the Roctest #1 piezometer.

While saturation problems were possible at R-1, the careful procedures used in installing the Roctest #1 at R-2 and R-3 seem to eliminate any possibility of loss of saturation during installation. The presence of a silt layer or clogging of the piezometer screens during pushing could cause the lack of response. Similar problems would be encountered

at the testing at Treasure Island in August 2000 and clogging of the piezometer screen was investigated again in November 2000 at Camp Hedding.

Based on discussions with the drillers during the April testing the hammer guide rods were changed to AW rods (1.719" OD and 1.219" ID). The smaller diameter of the AW rods allowed free fall of the hammer and the conical threads allowed longer hammer drops. An NQ drive head section was added above the anvil and a striker plate added for the hammer to land on (see Figure B.1).

Further modification included tying the output of the Roctest #1 signal conditioner into the LABVIEW logging system by taking the analog signal from the signal conditioner directly to the data block. This would allow the determination of the velocity of the signal, faster logging of the signal, and better resolution of the signal.

During the April testing, no transducer was placed in the signal well to determine the pressures being generated. It was not possible to determine the start times for the signal nor the magnitude of the initial signal. There was a need for measuring the pressure inside the signal well and determining the starting times for the signal.

APPENDIX B

CAMP HEDDING TESTING. JUNE AND JULY 2000

B.1-Signal generating system modification: The primary purpose of June and July testing at Camp Hedding was to test the modifications to the signal generation system made as a result of the April testing. An attempt to determine the initial starting times for the generation of the signal inside the signal well was to be made. The modified signal generating system is shown in Figure B.1. AW rods replaced the 2.75" hammer guide rod. A NQ drive head was attached to the top of the anvil and a striker plate added for the landing of the hammer. A Validyne transducer (Model DP15-50 with a 5000-psi diaphragm) was modified to measure the pressures inside the well screen and detect the start of the signal. The Validyne transducer is not submersible therefore a one-eighth inch diameter tube was run down the middle of the AW and NQ rods into the well screen under the surge block. The tube was saturated and the transducer was bled by drawing water from the well up through the transducer under an applied vacuum. Once the tube was saturated, the transducer bleed valve was closed and the water held under a slight vacuum. The initial reading on the transducer was negative and represented the height of the column of water above the water table (about 5 feet below the ground surface). The change in pressure was measured from the initial negative reading. At the end of the April testing the Keller 2 piezometer had been



Figure B.1-Camp Hedding testing June-July 2000: Modifications made to the signal generating system included using AW rods as guide rods for hammer and modifying anvil to include striker plates. A pelican hook is being used for releasing the hammer. A C-clamp is being used to hold up the anvil and surge block until the falling hammer strikes the anvil.

permanently installed at the K-4 location 20.3 feet from the signal well (see Figure IB.4) and at a depth of 20.5 feet bgs. Also used for measurement in this round of testing was the PVC well installed by the USGS located 32.3 feet from the signal well. The PVC well had previously been used for slug testing and a short pump test. The total depth of the well is 30 feet bgs. The USGS records indicate a 2-foot screen was installed in the bottom of the well. The Keller 1 transducer and protective tip, previously used in the tank testing, was placed in the PVC well during the June-July testing. The logging rate was increased in some of the tests to 5000 Hz in order to obtain more detail on the impact wave (P wave) that was being produced by the signal generating system.

B.2-Results: The Validyne was not suitable for determining the start of the pressure pulse in the signal well. In most cases, the pressure would start to rise in the Keller 2 piezometer and PVC well before the Validyne began to respond. Figure B.2, for 7-17-00, data 3, shows the response of all three transducers to the generated signal. The response of the Validyne followed the other two transducers by about 0.1 second. The Validyne transducer is the last to respond to the pressure change. This is likely caused by the lag time created by expansion of the tube leading from the well screen to the transducer.

Figure B.3 is an example of the unfiltered signal detected by the Keller 2 and Keller 1. Both the Keller 2 and Keller 1 in the PVC well detect two impact (P) waves. The unfiltered signal is dominated by the two sets of impact waves detected by the

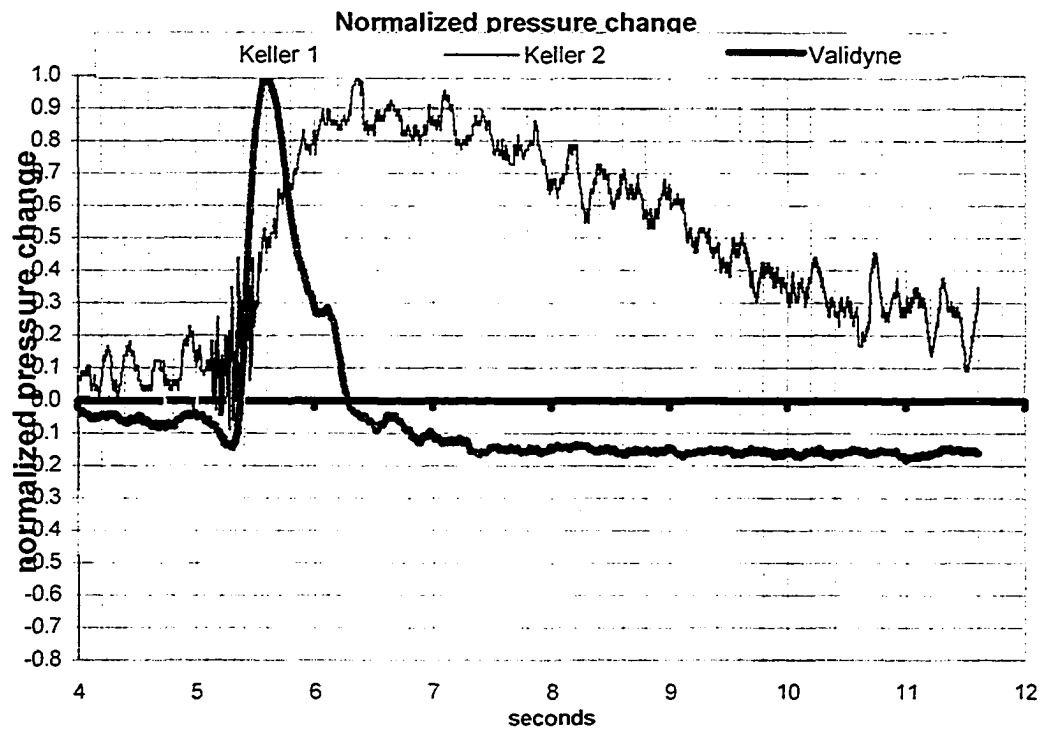


Figure B.2-The Validyne transducer is measuring the pressure change in the signal well. The Keller 2 piezometer is located 20 feet from the signal well. The Keller 1 piezometer is located in the PVC well 32 feet from the signal well. The pressures have been normalized by dividing each pressure change by the largest pressure change detected by each piezometer ($\Delta P / \Delta P_{\max}$).

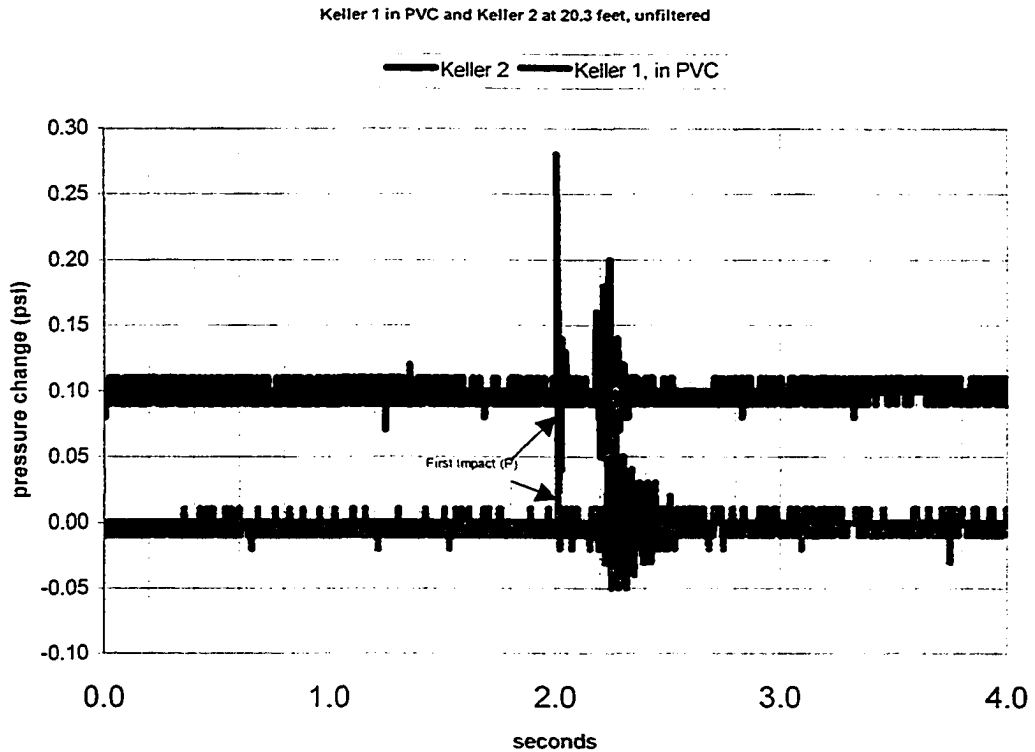


Figure B.3-Impact (P) waves for the Keller 2 piezometer located 20 feet from the signal well and the Keller 1 transducer located in the PVC well 32 feet from the signal well (6-28-00, Data 6). Both signals start at the same time. The impact waves are detected at both locations. The Keller 2 data has been offset vertically by +0.1 psi to show shapes of both signals.

piezometers. At the scale of the pressure changes for Figure B.3 the confined pressure waves are within what appears to be noise at this scale (Figure B.4 shows the confined pressure waves after the impact wave has been removed by filtering). The first set of impact (P) waves detected arrived at about 2 seconds and the second set of impact (P) waves arrived at about 2.18 seconds. The arrival times of the impact (P) waves at both transducers appear to be identical due to the short distance of travel and the logging speed. The pressure change data for Keller 2 was offset on Figure B.3 so that the coincidence of the impact (P) wave could better be shown. The data was logged at 500 Hz. If the velocity of the impact (P) wave is assumed to about 5000 ft/sec. then it would take about .002 second to traverse the 12 feet difference in distance between the two wells for the source well. This is about the spacing between individual data points when logged at 500 Hz.

The confined pressure wave, produced by water flowing out of the well casing, is shown on Figure B.4 after filtering the signal. The tails of both pressure waves were missed in the record. There appears to be about 0.6 to 0.8 seconds delay between the start of the rise in pressures between the transducers. The velocity of the confined pressure wave is therefore about 15 to 20 feet/second between Keller 2 and Keller 1.

B.3-Discussion: The change from 2.75" pipe to AW rod as guide for the hammer during the drop appears to have resulted in more of the energy from the hammer impact going into the impact (P) waves. The impact (P) waves are easily detected in the June and July results compared to the signals measured in the April testing. The increased

velocity of the drop afforded by the smaller guide rods appears to have resulted in a larger compressional wave moving down the rods and being transferred to the ground water. The increase in energy does not result in movement of the surge block because the water cannot get out of the way fast enough to allow the energy to be translated into movement of water out of the well screen. Therefore, the energy was translated into compressional energy. Since more energy is going into the impact (P) waves there is less energy being translated into the confined pressure waves. Referring back to Figure A.10 the pressure change observed in Figure B.3 for the Keller 2 at 20 feet is about half that measured in April testing for this instrument. Figure B.5 re-plots Figure A.10 with the additional data collected during the June/July 2000 testing at Camp Hedding.

Both Keller piezometers were capable of detecting the impact (P) waves and the confined pressure wave. Both the impact waves and the confined pressure waves can be detected up to 32 feet from the source well and could be detected in an open piezometer as well as by the buried piezometer.

The problem of obtaining reliable measurements of the pressures inside the well screen after the impact of the anvil by the hammer was not solved in the June and July testing. The result was that no well-screen pressure transducer could be checked prior to testing at Treasure Island in August 2000.

Keller 2 at 20'H, Keller 1 in PVC well at 33"H

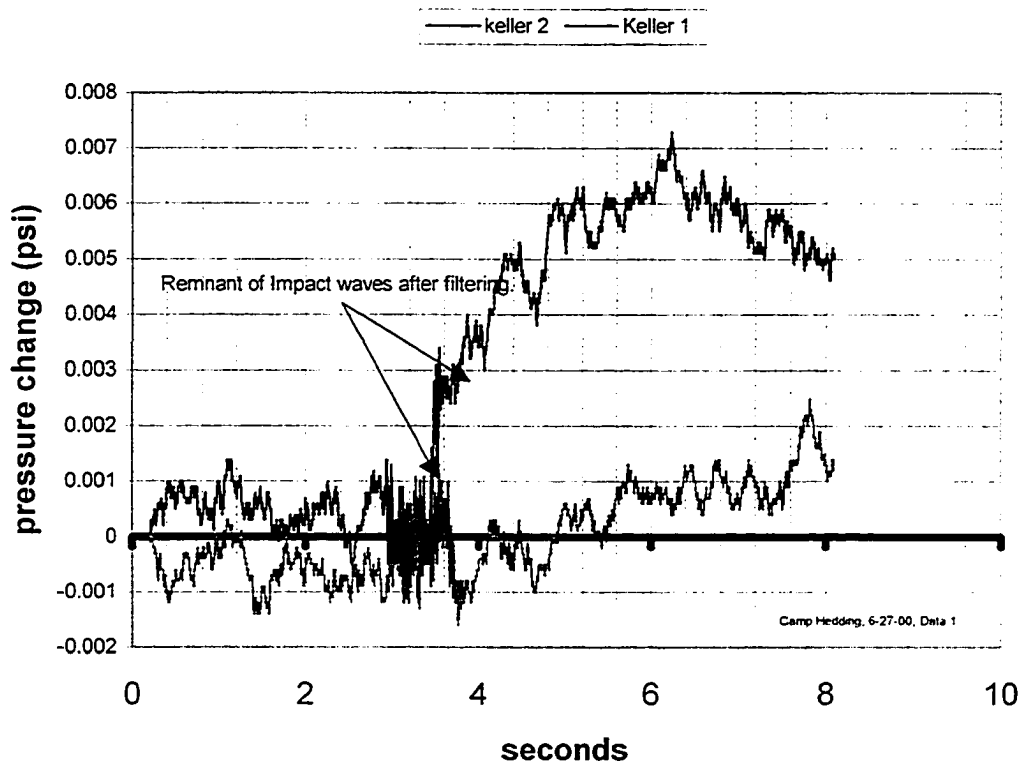


Figure B.4-Confined pressure waves for Keller 1 in PVC well 32 feet from the signal well and Keller 2 twenty feet from the signal well. The confined pressure waves begin about 0.6 to 0.8 seconds apart. The velocity between the two piezometers is about 15 to 20 feet/second.

April 2000 data compared to July/June 2000 data

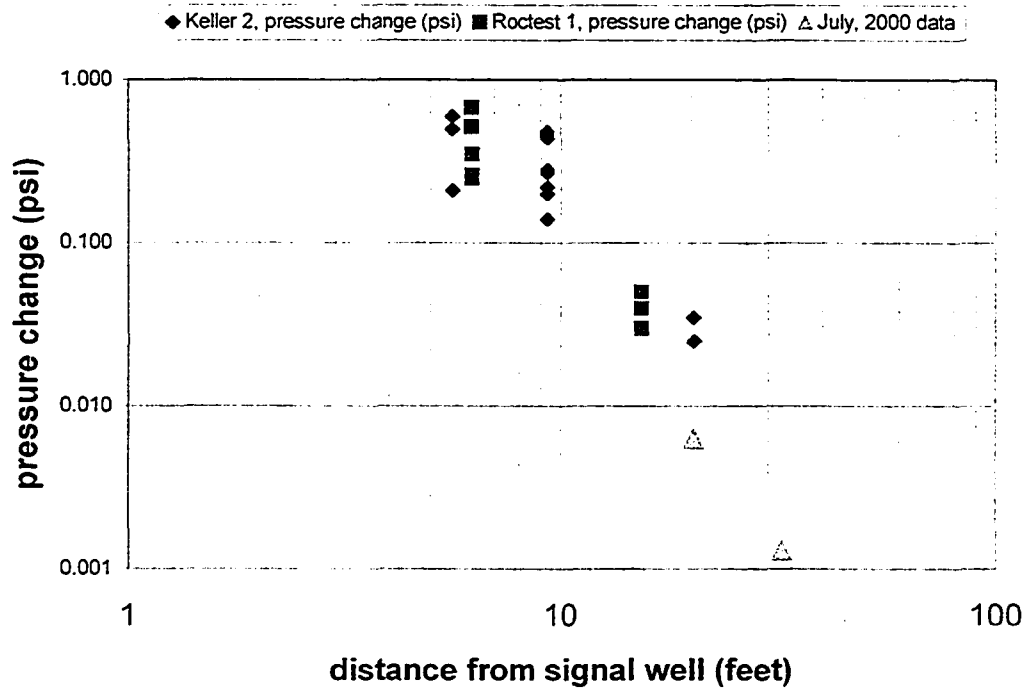


Figure B.5-Data for June-July 2000 testing has been added to Figure IB.10 of the April 2000 testing at Camp Hedding. The data has been plotted on a log/log scale for distance from the signal well and pressure change from the confined pressure wave. The July 2000 data is for the Keller 2 twenty feet for the signal well and the Keller 1 located in the PVC well 32 feet from the signal well.

APPENDIX C

TREASURE ISLAND TESTING, AUGUST 2000

C.1-Site Description: Treasure Island is located in the middle of San Francisco Bay, between San Francisco and Oakland. It is a northern extension of Yerba Buena Island (Figure C.1). In 1992, an earthquake instrumentation array was installed behind the Treasure Island Fire Station (Building 157) with NSF funding. The array includes 7 strong motion accelerometers distributed between the surface and a depth of 400 feet, and 8 piezometers in the hydraulic fill.

C.2-Surficial Geology: Treasure Island (TI) is a man-made island created by hydraulic filling of Bay sediments on to existing shallow shoal sediments (Lee and Praszker, 1969). The unconsolidated sediments extend to a depth of 260 feet below the Bay surface. The primary deposit of importance in this study is the shoal sand and hydraulic fill that is present from the ground surface to a depth of about 46 feet.

Grain size distribution curves on samples taken while drilling the signal well indicates that all the samples from the shoal sediments and fill material are generally poorly graded fine to very fine silty sand (SM). The boring log for the signal

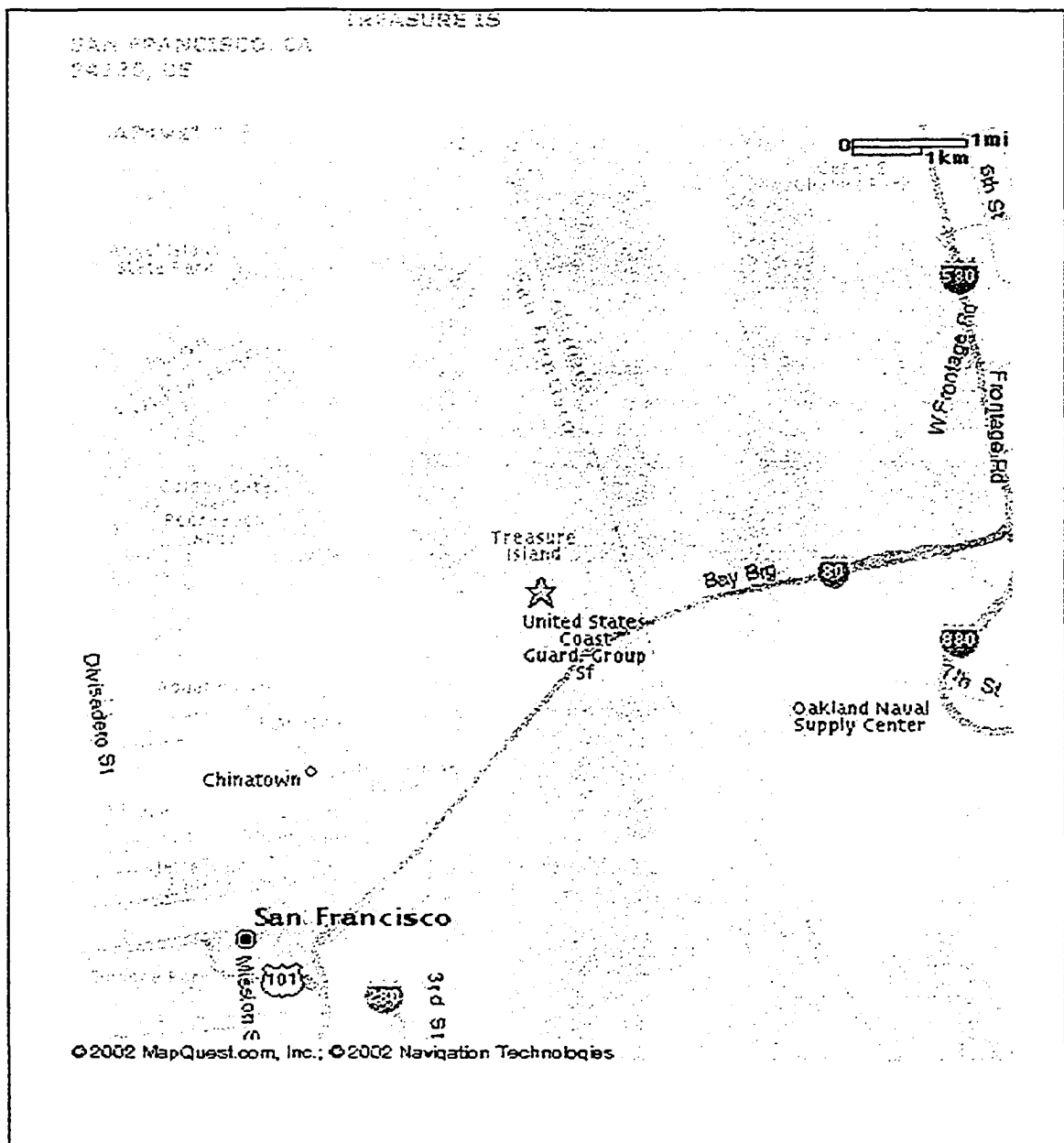
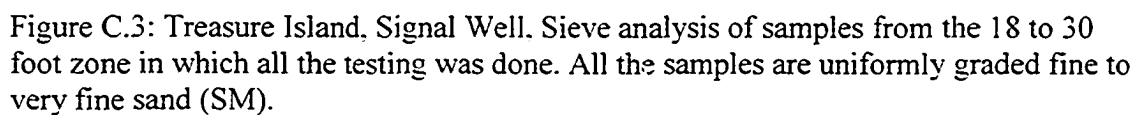


Figure C.1-Treasure Island, April 2000: Location map for Treasure Island.

Treasure Island	blows/6" hammer used is safely 140	Packer Drilling recovery (inches)	drillers: Roger	Field N-count	depth	Skempton's correction factor	short rod correction factor	Corrected and normalized N count	
depth (feet)			soil description	Nf		effect stress (tons/sq. ft. soil)	Cn	Cr	(Nf) ₆₀
5 to 6.5	1-4-4	10	Sand, medium sand, SP-SM, shells common, saturated. Sample 1	8	5.75	0.4656	1.365	0.665	7
7-8.5	1-4-5	9	Sand, medium sand, SP-SM, 1" for medium sand at bottom of sample, top 6" is shelly sand, Sample-2	9	7.75	0.5232	1.313	0.690	8
8.5 to 10	3-4-5	9	0-3"- medium sand, fine shell fragments common, 3-6" - alternating layers (3/8", 1/2", 1", 3/8", 3/8") of fine to medium sand, black color suggesting reduced conditions where shells are present; 6-9"-medium sand, fine shell fragments common. Sample 3	9	9.25	0.5664	1.277	0.766	8
10.33 to 11.52	4-4-4	9.5	Sand, medium to fine, large shelly zone at 6.5" from top of sample, bottom 6" is firmer than top 3", Sample 4	8	11.09	0.6191	1.235	0.731	7
11.83 to 13.5	5-4-3	11	Sand, medium, layers evident 0-3", 3-5", 5-7" and 7-11", the layer from 3-5" is firm and the separation between the layer at 7" is shelly zone, Sample 5	7	12.965	0.65475	1.201	0.750	6
13.5 to 15	2-4-2	8	0-5" medium sand; 6-7" silt/clay layer; 7 to 8" medium sand, Sample 6	6	14.25	0.7194	1.169	0.770	5
18 to 20.17	2-3-3(dropped about 8" under weight of hammers)	16	0-7"-black very fine sand to silt(30 to 40% fines, SM), slakes when shock (sample 7B); 7 to 18" sand, SM (sample 7B)	3	19.065	0.84695	1.081	0.829	3
20.17 to 21.57	weight of hammers-1-4	14	sand, Sample 8	5	20.52	0.9025	1.051	0.852	4
28 to 29.5	weight of hammers-2	16	0-4"-clay, no grit, layer 1/8" orange color; 4 to 18" medium sand, Sample 9B	2	29.75	1.128	0.940	0.948	2
29.5 to 31	1-5-4	8	0-7 sand green; 7-8" silt layer, Sample 10	9	30.25	1.1712	0.921	0.966	8

Figure C.2-Treasure Island, August 2000: Boring log for signal well.¹

¹ The field N-count, Nf, has been corrected for depth, $C_n = 1/(1 + \sigma'_{v0})$ (Skempton's correction factor). Short rod corrections (Cr) were made according to values suggested in Lew (2001). N_{f60} was calculated as $N_{f60} = N_f * C_n * C_r$ from Lew (2001). Because a safety hammer was used, no correction was made for energy.



The corrected SPT blow counts $[(N_1)_{60}]$ varied from as high as 12 blows/foot to as low as 2 blows/foot. The top 15 feet of sediments has higher blow counts than the sediments from 18 to 29.5 foot depth. Blow counts as low as 2 occur in this zone. In the sample

from 18 to 20.17 feet, the rods apparently hit a pocket and dropped about 8 inches. A rough estimate of the relative densities (D_r) according to Table 2.5 from Das (1999) would range from about 30% to 60% for the shallow sand between 5 and 15 feet. In the 18 and 29-foot zone, the relative densities could be as low as 0% to 5%.

C.3-Hydrology: The water table was present at a depth of 4.7 feet below the ground surface during the August 2000 testing. The water table was at 2.3 feet below the ground surface during the March 2001 testing. The hydraulic conductivity for the fine sand is estimated to be about 10^{-3} cm/sec. In situ falling head testing on the Keller transducer tip at a depth of 21.5 feet bgs indicated a hydraulic conductivity of 3×10^{-3} cm/sec..

C.4- Objectives: The primary objectives for testing at Treasure Island were to determine if the existing piezometer field could detect the signal generated by the pulse-generating system and to evaluate if the method of installation of a piezometer influences the signals which the piezometer detects. The existing piezometers at Treasure Island utilize Druck (model PDCR 940) transducers with a nylon protective tip installed using the method similar to that used for installing the Keller 2 at location K-1 at Camp Hedding. This installation method consisted of first boring to a predetermined depth. This depth was about a foot above the proposed final depth of the piezometer. The transducer, enclosed in its protective tip was then pushed to its final depth below the bottom of the casing. The native sediments were the only filter pack provided for the tip and there was no access to the tip once installed. There was no means available for developing the screens or a filter pack once the tip was installed. There was also no way to check the

calibration or sensitivity of the transducer once installed except by comparing the data to expected ambient conditions. As was shown previously in the installation of the Roctest#1 and Keller 2 at locations R-1 and K-1 at Camp Hedding it was possible for the piezometers to correctly measure hydrostatic water pressures and still not be able to detect low frequency pressure change at 2 to 10 Hz or the high frequency impact wave.

Figure C.4 shows the location of the existing Druck piezometer installations, as well as the inclinometer casing, signal well, water table monitoring well, and Keller 3 piezometer installation. All the existing piezometers used in this study are less the 20 feet from the signal well. The inclinometer casing, which is a 60-foot deep, was used at various times during the testing. The inclinometer casing provided a convenient means for quickly checking if a transducer was operating and to check its calibration by moving the transducer up and down in the water column in the inclinometer casing.

C.5-New instruments installed at TI in August 2000: A signal well was drilled and installed in a similar manner as the signal well at Camp Hedding. The signal well casing was four-inch ID schedule 40 PVC with two-foot screens installed at depths of 9.5' to 11.5', 19.5' to 21.5' and 29.5' to 31.5' below the ground surface. The screen slots were hand cut with a hacksaw so there was approximately a slot every 0.25 inches. The slots have an approximate width of a #50 slot (0.050-inch) screen. The filter packs and bentonite seals were place in a similar manner as at Camp Hedding (Chapter IV).

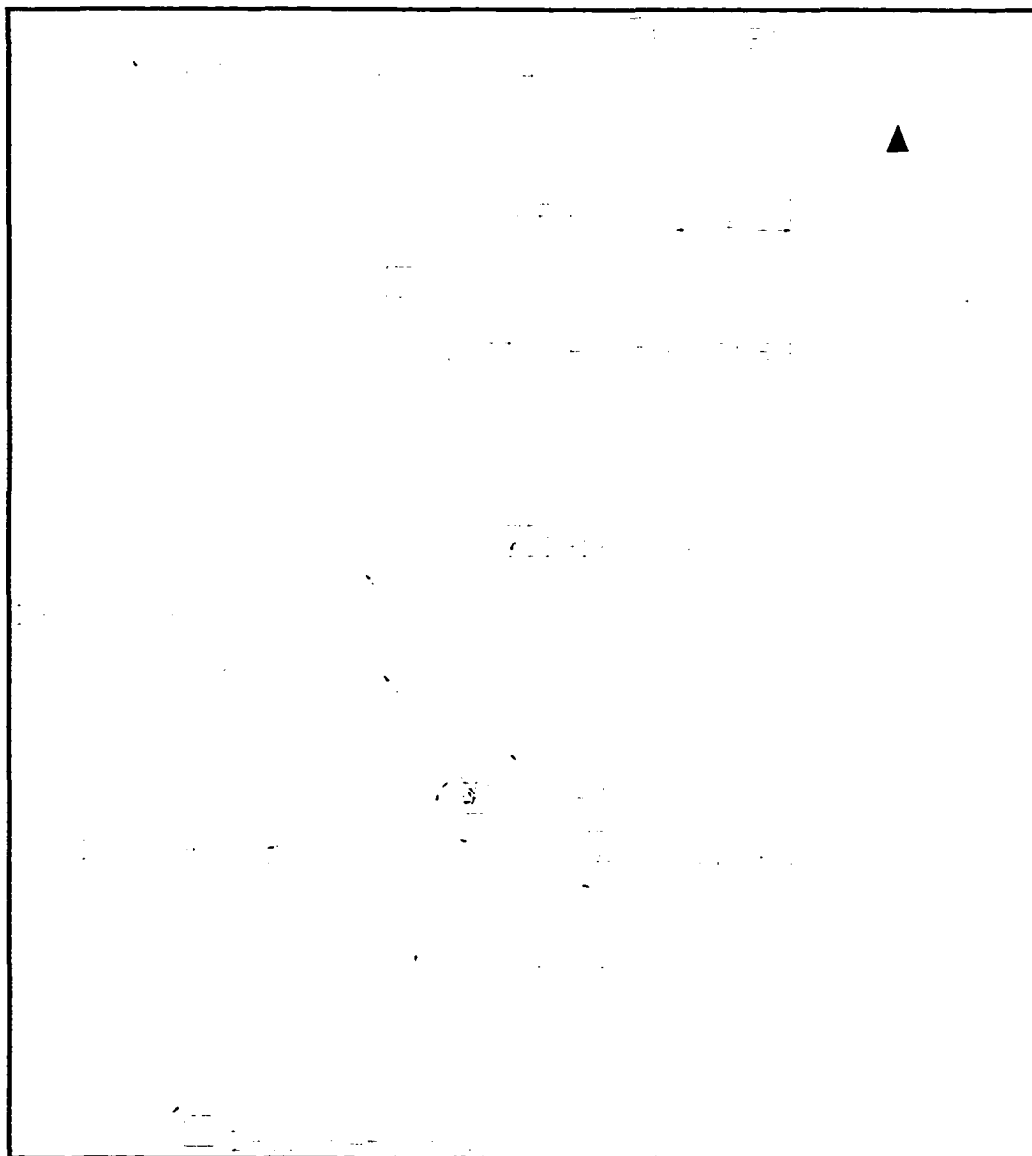


Figure C. 4-Treasure Island: Location map for wells and piezometers, Fire Station Site. Numbers in parentheses are CSMIP piezometer designation.

The Roctest #1 (Rt #1) transducer and drive point was installed 6.4 feet from the signal well. A 4-inch steel casing was advanced to below the water table and then washed out. The casing was filled with water to the top. The saturated Roctest #1 was placed in the casing below the water level in the casing and the protective latex membrane removed below the water surface in the casing. The drive point was advanced to a depth of 20 feet below ground surface. The hydrostatic pressure was checked and found to be consistent with the depth of installation below the water table. After several tests, Roctest #1 was pulled from this location, as it was not responding to the dynamic signal. It was then re-checked for calibration in the inclinometer casing, and then lowered into the inclinometer casing for the last day of testing (August 11, 2000).

The Keller 3 transducer and protective tip were the same design as the Keller 2 installed at Camp Hedding. The hydraulic conductivity of the screen on the protective tip was the same as the screen on the Keller 2 (from falling head tests done in the lab). The Keller 3 transducer was used in three different locations. The first was in the inclinometer casing located 34.3 feet from the signal well. The second location was in the water table well located 6.9 feet horizontally from the signal well. The Keller 3 was finally installed permanently in the same location as the Roctest#1 had been pushed, 6.4 feet horizontally from the signal well and to a depth of 20.5 feet. The installation and construction was the same as the final installation of Keller 2 at Camp Hedding (Location K-4).

C.6-Instruments previously installed at Treasure Island: The existing piezometers and installation were described in section C.4 and Chapter I. Only those Druck transducers

that the State of California, Bureau of Mines and Geology, Strong Motion Instrumentation Program determined were operating correctly were monitored during the signal testing at Treasure Island. These are the Druck installations shown on Figure C.4. Several previous designations have been applied to these transducers. For purposes of this investigation the transducers have been designated D followed with the depth of the screen below the ground surface. The earlier designation is shown in parentheses under the one used in this study.

According to discussion with Al Cramlet of the Strong Motion Instrumentation Program (personal communication, April 9, 2000), a transducer was determined to be operational by comparing current measurements with previous results. It was important that the results for the transducer reflected seasonal changes in water levels. In order to confirm this assumption, a check was made of the expected transducer reading based on the depth to the water table during the testing in August 2000. Table V.1 shows the average voltage reading for the Druck piezometers, the expected hydrostatic pressure reading based on the depth of the water table at that time, and measured pressure reading provided by the previous calibrations of the Druck transducer (de Alba, 1995). All transducers except D-10 show good agreement with the expected pressure reading for the depth of burial. The Druck 33 “near”, D-33 “far”, D-18, and D-17 were providing accurate data for the expected hydrostatic water pressure based on the elevation of the water table.

TABLE C.1
Calibration Check of Piezometers Based on Ambient Conditions

	Druck 33 "far"	Druck 18	Druck 17	Druck 10	Druck 33 "near"
Average background reading (mV)	0.931	0.680	0.679	0.603	0.910
Converted to psi	12.7	5.6	5.6	3.4	12.3
Depth of piezometer below water table (feet)	28	13	12	5	28
Expected pressure reading (psi)	12.1	5.6	5.1	2.1	12.1
Ratio of expected pressure to measured pressure	0.95	1.00	0.93	0.64	0.99

(The average reading is based on the first 30 readings at the start of DATA 10, 8/11/00. The depth of water at the time of the test was 4.7 feet below the ground surface in the signal well. A depth of 5 feet was used to calculate the amount of water above each piezometer.)

The background hydrostatic pressures measured by all piezometers declined slightly during the day of testing on August 11. This is believed related to the decline of the ground water level as the tide lowered during the day.

The work at Treasure Island occurred on August 9, 10, and 11, 2000. The 9th was used for the drilling, logging, and construction of the signal well. August 10th was used to integrate the logging of the in situ Druck piezometers with the LABVIEW system, and logging the advance of the Roctest (Rt#1) 6.4 feet from the signal well. Two tests were made to generate signals. August 11th was the primary day for testing. Table C.2 is the list of data sets that were collected during the August testing at Treasure Island.

Noise was a serious problem during the data logging at Treasure Island. An initial attempt was made to determine if there was less noise using a portable generator or available AC current (Data 1 and 2). The use of the generator produced less noise in the signal than did the AC power. Only Keller 3 and GEMS transducers could be run off the generator. However, the existing Druck transducers were wired in the local electrical system.

The signal generating systems used at Treasure Island was basically the same as that used for Camp Hedding testing described Chapters IV and V. This consisted of raising the hammer to the top of the guide rods then lifting the hammer, guide rods, anvil, NQ rods, and surge block an addition distance. The length of drop of the hammer was 7 feet for all the drops. The anvil drop was 18 inches for all but the last test (Data 14, Test 9) where the anvil drop was increased to 48 inches. The anvil, NQ rods, and surge block were held in place until the hammer hit the anvil by a C-clamp resting on the arrestor. All the tests except the last three used a pelican hook to lift and release the hammer. Tests 6, 7, 8, 9, and 10 used string the raise the hammer and anvil to the proper elevations. The string was then cut to release the hammer.

I.7-Results: No dynamic signal was received by the Druck 10 piezometer. The check made to determine if the piezometer was recording correctly the hydrostatic water pressure (Table 1, above) suggested the piezometer is reporting a value that is only about 64% of the expected pressure for the depth of the piezometer.

TABLE C. 2

Sequence of Testing at Treasure Island, August 10 and 11, 2000

Sequence of Testing at Treasure Island August 10 and 11, 2000	
August 10	
Data 1	Advancing Rt#1 from 7'5" to 10'7"
Data 2	Advancing Rt#1 from 10'7" to 13'11"
Data 3	Advancing Rt#1 from 13'11" to 20'6"
Test 1	5' hammer drop, 18" anvil drop, collection problems with all piezometers
Test 2	No data collected, wiring problem identified.
August 11	
Data 1	Background, house power for all piezometers
Data 2	Background, generator used for Rt#1, GEMS, and Keller #3 piezometers
Data 3, Test 1	7' hammer drop, 18" anvil drop, Keller 3 in inclinometer casing at 36'7", Rt#1 6.4 feet from SW at driven depth of 20'6"
Data 4, Test 2	Same except Keller 3 moved to depth of 25 feet in inclinometer casing.
Data 5, Test 3	Same except Keller 3 in water table well at 7' depth.
Data 6, Test 4	Same, repeat of Test 3
Data 7, Test 5	Same as Test 3 with a two string release of the hammer, anvil still held by C-clamp
Data 9, Test 6	Background with Keller 3 permanently replacing Rt#1 6.4' from SW at depth of 21.5'.
Data 10, Test 7	7' hammer drop, 18" anvil drop, Rt#1 in inclinometer casing at 21 feet.
Data 11, Test 8	Same as test 6
Data 12	Background checking operations of Rt#1 by rising and lowering in inclinometer casing.
Data 13, Test 9	Repeat test 6
Data 14, Test 10	7' hammer drop, 48" anvil drop, and Rt #1 failure.
Data 15	Background end of day.

Note: There is no Data 8.

Table C.2-Sequence of testing at Treasure Island August 10 and 11, 2000

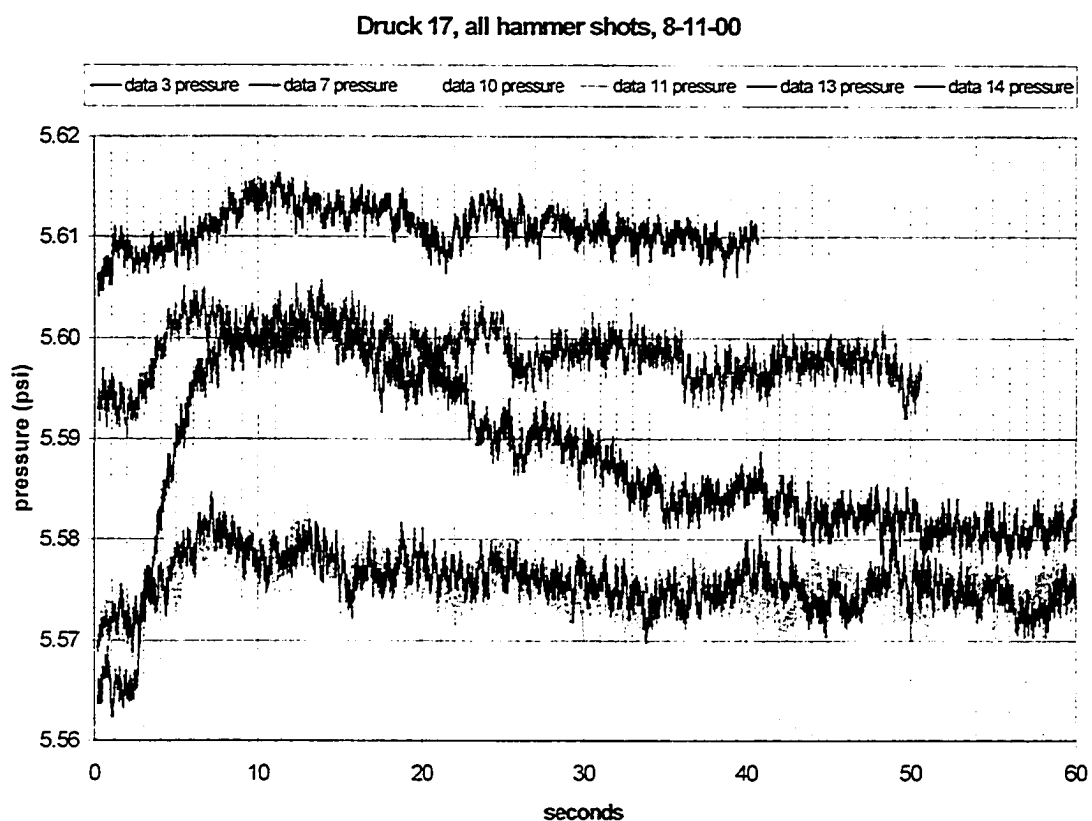


Figure C.5-Druck 17 (D-17) is located 7.7 feet from the signal well and is at a depth of 17 feet bgs. It takes up to 5 seconds for the pressure to rise from background to its peak. The dispersion of the pressure takes several minutes. The initial pressure changed during the day because of tidal changes. Only Data 14 had an anvil drop of 48 inches. All others were with anvil drops of 18 inches.

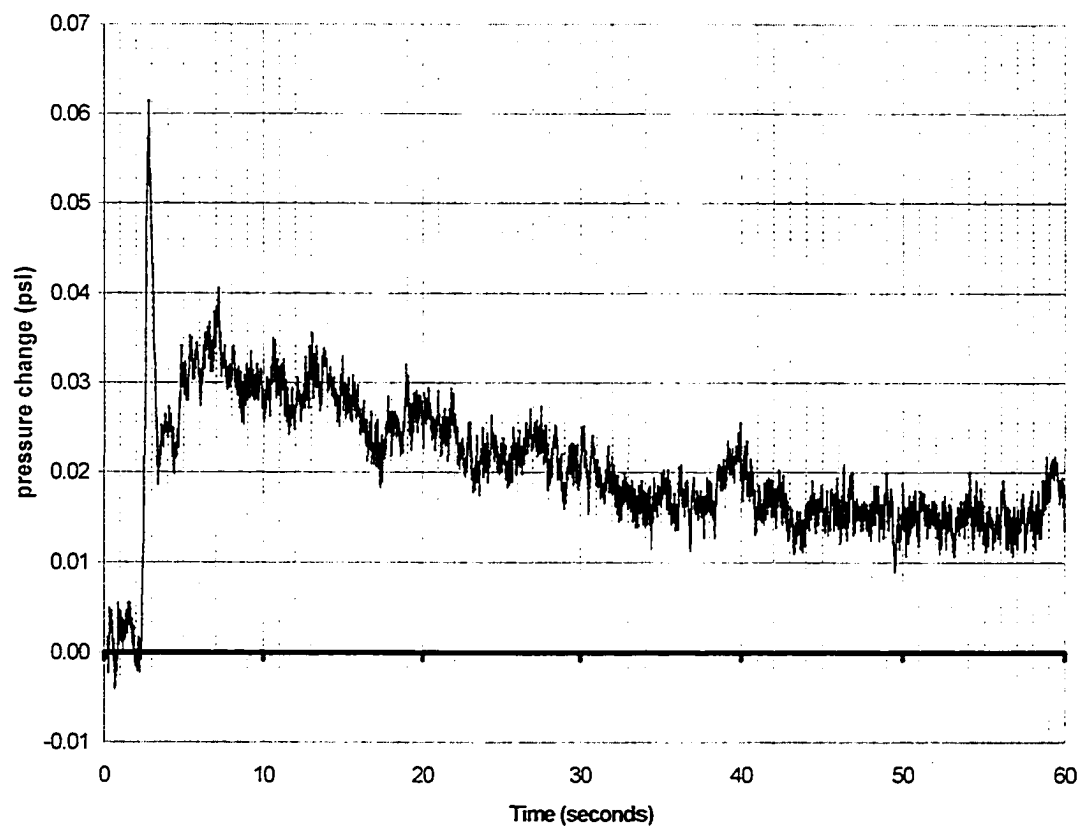


Figure C. 6-Druck 18, Data 14. Hammer drops 7 feet, anvil drop 48 inches. Logging speed is 500 cps. The first sharp rise is the confined pressure wave. The slower rise is the unconfined pressure wave.

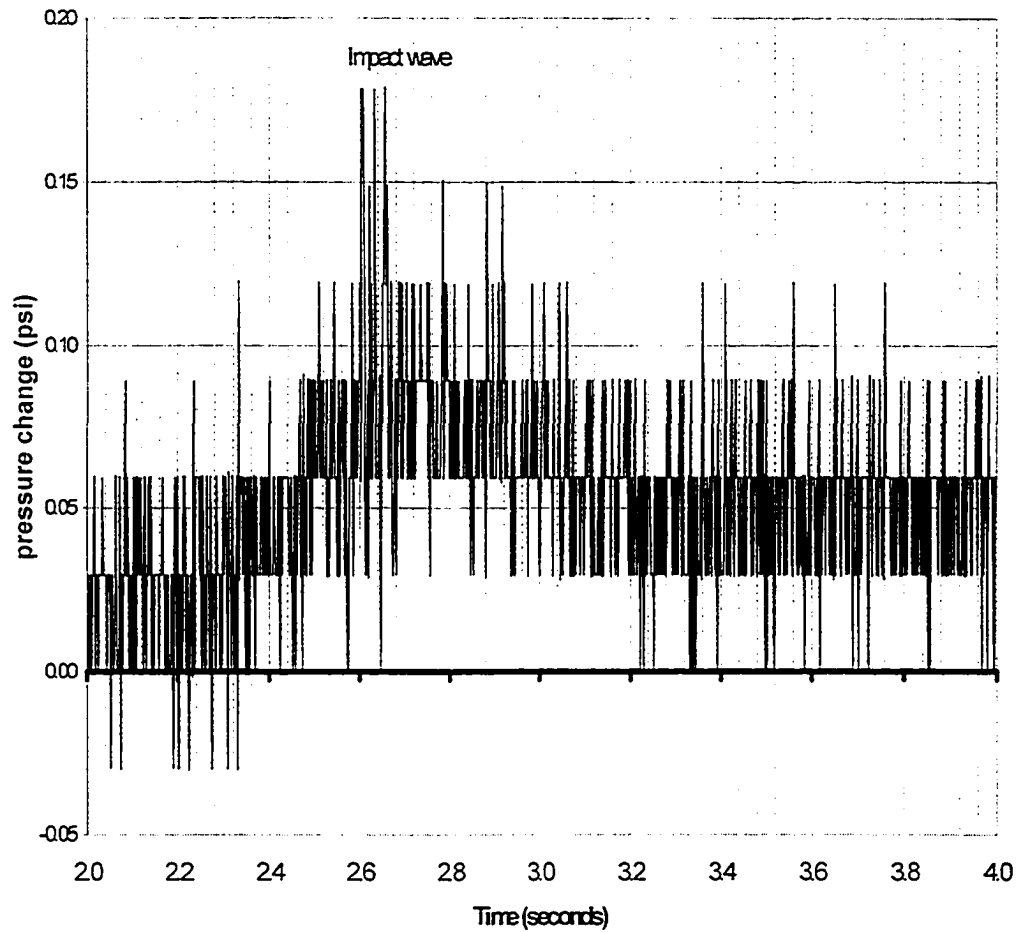


Figure C. 7- Druck 18 (Data 14, 8-11-00) is located 11 feet from the signal well. The impact wave is shown on the unfiltered data. The logging rate was 500 Hz.

The Druck 17 (D-17) is located 7.7 feet from the signal well and at a depth of 17 feet below the ground surface. Figure C.5 are filtered signals for five of the tests recorded with the D-17 on August 11 testing. The rise in the pressure from background to peak in D-17 is over about 5 seconds and dissipated over several minutes. Data 3 was the earliest test and Data 14 was the last test of the day. The background pore pressure recorded prior to each test decreased by about 1 inch during the day. The first four signals recorded by D-17 were for hammer drops of 7 feet and anvil drops of 18 inches. Data 14 was the signal for a hammer drop of 7 feet and an anvil drop of 48 inches. The signal received by D-17 is believed to be entirely the unconfined pressure wave.

The Druck 18 (D-18) is located 11 feet from the signal well and at a depth of 18 feet below the ground surface. Figure C.6 is the filtered signal for D-18 during the 14th test on August 11. There is an initial sharp spike followed by a slower rise over several seconds with a long delay. Figure C.7 shows an enlargement of the sharp peak in the unfiltered data. The initial sharp peak shown on Figure C.6 is a combination of the overlap of the impact wave with the confined pressure wave. The later rise, peaking at about 7 seconds is the unconfined pressure wave, which has a long decay tail. The logging rate is 500 Hz so the impact wave is not well defined. It took several minutes for the pressure to return to background levels.

The Druck 33 “near” is located 10.2 feet from the signal well and at a depth of 33 feet below the ground surface. The data for D-33 “near” is poor. Figure C. 8 shows the results for the D-33 “near” testing on August 11 for data 3 and data 14. It appears that a

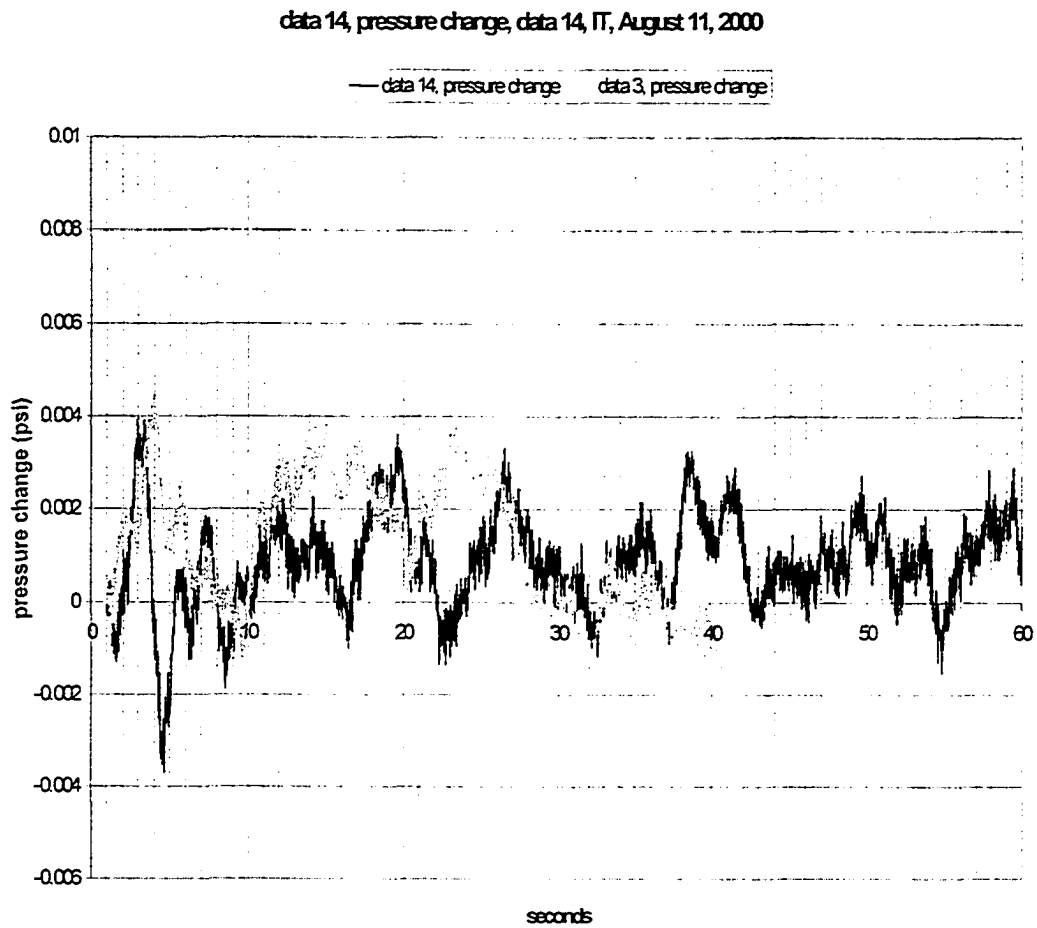


Figure C. 8-Druck 33 “near” is located 10.2 feet from the signal well at a depth of 33 feet bgs. The signal to noise ratio is very high. The sign for both tests appears to occur at about 3 to 4 seconds.

Druck 33 "far", data 14, 8-11-00

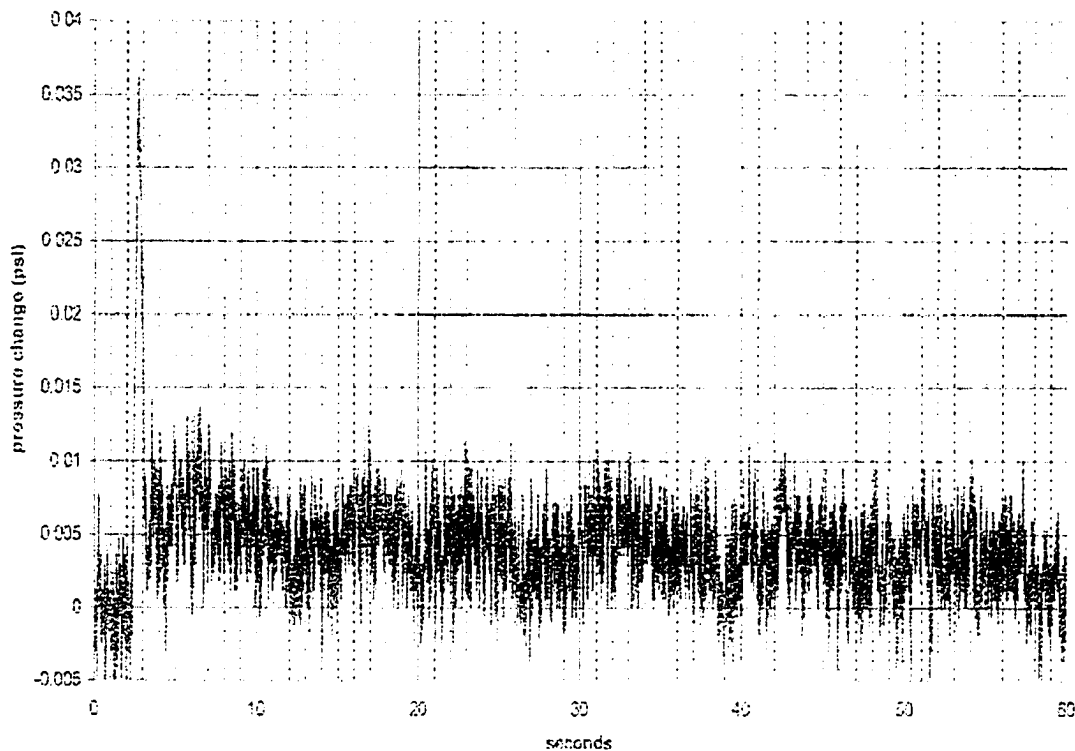


Figure C.9-Druck-33 "far" located 18.5 feet from the signal well and 33 feet bgs. The signal is a combination of a confined pressure wave (peak at 2.8 seconds) and an unconfined pressure wave (peak at about 6 to 7 seconds). The unconfined pressure wave dissipates over several minutes.

peak was detected at about 3 to 4 seconds for both data tests after filtering the data. It is difficult to separate the signal from the background noise. Not much analysis is possible with this high noise to signal ratio. The piezometer appears to be functioning and is likely detecting some signal.

The Druck 33 “far” (D-33 “far”) is located 18.5 feet horizontally from the signal well and about 12.5 feet deeper than the screen being used on the signal well. The signal detected by D-33 “far” shows a well-defined peak with a slight pressure rise following the peak. Data 14 on August 11 for D-33 “far” is shown in Figure C.9.

The Roctest #1 (Rt#1) was installed by pushing at the same location as the Keller 3 was eventually installed, 6.4 feet from the signal well, at a depth of 20.5 feet. The check of the hydrostatic water pressure indicated that Rt#1 provided the expected pressure reading for the depth it was pushed. The Rt#1 at this location did not detect a dynamic signal. Upon removal of the Rt#1, it was observed that the screens of the tip were completely clogged with silt/clay. The clogging on the screens appeared identical to that observed earlier at Camp Hedding. This clogging would have effectively sealed the piezometer tip not allowing rapid response of the transducer inside the screens to changes to pressure in the aquifer. Before test 10, Rt#1's calibration was checked and was determined to be operating correctly and in calibration. The Keller 3 piezometer was placed in inclinometer casing during the early testing on August 11 while testing Rt#1 at the pushed location 6.4 feet from the signal well. Keller

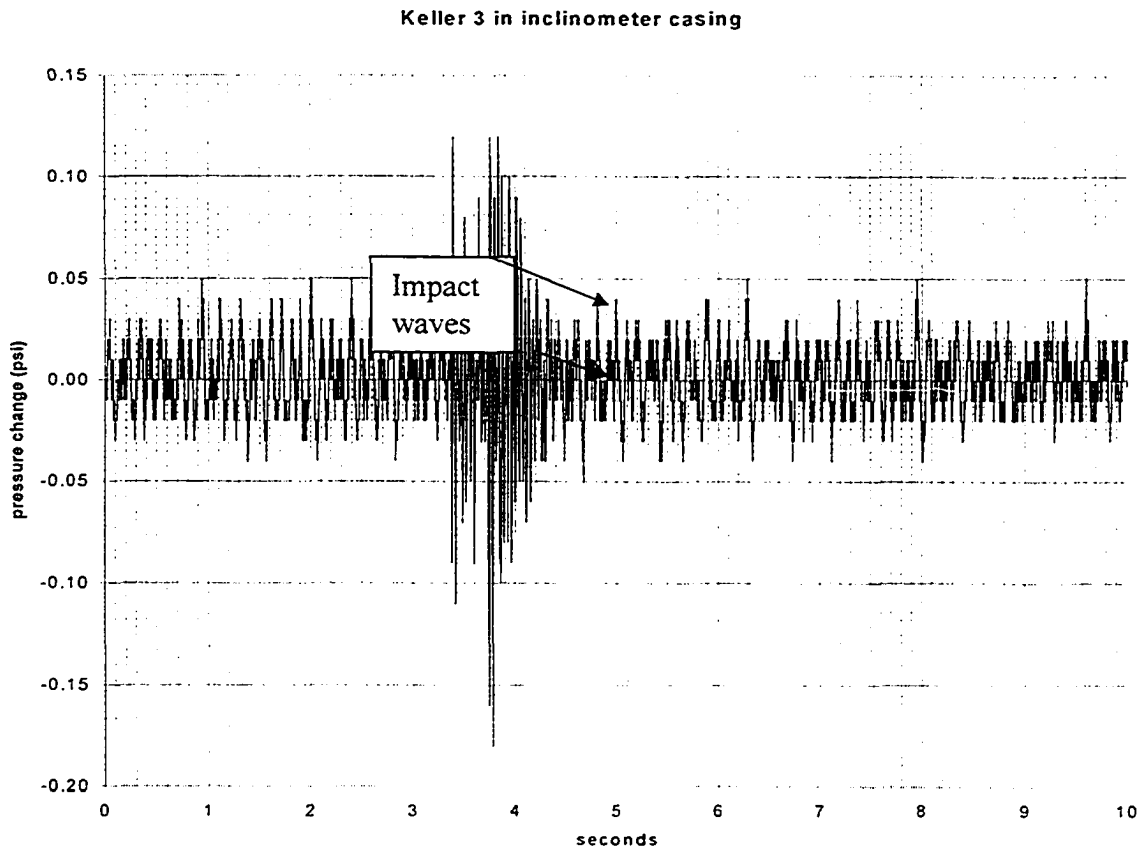


Figure C. 10-Treasure Island, August 2000: Keller 3 transducer in the inclinometer casing 33 feet from the signal well. Only impact waves are detected.

3 was later moved to the water table well 6.9 feet from the signal well and finally installed in the ground at the same location and depth that Rt#1 had previously been pushed. As shown in Figure C.10, the Keller 3 piezometer detected impact waves in the inclinometer hole 34.5 feet from the signal well. At least two cycles of impact wave are indicated. No confined pressure wave appears to have been detected.

The Keller 3 in the water table well, Figure C. 11, also detected two cycles of impact waves. The water table well is located 6.9 feet from the signal well. Again, no confined pressure wave was detected in the water table well. The impact waves detected in both locations has the same characteristics as the impact waves detected in the UNH pool and during the Camp Hedding testing. The two maximums followed by the decay of the cyclic signal are the same as seen in the pool testing (Chapter III) and are probably related to the multiple impacts of the hammer and anvil during each test.

The character of the detected signal changed considerable when the Keller 3 is installed in a filter pack at a new location 6.4 feet from the signal well (same location that Rt#1 was pushed in the earlier testing). The signal received by Keller 3, Figure C.12, is a very sharp spike with a long decay. It takes several minutes for the pressure to return to background. Details of the peak (Figure C.13) show that the peak has a spike at 2.6 seconds that probably reflects an impact wave. The earlier peak at 2.32 seconds suggests an impact wave but does not have the amplitude normally associated with the impact wave at this distance from the signal well. The logging rate for this signal is 500 Hz,

Keller 3, in the water table well, data 7, at 7 below ground surface

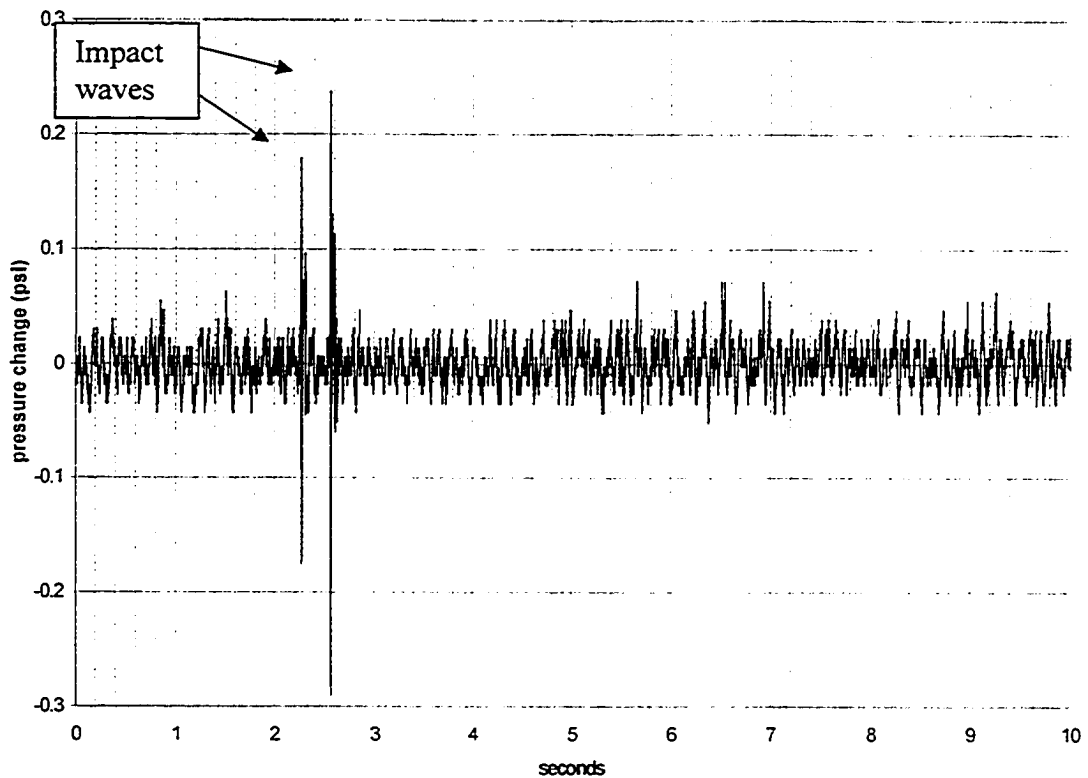


Figure C.11-Keller 3 located at a depth of 7 feet in the water table well. The water table well is located 6.9 feet from the signal well. Two impact waves are detected.

KELLER3, in new boring 6.4 feet from signal well, data 14

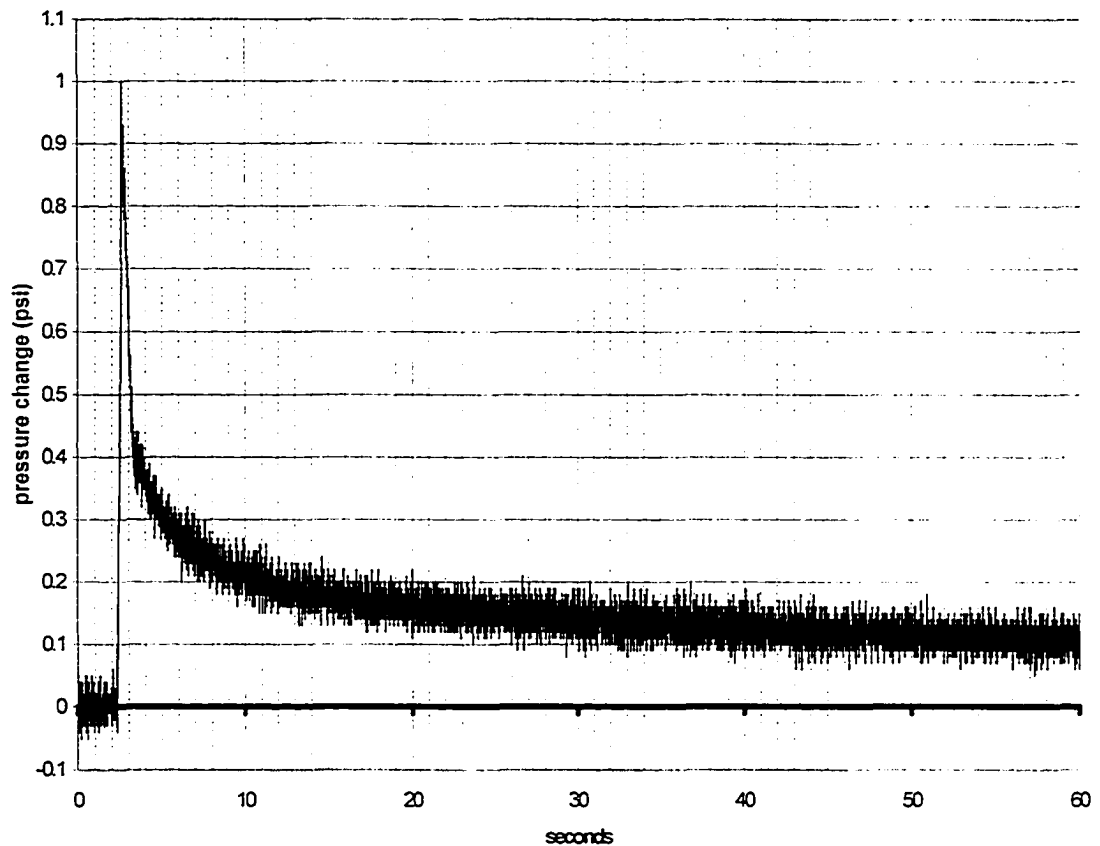


Figure C.12-Keller 3 piezometer is located in the new boring 6.4 feet from the signal well. This is the same location and depth Rt #1 had previously been located in earlier tests. The long decay curve takes several minutes to return to background levels. Details of the peak that occurs at 2.5 second are shown in Figure C.14.

KELLER 3, in new boring, data 14, expanded time scale

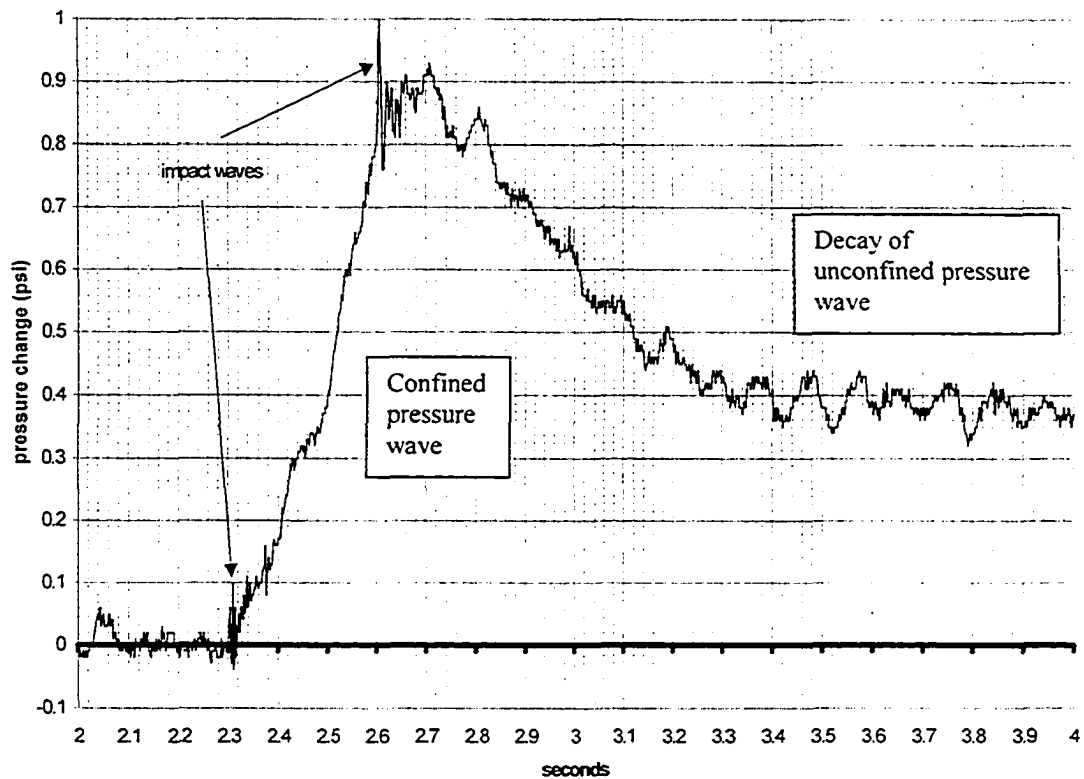


Figure C. 13-Enlargement of the large spike shown on Figure C.12. The impact waves are superimposed on the confined pressure wave signal and the maximum of the unconfined pressure wave is probably masked by the confined pressure wave. The long decay curve is probably the decay of the unconfined pressure wave. The proximity of the Keller 3 to the signal well causes all the signals to overlap.

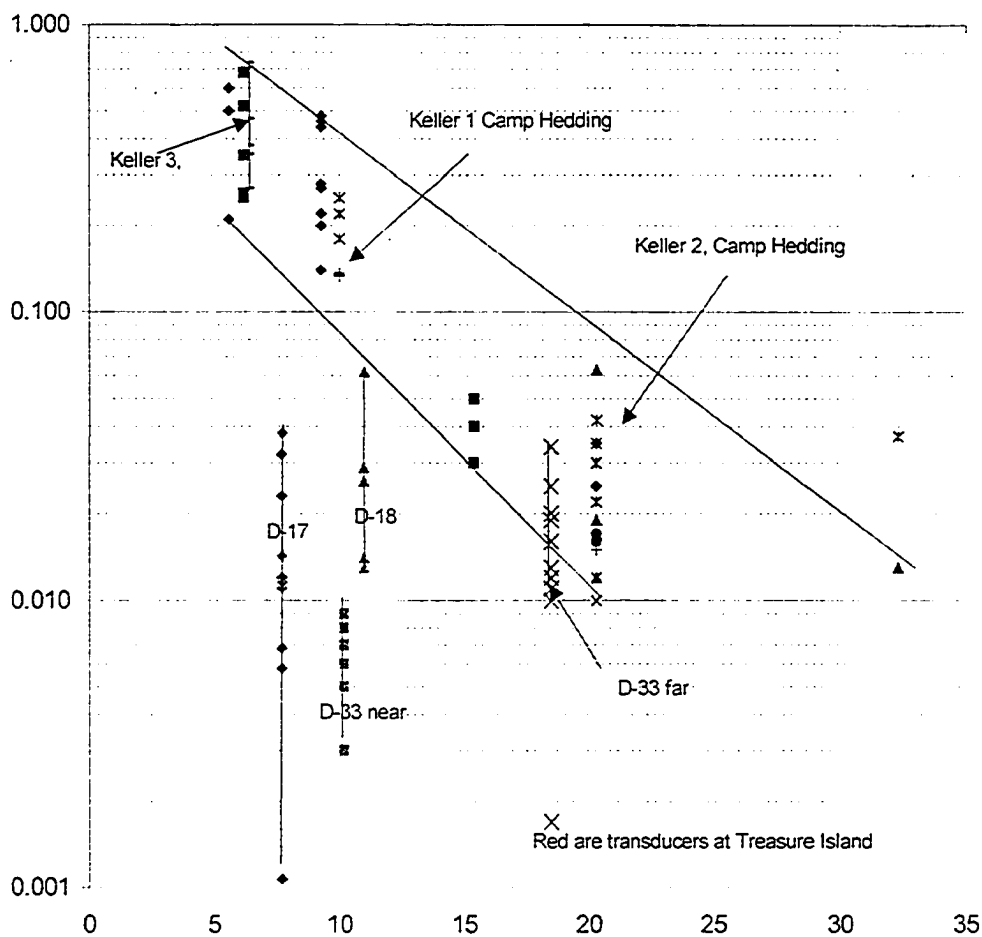


Figure C. 14- Change of signal strength with distance from the signal well. D-17 is probably just the confined pressure wave. D-33 “near” has very noisy signals. The data from Camp Hedding testing includes the data shown on Figure IV.10 for the April 2000 testing. Treasure Island data for Keller 3 and D-33 “far” generally fall in the same range of data as the data from Camp Hedding. The diagonal lines define the range of data from testing at Camp Hedding.

which is too slow for obtaining details of the impact wave. The most likely interpretation of the signal is two impact waves superimposed on a confined pressure wave with the unconfined pressure wave masked by the confined pressure wave. The long exponential decay is probably due to the unconfined pressure wave.

Figure C. 14 summarizes the signal strength of the confined pressure wave in psi (log scale) against the distance from the signal well. The lines bracket the range of data from Camp Hedding testing for each distance. The Keller 3 data fit the Camp Hedding data. D-33 “far”, at 18.5 feet also fit the data from Camp Hedding. D-17, D-33 “near”, and D-18 fall below the expect range of pressures for the distance from the source. It should be noted that Kellers 1, 2, and 3 are installed in filters packs.

C.8-Tentative conclusions based on August testing at TI: D-17 did not detect the impact wave or the confined pressure wave while it did detect the unconfined pressure wave. Of the Druck piezometers installed at Treasure Island, it appears D-33 “far” is detecting the impact wave as well as the confined pressure wave within the range of values consistent with those detected at Camp Hedding. D-18 and D-33 “far” are capable of detecting both the high frequency signal of the impact wave and the lower frequency signal of the confined pressure wave. D-18, D-33 “near”, and D-17 have responses well below the response expected for transducers at comparable distances at Camp Hedding. It is possible the differences are related to the sediments in which the piezometer are installed, to clogging of the screens over time after installation of the piezometers, and/or clogging during the pushing of the piezometer into place during initial piezometer

installation. From the available data collected in August 2000, it is not possible to assess the cause for the lower response of these piezometers.

The installation of the Rt#1 at both Camp Hedding and TI indicated that a piezometer advanced by pushing has a good chance of becoming clogged during installation. Two of the three occasions where Rt#1 was pushed at Camp Hedding (including an attempt in November 2000), the installation of Keller 2 at location K-1 at Camp Hedding, and the one installation of the Rt#1 at TI resulted in no responses or muted responses of the piezometer to rapid pressure changes created by the signal generation system (either the impact wave or the confined pressure wave). This is a high percentage of failure for pushed installations. Even when the screens were evidently clogged, as was observed when Rt#1 was retrieved at both TI and Camp Hedding, these pushed piezometers could successfully detect hydrostatic water pressures for the depth of installation. Therefore, using the response of the piezometer to changes in the hydrostatic water pressure as an indication of the ability of the piezometer to detect earthquake-like pore pressure changes is not valid for checking the health of an in situ piezometer.

C.5-Recommended changes based on testing at TI: The failure to correctly wire the GEMS pressure transducer emphasized the need to obtain a means for measuring the pressure inside the signal well screen and to provide a reliable starting time for the generation of pressure.

Discussion with the driller on-site emphasized the need for a consistent means for releasing the hammer. Based on these discussions it was decided to revisit the use of string to lift the hammer and to hold the surge block and anvil with string while the hammer is dropped. Cutting the string minimized the swing of the hammer created when the pelican hook was used to release the hammer. Starting with Data 7 on August 11, the hammer was raised by the use of string. The surge block and anvil were held by the C-clamp resting on the arrestor until the falling hammer struck the anvil.

APPENDIX D

CAMP HEDDING TESTING, NOVEMBER AND DECEMBER 2000

D.1-Objectives: The objectives for the November and December testing at Camp Hedding were to:

- 1) install a new piezometer midway between the signal well and Keller 2 in order to determine the velocity of travel of the impact wave and confined pressure wave,
- 2) investigate clogging of the Rt #1 screens during pushing,
- 3) change the mechanism of releasing the hammer and holding the anvil,
- 4) replace the packer with 3" PVC pipe to simplify the equipment, and
- 5) determine the pressure created within the well screen during a hammer drop.

D.2-New instruments installed: A new piezometer was installed 10 feet from the signal well. The location was midway between the signal well and the location of Keller 2 (see Figure A.4). A 3-inch ID PVC casing was wash bored to a depth of 10 feet. The casing was kept full of water at all times. The screens on the Rt#1 tip had previously been saturated and brought to the field under deair water. The Rt #1 piezometer was assembled under water in the casing and advanced by pushing to a depth of 20.5 feet below the top of ground. A check was made to insure that the piezometer was measuring the correct hydrostatic pressure at 20.5 feet. After reaching the desired depth, a number of signals were generated. No signal was detected by Rt #1 piezometer while other piezometers being used detected signals generated by the system. The Rt #1 was removed from the ground. The screens were found to be covered with silt/clay (Figure D.1).

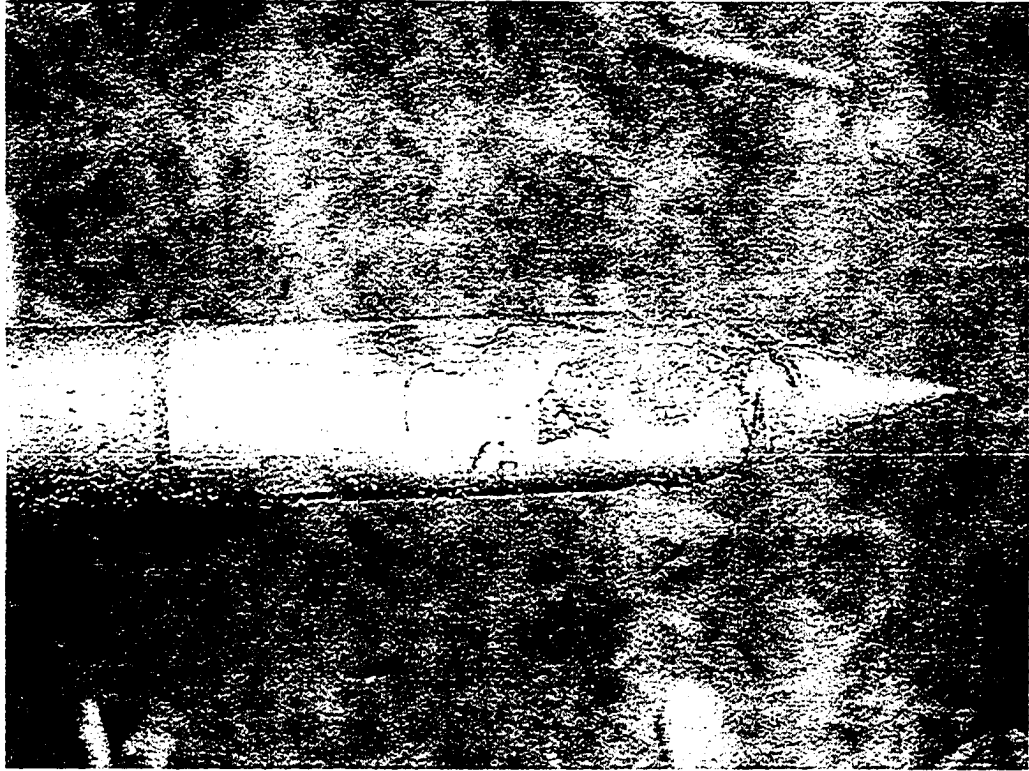


Figure D.1- The screen of Roctest #1 was clogged with silt/clay after being advanced to a depth of 20.5 feet. The starting depth for advancing the tip was 10 feet bgs. Hydrostatic water pressures could be measured but no dynamic signal was detected at this location.

The Keller 1 transducer and protective tip originally used in the pressure vessel testing were modified for use in the field. The lab protective tip was as shown in Figure II.5 for the pressure vessel testing earlier. This tip would not allow access and testing of the screens once installed in the field. Therefore, modifications were made to the tip (similar to the protective tip shown in Figure II.5) to provide access to the tip once installed. This was done by adding an additional 6-inch screen length to the protective tip with an access port drilled into the side of the new tip. A tube with a check valve was run from the access port to the ground surface, Figure D.2. The steel rod that was used to advance

the transducer when it was pushed into the pressure vessel was retained even though the method of installation no longer required pushing the transducer or tip.

In order to install the Keller 1, NQ casing was advanced though the bottom of the 3-inch PVC casing. The NQ casing was pushed 2 feet then washed out. Alternating pushing and washing was continued until the bottom of the casing was 20 feet below ground surface. The sand below the casing was washed out to a depth of 21.5 feet bgs. The hole below the casing stayed open therefore it was not necessary to advance the NQ casing further.

The screens on the Keller 1 were saturated as described earlier. The protective tips were brought to the field in deaired water and in protective membranes. The two protective tips were assembled to form the piezometer in the field. The assembly took place in the 3-inch casing below the water level in the casing. The protective membranes were not removed from the tips until both were below the water level in the 3-inch casing. After assembly, the Keller 1 was lowered through the middle of the NQ casing to the

open boring below the bottom of the casing. A filter pack was placed around the piezometer to hold it upright. The filter pack was poured into the NQ casing and then tamped with a half-inch fiberglass rod. Volume of material was accounted for as it was poured into the casing so that an approximate depth of the filter pack was known. This was confirmed during the tamping of the filter pack. This insured that no bridging was occurring in the NQ casing. The filter pack was added until there was a foot of filter material above the piezometer and the filter pack extended into the bottom of the NQ

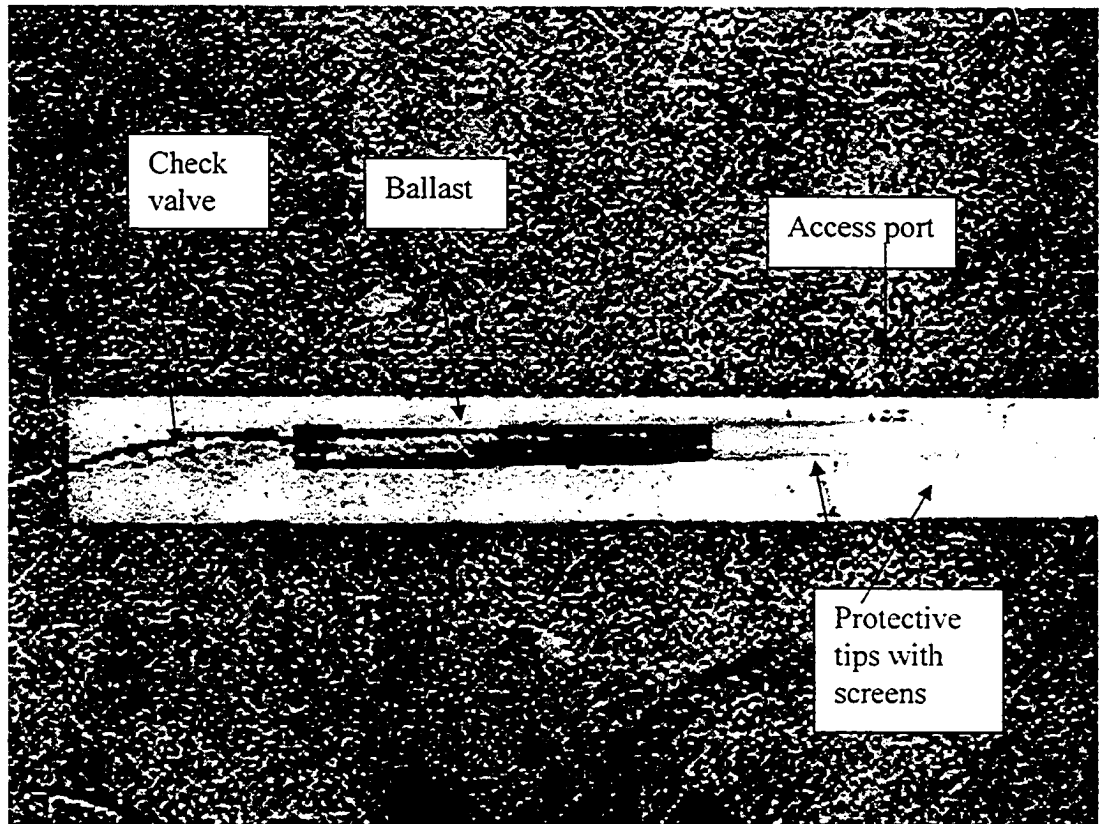


Figure D.2-The Keller 1 transducer and protective tip were modified for installation at Camp Hedding 10 feet from the signal well.

casing. Bentonite chips were added above the filter. The casing was pulled back and additional chips added until there were 3 feet of bentonite above the filter pack. The bentonite chips were also tamped as they were added and the volume of chips added was compared to the elevation at which the tamping was occurring. The NQ rods were then removed and the native sediments allowed to fill the boring. The tip was then developed (Figure D.3) by the injection of deaired water through the tip.

D.3-Modifications to hammer drop and signal well: In all the tests in November and December 2000 the anvil and surge block were held by strings until the impact of the falling hammer on the anvil broke the strings (Figure D.4). The hammer was lifted by strings and its release was achieved by cutting the strings holding the hammer (Figure D.5). The chain that had previously been used to lift the hammer was removed. The hammer drop could now be increased to eight feet by the addition of 2 more feet of AW rod to the guide rods. A 3-inch PVC plug replaced the inflatable packer previously used below the screened interval in the signal well. An assembly of 3-inch ID schedule 40 PVC pipes was lowered into the 4-inch signal well casing. The amount of 3-inch PVC pipe necessary to fill the casing from the bottom of the screen to the bottom of the signal well was placed in the signal well. A screw-on cap with a coupling for a 1" pipe was placed on the top of the 3-inch pipe. The pipe assembly was lowered and raised in the casing by the 1" pipes. The 1" pipes were removed during testing. This eliminated the many problems associated with the packer pressure line passing up through the middle of the NQ rods and out the top of the guide rod to the pressure tank. The signals

recorded by the piezometers were the same as previously recorded in the April and June/July 2000 testing at Camp Hedding.

D.4-Measuring pressure inside the signal well screen during hammer drops: Two different transducers were used in an attempt to measure the source pressures in the signal well. The GEMS transducer was used inside the signal well to measure the pressure. It was found, however, that it was possible to obtain only 1 or 2 tests a day from the GEMS before reliable signals could no longer be detected from the transducer. Drying the transducer out overnight restored the signal. Several different types of sealant were used in an attempt to prevent the wiring from becoming wet during impact of the hammer. The performance of the transducer deteriorated over time and it finally stopped working all together. The magnitude of the measured signals from this transducer are considered suspect. However, the signal from the GEMS transducer provided accurate determination of the start time for the impact of the hammer.

The second transducer used in the signal well was a PCB blast transducer (Model: W138A05/038CY050AC, Type: ICP, S/N 5206: used with Model 482A21 line power signal conditioner). It is a piezoelectric device that generates a current when the tourmaline crystal is caused to flex due to a rapid pressure change. The PCB was not designed to provide data on hydrostatic water pressure but would record dynamic pressure changes applied to the transducer.

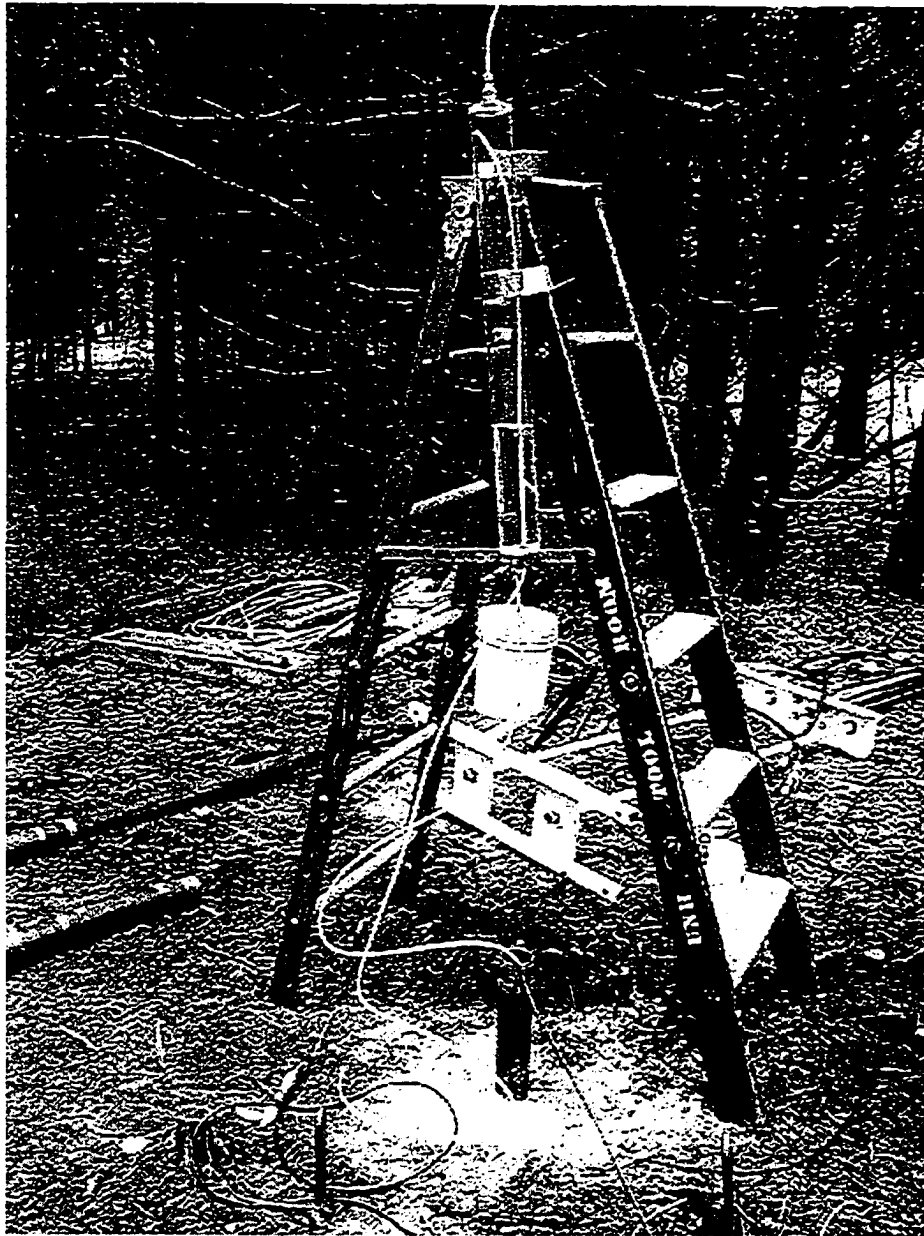


Figure D.3- The Keller 1 piezometer was developed by the injection of deaired water through the screens. Falling head tests were also performed using the access tube.



Figure D.4-The arrangement of strings used to lift and hold the 140 lb. SPT hammer. Another set of strings, attached to the horizontal rod through the top of the AW rod, held the surge block/anvil while the hammer dropped. The strings holding the surge block/anvil were broken when the hammer struck the anvil. The cable to the GEMS transducer emerges from the center of the AW guide rods.

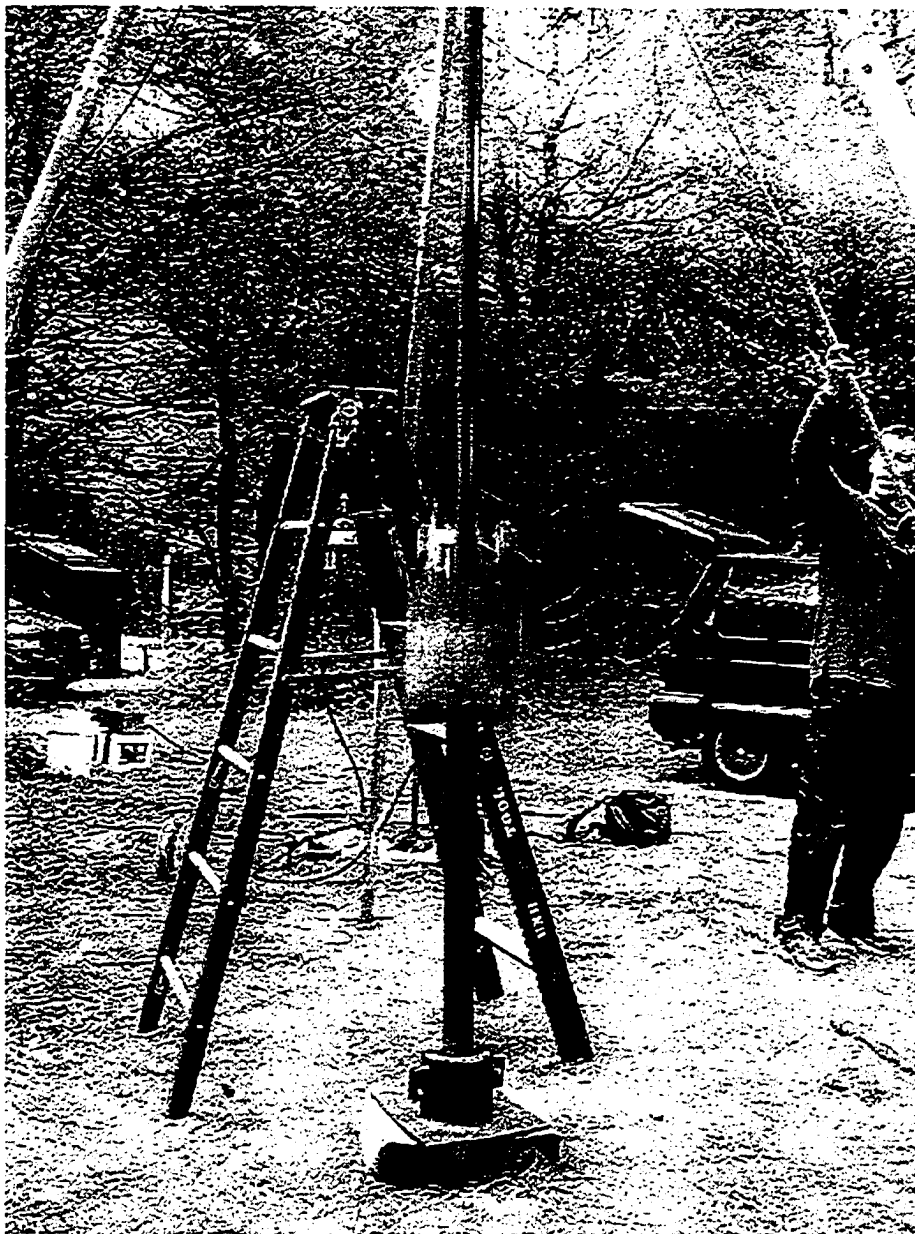


Figure D.5-Impact of hammer on anvil.

A calibration curve for the PCB transducer was provided with the transducer. The calibration of the transducer was checked in the lab by making rapid changes in pressure. In the field, the operation of the PCB transducer was checked by rapidly lowering the transducer to prescribed depths. In both cases, it was possible to confirm the calibration provided with the transducer.

The PCB transducer was initially placed in the open PVC well while the GEMS was being used in the signal well. After the GEMS failed, the PCB was placed in the signal well through the middle of the NQ rods (Figure D.6).

D.5-Results of measuring pressure inside the well screen in the signal well: The GEMS transducer provided data for some of the hammer drops during the tests in November. Several things appeared to occur to the transducer over time. There was a progressive drift of the base voltage reading, requiring progressive recalibration of the transducer after use. The slope of the calibration curve remained the same however. Apparently, as the transducer's electronics became wet during testing, the resulting signal underwent significant changes. This is shown in the series of signals figures from testing on 11-28-00. Figure D.7 has an initial oscillating signal at the beginning that goes from -770 psi to 420 psi. The full range of this signal is about 1200 psi. The signal remains negative

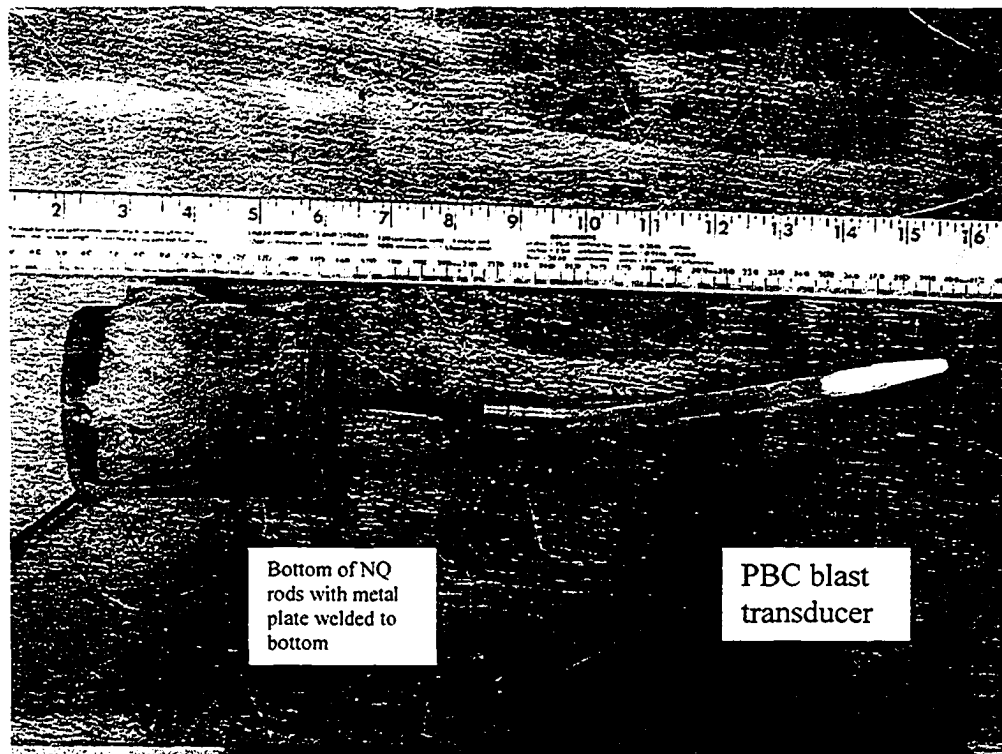


Figure D.6-The PCB transducer exited the bottom of the NQ rods through hole in the bottom plate. The transducer is suspended within the screened interval of the signal well below the surge block and above the 3 inch PVC plug.

as it decays back to zero. Figure D.8 shows a similar oscillating signal at the start but the pressure remains positive as it decays. As seen on both figures the base of the signal was shifted upward and did not return to the previous zero reading. The full range of the oscillations is about 1060 psi. Figure D.9 shows a large increase in the noise before the hammer impact. A sharp positive peak of about 1330 psi occurs with the impact of the hammer on the anvil. The decay is rapid compared to the earlier tests. No signal was detected by the GEMS piezometer on the last test on 11-28-00.

The one constant between the tests where a signal was detected is the large spike of about 1100 to 1200 psi. This would seem to be in agreement with values measured by the Rt #2 in the pool testing. The oscillation of the signal shown in Figures D.7 and D.8 would be consistent with a compressional wave traveling down the rods after impact. It is suspected the GEMS was failing during test 4 shown on Figure D.9.

The initial reading received by the PCB in the open PVC well seemed exaggerated. The recorded signal, Figure D.10, suggested a pressure change of up to 190 psi was being received. The transducer was returned to the company to check the calibration. They confirmed that the calibration included with the transducer was correct. The same pulse was recorded a few weeks later. The PCB transducer was moved to the screen of the signal well to record the pressures developed during the hammer drop. Figure D.11A (Data 2 on 12/6/00) is an example of signal recorded in the signal well. The pressure recorded full-scale (10 volts) 0.0008 seconds after hammer impact. A second large impact was recorded 0.17 seconds after the first. Full-scale reading would require a pressure of about 9100-psi according to the calibration curve. Other impacts record nearly identical signals but with the opposite sign. Figure D.11B for earlier tests is an example of recording in the opposite direction. Both signals go full scale of ± 10 volts corresponding to ± 9090 psi according to the calibration curve. This is far in excess of anything expected. It is believed that the PVC well casing would have failed under such pressures. The overburden pressure at 20.5 feet would be about 11 psi. There seems to

Pressures recorded by PCB and GEMS transducer, Data 2, 11-28-00

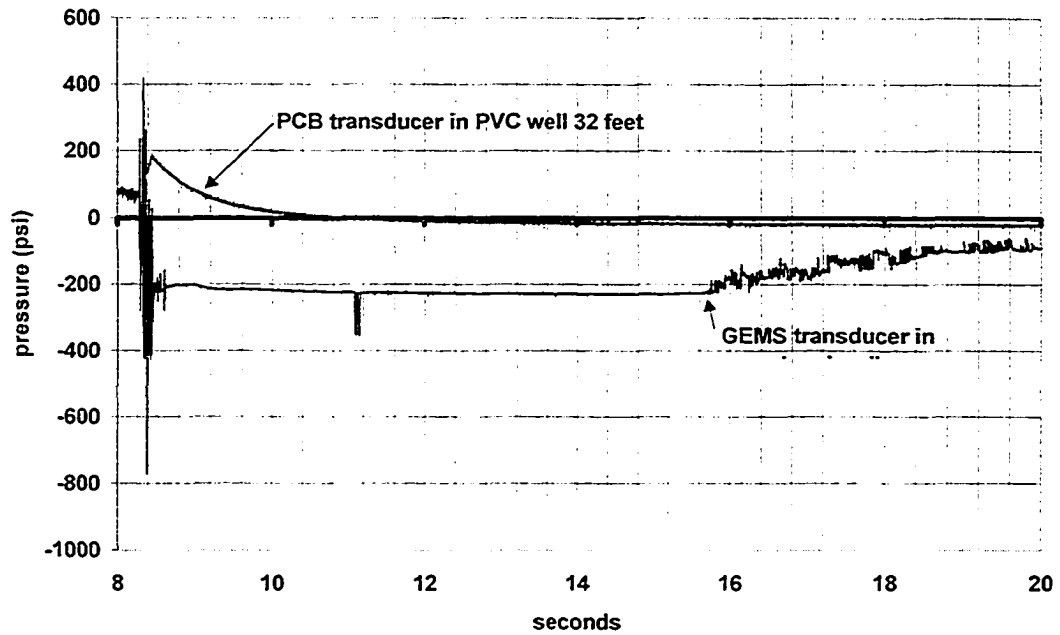


Figure D.7- The responses of the PCB transducer located in the PCB well and the GEMS transducer located in the signal well are compared. The PCB signal occurs 0.005 to 0.007 seconds after the GEMS signal begins.

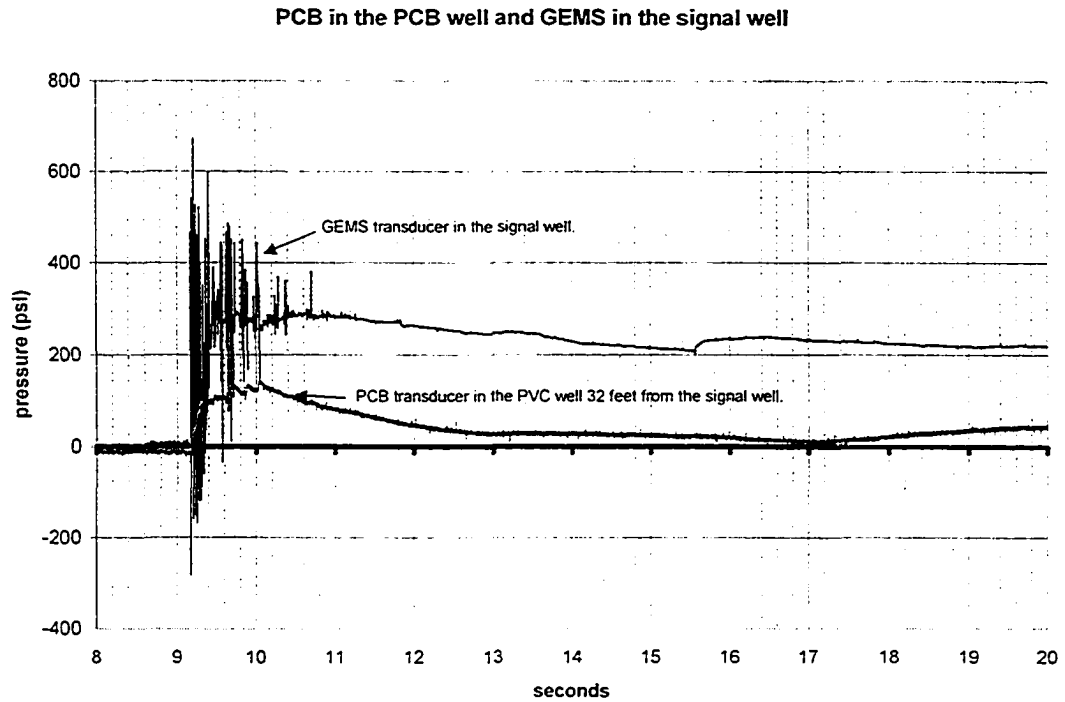


Figure D.8- Responses of the PCB transducer in the PVC well and the GEMS transducer in the signal well are compared. The time between the arrival at the PVC well and the start of the signal at the GEMS is about 0.008 seconds.

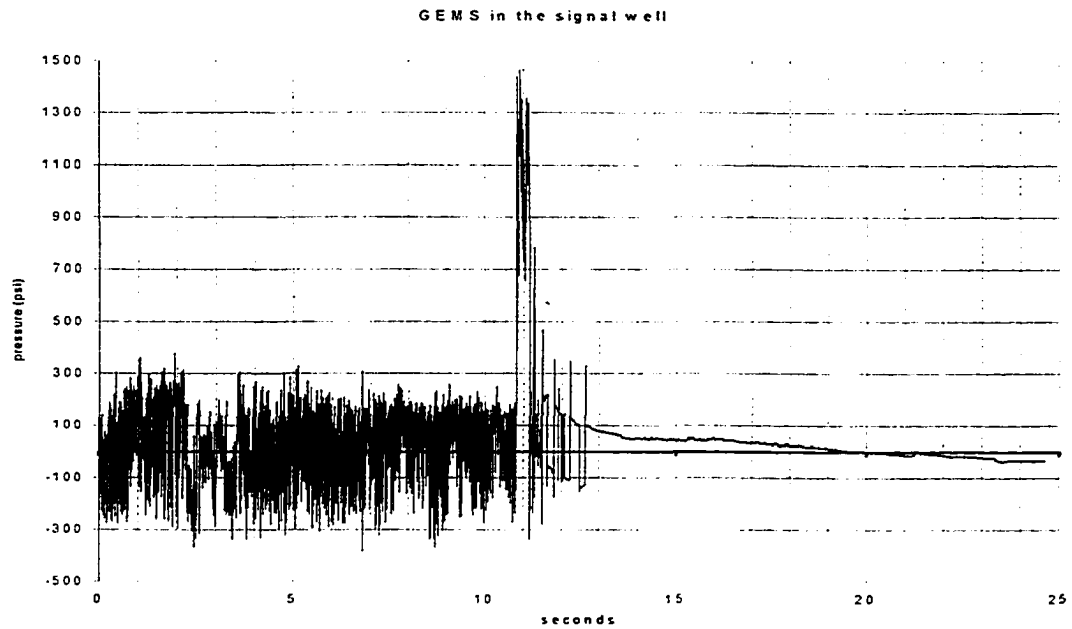


Figure D.9- The response of the GEMS transducer in the signal well.

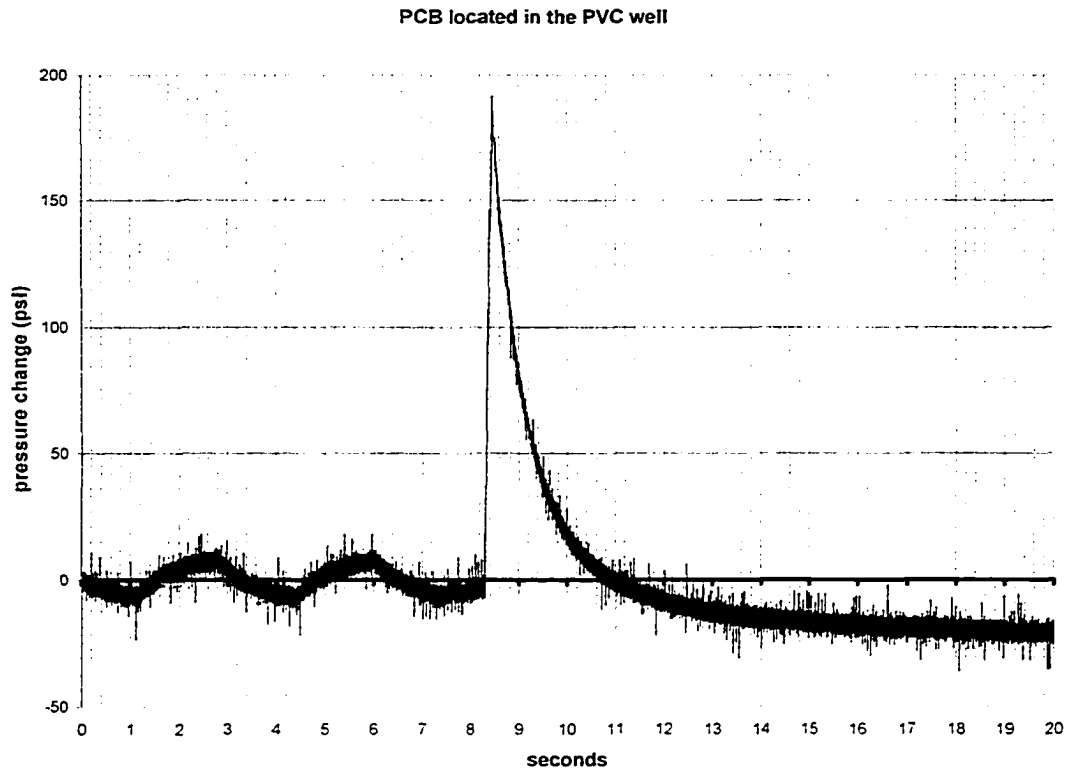


Figure D.10-Response of the PCB transducer located in the PVC well 32 feet from the signal well.

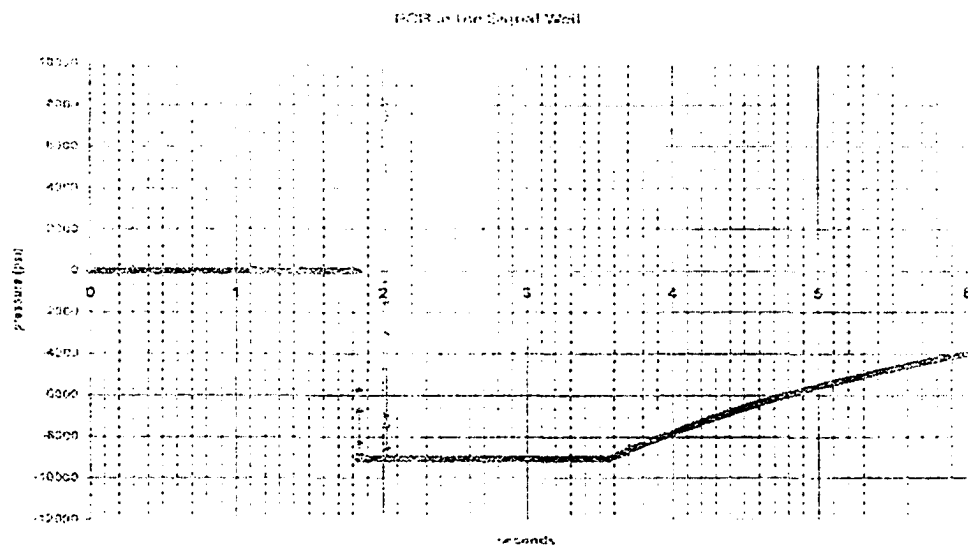
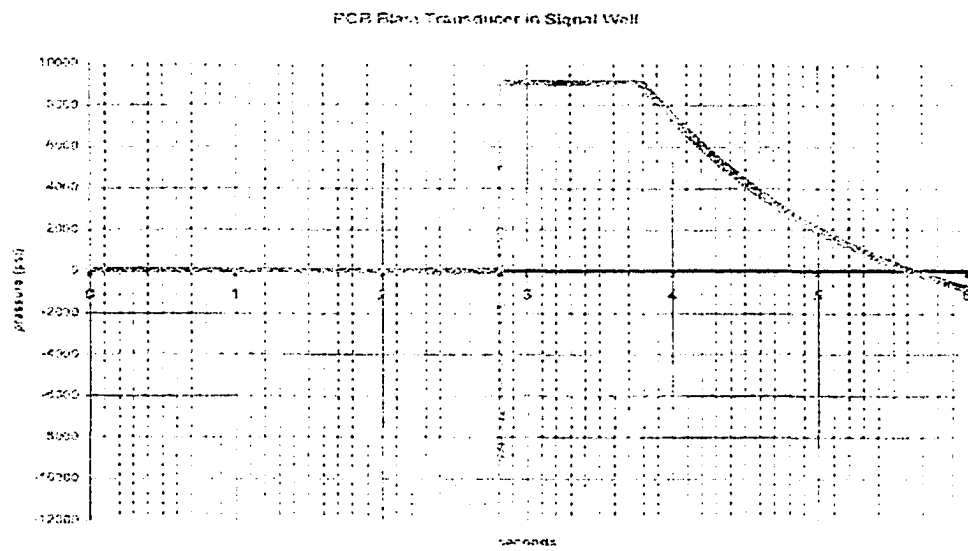


Figure D.11- Differences in the response of PCB transducer located in the signal well.

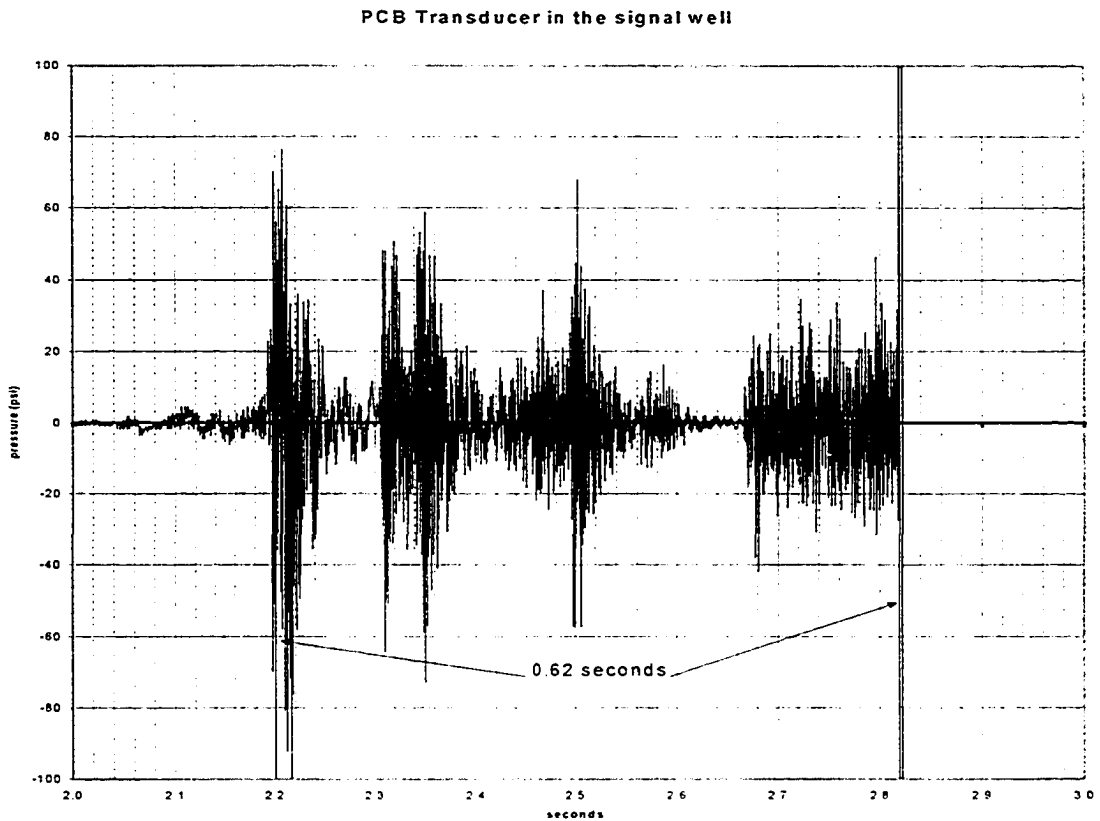


Figure D.12- The response of the PCB blast transducer located in the signal well. The initial 0.62 seconds corresponds to the time required for the hammer to drop after the string hold it was cut until it hits the anvil. This corresponds to 17 frames on the video of the drop.

be too much response for the system. However, the PCB transducer does provide a clear signal for the start of the pressure rise in the signal well.

An expansion of the initial part of the Figure D.11A, between 2.2 seconds and 2.8 seconds, is shown in Figure D.12. This interval corresponds to the travel of the hammer from the time of release until the impact with the anvil. The time for this travel time

corresponds well with the time interval suggested by counting frames on the video of the hammer drop. It takes about 17 frames for the hammer to reach the anvil or about 0.57 to 0.63 seconds (17/30 to 19/30 seconds, at 30 frames per second). Figure D.12 indicates 0.62 seconds for the hammer to reach the anvil. The first 0.62 seconds of the signal, prior to the large impulse at 2.82 seconds, is “rattling” of the hammer on the guide rods as the hammer drops. The impact or time where $t=0$ is at 2.82 seconds. It is not clear what pressures the PCB transducer is measuring. The pressures measured in the PVC well and in the signal well bear no relationship to pressures measured by other instruments placed in the same locations (Rt #2, GEMS, or Validyne).

D.6-In ground piezometer results: Keller 1 was installed 10 feet from the signal well. Figure D.13 is an example of an unfiltered signal received by the Keller 1 piezometer located ten feet for the signal well. The unfiltered signal is dominated by the two impact waves of the hammer and anvil. The first impact wave arrives before the confined pressure wave and the second impact wave overlaps with the confined pressure wave. Figure D.14 is the filtered signal showing the confined pressure wave. Only the slight dip at 1.83 seconds and at 2.23 seconds remain of the impact wave after filtering. The logging rate for these signals is 5000 Hz. The water pressure returns to background at about 5.6 seconds for a total pulse length of about 3.5 seconds.

The reproducibility of the signal by the Keller 1 piezometer is quite good. Figure D.15 is the results of five hammer drops on 11-15-00. Three of the five tests have nearly identical shapes and pressures developed. The other two tests have lower pressures

Keller 1, 10 feet from signal well

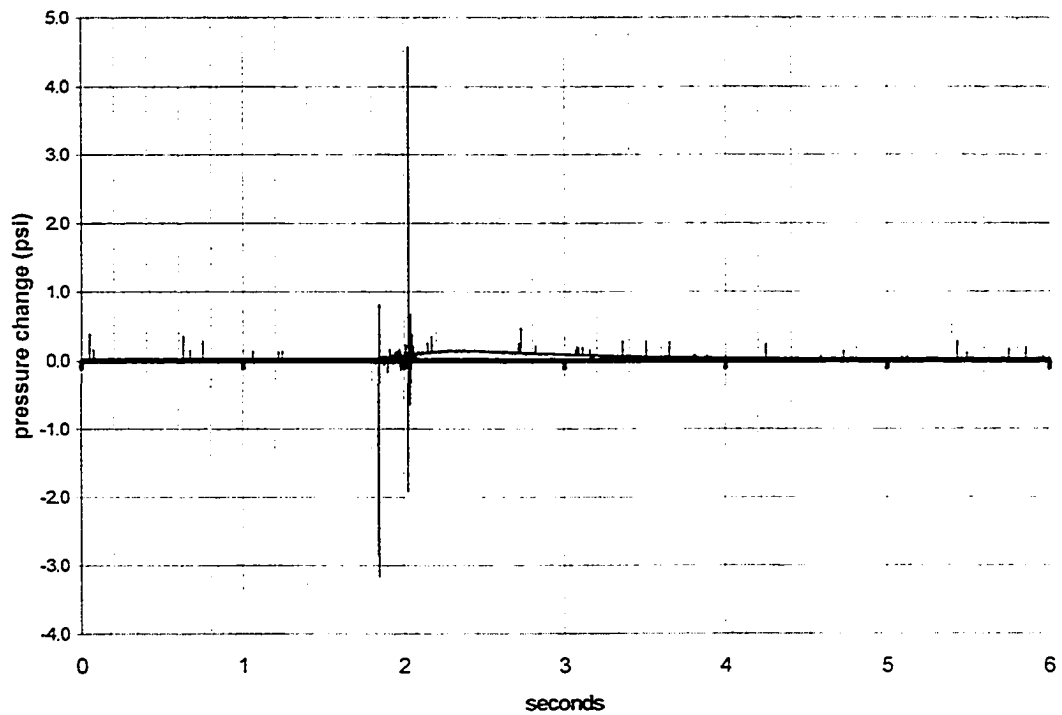


Figure D.13- Unfiltered signal received from the Keller 1 located 10 feet from the signal well. The two large peaks are the impact waves. The smaller rise is the confined pressure wave. The signal was logged at 5000 cps.

Keller 1, Camp Hedding, 10 feet from signal well

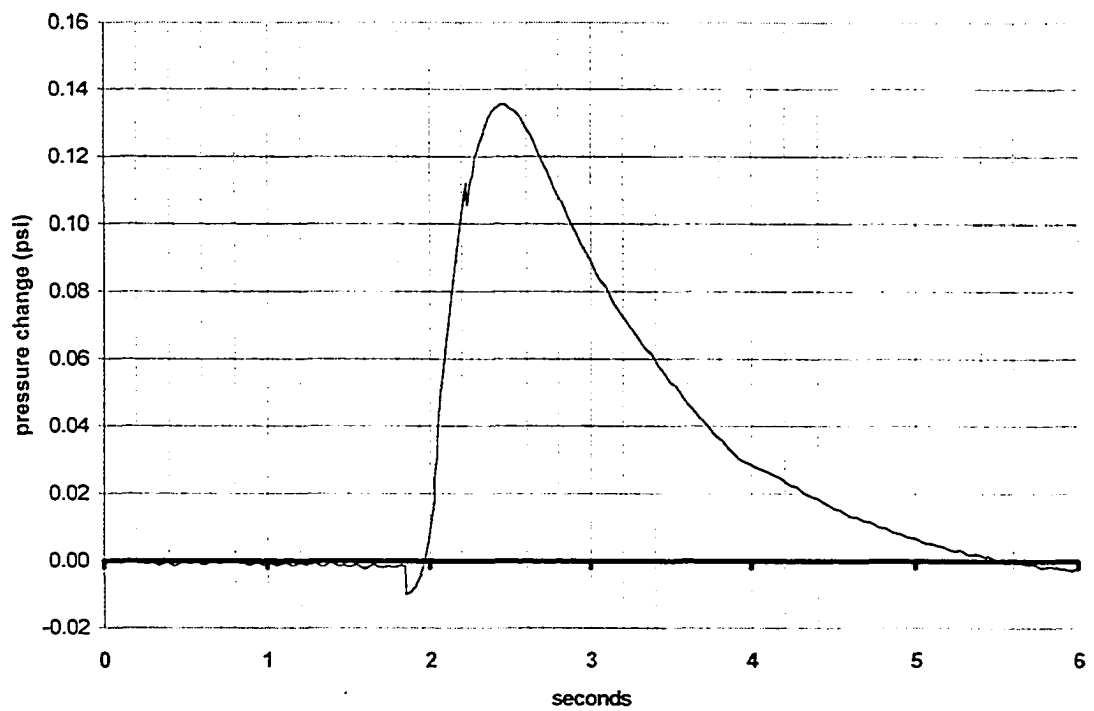


Figure D.14- Filtered signal from Keller 1 located 10 feet from the signal well. Logging rate was 5000 cps. Impact wave has essentially been filter out. The remaining signal is the confined pressure wave.

because the string restraining the anvil/surge block (see Figure D.4) broke before the hammer impact on the anvil. For data 5, the anvil reached the arrestor before being impacted by the hammer. During data 6, the hammer caught up with the anvil before the anvil hit the arrestor.

Keller 2 is located 20 feet from the signal well. The Keller 2 was installed for testing as part of the April 2000 testing. Figure D.16 is an unfiltered impact signal for Data 3 on 12-06-00. The unfiltered data is dominated by two impact waves. Both impact waves arrive before the confined pressure wave. The range of the pressures measured for impact waves for Keller 2 are about twice those measured by Keller 1. Figure D.17 is the filtered data used in Figure D.17. The confined pressure wave arrives at about 2.25 seconds. The signal is an order of magnitude lower than Keller 1, has a much slower rise to full pressure, and still has not returned to background pressures at the end of the recorded data.

D.7-Signal Velocities: The calculation of the signal velocities is discussed in Chapter IV comparing the data collected at Camp Hedding and at Treasure Island over time.

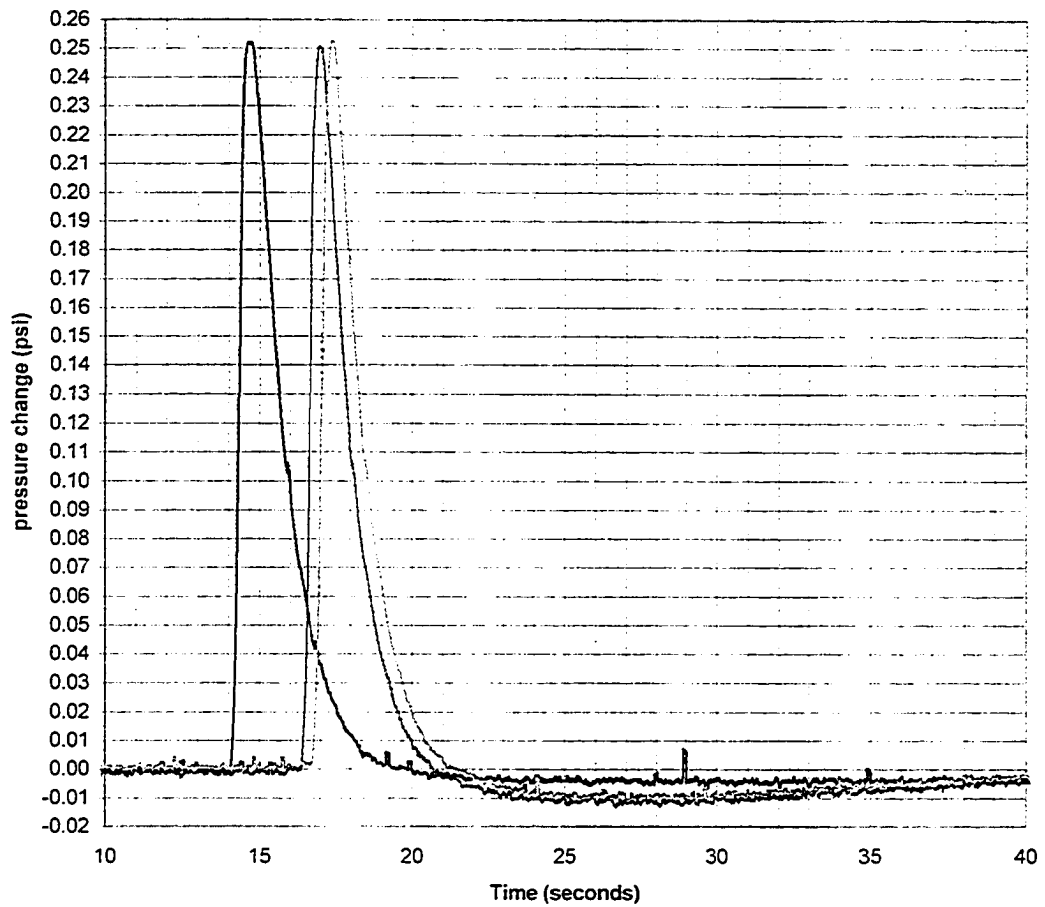


Figure D.15-Keller 1 signal detected on 11-15-00. Keller 1 is located 10 feet from the signal well. All signals were logged at 500 Hz. The signals have been spaced horizontally to allow comparison of their shapes.

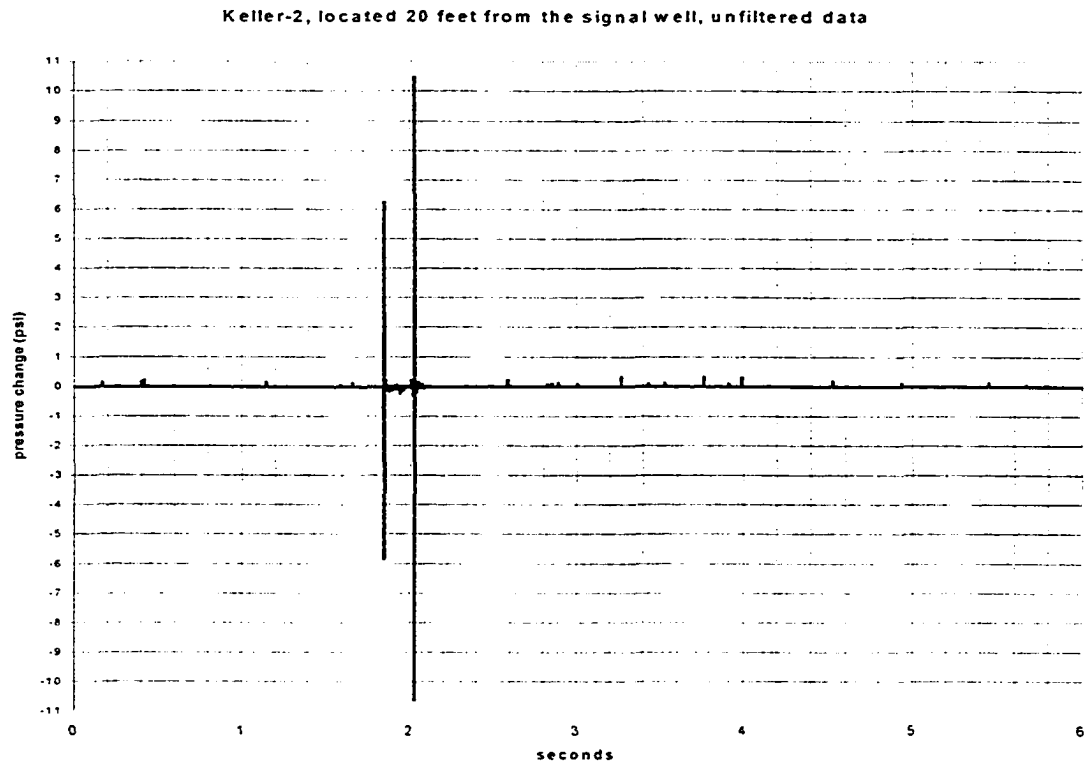


Figure D.16- Response of the Keller 2 piezometer located 20 feet from the signal well. The signal is unfiltered. The two impact waves are shown.

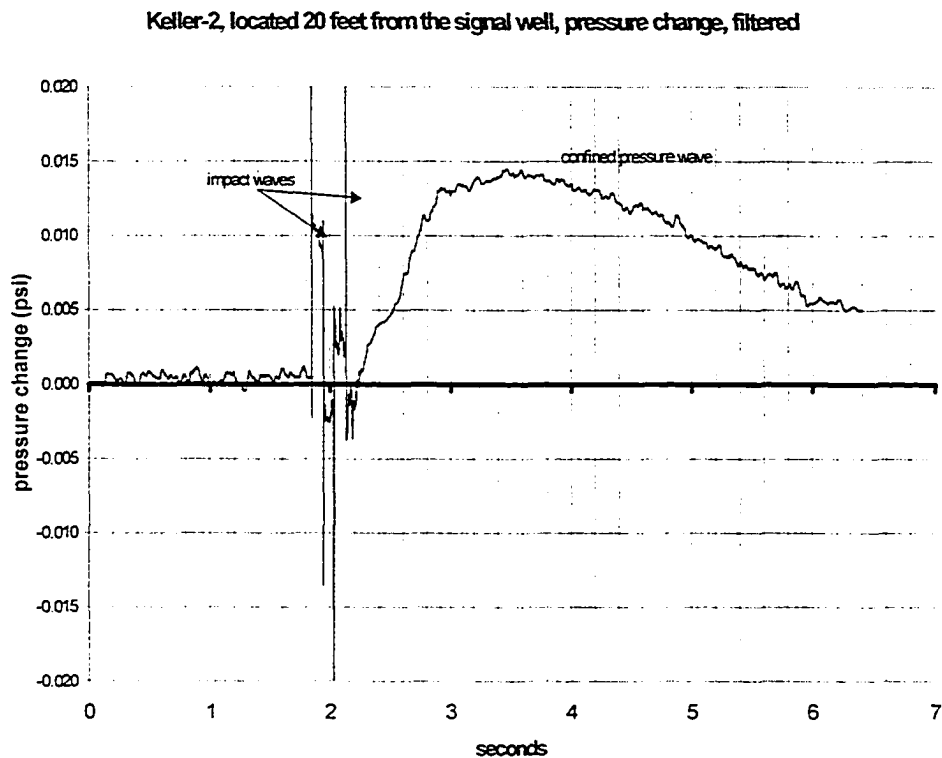


Figure D.17- Response of the Keller 2 piezometer located 20 feet from the signal well. The signal is filtered. The impact waves have been reduced by filtering the signal but are still clearly evident. The impact waves occur before the arrival of the confined pressure wave.

APPENDIX E

TREASURE ISLAND TESTING, MARCH 2001

E.1 Introduction: The testing at Treasure Island in March 2001 used the same equipment for signal generation as was used at Camp Hedding in December 2000, including the PVC pipe ‘plug’ below the screen. As during the previous testing in April 2000 at Treasure Island a drill rig was used to raise the hammer and the anvil/surge block. The setup of the drill rig over the signal well is shown in Figure E.1. All tests were carried out using the screen at 20-foot zone.

The purposes of testing at Treasure Island a second time was to:

- 1) determine if there would be any significant changes using the equipment modifications since the last testing round at TI, and
- 2) determine if there were any changes to the piezometers in the intervening time compared to the April 2000 testing.

Transducer layout is shown in Figure C.4. The previous testing had demonstrated that piezometer D-10 was not likely to be properly operating, therefore, D-10 was not included in this round of testing. D-33 “near” was not operational on March 14, 2001. The Rt#1 was not used in this round of testing. Only in situ piezometers were used for testing. No transducers were placed in the inclinometer pipe or in the water table well. Keller 3, D-18, D-17, and D-33 “far” were used to measure the signal. The PCB transducer was placed in the signal well to determine the start times. An initial check was made to determine if the transducers were accurately

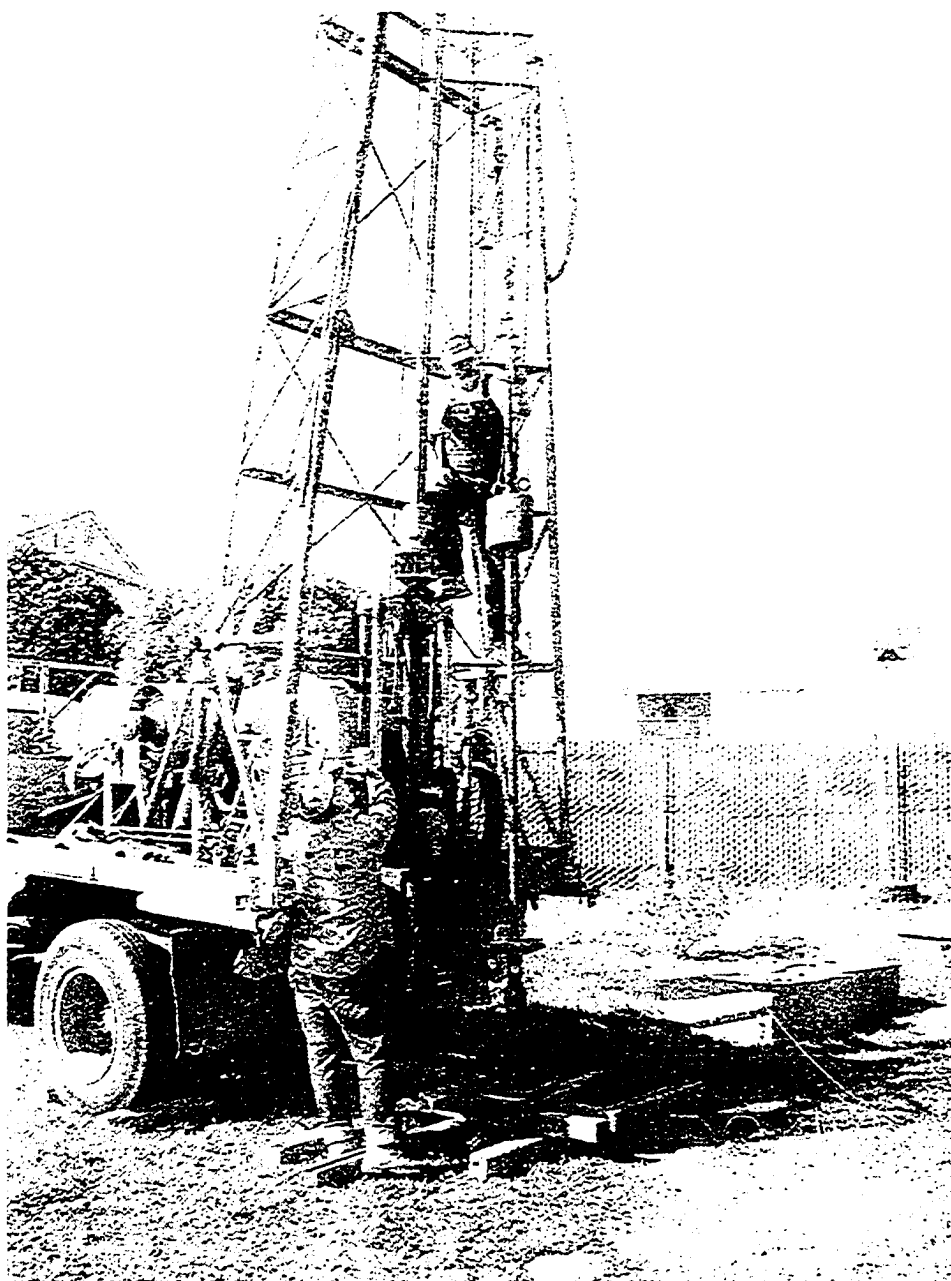


Figure E.1-Treasure Island Testing March 2001:Signal generating system set up over the signal well. A string is holding SPT hammer for a drop of 8 feet. A string holds the guide rods and anvil up until struck by the hammer. The anvil drop is 18 inches.

measuring hydrostatic conditions. D-33 “far” returned 104% of the expected hydrostatic pressure (30 feet of water about the transducer based on a measured water table of 3 feet on March 14, 2001). D-17 and D-18 returned 107% of the expected hydrostatic pressure and Keller 3 returned 97% of the expected value.

Noise was a serious problem with all the Druck transducer readings. A noise signal of approximately 0.133 Hz to 7 Hz most commonly occurred. Noise signals of frequencies of 8 Hz and 60 Hz were also present on occasion. The noise frequency was a function of the logging rate. The 4 Hz noise occurred when a logging rate of 3300 Hz was used (data 2, 3, and 4). The 60-Hz noise occurred when logging rates of 500 Hz. The 4 Hz noise was present in the Keller 3 signal at the 3300 Hz logging rate even though it was independently powered by a 12-volt battery pack. The Druck transducers are powered from AC current supplied to the site.

Logging speeds were initially 3300 Hz to obtain details of the impact wave. However, this did not provide sufficient time for the entire decay curve for the signal. The last tests were made at 500 Hz and logging was extended to over a minute. For all the tests at Treasure Island in March the hammer drop distance was 8 feet and the anvil drop was 18 inches.

E.2-Results:

E.2a-PCB transducer in signal well: The PCB signal was distinctly different from the signal at Camp Hedding. In the first two tests logged at 3300 Hz (data 2 and data 3 on Figure E.2¹), the pressure spiked at full range of 10 volts or over 9090 psi as at Camp Hedding. However, there was no decay tail. The remaining four test resembled Camp Hedding data but without the initial large off-scale spike (data 4 on Figure E.2 and data 5, 6 and 7 on Figure E.3). Two impacts are evident on all the figures for all the PCB transducer records. Although no video was made of these tests at Treasure Island, it is believed that, as at Camp Hedding, the initial peak corresponds to the first impact of the hammer and anvil after the hammer has dropped 8 feet. The second impact is the impact of the anvil on the arrestor and/or the second impact of the hammer on the anvil.

E.2b-Keller 3: In the signals recorded at 3300 Hz, two impact waves are present (Figure E.4). The time between the two impact waves for the Keller 3 correspond to the time between the impacts recorded by the PCB transducer for the same tests. The first impact wave arrives at the Keller 3 before the rise begins for the confined pressure wave. The second impact wave arrives near the peak of the confined pressure wave. Filtered data contained in Figure E.4 is shown in Figure E.5. The impact wave is lost during the filtering due to the oscillation of positive and negative pressures. The confined pressure wave is shown on Figure E.5.

¹ Note that in the follow figures, the received signals has been offset in time so that their shapes may be compared. This offset has no physical significance.

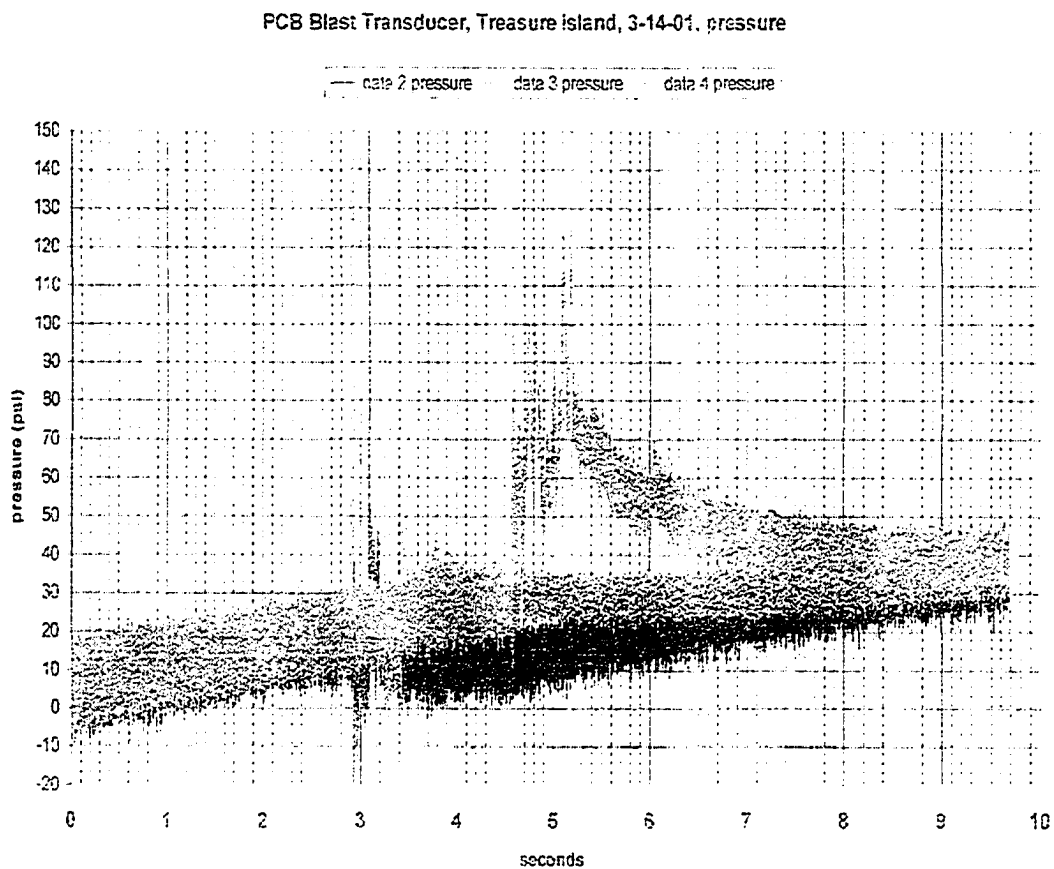


Figure E.2-PCB blast transducer located in the signal well. Recording rate was 3300 Hz. This is the unfiltered data. Time offset has no physical significance and depends on when logging started and hammer was dropped.

PCB, Blast Transducer, Treasure Island, 500 cps, 3-14-01

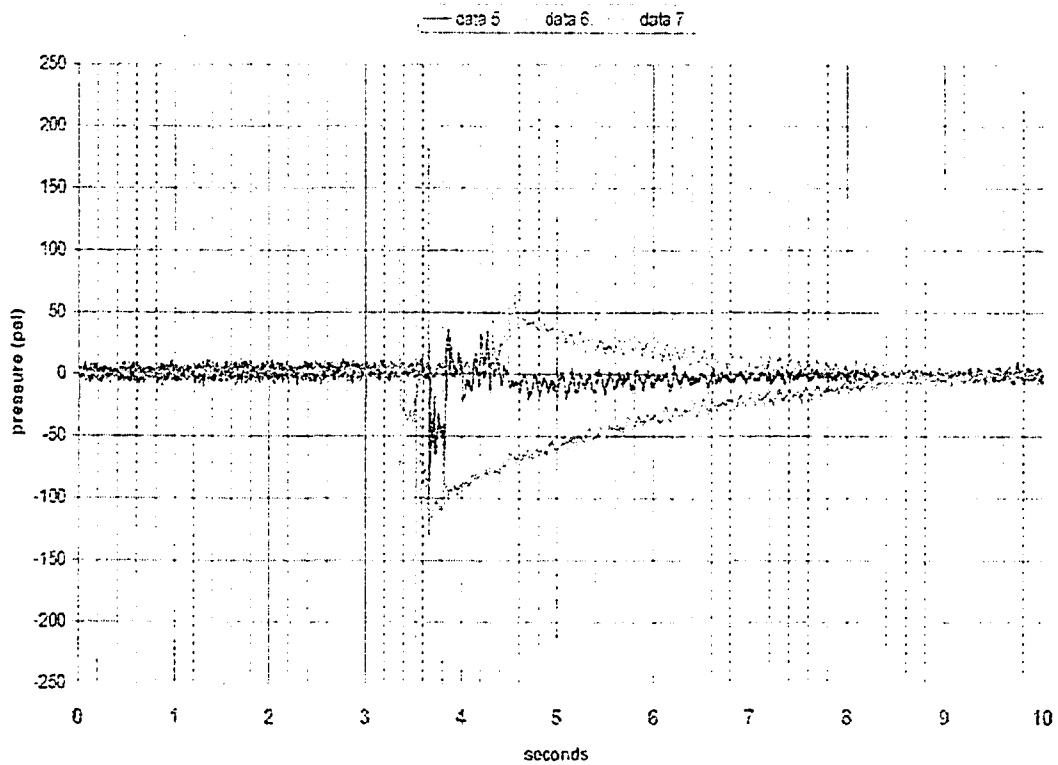


Figure E.3-PCB blast transducer located in the signal well. Signals were logged at 500 Hz. The figure shows the length of time for the pressure in the signal well to return to background.

Keller 3, located 6.4 feet from the signal well, Treasure Island, March 14, 2001

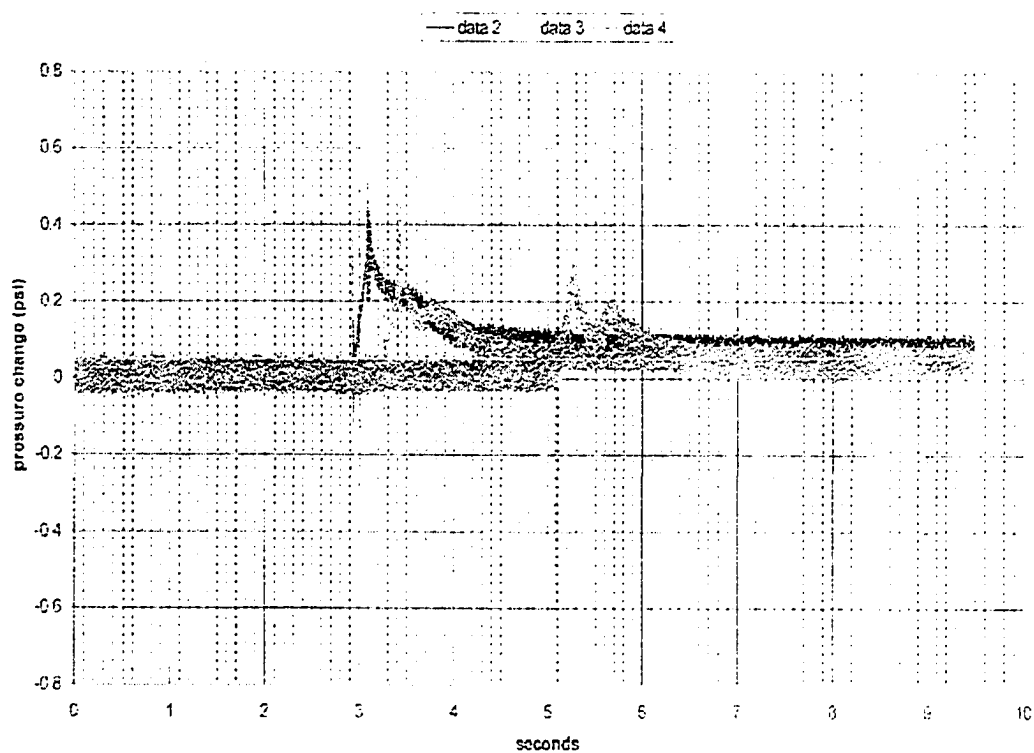


Figure E.4-Keller 3 data logged at 3300 Hz. Unfiltered signals.

Keller 3, filtered, 3300 cps data, 3-14-01, Treasure Island

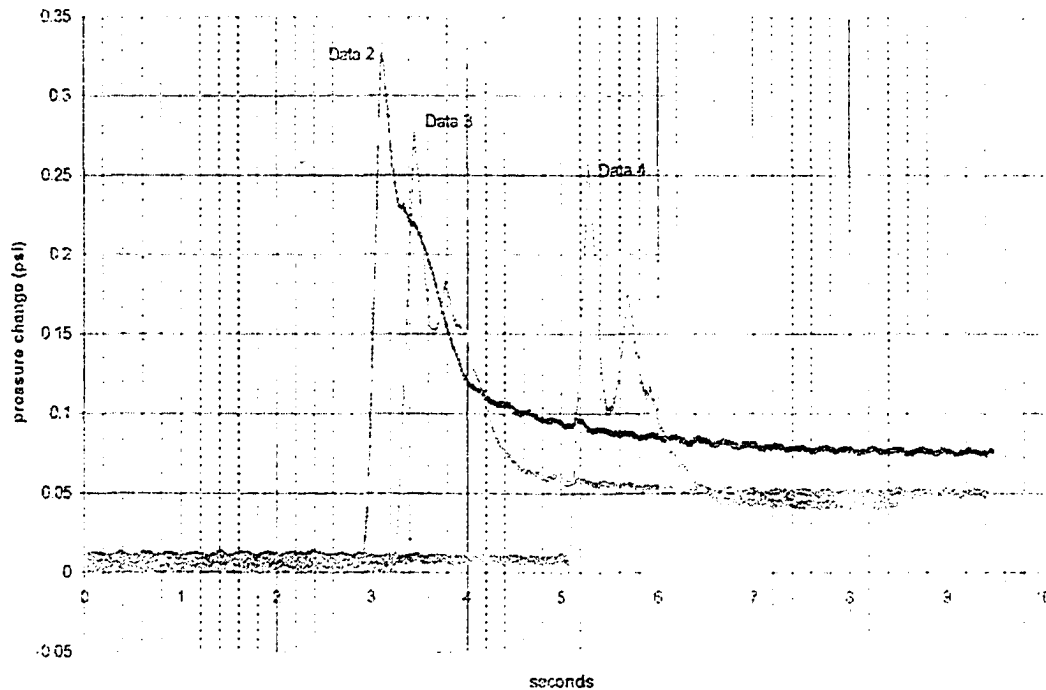


Figure E.5-Keller 3 located 6.4 feet from the signal well. The data is filtered and logging was done at 3300 Hz.

Data set 5, 6 and 7, recorded at 500 Hz, are shown filtered in Figure E.6. These data sets were recorded for over a minute to observe the decay of the signal. The filtered data show a long period wave peaking 15 to 20 seconds after the confined pressure wave. The long period wave is the unconfined pressure wave.

Falling head tests performed on the Keller 3 after testing gave an average hydraulic conductivity of 4.59×10^{-3} cm/second. This is nearly identical to the hydraulic conductivity of the Keller 2 measured in situ at Camp Hedding (4.1 to 4.7×10^{-3} cm/second on 4/13/00).

E.2c-D-18: The unfiltered data for D-18 are shown in Figures E.7 and E.8 for logging rates of 3300 Hz and 500 Hz respectively. There is no indication that the impact wave was detected by this piezometer. The confined pressure waves show up well at both logging rates, however, the shape of the pressure waves are distorted by the presence of cyclic noise which depends on the logging rate. The faster logging rate has a 4-Hz noise that is accentuated when filtered as shown in Figure E.9. The 500 Hz logging rates has an 8-Hz signal which is accentuated with filtering as shown in Figure E.10. Expanding the 500 Hz signal further in Figure E.11, showing the first 10 seconds of the data, shows there is a 7.5-Hz noise riding the longer frequency noise. Underneath these noisily overlays is the rapid rise of the confined pressure wave and the slower rise of the unconfined pressure wave that is shown in Figure E.11 for the 500 Hz logging rate.

E.2d-D-17: It is not clear that D-17 transducer was actually functioning properly during the testing. As shown in Figure E.12, there was continuous drift of the base pressure throughout the testing. There is a clear 4-Hz noise signal throughout the tests when logging at 3300 Hz. There is clearly a shape pressure rise of about 0.17 psi for data 2, 3, and 4. When logging rate is 500 Hz the drift in the base increases, Figure E.13. There is virtually no signal associated with the impact for data 5 and 6. Data 7 is enlarged in Figure E.14. A 0.05 psi rise is indicated

Keller 3, Tresure Island, 500 cps data, 3-14-01, filtered

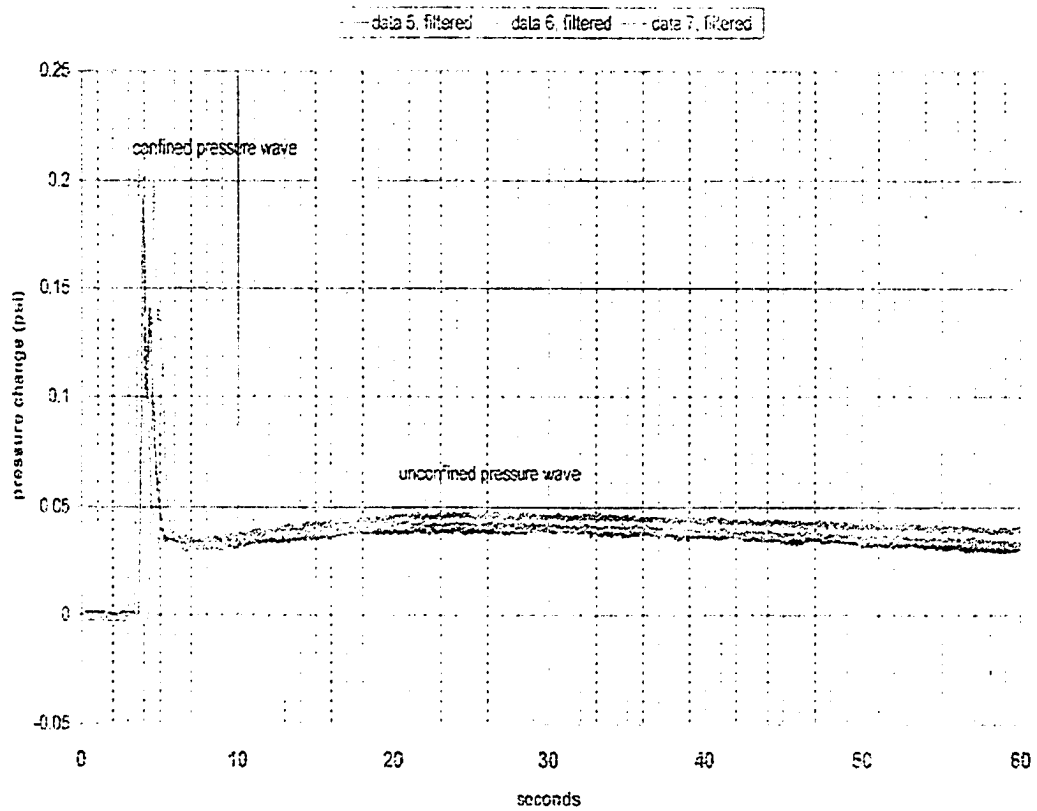


Figure E.6-Keller 3 data logged at 500 Hz. Data is filtered.

D-18. Treasure Island, 3300 cps data, 3-14-01

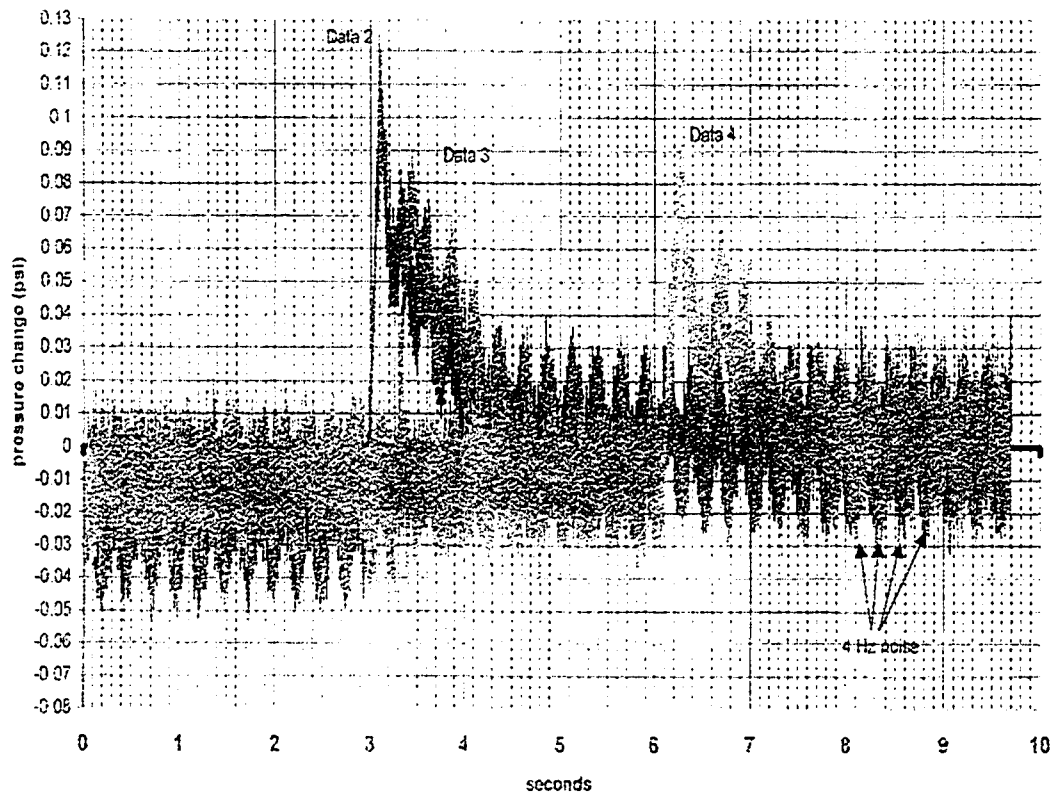


Figure E.7-Druck 18 located 11 feet from the signal well. Signals are logged at 3300 Hz. Unfiltered signals.

D-16, Treasure Island, 500 cps, 3-14-03

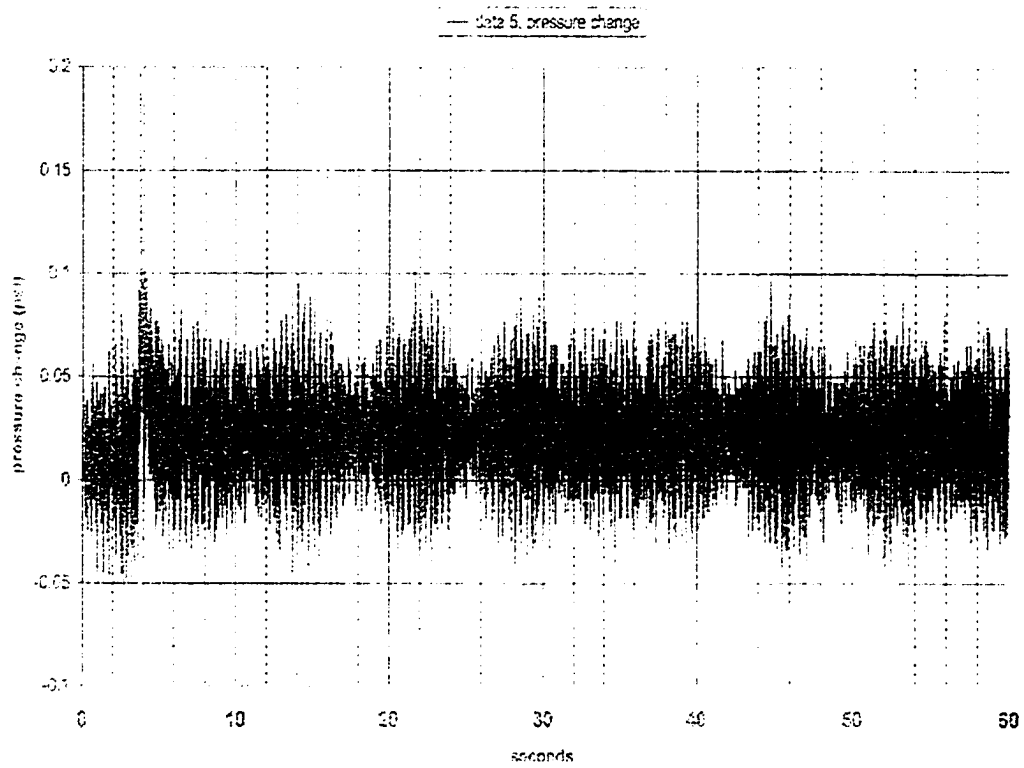


Figure E.8- Druck 18 logged at 500 Hz. Unfiltered data.

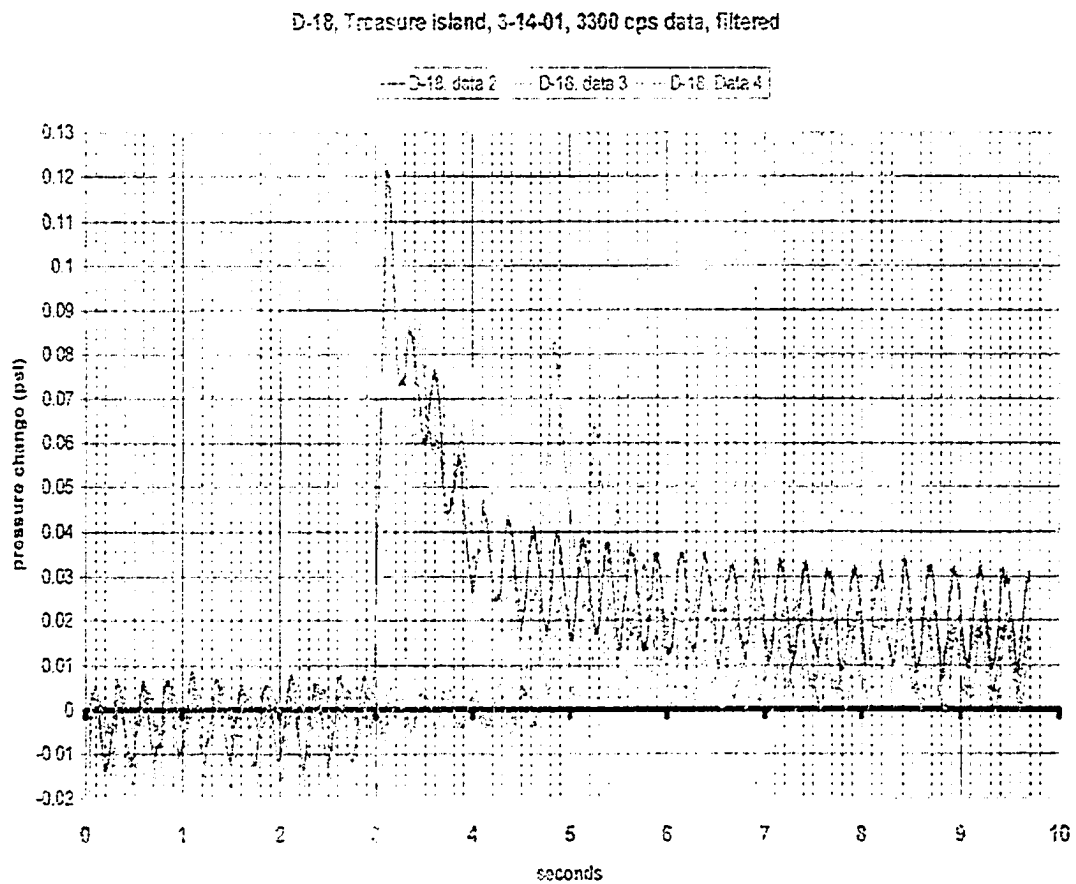


Figure E.9 Druck 18 logged at 3300 Hz. Filtered signals.

D-13, Treasure Island, 500 cps data, 3-14-01

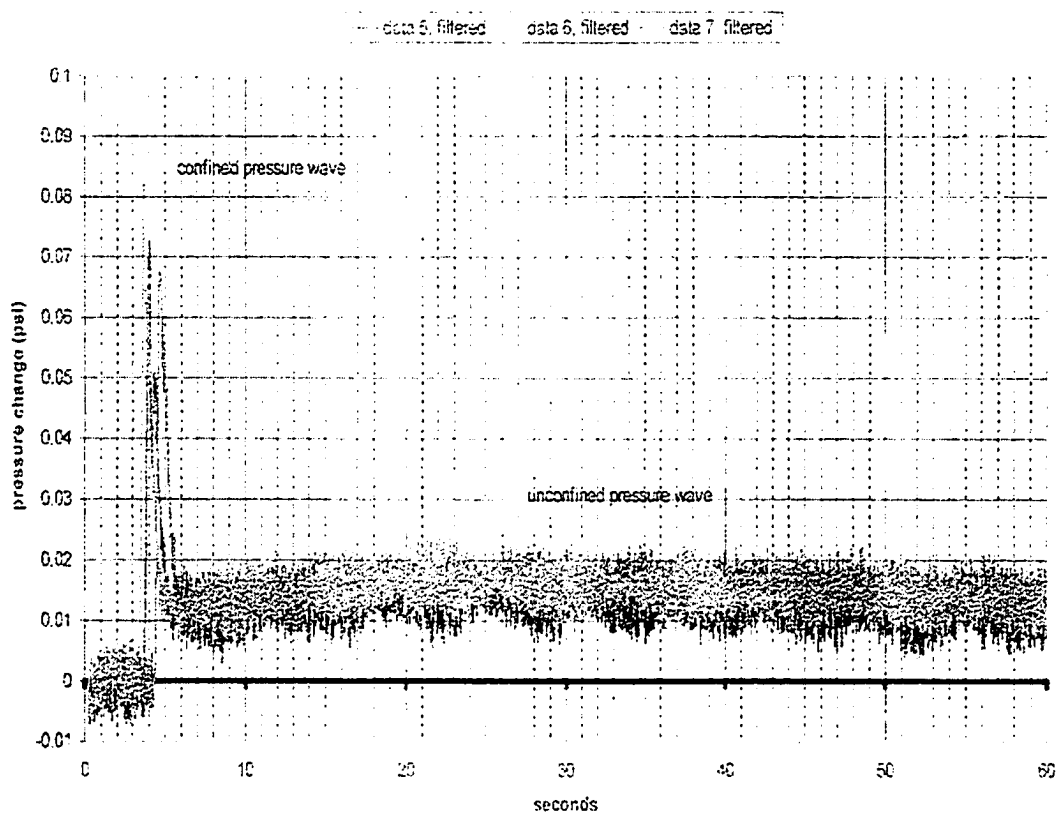


Figure E.10-Druck 18 data logged at 500 Hz and filtered.

D-18, Treasure Island, 500 cps data, 3-14-01

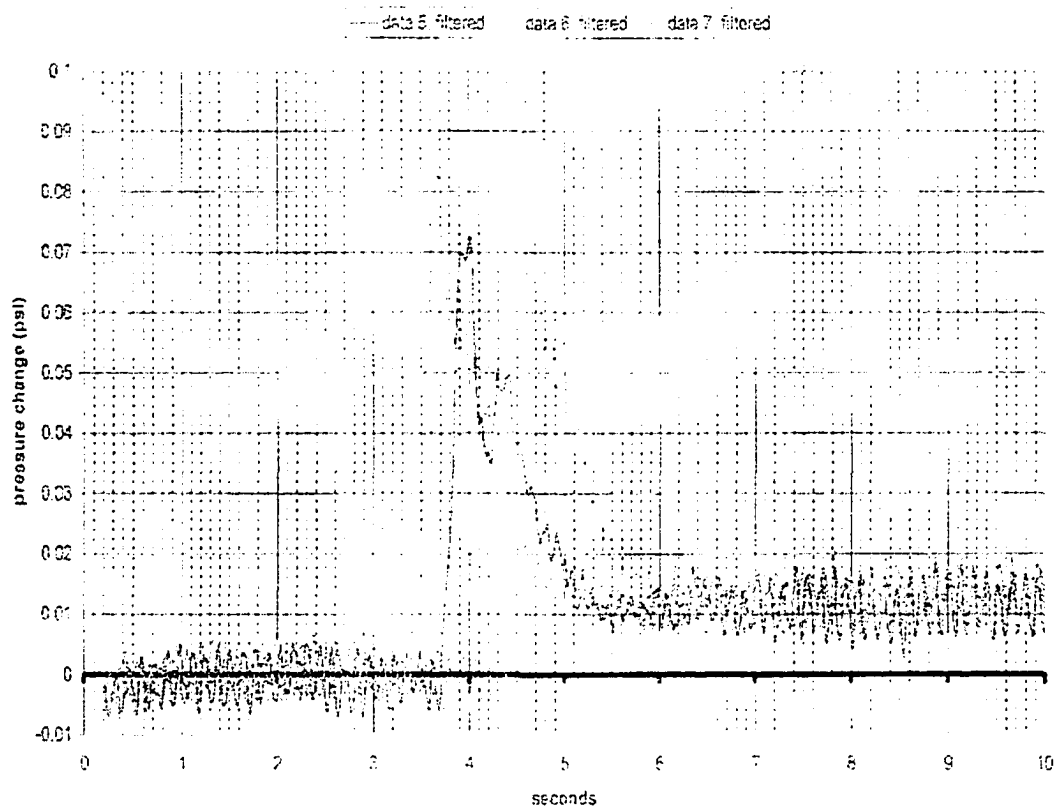


Figure E.11-Druck 18 data logged at 500 Hz. These are enlargements of the confined pressure waves.

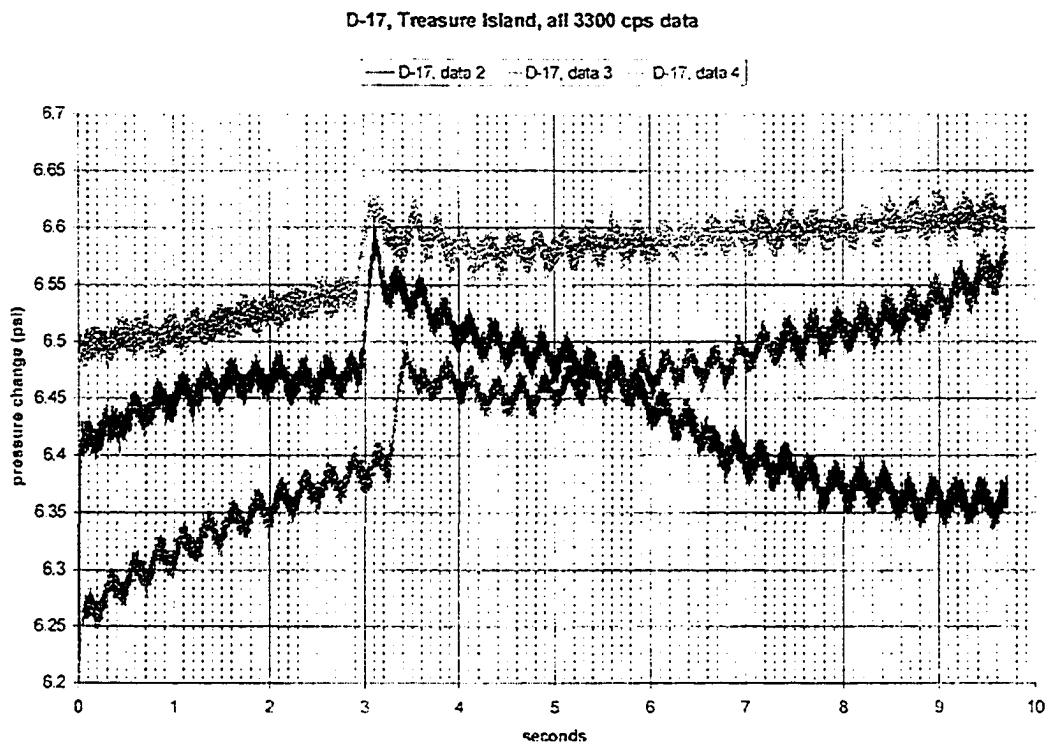


Figure E.12-Druck 17 pressure signal logged at 3300Hz.

above the background drift. The 4-Hz noise is also gone with the slower logging rates.

E.2e-D-33 “far”: The impact wave was detected at D-33 “far” on all the hammer drops at both logging rates, Figures E.15 and E.16. No confined pressure wave was evident either in the unfiltered or filtered data (Figures E.17 and E.18). The 4-Hz noise was present after filtering the 3300 Hz data.

E.3-Discussion: It is likely that D-17 was not operating properly on the day of the testing. It is unusual to detect the impact wave and not detect the pressure wave as occurred at D- 33 “far”. It would appear that D-33 “far” is operating correctly and can detect a signal if it reaches the piezometer because the impact wave was detected.

Placing the responses of the pressure wave on Figure E.19 indicates that Keller 3 responses are within the range of values expected based on the tests at Camp Hedding and on the August 2000 testing at Treasure Island. D-18 had higher responses than the August testing results and falls within the range of responses expected based on the testing at Camp Hedding. D- 33 “far” had no detectable pressure wave so the results are far below that of the August testing. The responses for D-17, where they are detected indicated on data 2, 3, 4, and 7 are in the same range observed in August. However, the drift of the signal at D-17 indicates a serious problem with the transducer.

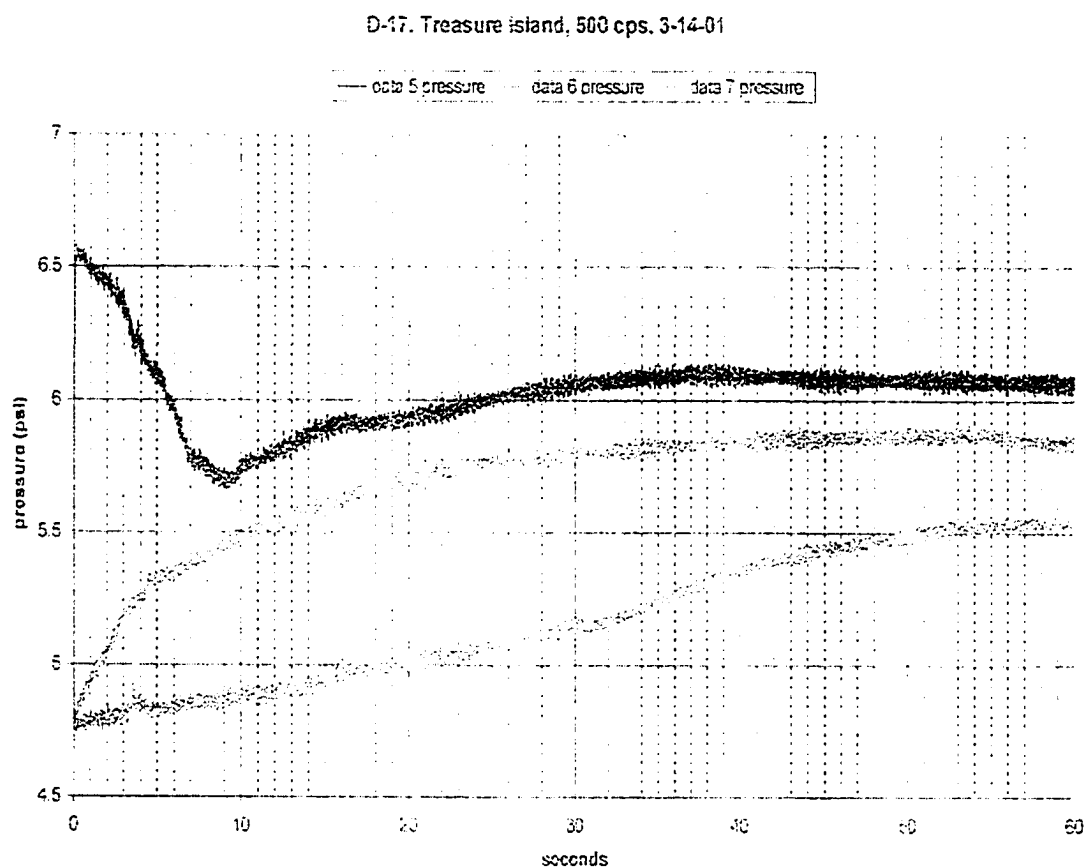


Figure E.13-Druck 17 data logged at 500 Hz. The base drift is shown.

Druck 17, Data 7, March 14, 2001

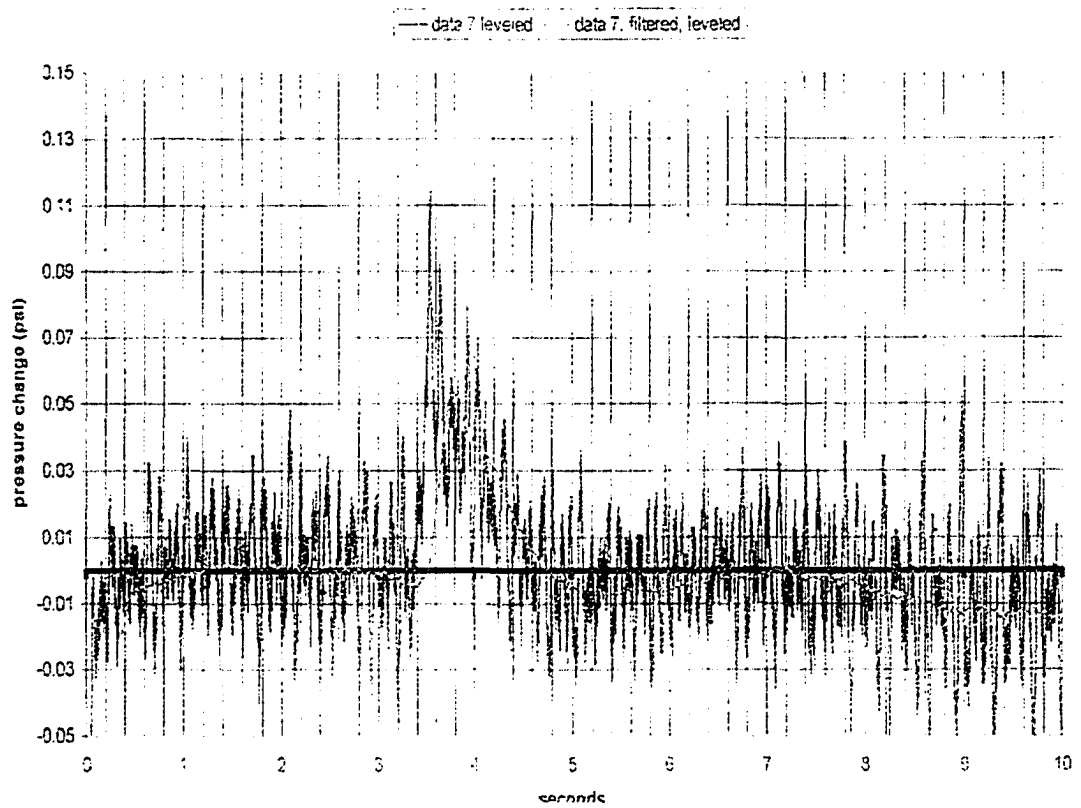


Figure E.14-Druck 17 data 7 corrected for drift in the base. Data was logged at 500 Hz.

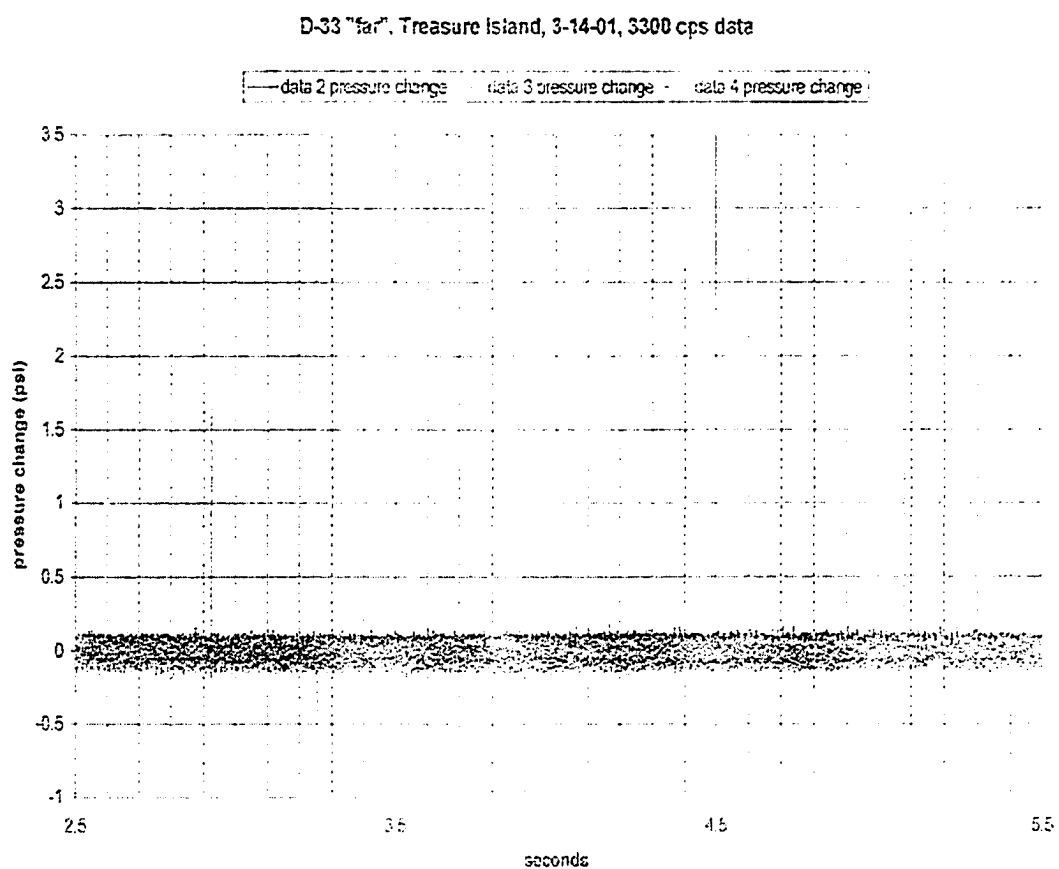


Figure E.15-Druck 33 "far" unfiltered data logged at 3300 Hz.

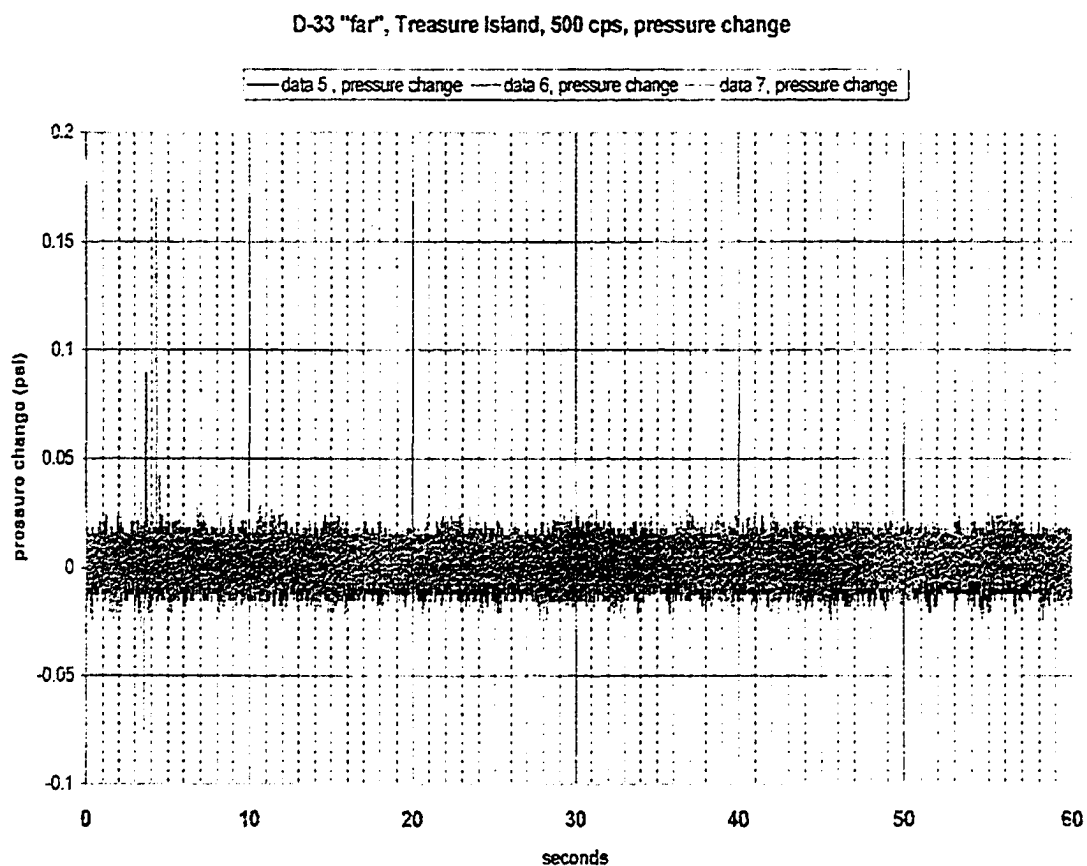


Figure E.16-Druck 33 "far" unfiltered data logged at 500 Hz.

D-33 "far", Treasure Island, 3-14-01, 3300 cps, filtered

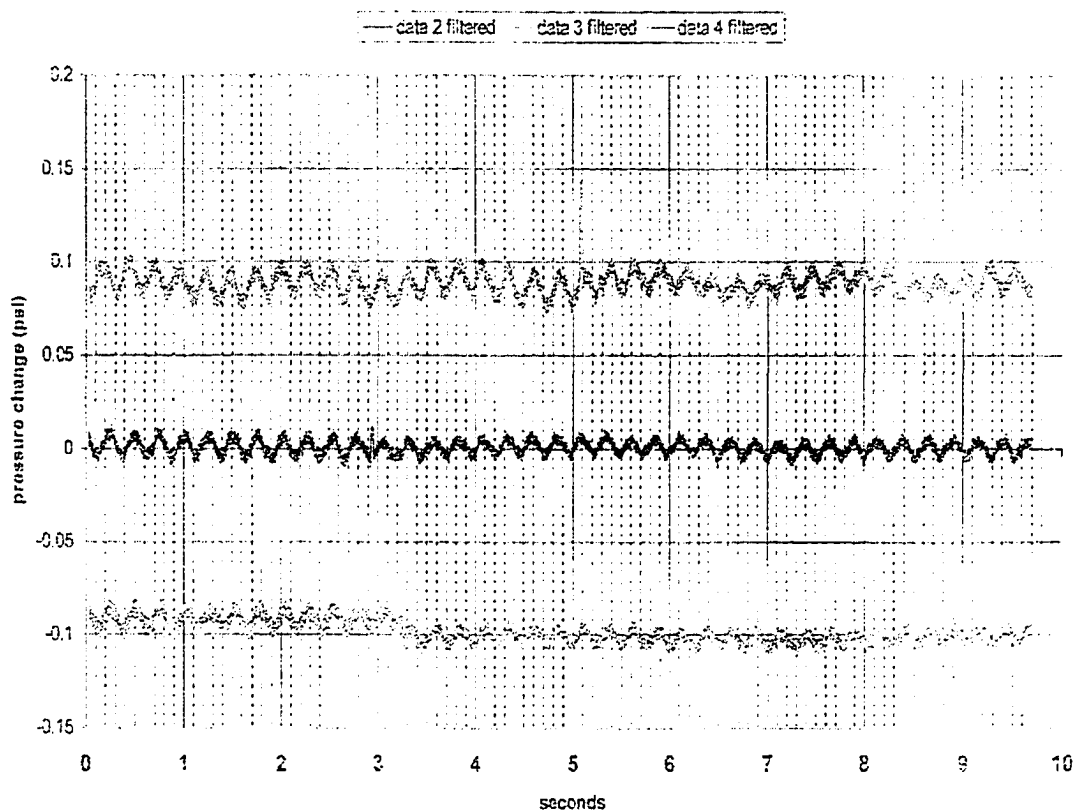


Figure E.17 Druck 33 "far" data logged at 3300 Hz and filtered. The impact wave is much reduced by filtering. Aside from the 4 Hz noise no other signal is evident in the data. The data sets were separated vertically for clarity.

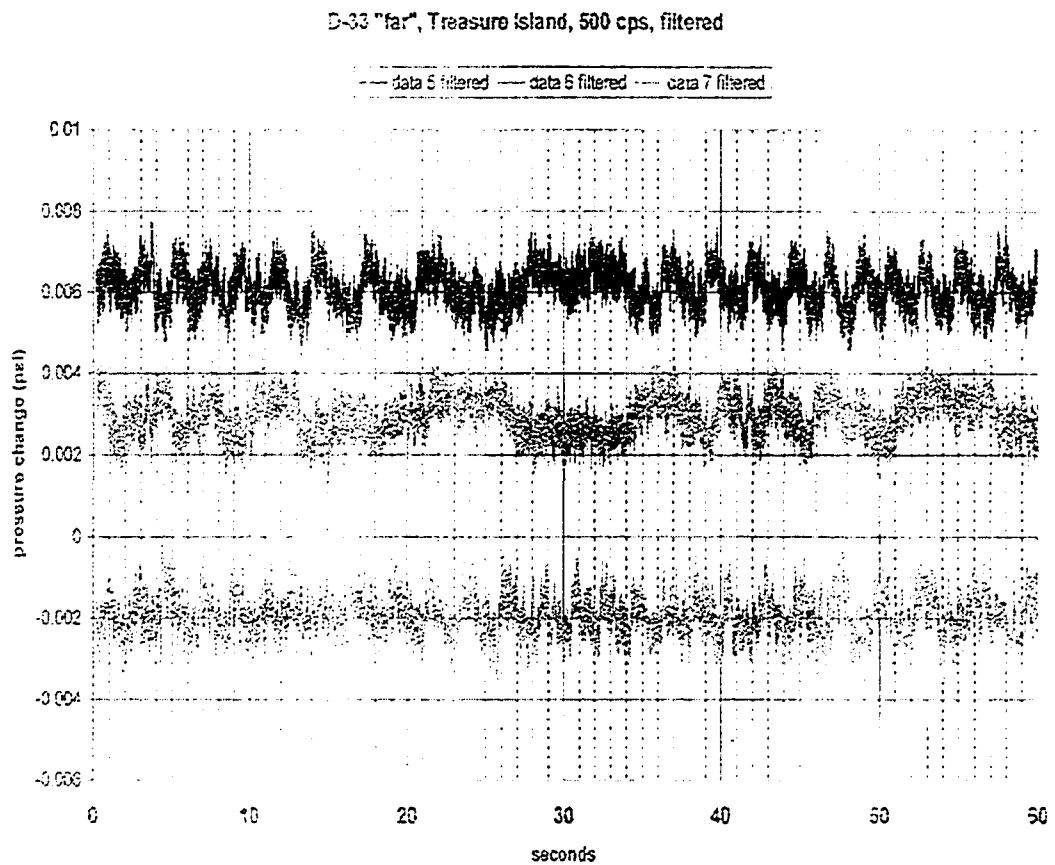


Figure E.18-Druck 33 "far" logged at 500 Hz. Vertical spacing has been added for clarity.

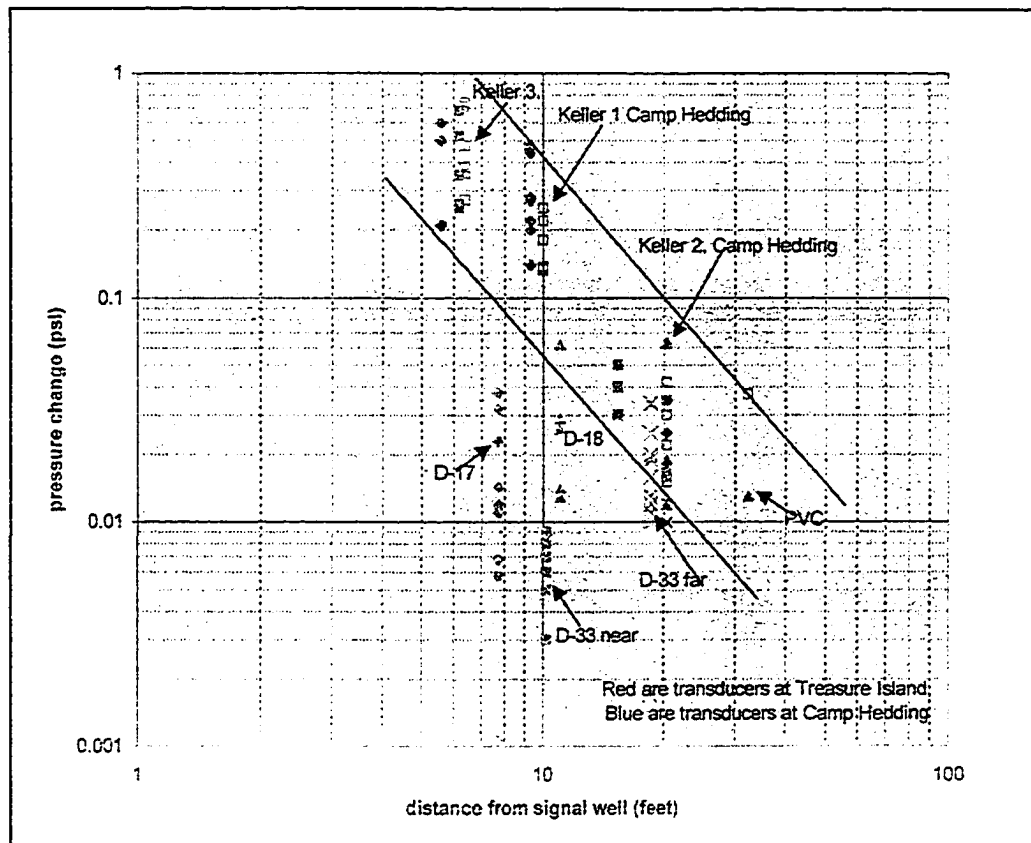


Figure E.19-Change of signal strength with distance from the signal well for all the testing at Camp Hedding and Treasure Island. All the data from the August 2000 and March 2001 testing at Treasure Island are shown together. The data from Camp Hedding testing is included for comparison. The lines bracket the range of Keller 1 and Keller 2 data from all testing at Camp Hedding. The Rt#1 data collected at Camp Hedding is shown in blue squares.

APPENDIX F

NUMERICAL SIMULATION

F.1-Introduction: Two different types of signal modeling were performed. Based on the review of the signal generated within the signal well and recorded by the transducers at various distances for the signal well, it was apparent that two different sets of signals were being generated by the hammer/anvil/surge block system. The following models are intended to demonstrate that the operations of the hammer/anvil/surge block system and the interaction of the surge block, water column, and aquifer ground water can be modeled in a rational way. Exact duplication of the detected signals is not intended in the modeling. Instead, it is expected that a reasonable variation of parameters around known, measured, or reasonably estimated values should bracket the observed responses in the transducers.

F.2-Raw Signal Description

F.2a: Signal Well: Measuring the pressure changes generated by the advancing surge block (Figure III.2) inside the signal well proved to be difficult. Four different transducers were used. All proved unsatisfactory in some way or another. The first transducer used was an optical fiber Roctest-500 psi transducer. The rise to peak value measured-800 psi- was less than $1/500^{\text{th}}$ of a second. Eight hundred psi, being the maximum reading allowed by the transducer before automatic protection, prevented higher readings. This signal was measured twice before the transducer was overstressed. The manufacturer indicated that pressures in excess of 1200 psi were

necessary to overstress the transducer. The pressure within the signal well was expected to be less than 500 psi and the initial recorded pressures were believed to be erroneous. Subsequent measurements and modeling have suggested otherwise.

A Validyne transducer (with a 3000 psi diaphragm, the electronics cannot be submerged, see Appendix B) was the second transducer used to measure pressures in the signal well. The transducer was attached to a stiff 1/8-inch plastic hose leading from the ground surface through the middle of the guide rods, anvil, and NQ rods to the screened interval in the well casing below the surge block. Drawing water from inside the signal well up through the transducer bleed hole in the transducer saturated the hose. The bleed hole was closed and the water in the hose maintained under slight vacuum created by the weight of water in the hose above the water table. The pressure measurements provided indication of the shape and duration of the pressure pulse created by the surge block. The maximum pressures measured by the Validyne transducer ranged from 12 psi to 140 psi. These pressures are considered to be minimum values because of the long column of water in the hose used to connect between the end of the surge block in the well and the transducer. It is believed that the hose, even though considered quite stiff, expanded slightly as the pressure pulse moved up the hose.

A GEMS 2000 psi transducer was the third transducer used to measure pressure within the signal well (discussed in Appendix D). The GEMS provided signals indicating maximum pressures generated in the signal well as ranging between 1200 and 1300 psi.

The GEMS failed to respond after one or two hammer shots during any given day of testing because of water being driven past the seals. It was possible to dry the transducer overnight and repeat the next day. Again, because of the performance of the transducer under the pressures generated by the surge block, the measured pressures are not considered reliable but do provide an indication of the timing of the pulse generated during the hammer shots when the GEMS transducer was functioning and the maximum pressures generated within the screen.

A PCB blast transducer was finally placed in the well screen interval below the surge block (discussed in Appendices D and E). A reproducible signal was generated. However, the transducer exceeded the full voltage range of 10 volts on every shot at Camp Hedding and 3 out of 7 shots at Treasure Island on March 14, 2001. A 10-volt change in pressure would suggest a pressure in excess of 9000 psi within the screened interval. Such high pressure is considered impossible without the destruction of the PVC well screen and well casing. Although these pressures are unrealistic, the transducer did provide reliable starting times for the signal in the tests in which it was used.

The data from the Roctest transducers appears to have provided the best indication of the magnitude of pressures generated by the hammer/anvil/surge block system in the signal well. The pressures, ranging from at least 800 psi to 1200 psi, appear to be generated in the screened interval by the surge block after being struck by the falling hammer. The generated pressures exceeded the maximum recording pressure allowed

by the transducer of about 800 psi. The transducer was overstressed on the second attempt but not of the first. This suggests the pressure actually generated must have been near or slightly above the maximum design pressure of the transducer of about 1200 psi. The suggestion being that if the pressure was significantly higher than the maximum over-pressure the transducer would have been overstressed on the first test rather than requiring two overpressures to be overstressed.

F.2b: Aquifer Signal-The raw signal received by the transducers in the aquifer (Figure F.1 is an example) consistently had two parts. There is an initial set of sharp, high frequency waves. FFT analysis indicates frequencies of this initial wave are about 900 to 1000 Hz. The velocity of these initial waves is about 4000 to 5000 ft/sec. As was stated in the Chapter IX, these velocities are approximate, since, given the short distance between the signal well and the piezometers, a change in one data point would result in a 900-ft/second difference in velocity. It is this signal that has been called the impact wave throughout this paper, is believed to be a compressional wave (P-wave) developed from the hammer driving the surge block into a standing column of water within the well casing. The measured velocities of the compressional waves are consistent with values given by Clark (1966) for water.

It is common to detect a second set of impact waves overlapping the confined pressure wave for the piezometers installed at Treasure Island and Camp Hedding. The video recordings of the hammer drops during the pool testing and at Camp Hedding showed the second set of impact waves was generated when the hammer again hits the anvil

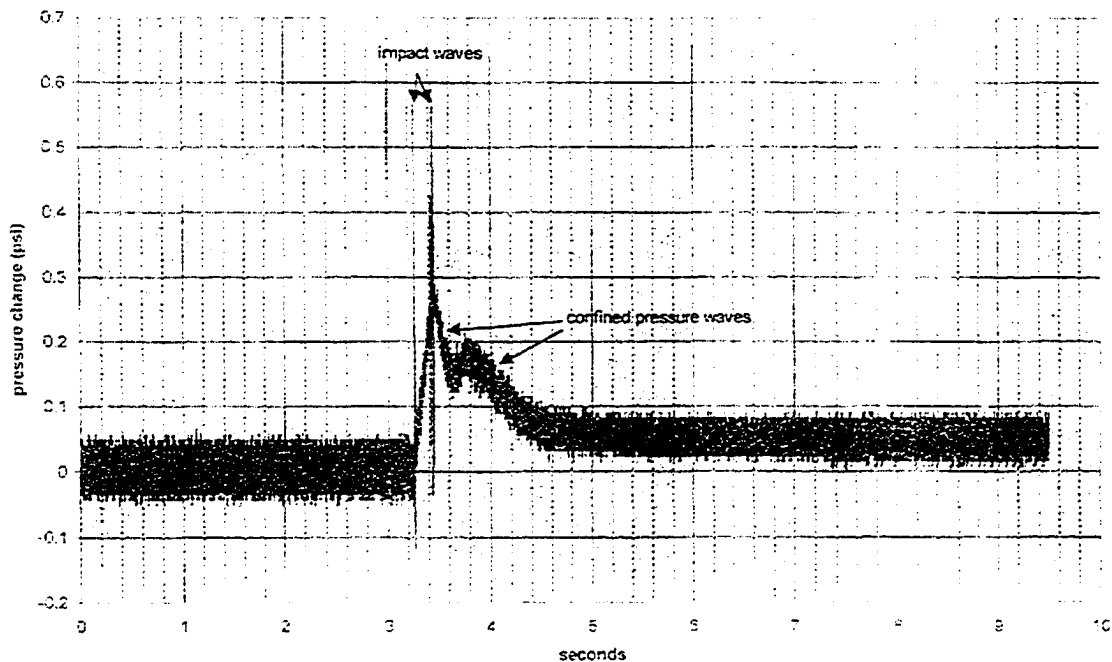


Figure F.1-Keller 3, Treasure Island, Data 3, 3-14-01, logging rate is 3300 Hz

after the anvil recoils off the arrestor. This second impact drives the surge block forward again creating another set of impact waves. During pool testing (see Figure III.8), where there is no interference created by the confined pressure wave, a third set of impact waves could be observed corresponding to another bounce and collision of the hammer and anvil.

The second part of the signal received by the piezometers installed in the aquifers is a “hydraulic pressure wave” or as called in this study, a confined pressure wave. This wave is created by the pushing out of a volume of water through the screen by the advancing surge block and rods (see Figure III.2). The length of advance was varied

from 12 inches to 36 inches. Most commonly, 18 inches was used as the distance the anvil drops and surges block advances before the anvil hits the arrestor. The effect of varying the length of the anvil/surge block drop had a larger effect on the results than varying the hammer drop. This was discussed in Appendix D. However, in order to compare repeated tests between sites and over time, an 18 inches anvil drop was adopted. The confined pressure wave has a much slower velocity than the impact wave. The velocity of the advancing confined pressure wave decreased with distance from the signal well (discussed in Chapter IV).

Both of these components of the signal were modeled separately. The impact wave was modeled using the equations developed for driving piles. The confined pressure wave was modeled using a common public domain ground water model.

F.3-Modeling the Rod Wave

The numerical model by Smith (1955) for the transmission of an impact to a stiff elastic rod is used to model the propagation of the impact energy of the hammer down the rods to the surge block. The model was set up as a spreadsheet using the equations presented by Smith. Initially the model was tested against the solution presented in Smith's paper for time steps of $1/3000^{\text{th}}$ second. The same model was changed to time steps of $1/5000^{\text{th}}$ second. Smith's Type VII impact (Direct impact between a ram and a long object) was selected as best representing the hammer/anvil/surge block system used to generate the signal. Table F.1 is the input data for the rod model. Figure F.2 is the

arrangement of the various parts of the hammer/anvil/rod system and the locations of the spring constants used in the model.

Table F.1

Input Data for Smith (1955) Model

m	unit	W _m (lbs) weight	K _m (lbs/in) Spring constant	R _m (resistance) (lbs)	Δt (sec)	T _{mR} critical time	Φ(T _m /Δt)
1	Hammer	140	1130557	0	1/5000		
						4.79E-4	2.395
2	Anvil	84	169160	0	1/5000		
						6.19E-4	3.93
3	Rod 1	26.2	39479	0	1/5000		
						1.23E-3	6.40
4	Rod 2	26.2	39479	0	1/5000		
						1.23E-3	6.40
5	Rod 3	26.2	39479	0	1/5000		
						1.23E-3	6.40
6	Rod 4	26.2	39479	0	1/5000		
						1.15E-3	5.72
7	Surge Block	10.6	172000	0	1/5000		

W_m is the weight of each segment. K_m is the spring constant between the segment m and the segment m+1 below. R_m is the resistance between the segment and the soil or, in this case the water, Δt is the time step. T_m is the travel time though each element and is equal to:

$$T_m = 1/19648 * \text{square root } (W_{m+1}/K_m).$$

T_{mR} is called the critical time and is equal to the smallest T_m . The smallest T_m or T_{mR} is used to evaluate if the chosen Δt is small enough.

According to Smith

$$\Phi = T_m/\Delta t$$

has to be greater than 1 for the model to work. All the Φ 's are well above 1 for the model.

Attempts were made to separate the anvil into the guide rods, striker plates, drive head and anvil mass. However, numerical instability resulted with various parts of the anvil oscillating between positive and negative values with each iteration. Therefore, the anvil was modeled as a single mass with only one spring constant as shown in Figure F.2 and on Table F.1.

The spring constant, K_m was determined using Smith's equation #6:

$$K_m = AE/l$$

where A is the contact area between the sections. E is Young's modulus, and l is the length of the section. For steel $E = 3.35E5$ lbs/in² was used.

The spring constant for the water column below the surge block was arrived at by two different methods. One method began with the compressibility of water:

$$\beta = 4.4E-10 \text{ m}^2/\text{N}.$$

Inverting and changing to English units

$$E = 329380 \text{ lbs/in}^2.$$

Using $l = 24$ inches (length of water column within the screened interval), an area of 12.56 in^2 (4" ID for a schedule 40 PVC well casing) the spring constant for water is $K_w = 172,375 \text{ lbs/in}$.

An alternative calculation of the spring constant is

$$K_m = DA/l$$

where D is the constrained modulus.

Lambe and Whitman's equation 12.8, pg. 153 for the constrained modulus is

$$D = E(1-\nu)/(1+\nu)(1-2\nu)$$

The bulk modulus $B = 312000 \text{ lbs/in}^2$ (Daily and Harleman, 1966) and using Lambe and Whitman's equation 12.6:

$$B = E/3(1-2\nu)$$

with ν being the Poisson's ratio, and plugging into equation 12.8 results in

$$D = 3B(1-\nu)/(1+\nu)$$

Using an estimated Poisson's ratio of 0.48 the spring constant is

$$K_m = 172,106 \text{ lbs/in}$$

The two spring constants are considered identical. A spring constant of 172000 lb/in was used in the model.

Figure F.3 is an example of the results of the Smith model. The maximum force delivered to the surge block about 0.015 seconds after impact of the hammer is about 20000 lbs.

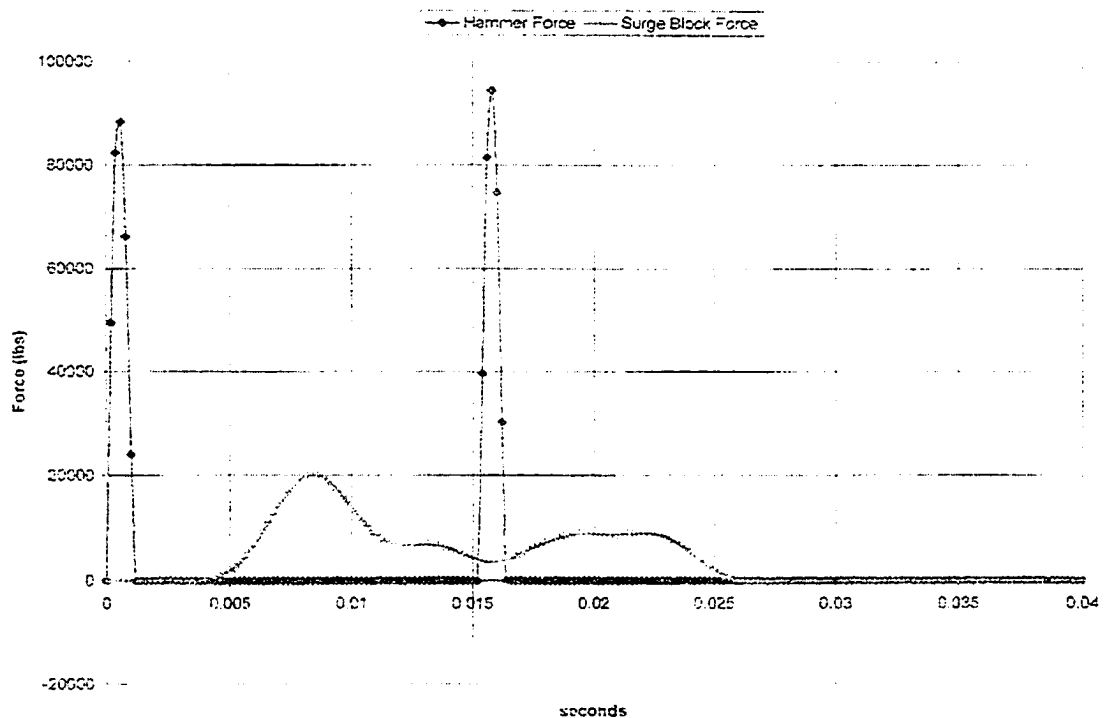


Figure F.3-Modeling results show the force generated by the hammer hitting the anvil being transferred down the NQ rods to the surge block. The result is the application of about 20000 lbs. to the top of the water column in the signal well.

Applying this force over the area of the surge block would result in about 1590 psi to the water column within the screened interval. This pressure is higher than measured values but within the range for values necessary to damage the Roctest transducer or about 1200 psi. Values of the pressure in the signal well in the range of 1000 psi to 1500 psi have been carried forward into the hydraulic pressure wave modeling.

F.4-Modeling the hydraulic pressure wave

The second part of the signal shown in Figure F.1 was believed to be a pressure wave generated by driving the water from the screened interval into the aquifer. The actual volume of water ejected through the screens is small. The volume ejected through the

screen is about 226 in³ (0.13 ft³ or 0.98 gallons based on 24" water column in a 4" well casing) and is injected into the aquifer in about 0.6 seconds (time from the impact of hammer until the anvil bounces off the arrestor). This is an equivalent injection rate of about 100 gpm.

Based on pump tests and slug tests at Hedding the hydraulic conductivity (K) is estimated to average 3E-3 cm/sec for the depth of 15 feet to 30 feet zone in the aquifer. The thickness of the aquifer (B) is estimated to be at least 70 feet from the boring log for the existing PVC well and refraction seismic work (see appendix B). The following estimated parameters were used in the first attempts to model the signal at Hedding:

$$\begin{aligned} K &= 3E-3 \text{ cm/sec.}, \\ S &= 0.0001 \text{ (S is storage coefficient)}, \\ B &= 70 \text{ feet, and} \\ \Delta t &= 2E-9 \text{ days (this is 0.0002 second or } 1/5000^{\text{th}} \text{ of a second)}. \end{aligned}$$

While the aquifer at Hedding would be considered as being a phreatic aquifer and for longer pumping periods it would be reasonable to assign a storage coefficient (S) of about 0.2. The generation of the pressure wave occurs so rapidly it is not possible for the aquifer and water to react as a phreatic aquifer. In this sense, the aquifer is acting similar to the initial part of a pump test before the transition can occur from undrained to drained conditions. A storage coefficient consistent with confined conditions was assigned in the model. The change in time, Δt , is selected based on the fastest logging rate used in the field and in the pool testing. Transmissivity (T) was set initially at 4450

gallons per day per foot (based on $T=KB= 3E-3 \text{ cm/sec} \cdot 70'$, and changing units to be consistent with those in the model of g/d/ft).

The computer code selected for modeling the system was PLASM (Prickett and Lonquist, 1971). This is a well-known public domain code. A 70x70 node grid with 1 foot spacing in both the x and y directions is used in the model. Based on the maximum rate of data sampling used of $1/5000^{\text{th}}$ of a second, the initial Δt was 0.0002 second. Thirty time steps are used in the model (this is the maximum number of time steps allowed with this version of the model) with a multiplication factor of 1.5 between time steps giving a total modeling time of 25 seconds. This means that the first time step is 0.0002 seconds, the second time step is $0.0002 \cdot 1.5 = 0.0003$ seconds, the third time step is $0.0003 \cdot 1.5 = 0.00045$ seconds, etc.

An example of the modeling results is shown in Figure F.4. The shape of the curve is similar to those measured in the transducers at both Hedding and Treasure Island (see Figure F.1). There is a rapid rise with a long tail of pressure decay. The shape and height of the curve can be adjusted by varying the transmissivity, storage coefficient, and pressure in the signal well. Examples of effect of these variations are shown in Figure F.5. Changing the T from 4500 g/d/ft to 500 g/d/ft delayed the time of the arrival (shown in Figure F.5 by the location of the maximum pressure rise) by a few seconds. However, a similar order of magnitude change in the storage coefficient delayed the arrival of the peak pressure by tens of seconds and beyond the modeled 22-second window.

F.4a-Arrival Time of the confined pressure wave: Comparison of the arrival times of the confined pressure waves between the model and the measured values are another important parameter necessary to demonstrate understanding of the signals being generated. This was done first by measuring the time difference between the initial input of the signal at the signal well and the initial start of the rise at the measuring point. The second measure of arrival time was a comparison between the ratios of the initial start time of the pressure rise at various distances for each other. At Camp Hedding, it was possible to consistently measure the second ratio because of the location of Keller transducers at 10 and 20 feet from the signal well on the same shot. For the first series of tests at Treasure Island there was no transducer or accelerometer working in the signal well that allowed the measurement of the start times necessary to calculate the first source-transducer arrival times. The measured arrival times were compared to the modeled arrival times.

Figure F.6 is an example of the measurement of the time of start of the signal generation in the signal well as measured by the PCB transducer at 0.147 seconds. The start of the times for rise at Keller 1 ten feet from the signal well and Keller 2 twenty feet from the signal well are 0.22 and 0.43 seconds respectively. Similar measurements were made for the Keller 3 and Druck transducers at Treasure Island.

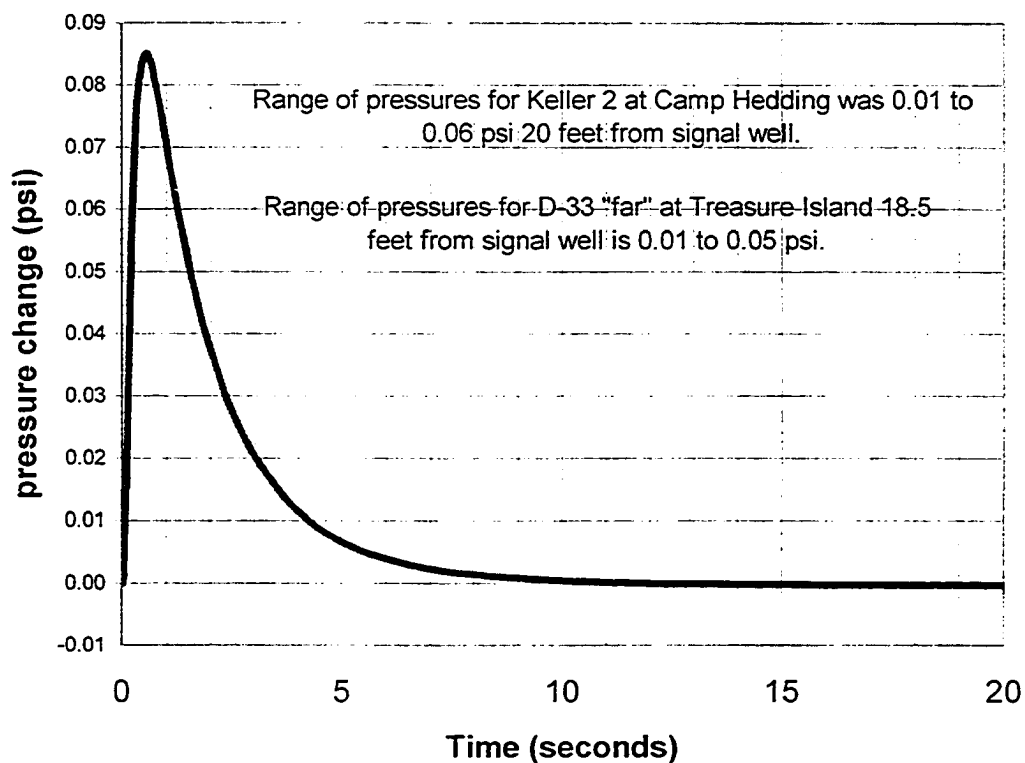


Figure F.4-Modeling: Modeling the signal generated 20 feet from the signal well. Modeling parameters at transmissivity (T) is 4500 gpd, the storage coefficients was 0.0001, and initial pressure in signal well was 310 psi. Similar curves could have been drawn from the modeling data for each distance. The Keller 2 piezometer at Camp Hedding is located 20 feet from the signal well. The most data over the longest period of time has been recorded for the Keller 2 piezometer at Camp Hedding.

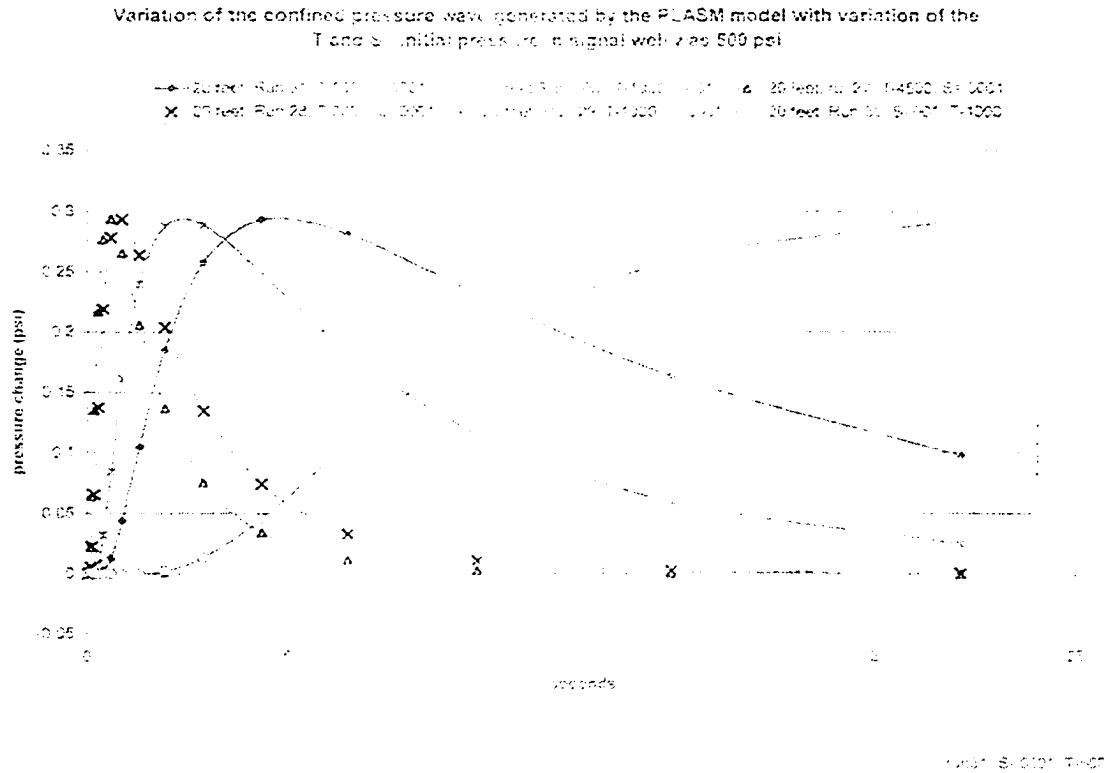


Figure F.5- Variation of parameters in the PLASM model to get different shape response curves 20 feet from the source. T is transmissivity in gallon/day/ft². S is the storage coefficient. The initial pressure at the signal well was assumed to be 500 psi for all the model runs above.

Varying T, S, and pressure within expected ranges of values for the aquifers at Hedding and Treasure Island, it is possible to duplicate the shape, arrival times, and change in water elevation found in all the Keller transducers (Keller 1, Hedding at 10 feet horizontal; Keller 2, Hedding at 20 feet horizontal; Keller 3, Treasure Island at 6.4 feet horizontal). The various transducers used in the signal well measured pressures that

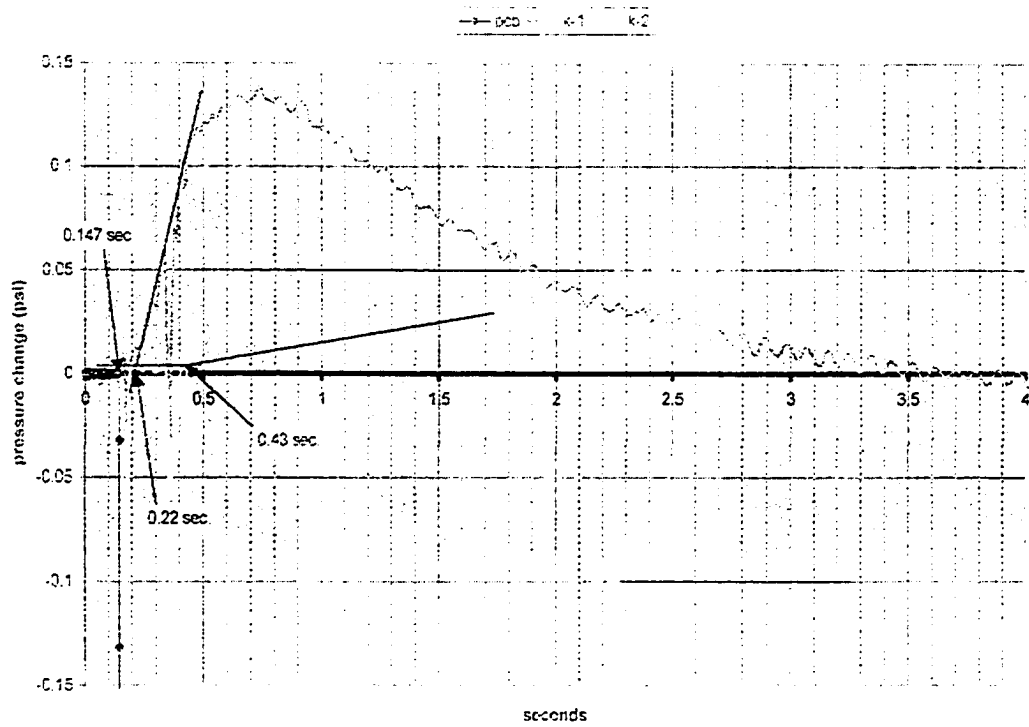


Figure F.6-Calculating the arrival times of the confined pressure waves at Keller 1 (10 feet from the signal well) and Keller 2 (20 feet from the signal well) at Camp Hedding. The initial change in the PCB transducer provides the starting time (0.147 seconds).

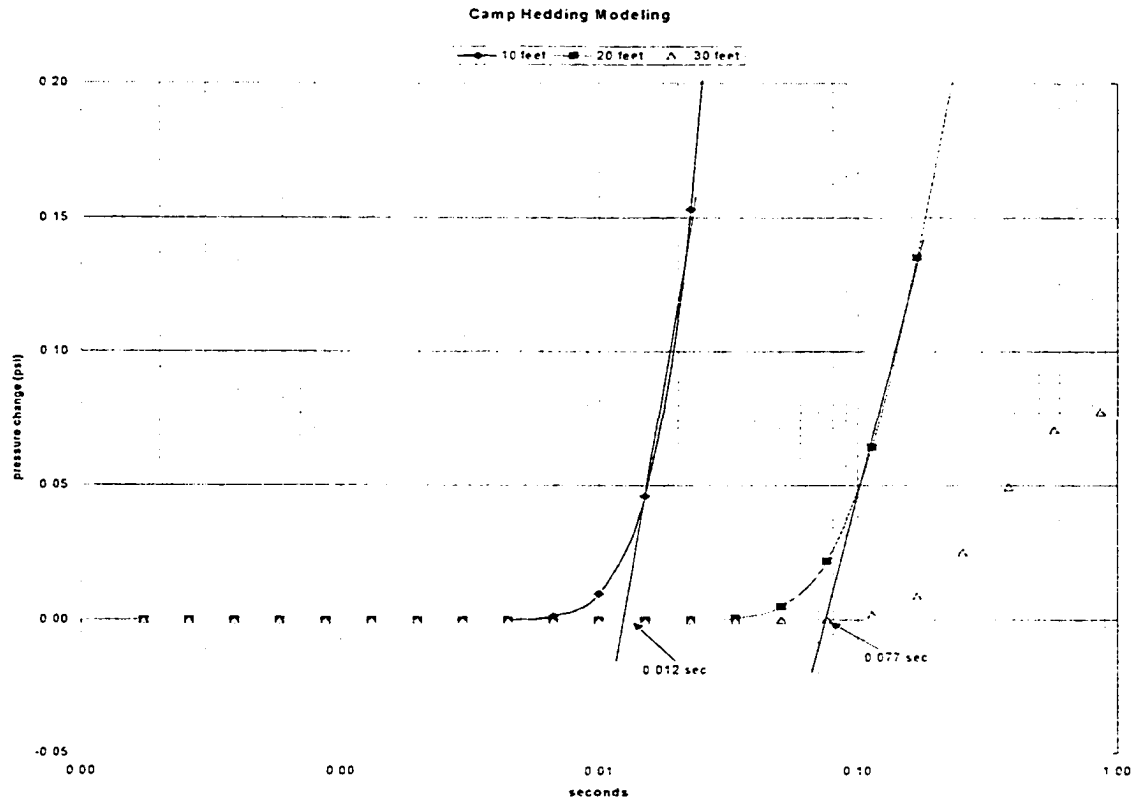


Figure F.7-Modeling: Modeling the confined pressure wave for T-4450 gpd. The velocity of the wave to 10 feet is 833 ft/sec. The velocity to travel a distance of 20 feet is 259 ft/sec.

ranged from 140 psi to over 9000 psi. The 140 psi is far too low based on all the other transducers and the way the Validyne transducer was set up. The upper range of 9000 psi is unrealistic because of the likely damage that would have occurred if such pressures were actually occurring. The rod model suggests an upper limit of about 1500 psi. The destruction of the Roctest transducer suggests a pressure of near 1200 psi was generated.

The uncertainty for transmissivity (T) would be an order of magnitude. For the storage coefficient (S) two orders of magnitude could reasonably be expected. However, the overall results from the modeling suggest that a $T=4500 \text{ g/d/f}$, $S=0.0001$, and pressures between 250 to 1000 psi in the signal well give good approximation of the pressure waves and arrival times at both Camp Hedding and Treasure Island. The transmissivity is in agreement with the insitu testing that was done at Camp Hedding and Treasure Island. The storage coefficient is a reasonable approximation of what should be expected if the fine sand aquifer acted as a confined aquifer for the first few seconds after the hammer shot. The modeled pressures are consistent with the measured pressures provided by the GEMS and Roctest transducers.

F.5-Conclusions for modeling signal: The rod modeling suggests that pressures of 1590 psi can be generated at the surge block using the recommended equations for calculating the spring constants and using the impact model suggested by Smith. This pressure is consistent with the pressures measured inside the signal well and projected from the damaging of a transducer. Further, using pressures in the same magnitude as suggested by the model along with the hydraulic conductivities measured in the field and the measured thickness of the aquifer provide reasonable agreement of the modeled confined pressure wave with actual measured confined pressure peaks and arrival time data. The model confirms the original hypothesis that the hammer first generates a compressional wave that is transferred down the rods to the surge block. The surge block hits the nearly confined column of water transferring the compressional wave to the aquifer. More than one impact may occur as the anvil rebounds off the arrestor. If

the anvil and rods are simply released without being struck by the falling hammer, no compressional wave is created. The speed of the compressional wave in ground water should be near 5000 ft per second. This velocity is near the limit of resolution of the arrival times for the compressional wave at 5, 10, and 20 feet from the signal well, but consistent with the measured signals.

The fall of the surge block, driven by the hammer, drives a surge of water out of the screened interval of the signal well. This surge is the 'hydraulic pressure' wave or 'confined pressure' wave that is measured in the transducers set at various distances from the signal well. Initially the aquifer compressibility and compressibility of the water transmit the pressure through the aquifer similar to a confined aquifer. As the aquifer has time to adjust to the initial pressure there is an actual transfer of water from the well casing into the aquifer. The aquifer acts more as an unconfined aquifer with larger storage coefficient. This 'unconfined pressure' wave was not modeled because in part the frequency of the signal is below any possible interest for earthquake induced liquefaction and a different model would have been necessary to allow changes in the storage coefficient with time during the modeling.